PLUTONIUM FUTURES
THE SCIENCE
26-29 September 2022
AVIGNON (France)

Book of Abstracts

Oral Talks

Plutonium Futures – The Science 2022

ORAL TALKS

Surface Science and Corrosion

	Conference room #1: CELLIER BENOIT XII
PLENARY TALK **09:50 – 10:40**	**Paul ROUSSEL (AWE)** *"The Pu4f line shape revisited"*
	Conference room #1: CELLIER BENOIT XII
INVITED TALK **11:10 – 11:40**	**Thomas GOUDER (European Commission - JRC)** *"Role of intermediate oxides in actinide corrosion"*
11:40 – 12:00	**Sandrine MIRO (CEA)** *"Alteration mechanisms of MOX samples: Studtite formation assessed by Raman Spectroscopy and 18O Isotopic Labeling"*
12:00 – 12:20	**Shohini SEN-BRITAIN (LLNL)** *"Hydrogen corrosion of uranium studied using in-situ and post-mortem analysis"*
	Conference room #1: CELLIER BENOIT XII
INVITED TALK **15:00 – 15:30**	**Lionel JOLLY (CEA)** *"Nature and growth of oxide scale on plutonium metal stabilized with 1 at% of gallium"*
15:30 – 15:50	**Brice RAVAT (CEA)** *"Ga Behavior during oxidation of a Pu alloy stabilized in delta phase"*
15:50 – 16:10	**Hélène ARENA (CEA)** *"Alpha dose rate and decay dose impacts on the long-term alteration of HLW nuclear glasses"*
INVITED TALK **16:40 – 17:10**	**Scott DONALD (LLNL)** *"Evolution of δ-Stabilized Pu-Ga Alloys during Oxidation"*
17:10 – 17:30	**D. Travis CARVER (LANL)** *"High Energy X-Ray Characterization of Microstructure at Macroscopic Depths in Pu Alloys"*
17:30 – 17:50	**Rafael CAPRANI (CEA)** *" Fission products speciation in high burnup SFR fuel: fabrication and experimental characterization of Pu-bearing simulated fuel"*
17:50 – 18:10	**Charles HOURS (CEA)** *"ESEM-monitored dissolution of (U,Th)O2 heterogeneous mixed oxides for spent fuel modeling"*

Chair persons:

Scott BAZLEY and François DELAUNAY

The Pu4f line shape revisited

P. Roussel [1], A. Nelson [2]

[1] AWE plc, Aldermaston, Reading, Berkshire. U. K. RG7 4PR
[2] Lawrence Livermore National Laboratory, Livermore, CA 94551 United States

paul.roussel@awe.co.uk

Quantitative X-ray Photoelectron Spectroscopy (XPS) requires the use Relative Sensitivity Factors (RSF). While it is possible to use theoretically calculated photoionization cross section values combined with the Inelastic Mean Free Path (IMFP) [1], this requires the intensity and energy response function of the electron spectrometer to be calibrated by the methods described by Seah [2]. The alternative and more common approach is to use experimentally determined RSF libraries which are supplied by most instrument manufacturers as part of their data reduction and analysis software. However, these libraries do not contain RSF values for plutonium. RSF values can be determined from a sample of the pure metal. High resolution XPS measurements have been acquired from electro-refined □-Pu. The peaks attributable to the Pu4f spin-orbit doublet comprise of an asymmetric line accompanied by a low intensity satellite approximately 2.5 eV to higher binding energy. To determine the RSF requires measurement of the Pu4f peak area and therefore an understanding of the satellite contribution is required. Mounted on the same platen was a sample of □-Pu(Ga) alloy and high resolution XPS data were acquired using identical spectrometer setting and parameters to be directly comparable to the □-Pu spectra. The differences in the Pu4f peak shape include a decreased satellite intensity and broader peak width in the □-Pu(Ga) alloy and highlights that the Pu4f peak shape in metal and alloys is still not fully understood.

In this presentation we will present an XPS characterization of these two plutonium samples. This includes X-ray induced Auger spectra, curve fitting parameters and RSF for the Pu4p3/2, Pu4d5/2, Pu4f and 6p3/2 transitions and quantification of the Pu4f line shape investigating the Pu4f satellite intensity.

[1] A. G. Shard, J. D. P. Counsell, D. J. H. Cant, E. F Smith, P. Navabpour, X. Zhang, C. J. Blomfield, Surf. Interface Anal., 51 (2019) 763.

[2] M. P. Seah, Surf. Interface Anal. 20 (1993) 243.

Role of intermediate oxides in actinide corrosion

T. Gouder [1], R. Eloirdi [1], M. Jonsson [2]

[1] *European Commission, Joint Research Centre (JRC), 76125 Karlsruhe, Germany*
[2] KTH Royal Institute of Technology, SE-100 44 Stockholm, Sweden

thomas.gouder@ec.europa.eu

Corrosion of actinides proceeds through surface adsorption of oxidants (O, OH, etc.) and incorporation into the lattice. Corrosion is a complex interplay between oxidants and reductants (H, e-, …) both being present at the surface. The early actinides have multiple oxidation states, making them easily available as adsorption sites. With increasing oxidation state, the tendency for oxidant adsorption decreases, while that of reductants increases. There may be formation of unreactive, stable (towards oxidation and dissolution) surface oxide layers. When this occurs, the surface is passivated, higher oxides no longer form, and corrosion stops. Study of the various oxides and their reactivity thus gives valuable information on the corrosion resistance of nuclear waste and fuel.

Surface oxidation and reduction can be studied by model experiments. The simplest reactants are atomic oxygen and hydrogen, which easily stick on the surface. Atomic oxygen reaction allows reaching the highest possible oxidation states (UO_3, Np_2O_5, PuO_2) and makes thus the entire oxide series available for surface science investigations (which are done under vacuum conditions). Diatomic gases (O_2 and H_2) need to dissociate previously, limiting the reaction kinetic. Precise dosage of the adsorbents allows producing intermediate oxides. These oxides have to be distinguished from inhomogeneous surface layers, produced by concentration gradient between highly reacted top surface and unreacted bulk. These are often encountered in classical corrosion studies, where bulk samples are exposed to oxidative environment at low temperatures. Using thin film systems (20nm and less), to avoid the bulk, and relatively elevated temperatures (300°C), to allow fast diffusion, guaranties homogenous reaction layers. We can thus distinguish concentration gradient inhomogeneity from mixed oxide formation.

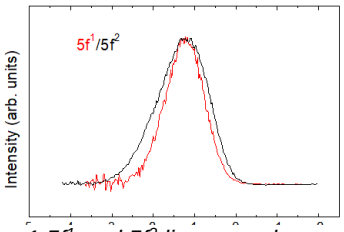

Fig. 1 $5f^1$ and $5f^2$ lines, as observed in $U^{4+}(UO_2)$ and U^{5+} (U_2O_5)

In this presentation, we will report on the surface oxidation and reduction of uranium by oxygen, hydrogen and water, present either as molecular gases or as atomic gases (generated by ECR plasma). Films are analysed in-situ by X-ray and Ultra-Violet Photoelectron Spectroscopy. Uranium oxidation states +4,+5 and +6 are observed and they correspond to $U5f^2$, $U5f^1$ and $U5f^0$ configuration respectively [1]. Analysis of the 5f lineshape allows to distinguish $5f^1$ and $5f^2$ configurations, and thus the +4 and +5 oxidation states (Fig. 1). In UO_2, oxidation with molecular oxygen takes place in 2 steps. First U^{4+} (UO_2) is oxidized to U^{5+}, relatively fast, after which the reaction slows down dramatically. Atomic oxygen oxidizes uranium readily to U^{6+}, which shows that chemisorption and dissociation of O_2 on the U^{5+}

surface layer is the rate-limiting step in surface oxidation of UO_2 by molecular oxygen. Surface reduction proceeds by reaction of hydrogen with the higher oxides. Molecular hydrogen does not react with pure oxides but needs a catalyst (e.g. epsilon particles) to react. Atomic hydrogen reduces UO_3 fast, but slows down on U_2O_5. The reason, still hypothetical, may be linked to the similar crystal structure of UO_3 and U_2O_5 with lower symmetry, which is different from that of UO_2. Further reduction of U_2O_5 to UO_2 thus involves reconstruction. Therefore, almost pure U_2O_5 was produced by UO_3 reduction (Fig. 2). Conversely, it is difficult to obtain pure U_2O_5 by UO_2 oxidation because once U_2O_5 is formed (involving surface reconstruction), oxidation readily continues to mixed oxides and finally UO_3.

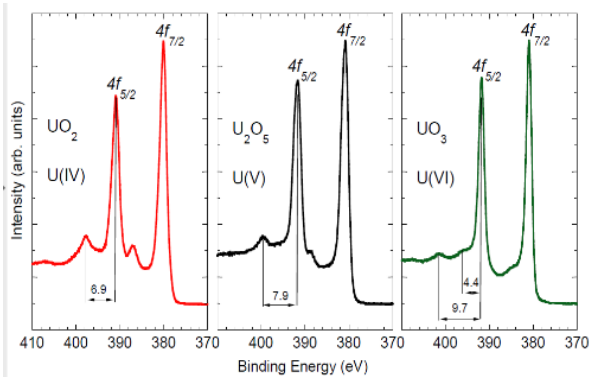

Figure. 2 XPS-U4f spectra of pure U^{4+}, U^{5+} and U^{6+}

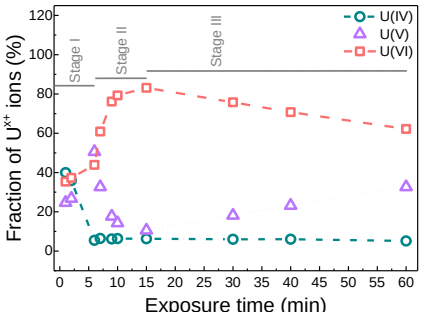

Figure. 3 Evolution of surface oxidation state with water plasma exposure time

Reaction with water plasma is complex, because of the presence of both oxidative (O, OH radicals) and reductive species (H radicals). Water plasma simulates to a certain extent water radiolysis by the radiation field (also producing oxidative and reductive species) and relevant for waste disposal and fuel safety studies. Initial reaction of UO_2 with water plasma leads to the formation of high oxidation state, close to UO_3. Then, the reaction reverses and the surface concentration of U^{5+} increases again (Fig. 3) [3]. This is highly surprising and has to be related to a slowly evolving nature of the oxide. We will discuss tentative explanations.

While we focus on the reaction with uranium, similar studies can also be performed on the other early actinides. Surface interaction of PuO_2 with atomic oxygen and hydrogen has been studied in the past. The results will be briefly recalled and compared to the more extensive studies of the uranium oxides.

[1] T. Gouder,.; R. Eloirdi, ; R. Caciuffo,. Scientific Reports 2018, 8 (1), 8306.
{2] G. El Jamal, T. Gouder, R. Eloirdi, and M. Jonsson, J. Nucl. Mater. 2022 (560), 153504.
[3] G. El Jamal, T. Gouder, R. Eloirdi, and M. Jonsson, Dalton Transactions 2021, 50 (14), 4796.

Alteration mechanisms of MOX samples: Studtite formation assessed by Raman Spectroscopy and ^{18}O Isotopic Labeling

S. Miro, C. Jégou, L. Sarrasin, V. Broudic, C. Marques, M. Tribet, S. Peuget

Commissariat à l'Énergie Atomique (CEA), DES, ISEC, DE2D, Marcoule, France BP 17171. F-30207 Bagnols-sur-Cèze Cedex

sandrine.miro@cea.fr

In the prospect of interim wet storage of the MOX spent fuel assemblies in water pools, the case of a defect affecting the clad must be considered. The high gamma irradiation field, slightly acidic pH of the aerated water (5 - 5.5) and presence of oxidizing species such as H_2O_2 arising from water radiolysis are so many parameters that need to be assessed in such a scenario [1]. The direct contact of the fuel with the pool water will lead to its oxidative dissolution and the formation of secondary phases that may affect the integrity of the assemblies. We aim in this study at understanding the mechanisms responsible for the formation of secondary phases on MOX fuels when in contact with radiolyzed water.

Non-irradiated MOX07 heterogeneous pellets (MIMAS MOX 7% Pu/(U+Pu)) were leached in aerated water under a gamma source (^{60}Co) in order to reproduce the interim storage environment in a hot cell. The initial pH of the solution was of 6.3 but was expected to acidify because of the oxic conditions. This experiment was followed by a second one performed in the same experimental conditions but with water enriched at 97% in ^{18}O. Samples were analysed using Raman spectroscopy over time during the 3 months of the experiments. Punctual spectra as long as mappings of the samples were acquired in order to follow the sample's evolutions and link it to their chemical compositions. The Raman spectroscopy being sensitive to mass variations, the ^{18}O of the second experiment act as a marker for the oxidation/phase formation at the sample's surface. These characterizations of the solids were combined with leachate analyses to follow the alteration markers.

During the leaching experiments, the uranium-rich zones are preferentially altered: they are dissolved prior to Pu-rich aggregates, which causes the appearance of holes at the surface of the samples. This result illustrates the preferential dissolution of the UO_2 grains in the presence of oxidizing species, the zones with a high plutonium content being much more stable with respect to dissolution.

In addition, we evidenced the heterogeneous formation of uranium peroxide at the surface of the samples accordingly to their chemical compositions (Figure 1). In the early stages of the precipitation, this selective dissolution of the UO_2 grains leads to a local precipitation of studtite on their surface and in the corrosion pits, indicating a localized process at the interface. Local supersaturation processes are possible, and preferential germination sites may be found in these corrosion pits. In the long term, the entire MOX fuel surface was covered, including the plutonium-enriched aggregates. We demonstrate here, thanks to Raman mappings, the local nature of the oxidative dissolution and secondary phases precipitation.

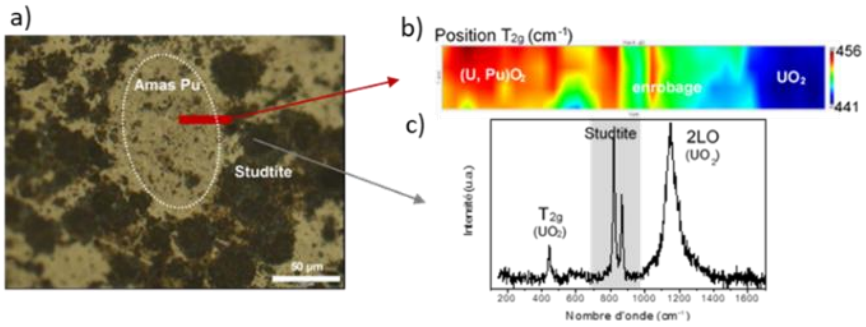

Figure 1: Heterogeneous precipitation of Studtite on U-rich zones of the MOX sample after 20 days of leaching in water with a natural isotopic composition; a) optical image b) Raman mapping and c) Raman spectra of the surface.

Concerning the formation of the uranyl and peroxide bonds, isotopic analysis of the Raman bands of the studtite precipitates highlighted very distinct exchanges (Figure 2). The oxygen atoms in the uranyl bond and in the peroxide bond do not have the same origin, which could be explained by the respective roles of radicals and hydrogen peroxide. The radicals would be mainly involved in the formation of the uranyl ion during the fuel surface oxidation, while the hydrogen peroxide would lead to the formation of peroxide bridges during the studtite precipitation. Finally, this work also demonstrated the feasibility of such an experimental approach, combining Raman imaging with isotopic labeling, to improve our understanding of dissolution mechanisms.

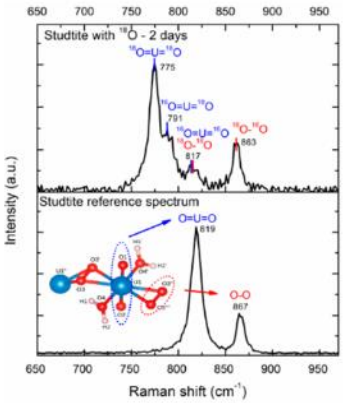

Figure 2: Raman spectra of studtite formed at the surface of the MIMAS MOX sample after two leaching days in ^{18}O-enriched water (top) and formed in water with a natural isotopic composition (bottom), with band assignments and ball-and-stick representation [2].

[1] M. Magnin et al., Journal of Nuclear Materials 462 (2015) 230–241.
[2] L. Sarrasin et al., The Journal of Physical Chemistry C 2021 125 (35), 19209-19218.

Hydrogen corrosion of uranium studied using *in-situ* and post-mortem analysis

Shohini Sen-Britain, Yaakov Idell, Wigbert Siekhaus, Kerri Blobaum, Bill McLean

Lawrence Livermore National Laboratory
7000 East Ave, Livermore CA 94550

senbritain1@llnl.gov

Introduction. Hydrogen corrosion of uranium is a destructive process caused by the following chemical reaction:

$$3H2\ (g) + 2U\ (s) \rightarrow\ 2UH3\ (s)$$

Hydrogen may become introduced into uranium metal during early-stage processing, machining, or storage near hydrogen-generating sources. Uranium hydride (UH_3) precipitates form over time and have lower density than uranium metal. Over time, precipitates that have grown near or below the surface will cause partial or complete spallation of the surface via plastic deformation to relieve stress, and result in component failure [1]. In this paper and presentation, we will report correlations between surface chemical impurities, oxide chemistry, and spallation due to UH_3 precipitation.

Methods. In this work, we have used white-light interferometry (WLI) to observe formation of UH_3 precipitates *in-situ* after introduction of H_2 gas at 2 psi into an environmental gas cell containing a depleted uranium (DU) sample under high vacuum at 35C (Figure 1A). After overnight monitoring, the corroded sample was brought up to atmosphere and the expelled UH_3 precipitates were collected for x-ray diffraction (XRD) analysis. The hydrided sample was then analyzed using time-of-flight secondary ion mass spectrometry (ToF-SIMS) for ion imaging of spalled and partially spalled regions. Edges of a partially spalled and completely spalled region were then removed from the sample using a focused ion beam (FIB) and imaged using transmission electron microscopy (TEM) and energy dispersive spectroscopy (EDS).

Results. ToF-SIMS imaging of spalled and partially spalled regions captured by WLI (Figure 1B) indicates that surface eruption occurs at or near carbide inclusions of the DU surface. Aluminide precipitates are found surrounding partially and completely spalled regions (Figure 1C). STEM/EDS of FIB lift-outs showed that spalled regions contain a surface layer of uranium hydride and a buried layer of uranium oxide while partially spalled regions contain a surface layer of uranium oxide and a buried layer of uranium hydride (Figure 1D). These results were confirmed by ToF-SIMS depth profiles of edges of spalled and partially spalled regions. X-ray diffraction (XRD) analysis of expelled UH_3 precipitates indicated that both the alpha and beta phases of UH_3 is present. The UH_3 precipitates also grew a surface layer of UO_2 (Figure 1E).

Summary. To summarize, this combination of *in-situ* monitoring and post-mortem analysis of hydrogen corroded uranium allows us to monitor initial form of precipitates, distinguish surface chemistry of fully and partially spalled regions, and identify buried layers of UH_3 under partially spalled regions to provide novel insight into hydrogen corrosion.

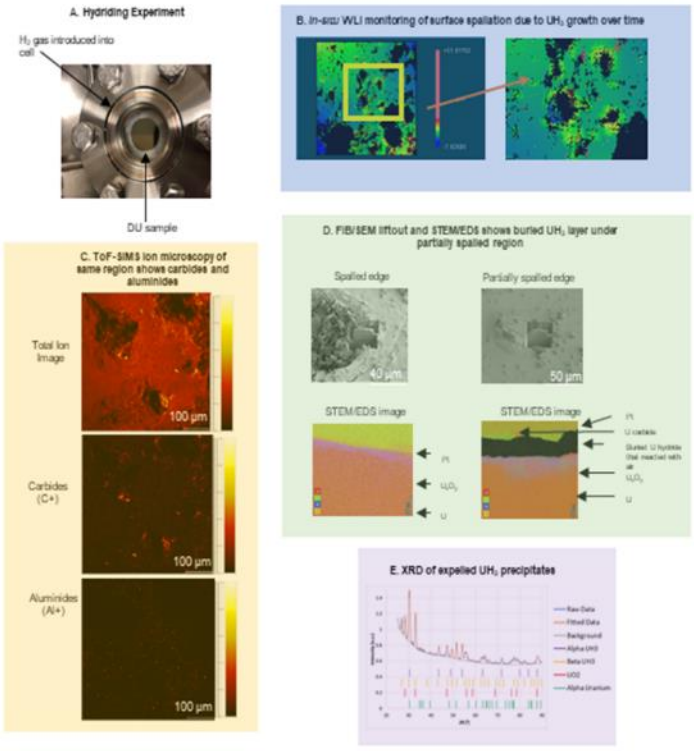

Figure 1. A) Experimental setup, B) WLI monitoring, C) ToF-SIMS analysis, D) FIB/SEM and STEM/EDS analysis, and E) XRD analysis.

Acknowledgements. This work was performed under the auspices of the U.S. Department of Energy by Lawrence Livermore National Laboratory under contract DE-AC52-07NA27344.

[1] A. Loui, "*The Hydrogen Corrosion of Uranium: Identification of Underlying Causes and Proposed Mitigation Strategies*," LLNL-TR-607653, (2012)

Nature and growth of oxide scale on plutonium metal stabilized with 1 at% of gallium

L. Jolly [1], N. Favart [1,2], B. Ravat [1], B. Oudot [1], I. Zacharie-Aubrun [3], P. Martin [4], F. Delaunay[1], I. Popa [2] , S. Chevalier [2]

[1] CEA, Centre de Valduc, 21120 Is sur Tille, France
[2] ICB UMP 6303 CNRS Université de Bourgogne Franche-Comté, 9 avenue Savary, 21078 Dijon, France
[3] CEA, Centre de Cadarache, 13108 St Paul lez Durance, France
[4] CEA, DES, ISEC, DMRC, Université Montpellier, Marcoule, France

lionel.jolly@cea.fr

Plutonium metal is particularly sensitive to corrosion even at ambient temperature. Therefore, the corrosion control during storage is essential. Even if the plutonium metal oxidation is widely treated in the literature, the oxidation of this metal is still difficult to predict due to an extreme sensitivity to a wide range of parameters as nature of atmosphere, temperature, chemical nature of the surface.

As admitted in the literature, the oxidation produces an external PuO_2 layer covering a Pu_2O_3 layer in presence of oxidant atmosphere around ambient temperature and pressure. The oxidation kinetics are interpreted in terms of a parabolic rate law driven by Pu_2O_3 formation followed by a linear rate law connected to PuO_2 growth [1,2].

The purpose of the presented work is to describe in detail the morphology of the oxide scale and to study the parabolic rate law part of the oxidation kinetics of the δ-stabilized plutonium alloy with 1at.% of gallium.

Regarding the structures formed after oxygen exposure of a $PuGa_{1\%at.}$, XRD analyses show that 5 different structures may coexist: α-PuO_2, α-Pu_2O_3, β-Pu_2O_3, β-Pu (or γ-Pu, depending on the temperature of exposition) and δ-Pu. In order to describe the morphology composed of these different phases in the material, FIB-SEM and Raman Microscopy experiments were performed. The comparison of these different analyses led to a fine description of the oxide scale arrangement and morphology which were compared with recent work [3].

Additionally, the oxidation kinetics dependence on temperature and oxygen partial pressure was investigated using original XRD patterns analysis allowing the monitoring of each oxide growth [2]. The oxidation kinetics clearly show that Pu_2O_3 drives the growth of the oxide scale in the parabolic rate law part while PuO_2 drives the growth of the oxide scale in the linear rate law part. In order to model the parabolic kinetics, the Wagner's theory, based on growth of oxide scales by lattice transport, is used [4]. This model depends on parameters such as the nature of the main defect driving the oxidation and its self-diffusion coefficient. These parameters were determined for Pu_2O_3. Oxygen interstitials were identified as main defects since the oxidation kinetics depends on the oxygen pressure and as the oxide growth is anionic revealed by inert marker localisation in the oxide scale using SEM observation of FIB cross section. The self-diffusion coefficient of oxygen was determined by XPS analyses of self-reduction process of PuO_2 into Pu_2O_3 at ambient temperature under ultra-high vacuum.

However, the oxidation kinetics is modified in the presence of a carbide/oxicarbide (PuC/PuCxOy). Indeed, heating the alloy under vacuum, with carbon impurities, may form a thin layer of oxicarbide. By performing in-depth profiling by Ar^+ sputtering, respectively AES [5] and XPS [6] analyses show that this layer is located between the sesquioxide and the metal. The presence of this oxycarbide reduces drastically the oxidation of plutonium alloy.

[1] J.M. Haschke et al., Los Alamos Sci. 26 (2000), 252-273

[2] B. Ravat *et al.*, Corrosion Sci. 138 (2018), 66-74

[3] S. Donald *et al.* Corrosion Sci. 194 (2022), 109923

[4] C. Wagner, Zeitschrift für Phys. Chemie B, 21 (1933), 25-41

[5] S. Donald *et al.* J. Vac. Sci. Technol. A 36, 03E104 (2018)

[6] N. Favart *et al.*, Oxidation of Metals (2021), 96:271–281

Ga Behavior during oxidation of a Pu alloy stabilized in δ–phase

B. Ravat [1], L. Jolly [1], N. Favart [1], D. Menut [2], B. Oudot [1], F. Delaunay [1], I. Popa [3], S. Chevalier [3]

[1]CEA centre de Valduc, 21120 Is-sur-Tille, France
[2] Synchrotron SOLEIL, Ligne de lumière MARS, L'Orme des Merisiers, Saint Aubin – BP 48, 91192 Gif-sur-Yvette, France
[3] ICB UMP 6303 CNRS Univ. Bourgogne Franche-Comté, 9 avenue Savary, 21078 Dijon, France

brice.ravat@cea.fr

Introduction.

Understanding Plutonium alloy oxidation related to safe and long term storage is essential. Therefore, many studies deal with the reactivity of highly metastable δ-Pu alloy under controlled dry oxygen atmosphere at different temperatures and pressures [1-2]. Other parameters may also impact the oxidation kinetics. Indeed, according to the literature [3], the presence of Ga atoms, used as δ-stabilizer in Pu alloys, seems to decrease the oxidation rate. But the precise role played by this solute element during oxidation is not really understood. Does it diffuse out of the oxide scale to be oxidized instead of plutonium atoms limiting the formation of the plutonium oxide scale? Does it stay in the oxide scale and where? Although significant experimental and theoretical results [4-6] were recently published about this topic, several questions remain unanswered. Thus, the purpose of this work is to bring new insights into Ga behaviour during the oxidation process of δ-Pu alloy. The originality of this study lies in the combination of GIEXAFS (Grazing Incidence Extended X-ray Absorption Fine structure) experiments performed at SOLEIL synchrotron coupled with EXAFS data analysis using a Reverse Monte Carlo method which is an atomistic simulation technique allowing to reconstruct the 3D atomic structure of by minimizing differences between experimental and simulated EXAFS spectra.

Experimental details and analysis method.

Experimental study was carried out on a fully homogenised δ- PuGa alloy with a gallium content of 1 at.%. at a limit of δ-metastability. Samples were oxidised at high temperature under dry oxygen atmosphere in a temperature chamber mounted on a classical θ/θ diffractometer. GIEXAFS analyses were performed at MARS beamline of SOLEIL synchrotron. Samples were confined in a sample-holder composed of a double dome which was specifically designed for EXAFS analysis in grazing Incidence. EXAFS measurements were performed in fluorescence mode at the Ga K-edge and Pu L_{III}-edge. Experimental data were analysed by using EVAX code (Evolutionary Algorithm for eXafs analysis) which is a program for the analysis of EXAFS data using reverse Monte Carlo (RMC) and evolutionary algorithm (EA) methods [7].

Results.

As first results, the detection of florescence signal at the Ga K-edge in grazing incidence mode performed to only analyse the oxide scale have confirmed that Ga atoms were effectively present in both Pu_2O_3 and PuO_2 oxide layers. Furthermore, classical EXAFS analyses have revealed that Ga atoms

are surrounded by oxygen atoms as the first coordination shell. But the comparison of EXAFS spectra of the oxide scale formed on δ-Pu alloy and a Ga_2O_3 standard have shown that Ga atoms do not seem to form Ga oxides since no second shell composed by Ga atoms was observed. This means that Ga atoms remain in crystalline structure of Pu oxide scale.

In order to go further in the understanding of Ga behaviour in the oxide scale, investigations were focalized specifically on the analysis of PuO_2 layer to determine precisely in which crystallographic site of PuO_2 lattice Ga atoms could be localized. Thus, analysis of Ga K-edge and Pu L_{III}-edge EXAFS using Reverse Monte Carlo method was carried out. The RMC approach consists in randomly modifying all of the atomic positions of all elements until the spectra calculated from the atomic configuration matches the experimental ones. In this calculation, an atomic configuration including 5×5×5 supercells of 2×2×2 unit cells of PuO_2 was used. Periodic boundary conditions were also taken into account. In PuO_2 supercells, Ga atoms were initially localized at different high-symmetry sites such as in substitution of Pu or O atoms or in insertion in the lattice in the octahedral site. After running RMC simulation, good agreements between calculated and experimental EXAFS data were achieved when Ga atoms were originally placed either in Pu substitutional site (Figure 1) or in insertion in the octahedral site of PuO_2 lattice. The former is in good agreement with DFT calculations performed by Hernandez *et al.* [5] and Ao *et al.* [6]. Moreover, the analysis of this resulting atomic configuration actually show that Ga atoms do not remain in their initial crystallographic site, but they move some tenth of Å (Figure 2) to get closer to a few of the 8 O atoms which initially compose the first coordination shell (Figure 3).

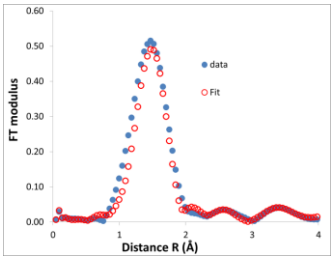

Figure 1: Fourier Transform modulus of simulated and experimental Ga K-edge EXAFS data

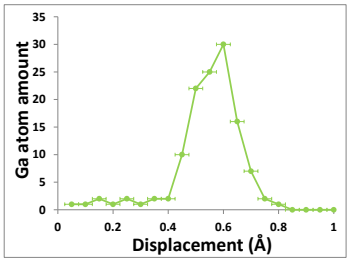

Figure 2: Displacement of Ga atoms from their initial Pu substitutional site

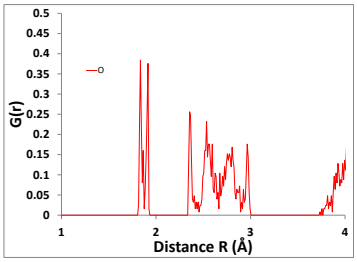

Figure 3: Radial distribution function of O atoms around Ga atoms

References

[1] Stakebake *et al.*, Journal of Less Common Metals, 136(1988) 349-366.
[2] Ravat *et al.*, Corrosion Science, 138 (2018) 66-74.
[3] Haschke *et al.*., Los Alamos Science (2000) 252-272.
[4] Donald *et al.*, Corrosion Science, 194 (2022) 109923.
[5] Hernandez *et al.*, Journal of Physical Chemistry, C 120 (2016) 13095 − 13102.
[6] Ao *et al.*, Computational Materials Science 122 (2016) 263 − 271.
[7] Timoshenko *et al.*, J. Phys.: Condens. Matter 26 (2014) 055401.

Alpha dose rate and decay dose impacts on the long-term alteration of HLW nuclear glasses

M. Tribet[1], H. Aréna[1], C. Marques[1], S. Mougnaud[1], V. Broudic[1], C. Jegou[1], S. Peuget[1]

[1] Univ Montpellier, CEA, DES, ISEC, DE2D, Montpellier, France

magaly.tribet@cea.fr

In the prospect of deep geological disposal, the long-term behavior of high-level nuclear glasses has to be investigated regarding alpha radiation induced by long-life minor actinides. The present study focuses on the effects of alpha radiation on the long-term chemical reactivity of R7T7-type glasses, by separately considering the alpha dose rate and the alpha decay dose. Old SON68 glasses doped with $^{238/239}PuO_2$ or $^{244}CmO_2$ were studied to simulate high alpha dose rates corresponding to an early water ingress and a high level of alpha decay doses corresponding to long-term disposal conditions. A part of the $^{238/239}$Pu-doped glass block was annealed to fully recover the irradiation-induced damage accumulated since the glass was fabricated and to dissociate the effect of the alpha dose rate from that of the alpha decay dose. The glasses were then leached under static conditions at 90 °C for several years. The results showed that the residual alteration rate is not affected by the alpha dose rate over a wide range of dose rate values expected under disposal conditions: this glass remained relatively insensitive to the alpha radiolysis phenomena at the glass - water interface. However, over the duration of the experiments, the residual alteration rate of the damaged $^{238/239}$Pu-doped glass was enhanced compared to that of the annealed glass (Figure 1). This result, underlying the role of the damaged glass structure on its macroscopic behavior, is in agreement with those obtained on previous studies on a ^{244}Cm-doped glass [1] and with leaching behavior of simplified externally irradiated glasses [2-3], indicating that the ballistic effects of the recoil nuclei are responsible for this increase in the residual alteration rate.

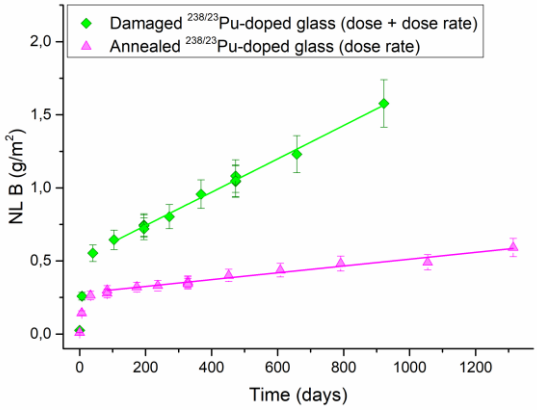

Figure 1: Boron normalized mass loss (NL B) versus time for annealed (pink triangles) and damaged (green diamonds) $^{238/239}$Pu-doped glass leaching tests.

[1] Peuget, S., Delaye, J. M. & Jegou, C. Specific outcomes of the research on the radiation stability of the French nuclear glass towards alpha decay accumulation. J. Nucl. Mater. 444, 76-91 (2014).
[2] Tribet, M. et al. Irradiation Impact on the Leaching Behavior of HLW Glasses. Procedia Materials Science 7, 209-215 (2014).
[3] Mougnaud, S. et al. Heavy ion radiation ageing impact on long-term glass alteration behavior. J. Nucl. Mater. 510, 168-177 (2018).

Evolution of δ-Stabilized Pu-Ga Alloys during Oxidation

Scott B. Donald, J. A. Stanford, W. McLean *and B. Chung*

Lawrence Livermore National Laboratory, 7000 East Avenue, Livermore, CA 94550

donald3@llnl.gov

The corrosion of metals by atmospheric gases, particular water vapor and oxygen, continues to garner interest for establishing safe handling and storage procedures. In the case of plutonium, the consequences to both human and environmental health are amplified by its toxic and radioactive nature, and the absence of a predictive capability to understand the characteristics and properties of the products resulting from exposure to common atmospheric conditions can lead to unintended outcomes. Metallic plutonium has been shown to readily oxidize when exposed to atmospheric conditions, forming a tetravalent dioxide (*i.e.,* PuO_2) with a trivalent sesquioxide (*i.e.,* Pu_2O_3) arising at the oxide metal interface due to thermodynamic constraints. While clarity on the oxidation kinetics of plutonium metal and its alloys has improved with time, less clear is the fate of the alloying element during the formation of an oxide on the metal. Historical studies have focused on gallium as the primary solute element used to stabilize the delta phase and, with few exceptions, understanding the role it plays during formation of an oxide scale remains relatively undeveloped.

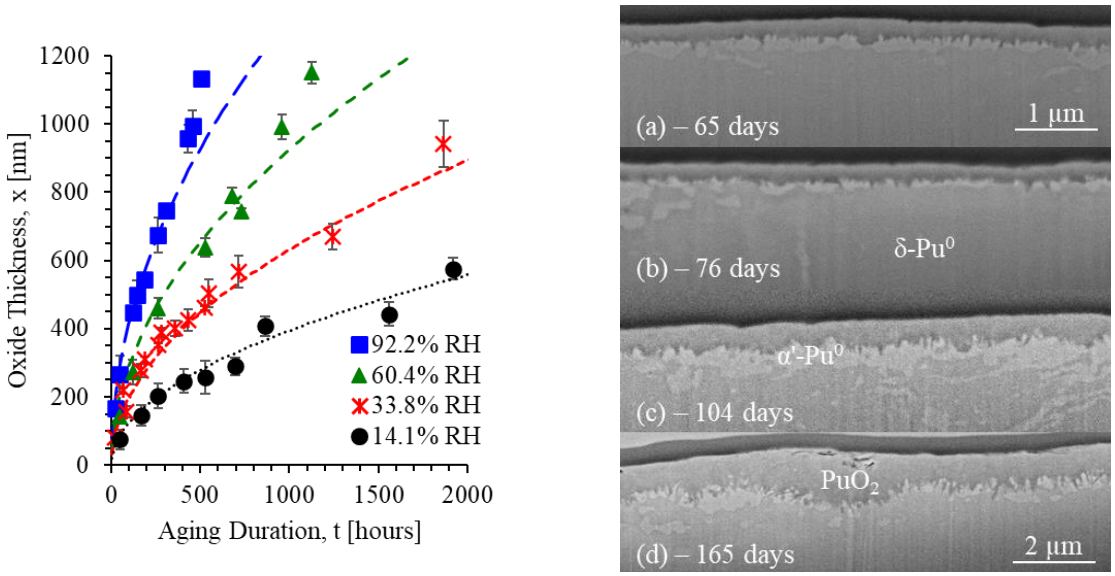

Figure 1: (left) Change in average oxide thickness formed on a delta-stabilized Pu-Ga alloy as a function of time and relative humidity at 25 °C. The dashed lines are parabolic fits to the experimental data. (right) SEM images of FIB cross-sections showing the evolution of the oxide formed on a delta-stabilized Pu-Ga alloy.

When performing investigations on the initial oxidation of δ-Pu, it is important to ensure that all the α`-Pu phase caused by sample preparation has been eliminated. While initial electropolishing has been shown to be sufficient to remove the oxide layer, a more rigorous electropolishing was necessary to completely remove the α` phase. Interestingly, XRD patterns taken following oxidation and growth of an ~1.2 µm thick PuO_2 layer indicated, in addition to the expected PuO_2 and δ-Pu peaks, an α-Pu phase was once again present. Investigation of the subsurface structure and chemistry of the oxide scale and

bulk metal was carried out by ion milling using FIB and subsequent analysis of the cross-section using SEM and AES. As displayed in the SEM images above, a continuous layer of lower-density plutonium dioxide can be identified by the darker region when compared to the brighter regions of the higher-density α`- and δ- plutonium metal phases. The observed oxidation of the stabilizing element by AES indicates the oxidation process may be influenced not only by the inward diffusion of oxygen ions, but also the outward diffusion of gallium ions.

The results of this study indicates the following occurred during growth of the oxide scale on the 1.5 at.% Ga samples studied: 1) there was significant enrichment of gallium on the surface of the sample, and it exists chemically as Ga_2O_3, 2) at a minimum, gallium was also present in the oxide scale at a similar concentration, measured relative to plutonium, as seen for the bulk metal and was determined to also exist chemically as Ga_2O_3, and 3) gallium was non-homogenously depleted at the oxide / metal interface in a layer up to ~1 µm thick, with the thickness of this layer observed to be independent with respect to oxide thickness. The preferential oxidation of the solute δ-stabilizer was found to occur at a sufficient degree to allow for destabilization of the δ-phase and formation of α-phase plutonium.

This work was performed under the auspices of the U.S. Department of Energy by Lawrence Livermore National Laboratory under Contract DE-AC52-07NA27344. This support does not constitute an express or implied endorsement on the part of the government. LLNL-ABS-832116

[1] J. M. Haschke et. al., Journal of Alloys and Compounds **271** (1998) 211

[2] B. Ravat et. al.., Corrosion Science **138** (2018) 66

[3] S. B. Donald et. al., Corrosion Science **187** (2021) 109527

[4] S. B. Donald et. al., Corrosion Science **194** (2022) 109923

High Energy X-Ray Characterization of Microstructure at Macroscopic Depths in Pu Alloys

D.T. Carver,[1] D. W. Brown, [1] T. R. Jacobs, [1] A.I. Smith,[1] J-S Park, [2] P. Kenesei[2]

[1] Materials Science and Technology Division, Los Alamos National Laboratory
[2] X-ray Sciences Division, Argonne National Laboratory

Plutonium is often alloyed with tri-valent elements, such as Aluminum or Gallium, to stabilize the more ductile d-phase at room temperature. These alloys have very rich phase diagrams and, moreover, the kinetics of the phase transformations are very sensitive to defects in the microstructure. As Pu alloys accumulate defects with time naturally through fission events, the phase transformation behavior, as well as mechanical properties) of Pu alloys evolves with age. Study of these phenomenon with traditional means, e.g. optical and electron microscopy, are made difficult by the safety precautions necessary when preparing samples. Benchtop X-ray sources, with energies of 30 keV or less, penetrate on a few microns into Pu. Neutrons, the usual fall-back probe for high-Z materials also only penetrate ^{239}Pu to a few 10's of microns. The advent of 3rd generation synchrotron X-ray sources with beamlines optimized for high energy (70-130 keV) X-rays is a game changer for the study of the phase transformations of Pu and its alloys. We will show first of their kind bulk transmission x-ray micro-tomography (mCT) and high energy X-ray (HEXRD) diffraction measurements on four Pu alloy samples with thickness of order 0.5 mm. The four samples had 2 distinct alloy contents and different histories (age and deformation). Measurements at ambient conditions provide texture, dislocation density, and phase information prior to in-situ measurements collected during cooling to 10K and back to room temperature.

Fission products speciation in high burnup SFR fuel: fabrication and experimental characterization of Pu-bearing simulated fuel

Rafael Caprani [1,2]*, Philippe Martin[1], Damien Prieur[2], Julien Martinez[1], Florent Lebreton[1], Nicolas Clavier[3]

[1] CEA/DES/ISEC/DMRC, Univ Montpellier, Marcoule, France
[2] HELMHOLTZ ZENTRUM DRESDEN ROSSENDORF (HZDR), Dresden, Germany
[3] Institut de Chimie Séparative de Marcoule, Univ Montpellier, CEA, CNRS, ENSCM, Marcoule, France

* E-mail: rafael.caprani@cea.fr

Introduction

In the context of Generation IV Sodium-cooled Fast Reactors (SFR), $U_{y-1}Pu_yO_{2-x}$ Mixed Oxides (MOx) with y ranging from 19 to 40%, are currently considered as the most suitable fuel. These materials have to meet precise physico-chemical properties, which are known to change drastically during irradiation, notably due to the formation of Fission Products (FPs) and their subsequent interaction with the $(U,Pu)O_2$ matrix. Some FPs accommodate into the MOx matrix, while others precipitate into metallic or oxide phases, affecting all fuel physical and chemical properties. Investigating the FPs behaviour is thus of the utmost importance for the understanding of the evolution of the fuel properties during irradiation [1,2].

Considering both high radiotoxicity and complex chemical composition of the spent fuel, model materials called SIMfuel have been developed in the last decades [3-5]. These materials have been shown to be representative of real spent fuel, but with several advantages. First, SIMfuels are constituted by fresh fuel doped with stable FPs isotopes, thus significantly reducing the associated radiological risk during the experimentation. Furthermore, the FPs chemical inventory of these materials can be adjusted to study specifically the effect of selected FPs.

Until now, only UO_2 based SIMfuel have been studied, so their applicability to spent MOx fuel is limited. In the course of this work, we developed a fabrication route to synthesize Pu-bearing SIMfuel (SIMMOx) samples. We further characterized them to study the FPs behaviour and their impact on the $(U,Pu)O_2$ microstructure in several conditions characteristic of different fuel life stages.

Results

In this work, we developed an efficient synthesis method for the fabrication of FPs-doped $U_{0.74}Pu_{0.26}O_{2-x}$ (SIMMOx). Three different batches were prepared, depending on the dopants nature:

- Batch “S”, containing only « soluble » FPs (Ce, La, Nd, Sr, Y, Zr),
- Batch “M”, adding FPs known to form metallic precipitates (same as “S” + Mo, Pd, Rh, Ru),
- Batch “B”, adding Ba as precursor of typical oxide precipitates (same as “M” + Ba).

According to chemical analysis, the samples are representative of real irradiated fuel with a burn up of 13 at. %.

After sintering, different thermal treatments were applied to simulate conditions of engineering interest in both regular and accidental scenarios such as: *in-pile* hypostoichiometric fuel (O/M<2), *in-pile* stoichiometric fuel (O/M=2.00), Loss Of Coolant Accidents (LOCA), and failure of final geological confinement. The evolution of the chemical behaviour of both actinides (U, Pu, Am) and fission products (Ba, Ce, La, Mo, Nd, Pd, Rh, Ru, Sr, Y, Zr) has been followed through several characterization techniques.

XRD and EPMA showed a globally monophasic and homogeneous $(U,Pu)O_2$ matrix typical of SFR fuel, with various FP-based precipitates. Under the most oxidizing conditions, the matrix is shown to oxidize and become biphasic. Oxidation resistance has been observed to depend significantly on the dopants nature, varying among batches S, M, and B. EPMA found small (<30µm) Pu-enriched zones in the matrix containing higher FPs concentration, showing that this phenomenon is due only to thermodynamics and not only to burnup, as previously believed. Through the coupling of EPMA with Raman, we were able to correlate the local FPs enrichment with the changes in the Raman spectra (and thus in local symmetry) on a µm scale. The FP has been found to have a significant effect on the anionic sublattice, which is reflected on all the observed Raman bands. Synchrotron XAS experiments performed at ESRF-ROBL, supplied crucial information on the fission products speciation, determining the prevalent chemical form of each dopant in the samples. HERFD-XANES performed at SOLEIL-MARS allowed for a precise determination of the chemical form of some FP (Ba + Lanthanides), and the actinides oxidation state, thus providing the O/M ratio of the matrix.

Conclusion

We developed, for the first ever in literature, a synthesis method for $(U,Pu)O_2$ SIMfuel samples (SIMMOx), and thoroughly characterized them to study the FPs behaviour. XRD, EPMA, Raman, and XAS were combined to perform a microstructural characterization of *as-sintered* and annealed samples. The overall material is representative of real irradiated $U_{0.74}Pu_{0.26}O_{2-x}$ fuel, in both chemical composition and microstructure.

The evolution of the FPs chemical behaviour has been followed through different thermal treatments simulating various normal and accidental conditions highlighting their rich interaction with the MOx matrix.

[1] Y. Guerin, Compr. Nucl. Mater., Elsevier, Oxford, 2012.
[2] K. Samuelsson et al., J. Nucl. Mater. 532, 2020, 151969.
[3] C. Le Gall, PhD Thesis, Université Grenoble Alpes, 2018.
[4] E. Geiger, PhD Thesis, Université Paris-Saclay, 2016.
[5] P.G. Lucuta et al., J. Nucl. Mater. 178, 1991, 48-60.

ESEM-monitored dissolution of $(U,Th)O_2$ heterogeneous mixed oxides for spent fuel modeling

C. Hours [1], L. Claparede [2], I. Viallard [3], N. Reynier-Tronche [1], É. Castelier [3], N. Dacheux [2]

[1] CEA, DES, ISEC, DMRC, Univ Montpellier, Marcoule, France [2] ICSM, CEA, CNRS, ENSCM, Univ Montpellier, Marcoule, France [3] CEA, DES, IRESNE, DEC, Cadarache, France.

nathalie.reynier-tronche@cea.fr

Introduction

Sodium-cooled fast neutrons reactors (SFR) are among the concepts of reactors developed in the Generation IV International Forum. The capacity of these reactors to split transuranic elements allows for better resources management, for control of plutonium stocks and for the reduction of waste toxicity. Fuels for these SFR reactors are Mixed OXide (MOX) with higher plutonium content than in the MOX fuels dedicated to LWR reactors. They induce significant challenges for the reprocessing step due to the refractory nature of plutonium dioxide in nitric acid medium.

One part of the research carried out for SFR MOX fuels relies on the development of modeling tools able to reproduce their dissolution behavior. In particular, Pu-enriched heterogeneities present in small quantities in SFR oxide fuels are expected to significantly participate in the final balance of residues of dissolution. Furthermore, SFR spent fuels also contain refractory metallic inclusions (mainly composed of Ru, Rh, Pd, Tc and Mo) which can influence the dissolution at the solid/liquid interface and in solution.

For these reasons, characterization of such Pu-rich heterogeneities and metallic inclusions was required in order to study their impact on the dissolution behavior of SFR oxide fuels in order to improve the current modeling tools regarding dissolution.

Methods

Using thorium as a plutonium surrogate, heterogeneous $U_{1-x}Th_xO_2$ samples including platinum group elements (Ru, Rh, Pd) and Mo have been synthetized by wet chemistry route. Several $U_{1-x}Th_xO_2$ powders containing various thorium contents have been prepared by hydroxide precipitation from mixtures of cations in solution [1]. The powders were mixed then sintered through a two-step procedure involving uniaxial pressing at room temperature followed by a heat treatment at 1600 °C under reducing conditions. Through this sintering step, metallic inclusions were formed in the materials while the pellets also contained heterogeneities in terms of U/Th mole ratios.

The microstructure, metallic inclusions and heterogeneities spatial distribution were then characterized using image analysis and geostatistical tools (a set of mathematical techniques well suited for image analysis of spatialized phenomena like heterogeneities distribution [2]) for validation of their ability to mimic SFR spent fuel.

Dissolution experiments consisted of both a set of macroscopic static dissolutions in concentrated nitric acid and a coupled localized operando ESEM-monitored dissolution tests (Figure 1). Images

obtained from ESEM-monitoring were then used to reconstruct the observed surface in 3D and determine a localized dissolution behavior [3]. The combined use of data obtained from the characterization of the pellets, the dissolution results and the 3D reconstructions allows for a better understanding of the heterogeneous mixed oxides fuel dissolution behavior in typical spent fuel recycling conditions.

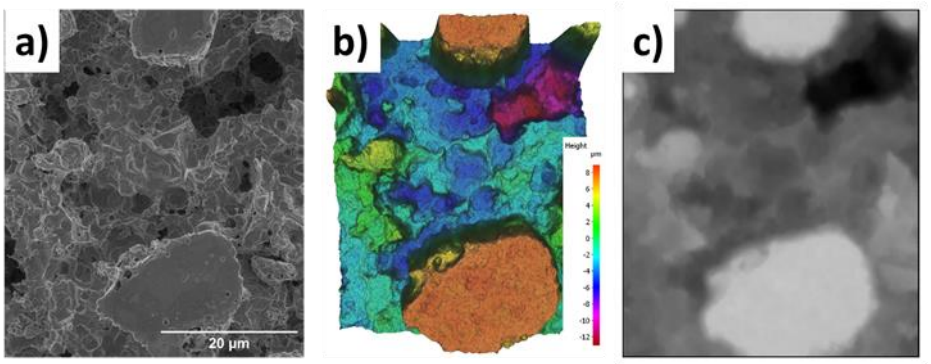

Figure 1: SEM micrography of an heterogeneous (U,Th)O_2 pellet after 108h of dissolution (60 °C; [HNO3] 2M) (a) ; 3D reconstruction of the microstructure (b) and height map generated with the 3D reconstruction (c).

[1] J. Martinez *et al.*, « An original precipitation route toward the preparation and the sintering of highly reactive uranium cerium dioxide powders », *J. Nucl. Mater.*, nº 462, p. 173-181, 2015.
[2] M. A. Oliver et R. Webster, « A tutorial guide to geostatistics: Computing and modelling variograms and kriging », *CATENA*, vol. 113, p. 56-69, févr. 2014.
[3] R. Podor *et al.*, « 3D-SEM height maps series to monitor materials corrosion and dissolution », *Mater. Charact.*, vol. 150, p. 220-228, avr. 2019.

Solution and Gas-phase Chemistry

	Conference room #2: CHAMBRE DU TRÉSORIER
INVITED TALK **11:10 – 11:40**	**Florent RÉAL (University of Lille)** *"Challenges in relativistic electronic structure calculations of gas-phase reactivity and thermodynamics of actinide species"*
11:40 – 12:00	**Gauthier DEBLONDE (LLNL)** *"Unravelling the heavy side of radiochemistry: macrochelators unlock novel actinide chemistry"*
12:00 – 12:20	**Norbert JORDAN (HZDR)** *"Complexation of Cm (III) with aqueous phosphates at elevated temperatures: a luminescence, thermodynamic, and ab initio study"*
PLENARY TALK **14:00 – 14:50**	*Conference room #1: CELLIER BENOIT XII* **Amy HIXON (University of Notre Dame)** *"Speciation in the Pu (VI)-oxalate System"*
	Conference room #2: CHAMBRE DU TRÉSORIER
INVITED TALK **15:00 – 15:30**	**Rebecca ABERGEL (UC Berkeley / LBNL)** *"From actinium to einsteinium: Expanding the synthetic and structural toolkit for actinide coordination"*
15:30 – 15:50	**Damien TOLU (CEA)** *"Simulation of alpha radiolysis in organic solution with plutonium at ultrashort time scales"*
15:50 – 16:10	**Melody MALOUBIER (CNRS)** *"First M4-edge RIXS measurement on Pa (V) complexes in aqueous solution"*
INVITED TALK **16:40 – 17:10**	**Enrique BATISTA (LANL)** *"New Methodology for Large-Scale Molecular Dynamics Simulation of Actinides in Solution"*
17:10 – 17:30	**Stefan MINASIAN (LBNL)** *"The Role of Orbital Overlap in Chemical Bonding for Actinide Hexafluoride Complexes"*
17:30 – 17:50	**Loïc DARONNAT (CEA)** *"Effect of Calmodulin variants on the redox behaviour of Pu (IV)"*
17:50 – 18:10	**Nicholas CICCHETTI (University of Nevada, Las Vegas)** *"Stabilization and Characterization of Heptavalent Neptunium in Acid"*

Chair persons:

Annie KERSTING & Christophe DEN AUWER

Challenges in relativistic electronic structure calculations of gas-phase reactivity and thermodynamics of actinide species

Florent Réal [1], Valérie Vallet [1], André Severo Pereira Gomes [1], Sophie Kervazo [1], Mohammad Saab [1,2], François Virot [2], Yu Gong [3], John K. Gibson [3]

[1] Univ. Lille, CNRS, UMR 8523 - PhLAM - Physique des Lasers Atomes et Molécules, F-59000 Lille, France
[2] Chemical Sciences Division, Lawrence Berkeley National Laboratory, Berkeley, California 94720, United States
[3] Institut de Radioprotection et de Sûreté Nucléaire (IRSN) PSN-RES, Cadarache, Saint Paul Lez Durance 13115, France

florent.real@univ-lille.fr

Probing the electronic structures, reactivity and thermodynamics properties of early actinide (U, Np, Pu) elements is a key fundamental aspect of actinide physical-chemistry, in order to elucidate to which extent their properties differ from one element to the other. When studied in the gas phase, it is possible to probe oxidation states that might not be readily accessible in condensed phase. However, these properties are strongly dependent on the correct description of the electronic ground state of the molecule or complex.

In this presentation, we will first discuss the reactivity of pentavalent actinyl $AnO_2^{(V)}$ sulfinate complexes $[(An^{V}O_2)(CH_3SO_2)_2]^-$ or $[(An^{V}O_2)(C_6H_5SO_2)_2]^-$ to investigate on the one side how Np and Pu complexes might differ from U ones, and on the other side, how the relative strengths of C-S mond in methanesulfinate and benzesulftinate impact the fragmentation pathways. To answer these questions, we have confronted the results of collision induced dissociation experiments to relativistic multi-reference electronic structure calculations [1].

The second focus will be on the thermodynamics properties of gas-phase volatile plutonium species, PuO_2, PuO_3, and $PuO_2(OH)_2$, in their neutral and ionic forms. We showcase the use of relativistic quantum chemical methods to predict the forms and quantities of the released plutonium species under accidental conditions [2, 3].

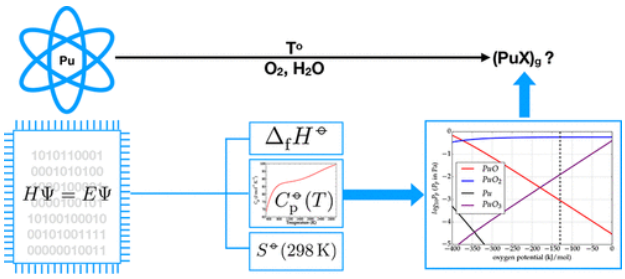

Figure 1: Ab initio prediction of Pu oxide thermodynamic properties

[1] V. Vallet, Y. Gong, M. Saab, F. Réal, J. K. Gibson, *Dalton Trans*. **49**, 3293–3303 (2020)
[2] K. Boguslawski, F. Réal, P. Tecmer, C. Duperrouzel, A. S. P. Gomes, Ö. Legeza, P. W. Ayers, and V. Vallet, *Phys. Chem. Chem. Phys.* **19**, 4317 (2017)
[3] S. Kervazo, F. Réal, F. Virot, A. S. P. Gomes, V. Vallet, *Inorg. Chem.* **58**, 14507–14521 (2019)

Unravelling the heavy side of radiochemistry: macrochelators unlock novel actinide chemistry

G. J.-P. Deblonde,[1] C. Colla,[1] I. Colliard,[2] J. Cotruvo Jr.,[3] Z. Dong,[1] A. B. Kersting,[1] J. Lee,[1] H. Mason,[1] J. Mattocks,[3] K. Morrison,[1] M. Nyman,[2] A. Sawvel,[1] P. T. Woody,[1] M. Zavarin[1]

[1] Lawrence Livermore National Laboratory, Livermore, California 94550, USA
[2] Oregon State University, Corvallis, Oregon 97331, USA
[3] The Pennsylvania State University, University Park, Pennsylvania 16802, USA

Deblonde1@LLNL.gov

The vast majority of the literature on actinide solution-state and solid-state chemistry is focused on small compounds (i.e., metals, oxides, small inorganic salts, metal ion complexes with small organic ligands). The recent emergence of new f-element radioisotopes for use in medicine, such as actinium [1], combined with a continued push to understand and predict the behavior of nuclear waste in the environment [2], call for the expansion of actinide and lanthanide chemistry to novel chelators, beyond the classic small molecules.

This presentation will detail a novel strategy explored by our team which consists of using macrochelators, whether natural or synthetic, for targeting actinides, including the most elusive ones [3–5]. Our multi-pronged strategy led us to investigate the solution-state chemistry of actinium and transuranic elements in the presence of a recently discovered metalloprotein, lanmodulin [6]. Our comprehensive thermodynamic and spectroscopic studies revealed potential new mechanisms for actinide migration in the environment as well as innovative separation pathways for radioisotopes. Our approach also leveraged polyoxometalate macroligands to isolate and characterize f-elements, and revealed otherwise unnoticeable differences between solution-state versus solid-state actinide chemistry, as well as actinide versus lanthanide chemistry. These investigations demonstrate that, contrary to small ligands, macromolecular chelators possess an expanded and yet unexplored repertoire of photophysical properties that can benefit radiochemical studies, from the fundamental chemistry of f-elements to the production/purification of radionuclides and environmental studies on nuclear materials.

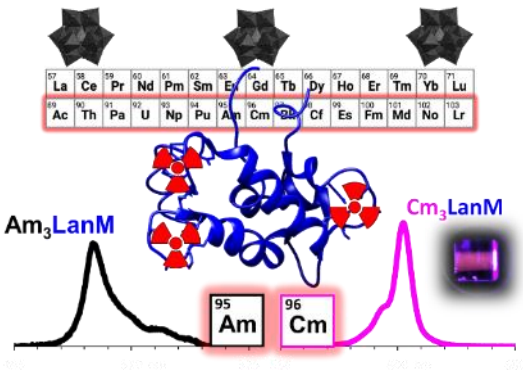

Figure 1: Investigations of macromolecular ligands, from metalloproteins to polyoxometalates, gave another perspective on the behavior of lanthanide and actinide elements, for both solution-state and solid-state chemistry.

References:

[1] G.J.-P. Deblonde, M. Zavarin, A.B. Kersting, The coordination properties and ionic radius of actinium: A 120-year-old enigma, Coordination Chemistry Reviews. 446 (2021) 214130. https://doi.org/10.1016/j.ccr.2021.214130.
[2] G.J.-P. Deblonde, A.B. Kersting, M. Zavarin, Open questions on the environmental chemistry of radionuclides, Commun Chem. 3 (2020) 1–5. https://doi.org/10.1038/s42004-020-00418-6.
[3] G.J.-P. Deblonde, J.A. Mattocks, Z. Dong, P.T. Wooddy, J.A. Cotruvo, M. Zavarin, Capturing an elusive but critical element: Natural protein enables actinium chemistry, Science Advances. 7 (2021) eabk0273. https://doi.org/10.1126/sciadv.abk0273.
[4] G.J.-P. Deblonde, J.A. Mattocks, H. Wang, E.M. Gale, A.B. Kersting, M. Zavarin, J.A. Cotruvo, Characterization of Americium and Curium Complexes with the Protein Lanmodulin: A Potential Macromolecular Mechanism for Actinide Mobility in the Environment, J. Am. Chem. Soc. 143 (2021) 15769–15783. https://doi.org/10.1021/jacs.1c07103.
[5] I. Colliard, J. Lee, C. Colla, A.M. Sawvel, H. Mason, M. Zavarin, M. Nyman, G.J.-P. Deblonde, Exploiting polyoxometalate ligands to complex, isolate, and characterize actinides, (2022).
[6] J.A.Jr. Cotruvo, E.R. Featherston, J.A. Mattocks, J.V. Ho, T.N. Laremore, Lanmodulin: A Highly Selective Lanthanide-Binding Protein from a Lanthanide-Utilizing Bacterium, J. Am. Chem. Soc. 140 (2018) 15056–15061. https://doi.org/10.1021/jacs.8b09842.

This work was performed under the auspices of the U.S. Department of Energy by Lawrence Livermore National Laboratory under Contract DE-AC52-07NA27344.

(Release number: LLNL-ABS-832637)

Complexation of Cm(III) with aqueous phosphates at elevated temperatures: a luminescence, thermodynamic, and *ab initio* study

N. Jordan [1], N. Huittinen [1], I. Jessat [1], F. Réal [2], V. Vallet [2]

[1] Helmholtz-Zentrum Dresden-Rossendorf e.V., Institute of Resource Ecology, Bautzner Landstraße 400, D-01328 Dresden, Germany
[2] Université de Lille, CNRS, UMR 8523 – PhLAM – Physique des Lasers Atomes et Molécules, F-59000 Lille, France

n.jordan@hzdr.de

The incorporation of actinides in lanthanide phosphate matrices crystallizing in the monazite structure has been intensely investigated in the past decades due to the relevance of these monazites as potential ceramic host phases for the immobilization of specific high level radioactive waste (HLW) streams [1-3]. In recent years, understanding the incorporation behaviour of trivalent dopants in the $LnPO_4 \bullet xH_2O$ rhabdophane structure has been given more attention [4,5]. Rhabdophane is the hydrated phosphate precursor in the synthesis of monazites through precipitation routes and a potential secondary mineral controlling actinide solubility in dissolution and re-precipitation reactions of monazite host-phases. Despite the large interest in lanthanide phosphates and the interaction of actinides with these solids, very little data [6-8] is available on the complexation of lanthanides and actinides with aqueous phosphates, even though these complexation reactions precede any aqueous synthesis of monazite ceramics and are expected to occur in natural waters as well as in the proximity of monazite-containing HLW repositories. In many cases, an independent spectroscopic validation of the stoichiometry of the proposed complexes, is also missing. Both from the perspective of aqueous rhabdophane synthesis, which is often carried out at elevated temperatures, and heat-generating HLW immobilization in monazites, the lanthanide and actinide complexation reactions with aqueous phosphates under ambient conditions should be complemented with data obtained at higher temperatures.

In the present work, laser-induced luminescence spectroscopy was used to study the complexation of Cm(III) (1.15×10^{-8} to 1.15×10^{-7} M) as a function of total phosphate concentration (0 to 0.08 M) in the temperature regime 25-90 °C, using $NaClO_4$ as a background electrolyte (I = 0.5 to 3.0 M). These studies have been conducted in the acidic pH-range ($-\log_{10}[H^+]$ = 1.00, 2.52, 3.44, and 3.65) to avoid precipitation of solid Cm rhabdophane. For the first time, in addition to the presence of $CmH_2PO_4^{2+}$ already evidenced before [6,7], the formation of $Cm(H_2PO_4)_2^+$ was unambiguously established from the luminescence spectroscopic data collected at the various H^+ concentrations previously mentioned [8].

The conditional complexation constants of both aqueous complexes were found to increase upon rising ionic strength and temperature. Extrapolation of the obtained complexation constants to infinite dilution at 25 °C was performed by applying the Specific Ion Interaction Theory (SIT) [9]. The obtained $\log_{10} \beta°$ values for $CmH_2PO_4^{2+}$ and $Cm(H_2PO_4)_2^+$ were 0.45 ± 0.04 and 0.08 ± 0.07 [8], respectively, for reactions 1 and 2 below:

$$Cm^{3+} + H_3PO_4 \rightleftharpoons CmH_2PO_4^{2+} + H^+ \quad (1)$$

$$Cm^{3+} + 2\ H_3PO_4 \rightleftharpoons Cm(H_2PO_4)_2^{+} + 2\ H^+ \quad (2)$$

The ion interaction coefficients $\varepsilon(CmH_2PO_4^{2+};ClO_4^-) = 0.17 \pm 0.04$ and $\varepsilon(Cm(H_2PO_4)_2^{+};ClO_4^-) = -0.10 \pm 0.06$ were derived at 25 °C [8].

Temperature-dependent conditional complexation constants for the identified species were obtained from the recorded luminescence emission spectra. They were subsequently extrapolated to I =0 M, assuming that the ion interaction parameters obtained at 25 °C are not significantly impacted by the temperature increase from 25 °C to 90 °C [6]. Using the integrated van´t Hoff equation, both the molar enthalpy of reaction $\Delta_rH_m°$ and entropy of reaction $\Delta_rS_m°$ values were found to be positive for the two complexes, namely $CmH_2PO_4^{2+}$ and $Cm(H_2PO_4)_2^{+}$ [8].

Relativistic quantum chemical investigations revealed a monodentate binding of the $H_2PO_4^-$ ligand to the central Cm^{3+} ion to be the most stable configuration for both complexes. By combining *ab initio* calculations with a thorough analysis of the obtained luminescence spectroscopic data, both $CmH_2PO_4^{2+}$ and $Cm(H_2PO_4)_2^{+}$ complexes with an overall CN of 9 were shown to be stable in solution at 25 °C. However, a different temperature-dependent evolution of the coordination of the Cm^{3+} ion to hydration water molecules could be derived from the electronic structure of the Cm(III)-phosphate complexes. More specifically, an overall coordination number of 9 was retained for the $CmH_2PO_4^{2+}$ complex in the investigated temperature range (25 to 90 °C), while a coordination change from 9 to 8 was established for the $Cm(H_2PO_4)_2^{+}$ species with increasing temperature [8]. This change of coordination upon increasing temperature, which has not been investigated in detail in the past, might also be relevant in the complexation of other f-elements with inorganic and/or organic ligands and deserves further exploration.

[1] R. C. Ewing, Proc. Natl. Acad. Sci. USA 96, 3432 (1999).
[2] D. Bregiroux et al., J. Nucl. Mater. 366, 52 (2007).
[3] N. Huittinen et al., J. Nucl. Mater. 486, 148 (2017).
[4] E. Du Fou de Kerdaniel, J. Nucl. Mater. 362, 451 (2007).
[5] N. Huittinen et al., Inorg. Chem. 57, 6252−6265 (2018).
[6] H. Moll et al., Radiochim. Acta, 99, 775−782 (2011).
[7] N. Jordan et al., Inorg. Chem. 57, 7015-7024 (2018).
[8] N. Huittinen et al., Inorg. Chem. 60, 10656−10673 (2021).
[9] I. Grenthe et al., Second update on the chemical thermodynamics of uranium, neptunium, plutonium, americium and technetium, OECD Nuclear Energy Agency Data Bank, Eds., OECD Publications, Paris, France, (2020).

Speciation in the Pu(VI)-oxalate System

A. Kirstin Sockwell [1], Nicole A. DiBlasi [1,2], and Amy E. Hixon [1]

[1] Department of Civil & Environmental Engineering & Earth Sciences, University of Notre Dame, Notre Dame, IN 46556 USA [2] Karlsruhe Institute of Technology, Institute for Nuclear Waste Disposal, Hermann-von-Helmhotz-Platz 1, Eggenstein-Leopoldshafen 76344 Germany

ahixon@nd.edu

The presence of plutonium in the geosphere poses a long-term environmental concern due to its toxicity and the long half-lives of several isotopes. Although there is global consensus that geologic disposal is the safest existing approach to dealing with used nuclear fuel and high-level nuclear waste, only a few nations are moving towards implementing a geologic repository due to technical and political barriers. Understanding the factors that affect the mobility of plutonium in the subsurface environment is critical to support the development of such repositories and will be essential for remediating locations contaminated as a result of nuclear weapons production and testing.

Although oxidation state is the primary factor in determining the mobility of plutonium in the subsurface environment [1], other important factors include pH and the presence of aqueous complexing ligands, such as oxalate ($(C_2O_4)^{2-}$). Oxalate is introduced into the nuclear fuel cycle at multiple points, including during reprocessing of used nuclear fuel and as a by-product of radiolytic degradation of waste conditioning, ion-exchange materials, and natural organic matter [2-3]. Growing interest in the development and use of mixed-oxide fuels, as well as the ongoing environmental remediation of legacy nuclear waste sites and planning for geologic repositories for used nuclear fuel, necessitates a deeper understanding of the plutonium oxalate system.

This work describes the behaviour of aqueous Pu(VI) in the presence of oxalate as a function of pH (1, 3, > 6) and metal to ligand ratio (M:L) (1:10–10:1) in order to determine the effect of the protonation state of oxalate and the potential formation of multiple Pu(VI)-oxalate complexes in solution. All experiments were conducted in a hood under ambient laboratory conditions at constant ionic strength (I = 0.1 M NaCl). The oxalate concentration was varied (0–10 mM) using a 20 mM oxalic acid stock in 0.1 M NaCl that was initially adjusted to pH 8 with 0.1 M NaOH. For each sample, an aliquot of the oxalic acid stock was adjusted to the target pH value (1, 3, > 6). Once the appropriate pH was achieved, the sample was spiked with weapons-grade Pu(VI) such that the initial plutonium concentration was 1 mM. Each sample was analysed using UV-vis-NIR spectrophotometry as soon as possible after the addition of plutonium. Aqueous plutonium concentrations were monitored by liquid scintillation counting.

Figure 1 shows the absorption spectra of Pu(VI)-oxalate solutions as a function of pH and M:L ratio. Varying the pH impacts the free Pu(VI) in solution as well as the formation of Pu(VI)-oxalate complexes. At pH 1, the oxalate ion is expected to be fully protonated. Although the Pu(VI) aquo ion remains an important species even at M:L = 1:10 (as indicated by the peak at 831 nm), complexation does appear to occur, as indicated by the in-growth of a peak at 839 nm. Previous studies suggest the formation of 1:1 and 1:2 Pu(VI)-oxalate complexes under these conditions [4]. At higher pH values, partial (pH = 3) or full (pH > 6) deprotonation of the oxalate is expected. The complete loss of the Pu(VI)-aquo peak at pH 3 (831 nm) and pH > 6 (850 nm) with increasing oxalate concentration suggests a loss of the

uncomplexed Pu(IV) aquo ion or hydrolysis complex, respectively. The new peak at 849 nm might suggest the formation of 1:2 or 2:3 Pu(VI)-oxalate complexes.

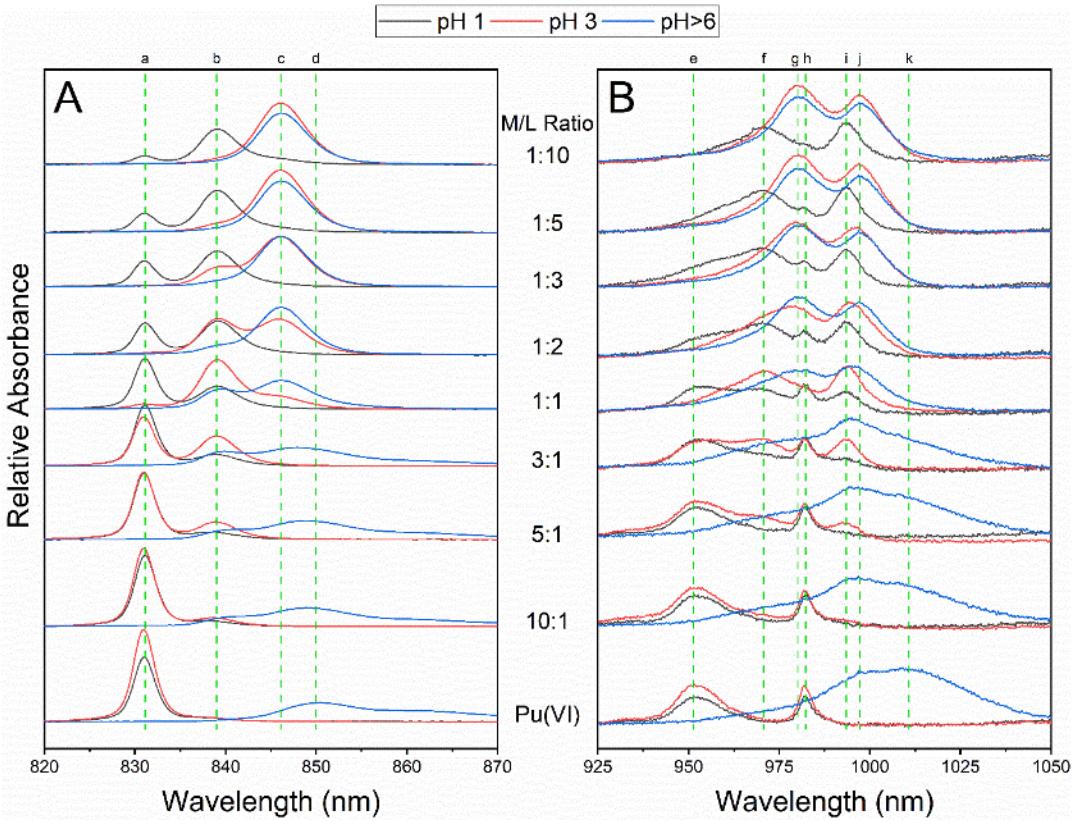

Figure 2. UV-vis-NIR spectra from (A) 820–870 nm and (B) 900–1050 nm at pH 1 (black trace), pH 3 (red trace), and pH > 6 (blue trace) as a function of M:L ratio at t < 15 min. Dashed vertical green lines represent peaks which have been assigned.

The results from UV-vis-NIR spectrophotometry were coupled with the total aqueous Pu concentrations from LSC analyses to calculate molar extinction coefficients (ε) for the Pu(VI) aquo ion and Pu(VI)-oxalate complexes. Subsequently, formation constants were calculated by using the oxalate protonation constants from Hummel et al. [5]. Free proton concentrations were based on experimentally-measured pH values, and ionic strength corrections were made based on the Specific Ion-interaction Theory (SIT) activity model.

The reduction of plutonium to the tri- or tetravalent oxidation state in the presence of oxalate has been heavily used for industrial purification of plutonium from waste mixtures. This reduction pathway has been studied for decades, but only under limited conditions compared to similar work with the uranium oxalate system. Our related work on the Pu(VI)-oxalate system suggests that a photocatalytic process may be involved in the reduction of Pu(VI) to Pu(IV) oxalate. Therefore, an additional aspect of this contribution will be a discussion of ongoing work targeted at understanding the impact of light exposure and M:L ratio on the speciation of the plutonium-oxalate system.

[1] A. E. Hixon and B. A. Powell, *Environ. Sci: Process Impacts*, **2018**, 20, 1306-1322.
[2] J. F. Facer, Jr. and K. M. Hannon, Precipitation of Plutonium(IV) Oxalate. Richland, WA, USA, **1954**.
[3] D. T. Reed et al., *Radiochim. Acta* **1998**, 82, 109-114.
[4] A. A. Bessonov et al., *Radiochemistry* **1996**, 38, 223-225. [5] W. Hummel et al., *Chemical Thermodynamics* Vol. 9, **2005**.

From actinium to einsteinium: Expanding the synthetic and structural toolkit for actinide coordination

J. N. Wacker [1], A. N. Gaiser [1], K. P. Carter [1], K. M. Shield [1,2], L. Arnedo-Sanchez [1], K. Smith [1], L. Moreau [1], G. J.-P. Deblonde [1], A. Mueller [3], P. Ercius [3], A. Minor [3], S. A. Kozimor [4], C. H. Booth [1], R. J. Abergel [1,2]

[1] Chemical Sciences Division, Lawrence Berkeley National Laboratory
[2] Department of Nuclear Engineering, University of California, Berkeley
[3] Molecular Foundry, Lawrence Berkeley National Laboratory
[4] Chemistry Division, Los Alamos National Laboratory

abergel@berkeley.edu

Structural characterization of actinide elements from actinium to einsteinium can be a challenging task due to the high radioactivity and limited availability of some of the isotopes of interest. However, significant work is needed to address a certain lack of understanding of the fundamental bonding interactions between those metal centers and selective ligands. Such understanding presents a rich set of scientific challenges and is critical to a number of applied problems including the development of new separation strategies for the nuclear fuel cycle, the need for decontamination after a nuclear accident or the use of radio-isotopes for new cancer treatments. Our studies utilize luminescence sensitization, UV-Visible, X-ray absorption, and X-ray diffraction spectroscopic techniques as well as transmission electron microscopy to investigate specific heavy actinide coordination features. Using simple inorganic complexes but also strong hard oxygen-donor ligands as well as more elaborate higher molecular weight protein assemblies allows the differentiation of heavy actinide species even when limited to minute amounts of materials. We will discuss some innovative ligand synthetic pathways linking specific metal binding units to polyamine, macrocyclic, and polymeric peptoid scaffolds, which, combined with advanced structural characterization techniques based on X-ray absorption, X-ray diffraction and electron microscopy, are used to derive coordination trends in the later 5f-element sequence.

This work is supported by the U.S. Department of Energy (DOE), Office of Science, Office of Basic Energy Sciences, Chemical Sciences, Geosciences, and Biosciences Division at the Lawrence Berkeley National Laboratory under Contract DE-AC02-05CH11231. Uses of the Advanced Light Source and of the Molecular Foundry is supported by the Office of Science, Office of Basic Energy Sciences, of the DOE under Contract No. DE-AC02-05CH11231. Use of the Stanford Synchrotron Radiation Lightsource, SLAC National Accelerator Laboratory, is supported by the U.S. DOE, Office of Science, Office of Basic Energy Sciences under Contract No. DE-AC02-76SF00515.

Simulation of alpha radiolysis in organic solution with plutonium at ultrashort time scales

Damien Tolu [1,2], Dominique Guillaumont [1], Aurélien de la Lande [2]

[1] CEA, DES, ISEC, DMRC, Univ Montpellier, Marcoule, 30207 Bagnols sur Cèze, France
[2] Institut de Chimie Physique, CNRS, Université Paris Saclay (UMR 8000), 15 Avenue Jean Perrin, 91405, France

---

Recycling spent nuclear fuel is a major issue in the power plant industry. Selective separation of actinides can be achieved through liquid-liquid extraction where the spent fuel is dissolved into concentrated nitric acid, and suitable organic ligands are used to extract actinide cations into an organic solution. PUREX process employs tributyl phosphate (TBP) to achieve plutonium and uranium extraction. However, the radioactivity causes radiolysis of both extractant and the diluent molecules, and forms unwanted products. Understanding such radiolysis phenomena is a necessary condition for the development and the improvement of new recycling processes. To date, one can isolate the degradation products with experimental methods such as mass spectrometry or gas chromatography analysis while others experimental technics, pulsed radiolysis for instance, give access to their formation mechanisms at the picosecond time scale. However, the sub-femtosecond time scale is totally out of range for experimental studies and the phenomena that happen at this time scale are not well understood.

The aim of this work is to model alpha radiolysis in organic phases with plutonium at ultrashort time scales through numerical simulations, with quantum chemistry tools. To this end, Real-Time Time-Dependent Density Functional Theory (RT-TD-DFT) [1] was applied to give access to the deposit energy and the charge variations during the electronic dynamics.

In order to understand the radiation effects on organic molecules, samples of deposit energies on TBP are simulated using alpha particles of 5 MeV energy. A large range of energies are observed along the projectile trajectory and near the point of impact, from a few electron-volts to hundreds electron-volts. These simulations were performed in the gas phase on neat TBP as well as with $Pu(NO_3)_4(TBP)_2$ complex to evaluate the influence of ligands on the charge transfers and the stability of TBP.

[1] X Wu, JM Teuler, F Cailliez, C Clavague´ra, DR Salahub, A de la Lande, J. Chem. Theor. Comput. 2017,13, 3985-4002.

First M4-edge RIXS measurement on Pa(V) complexes in aqueous solution

M. Maloubier [1], L. Meng [1], B. Siberchicot [2], M.O.J.Y Hunault [3], C. Le Naour [1]

[1] IJCLab, CNRS-IN2P3, Université Paris-Saclay, 91406 Orsay Cedex, France
[2] CEA, DAM, 91297 Arpajon, France
[3] Synchrotron SOLEIL, L'Orme des Merisiers, Saint-Aubin, BP 48F-91192, Gif-sur-Yvette Cedex, France

maloubier@ijclab.in2p3.fr

The actinide chemistry is known to be governed by the contribution of their 5f and 6d orbitals in the chemical bonding. Among the actinides, protactinium is at a key position in the series, between the "transition-metal-like" actinides and the "f-elements", giving its particular properties that are still unpredictable. Thus, protactinium is considered as the first actinide with 5f orbitals involved in bonding. Understanding of the Pa chemistry is of fundamental interest for improving our knowledge on chemical bonding in actinides complexes but also to better predict the Pa behavior in the environment or in the nuclear cycle (presence of Pa in uranium mine tailing, in thorium-based fuel reactor).

In aqueous solution, the existence of $Pa^{V}O_2^{+}$, a form analogue to $U^{VI}O_2^{2+}$ and $Np^{V}O_2^{+}$ has been unambiguously ruled out and the presence of a mono-oxo species, firstly postulated from UV spectrophotometric measurements, was then confirmed by X-ray Absorption Spectroscopy at the Pa L_{III} edge combined with DFT calculations in sulfate and oxalate complexes[1,2]. However, the Pa=O bond is not so stable and can vanish upon complexation, which is the case in presence of fluoride[2,3].

The current structural data on Pa(V) complexes are rather scarce, especially for predicting the presence or not of this mono-oxo bond. In fact, experimental difficulties occur when isolating significant amount of this actinide, and Pa(V) has a remarkable propensity towards hydrolysis and polymerization[4]. Moreover, the presence of the mono-oxo bond in Pa complexes cannot be deduced from XANES spectra collected at the Pa L_{III} edge, unlike the translinear dioxo cation present for other actinides (V) and (VI).

Several studies have proved now that high energy resolution fluorescence detection (HERFD) X-Ray absorption spectroscopy and resonant inelastic X-Ray scattering (RIXS) could be a powerful technique for characterizing the electronic structures of actinides, but were never used in the case of protactinium[5-7]. For the first time, we used HERFD-XANES and RIXS at the Pa M_4-edge, to probe the electronic structure of protactinium(V). The study has been conducted on $Pa^{V}F_7^{2-}$ and $Pa^{V}O(C_2O_4)_3^{3-}$, two Pa(V) complexes of which the structure is already known[2,3]. Experimental spectra, collected at the MARS beamline at SOLEIL synchrotron, have been compared to spectra simulated using different theoretical approaches. The insights provided on the role of 5f orbitals in the chemical bonding on Pa(V) will be discussed in light of these new results.

[1] Le Naour, C., Trubert, D., Di Giandomenico, M.V., Fillaux, C., Den Auwer, C., Moisy, P. and Hennig,C. Inorg. Chem. (2005) 44, 9542-9546
[2] Mendes, M., Hamadi, S., Le Naour, C., Roques, J., Jeanson, A., Den Auwer, C., Moisy,P., Topin, S.,Aupiais, J., Hennig, C., Di Giandomenico, M.V. (2010). Inorg. Chem. 49 9962-9971
[3] Le Naour, C., Roques, J., Den Auwer, C., Moisy, P. and Aupiais, J. (2019) Radiochim. Acta 107, 979-991
[4] Guillaumont, R., (1966). Revue de Chimie Minérale, 3, 339-373

[5] Butorin, S. M. (2020). Inorg. Chem. 59(22), 16251-16264.
[6] Butorin, S. M., Kvashnina, K. O., Vegelius, J. R., Meyer, D., & Shuh, D. K. (2016). Proceedings of the National Academy of Sciences, 113(29), 8093-8097.
[7] Vitova, T., Pidchenko, I., Fellhauer, D., Bagus, P. S., Joly, Y., Pruessmann, T., Bahl, S., Gonzales-Robles, E., Rothe, J., Altmaier, M., Denecke, M.A., Geckeis, H. (2017). Nature communications, 8(1), 1-9

New Methodology for Large-Scale Molecular Dynamics Simulation of Actinides in Solution

Enrique R. Batista, Rebecca K. Carlson, Danny Perez, Marc Cawkwell, and Ping Yang

Theoretical Division, Los Alamos National Laboratory, Los Alamos, NM 87545, USA

erb@lanl.gov

Actinide chemistry in solution is very intricate in nature. Based on calculated Pourbaix diagrams, depending on pH, temperature, and the type of ions present in solution, the stable phases of U or Pu, for example, can change within less than one pH unit. The solubility of actinides also depends on oxidation state and age of sample. For example, stable oxidation states of U in solution are U(IV) and U(VI) and sometimes U(V). These ions can undergo various physical and chemical processes such as hydration or hydrolysis and it can be difficult experimentally to unambiguously determine coordination and structure. Depending on reaction conditions, there may be an equilibrium between multiple hydrolyzed species or multiple polynuclear uranyl clusters forming in solution. Even more complex is the picture when multiple species are present in solution, indicating that binary complexes is rather the exception than the rule, as ternary and quaternary species have been crystalized and identified. Computational studies of these complex and complicated environments must rely on relied on first-principle electronic structure calculations in order to be predictive with respect to charge migration, bond formation and bond dissociation. To date the computational studies, focus of molecular systems with at most the first coordination shell compared and contrasted with crystal structures obtained in the laboratory. Few are the calculations carrying out molecular dynamics in solution and these are usually small simulation cells with binary systems (see Figure. 1). In order to shake hands with liquid-chemistry experiments one needs a methodology that can simulate large scale systems in the liquid phase for extended time scale.

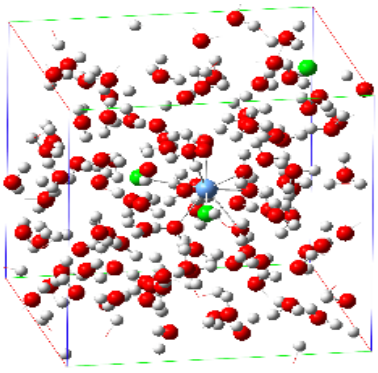

Figure 1: Example of State-of-the-art AIMD simulation we can carry out with BO MD for 4ps. Only one Ac ion in solution can be treated therefore no dimers are allowed in the simulation.[1]

Since density functional theory cannot handle the system sizes and time scales needed, we have been developing the self-consistent tight-binding approach for modeling actinides in solution. This approach is based on electronic structure and, due to its parameterized Hamiltonian, is much faster than density functional MD. In this talk we will present our first results that are for actinides in aqueous solution. Our parameterization has been made to fit the predictions of hybrid density functional theory for a good description of the potential energy surface. We will present performance evaluation of DFTB on prediction of molecular structural parameters of molecular clusters, a variety of chemical reaction free energies, and various solution environments.

The Role of Orbital Overlap in Chemical Bonding for Actinide Hexafluoride Complexes

S. G. Minasian [1], R. J. Abergel [1], J. Arnold [1], J. Autschbach [2], E. R. Batista [3], J. A. Bradley [3], J. Branson [1], A. S. Ditter [1], A. Gaiser [1], O. S. Gunther [1], J. Kasper [3], A. A. Peterson [1], S. A. Kozimor [3], W. W. Lukens [1], D.-C. Sergentu [2], D. K. Shuh [1], P. Yang [3]

[1] Lawrence Berkeley National Laboratory, Berkeley, CA 94720
[2] University at Buffalo, Buffalo, NY 14260
[3] Los Alamos National Laboratory, Los Alamos, NM 87545

sgminasian@lbl.gov

Controlling the outcome of chemical processes involving plutonium requires accurate, predictive models of molecular structure and bonding. Towards this goal, recent chlorine K-edge X-ray absorption spectroscopy (XAS) studies on molecular actinide hexachlorides, $AnCl_6^{n-}$ (An = Th to Am; n = 1-3), provided direct and quantitative evidence of mixing between the 5f- and Cl 3p-orbitals, and helped resolve long-standing debates regarding the mere existence of covalent bonding for actinides [1,2]. Furthermore, these studies demonstrated the relationship between the extent of 5f-orbital mixing and the relative energy of 5f- and ligand-based orbitals. However, because the 5f-orbitals are contracted for plutonium and overlap with ligand orbitals is small, these studies suggest that the relationship between 5f-orbital covalency and stability may be more complicated for heavier actinides such as plutonium. Quantum theory of atoms-in-molecules (QTAIM) calculations reported by Kerridge and Kaltsoyannis lend validity to these hypotheses by showing that increases in 5f-orbital mixing are rarely tied to a large build-up of charge at the bond midpoint [3,4]. To understand the possible link between 5f-orbital mixing and the chemical behaviour of plutonium and other actinides, we conducted F K-edge XAS and electron density mapping studies of the hexafluorides, AnF_6^{n-}. Because values for the F and Cl valence orbital ionization potentials are known precisely, these comparisons provide an opportunity to control for changes in orbital energy and show if covalency is affected by overlap (Fig. 1).

Results are compared to Cl K-edge XAS experiments on the analogous compounds, such as UCl_6^{1-} and $PuCl_6^{2-}$. Although AnF_6^{n-} are structurally similar, the extent of An–F bonding is anticipated to vary significantly as 5f-orbital energies and occupancies change with oxidation state and/or the identity of the actinide (Fig. 2). For example, comparisons between UF_6^{1-} ($5f^1$), NpF_6^{1-} ($5f^2$), and PuF_6^{1-} ($5f^3$), or between PuF_6^{2-} ($5f^4$), PuF_6^{1-} ($5f^3$) will show how decreasing 5f-orbital energies may result in increased An 5f and F 2p orbital mixing. To quantify the role of orbital overlap, we will compare these results with reported Cl K-edge XAS experiments on the analogous compounds, such as UCl_6^{1-} and $PuCl_6^{2-}$, among others. Interpretations of the F K-edge XAS will be facilitated by electronic structure calculations (in collaboration with Batista and Yang, LANL), and the percentage of F 2p character determined experimentally will be related to theoretical values determined from the Mulliken population analyses provided by ground-state DFT.

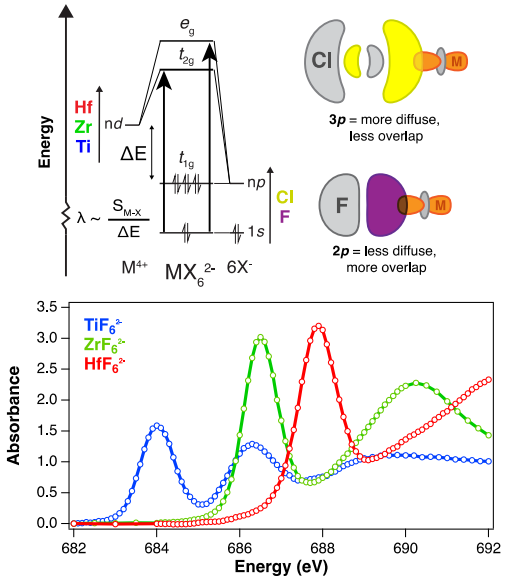

Fig 1. Bonding models used to interpret the F K-edge XAS. The XAS results show a larger amount of mixing in the M orbitals of t_{2g} symmetry for fluorides. Since the F 2p orbitals are lower in energy than the Cl 3p orbitals, this suggests that there is greater overlap in the M–F bonds.

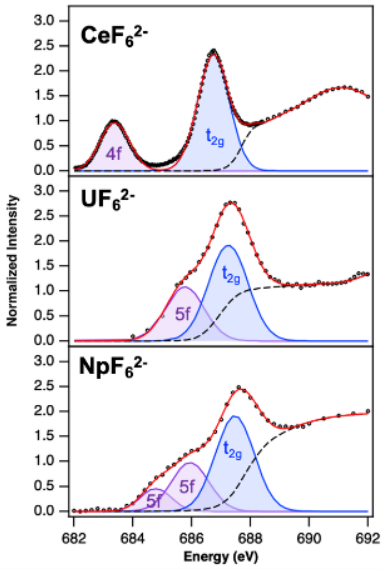

Fig 2. Fluorine K-edge spectra for MF_6^{2-} complexes where M = Ce, U, and Np

Results from the F K-edge XAS and DFT calculations are compared to experimental charge-density studies from single-crystal x-ray diffraction. Through this comprehensive approach, we show that enhancements in actinide overlap are reflected by the build-up of electron density at the bond midpoint. This presentation will also discuss these results, as well as our more recent efforts to achieve long-term goals including preparation and characterization of the BkF_6^{2-} molecule using a recently obtained supply of 249-Bk from Oak Ridge National Laboratory.

[1] Minasian, S. G.; Kieth, J. M.; Batista, E. R.; Boland, K. S.; Christensen, C. N.; Clark, D. L.; Conradson, S. D.; Kozimor, S. A.; Martin, R. L.; Schwarz, D. E.; Shuh, D. K.; Wagner, G. L.; Wilkerson, M. P.; Wolfsberg, L. E.; Yang, P. Determining Relative f and d Orbital Contributions to M–Cl Covalency in MCl_6^{2-} (M = Ti, Zr, Hf, U) and $UOCl_5^{1-}$ using Cl K-edge X-Ray Absorption Spectroscopy and Time-Dependent Density Functional Theory. *J. Am. Chem. Soc.* **2012**, *134*, 5586-5597.
[2] Su, J.; Batista, E. R.; Boland, K. S.; Bone, S. E.; Bradley, J. A.; Cary, S. K.; Clark, D. L.; Conradson, S. D.; Ditter, A. S.; Kaltsoyannis, N.; Keith, J. M.; Kerridge, A.; Kozimor, S. A.; Löble, M. W.; Martin, R. L.; Minasian, S. G.; Mocko, V.; La Pierre, H. S.; Seidler, G. T.; Shuh, D. K.; Wilkerson, M. P.; Wolfsberg, L. E.; Yang, P. Energy-Degeneracy-Driven Covalency in Actinide Bonding. *J. Am. Chem. Soc.* **2018**, *140*, 17977-17984.
[3] Kaltsoyannis, N. Does Covalency Increase or Decrease across the Actinide Series? Implications for Minor Actinide Partitioning. *Inorg. Chem.* **2013**, *52*, 3407-3413.
[4] Lu, E.; Sajjad, S.; Berryman, V. E. J.; Wooles, A. J.; Kaltsoyannis, N.; Liddle, S. T. Emergence of the structure-directing role of f-orbital overlap-driven covalency. *Nat. Commun.* **2019**, *10*, 634.

Effect of Calmodulin variants on the redox behaviour of Pu(IV)

L. Daronnat[1], V. Holfeltz[1], L. Berthon[1], N. Boubals[1], T. Dumas[1], P. Moisy[1], S. Sauge-Merle[2], D. Lemaire[2], C. Berthomieu[2]

1. CEA, DES, ISEC, DMRC, Univ Montpellier, Marcoule, France
2. CEA, DRF, BIAM, IPM, Univ Aix-Marseille, Cadarache, France

loic.daronnat@cea.fr

Pu is an actinide of major societal relevance due to its large stock worldwide and its key role in the cleanup challenges of legacy nuclear sites. Although its physiological impact has been widely investigated, understanding its interactions with biological molecules remains limited. The knowledge relative to actinide transportation mechanism, and in particular, the direct interaction of Pu at the molecular scale with proteins is still unclear. Recent publications have pointed that Pu interaction with transferrin or ferritin [1], an iron carrier of blood, could be at the origin of its internalization in cells [2] and that calcium-binding proteins are possible Pu targets, Figure 1(because as Pu, Ca is hard cation – strong Lewis acid) [3].

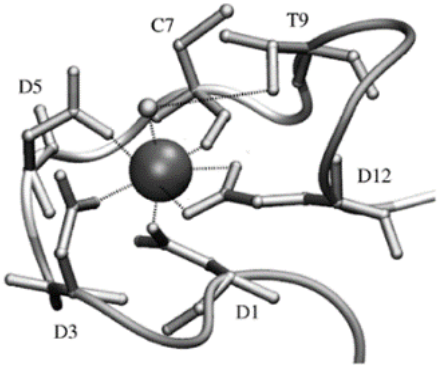

Figure 3 Complex calmodulin-plutonium

This work aims at investigating the interaction between actinide *elements*, and more specifically plutonium, and biological molecules. [4-6] Calcium-binding EF-hand protein motifs of the calmodulin N-terminal domain, which contains seven coordination sites were chosen for this study. Calmodulin is an important protein expressed in all eukaryotic cells and is involved in a large number of signal transduction pathways.

In vivo, plutonium is mainly present at oxidation state +IV, and at this oxidation state, plutonium is a very high hydrolyses propensity. In this work, we will focus on the interaction of the plutonium (IV) with two variants of the calmodulin. CaM-WT, which is the wild type calmodulin, and CaME variant in which one threonine is replaced by one glutamate, thus increasing the number of hard donor carboxylate ligands in the binding site. Different routes taking into account the constraints due to the hydrolysis of plutonium (IV) at physiological pH have been used and will be discussed.

The interactions between Pu and calmodulin ligand were then characterized using visible and X-ray absorption spectroscopies and ESI-MS. Complexing CaM-E and CaM-WT with plutonium IV, two different types of behaviour were observed.

[1] Zurita et al., Chemistry- A European Journal, **2020**, 27,2393-2401
[2] Jensen et al., Nature Chem. Biol., **2011**, 7, 560
[3] Aryal et al., J. Proteomics, **2012**, 75, 1505
[4] Sauge-Merle et al. Dalton Trans **2017**, 46, 1389-1396
[5] Vidaud et al. Scientific Reports **2019**, 9, 17584
[6] Sauge-Merle et al. Chemistry, A European Journal, **2017**, 23, 15505-15517

Stabilization and Characterization of Heptavalent Neptunium Under Mildly Acidic Conditions

N. Cicchetti [1,P], B. Khavkin [1], A. Gelis [1]

[1] Radiochemistry, Department of Chemistry. University of Nevada, Las Vegas. 4505 S. Maryland Pkwy, Las Vegas, NV 89154

artem.gelis@unlv.edu

The heptavalent form of neptunium is known to be stable under strongly alkaline conditions, but has not yet been stabilized in acidic media. Musikas et al. published voltammetry studies indicating oxidation to Np(VII) in a weak acid[1], but this has not been verified spectrophotometrically. Previous efforts to characterize the reduction potential and UV-vis spectrum of Np(VII) in acid start by preparing Np(VII) in alkali and acidifying it before measurement[2,3]. Np(VII) will rapidly reduce to Np(VI) under these conditions, making its precise concentration hard to determine and limiting the accuracy of any reduction potential or extinction coefficient determined via this method. This presentation details a method for stabilizing heptavalent neptunium under mildly acidic conditions, as well as spectroscopic measurements of the stabilized Np(VII). The molar absorptivity is reported, and further characterizations of this species using electrochemical methods are also discussed.

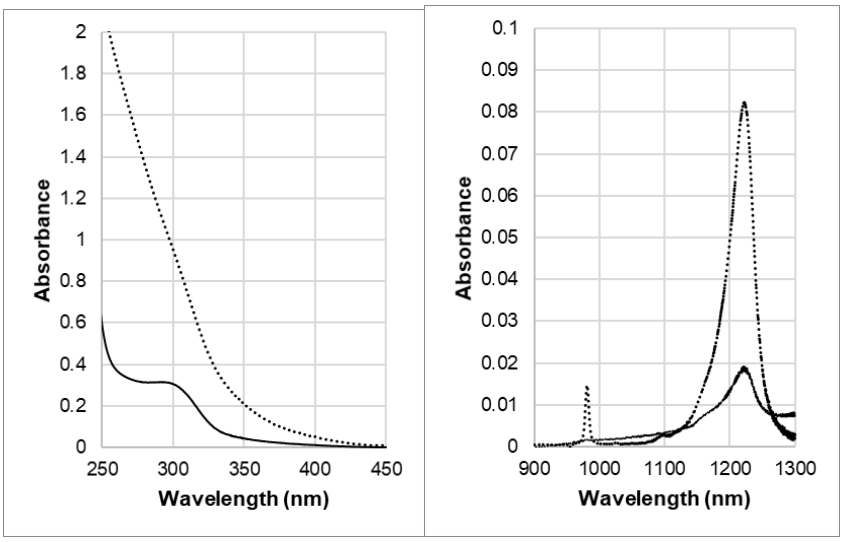

Figure 1: *UV-vis absorbance spectrum of stabilized Np(VII) in perchloric acid at pH 4.1 (solid line), compared with spectrum of combined Np(V) and Np(VI) starting material (dotted line). Left: Absorbance in UV drops, and a new peak at 300 nm appears after treatment. Right: NIR signal from Np(V) at 980 nm disappears when the solution is treated, and Np(VI) signal at 1220 nm is reduced. The spectra were collected in a conventional 1 cm quartz cell.*

[1] Musikas, C.; Couffin, F.; Marteau, M. On Neptunium (VII) Ions in Aqueous Acid Solutions. *J. Chemie Phys.* **1974**, *71* (5).

[2] Cohen, D. The Absorption Spectrum of Np(VII) in Acid Solution. *Inorg. Nucl. Chem. Lett.* **1976**, *12* (8), 635–637. https://doi.org/10.1016/0020-1650(76)80082-7.

[3] Lemire, R. J.; Fuger, J.; Spahiu, K.; Sullivan, J. C.; Nitsche, H.; Ullman, W. J.; Potter, P.; Vitorge, P.; Rand, M. H.; Wanner, H.; Rydberg, J. *Chemical Thermodynamics of Neptunium and Plutonium*; 2001; Vol. 4.

Compounds, Complexes And Coordination Chemistry

	Conference room #1: CELLIER BENOIT XII
PLENARY TALK **9:00 – 09:50**	**Thomas ALBRECHT-SCHOENZART (Florida State University)** *"The Quest for Californium (II) and the Importance of Trail Markers from Other Transuranium Elements and Lanthanides"*
	Conference room #1: CELLIER BENOIT XII
INVITED TALK **10:00 – 10:30**	**Andrew GAUNT (LANL)** *"Molecular Synthetic Transuranium Chemistry"*
INVITED TALK **11:00 – 11:30**	**Juliane MÄRZ (HZDR)** *"In Search of Covalency in Tetravalent Actinide (Th - Pu) Monosalen Complex Series"*
11:30 – 11:50	**Ashley HASTINGS (University of Notre Dame)** *"Plutonium Metal–Organic Frameworks: a Platform to Harness Hydrolysis and Probe Structural Radiation Stability"*
11:50 – 12:10	**David FELLHAUER (KIT)** *"Synthesis and characterization of ternary M-Pu (VI)-O (H) solid phases in alkaline electrolyte solutions"*
12:10 – 12:30	**Henry LA PIERRE (Georgia Institute of Technology)** *"High-Valent U, Np, and Pu Imidophosphorane Mono-Oxo Complexes"*
	Conference room #1: CELLIER BENOIT XII
INVITED TALK **15:00 – 15:30**	**Ping YANG (LANL)** *"Electronic Structure of Molecular Plutonium and Actinide Complexes"*
15:30 – 15:50	**Jennifer WACKER (LBNL)** *"Complexation of Actinides with Biologically-Inspired Chelators"*
16:20 – 16:40	**Jesse MURILLO (LANL)** *"Synthesis and Study of Isostructural F-Block Complexes Featuring eta (6)-Arene Interactions"*
16:40 – 17:00	**Kirstin SOCKWELL (University of Notre Dame)** *"The first crystal structure of Pu $(C_2O_4)_2$ and insight into the structural ambiguity of An$(C_2O_4)_2$ sheets – U$(C_2O_4)_2 \cdot 6H_2O$, Np$(C_2O_4)_2 \cdot 6H_2O$ and Pu$(C_2O_4)_2 \cdot 6H_2O$"*
17:00 – 17:20	**Alyssa GAISER (Michigan State University)** *"Investigation of the f-Block Elements with the Biological Ionophore Valinomycin"*

Chair persons:

Ping YANG and Nicolas DACHEU

The Quest for Californium(II) and the Importance of Trail Markers from Other Transuranium Elements and Lanthanides

Thomas Albrecht-Schoenzart

Department of Chemistry and Biochemistry, Florida State University, Tallahassee, Florida 32306

tschoenzart@mines.edu

The standard reduction potential of californium(III) to californium(II) has been measured to be anomalously low compared to both earlier actinides and to lanthanides with either similar ionic radii or the same number of *f* electrons. This potential (vs SHE) is similar to that of Sm(III) to Sm(II) and thus provides a potential electrochemical analog for fine-tuning the challenging reduction chemistry. However, Sm(II) should be considerably larger than Cf(II) and the coordination chemistry might be different enough that smaller Ln(II) cations are needed to guide ligand design. Moreover, directions provided by Ln(II) cations can still lead one down the wrong path because they do not account for radiolytic reactions or the contracted bond distances observed with actinides. By combining both Ln(II) and earlier actinide chemistry, we have finally isolated a Cf(II) molecule and now understand why it has been so elusive. This talk with detail that journey to discovery.

Molecular Synthetic Transuranium Chemistry

A. J. Gaunt [1], J. Murillo [1], C. A. P. Goodwin [1,2], L. Stevens [1], B. L. Scott [1], S. A. Kozimor [1], P. Yang [1], E. R. Batista [1], A. M. Tondreau [1], M. T. Janicke [1], S. T. Liddle [2], A. Wooles [2], N. Kaltsoyannis [2], W. J. Evans [3], J. C. Wedal [3], S. R. Ciccone [3], F. Furche [3], T. E. Albrecht-Schönzart [4], S. Fortier [5], T. W. Hayton [6], S. L. Staun [6], D. J. H. Emslie [7], N. A. G. Gray [7]

[1] Los Alamos National Laboratory, Los Alamos, NM 87545, USA | [2] Department of Chemistry, University of Manchester, Manchester M13 9PL, United Kingdom [3] Department of Chemistry, University of California – Irvine, Irvine, CA 92697-2025, USA [4] Department of Chemistry and Biochemistry, Florida State University, Tallahassee, FL 32306, USA [5] Department of Chemistry and Biochemistry, University of Texas at El Paso, El Paso, TX 79968, USA [6] Department of Chemistry and Biochemistry, University of California – Santa Barbara, CA 93106, USA [7] Department of Chemistry and Chemical Biology, McMaster University, Hamilton, Ontario, L8S 4M1, Canada

gaunt@lanl.gov

With the goal of gaining a better comprehension of transuranium electronic structure, bonding and redox behaviour, well-defined homologous series of organometallic and non-aqueous complexes have been synthesized and characterized. The actinide elements studied span from thorium to californium, and have been compared to lanthanide congeners. An inert atmosphere negative pressure glovebox supports the synthetic chemistry capability with transuranium isotopes (of Np, Pu, Am, and Cf) to selectively isolate molecules that will yield controlled, systematic, insight into bonding and electronic structure as the 4f/5f series are traversed. Development of new entry routes and isolation of additional starting materials has gone hand-in-hand with identification of target molecules, many of which were not optimally served by the limited range of existing synthons for non-aqueous transuranium chemistry. A broad range of chemical systems have been studied spanning f-element soft-donor chemistry, multiply-bonded motifs, utilization of organometallic frameworks to elucidate bonding trends and redox stability across the 5f block, and metal-encapsulating O/N donor macrocycles. Analysis of experimental structural metrics and spectroscopic data, in conjunction with computational modelling, has afforded detailed bonding and electronic structure descriptions, with comment on metal-ligand valence orbital mixing where appropriate. Experimental characterization techniques to be presented are a combination of single-crystal X-ray diffraction, solid and solution phase UV/vis/NIR, and solution NMR spectroscopies, along with electrochemical cyclic voltammetry measurements. These studies spotlight the usefulness of generating homologous series of molecules across the 4f/5f series in the quest to accurately map subtle bonding changes as a function of metal and donor-class identity.

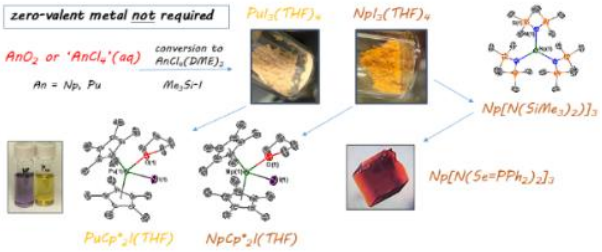

Figure 1: Example of the general synthetic utility of transuranium halide precursors in targeting a range of non-aqueous molecules.[1]

[1] "[AnI$_3$(THF)$_4$] (An = Np, Pu) Preparation Bypassing An^0 Metal Precursors: Access to Np^{3+}/Pu^{3+} Nonaqueous and Organometallic Complexes" Goodwin, C. A. P.; Janicke, M. T.; Scott, B. L.; Gaunt, A. J., J. AM. CHEM. SOC., **2021**, *143*, 20680-20696. **DOI**: 10.1021/jacs1c07967

In Search of Covalency in Tetravalent Actinide (Th - Pu) Monosalen Complex Series

M. Blei [1], M. Patzschke [1], K. O. Kvashnina [1, 2], L. Waurick [1], M. Schmidt [1], T. Stumpf [1], J. März [1]

[1] Helmholtz-Zentrum Dresden-Rossendorf, Institute of Resource Ecology, Bautzner Landstraße 400, 01328 Dresden, Germany

[2] The Rossendorf Beamline at ESRF at the European Synchrotron, CS40220,

38043 Grenoble Cedex 9, France

j.maerz@hzdr.de

Actinides play an important role in chemical engineering and environmental science related to the nuclear industry or nuclear waste repositories.[1] One of the major tools to obtain a profound basic knowledge about actinide (An) binding is the coordination chemistry of An using model ligands. However, fundamental An chemistry is still relatively little explored. Characteristic of the actinides is their huge variety of possible oxidation states, typically ranging from +II to +VII for early An, making their chemistry complex but interesting. A suitable approach to explore fundamental physico-chemical properties of the actinides is to study series of isostructural An compounds in which the An is in the same oxidation state.[2] Observed changes in e.g. the binding situation or magnetic effects among the An series may deliver insight into their unique electronic properties mainly originating from the *f*-electrons. A question still remaining in the field of An chemistry is the degree of "covalency" in compounds across the An series,[3] which may be addressed by systematic studies on series of An compounds, including transuranium (TRU) elements.

In this study we investigate the coordination chemistry of tetravalent actinides (An(IV)), which are dominant particularly under anoxic environmental conditions, using the organic salen ligand (salen = *N*,*N'*-bis(salicylidene)ethylenediamine) as a small *N*,*O* donor.[4] In addition, we change halogen (F, Cl, Br, I) and solvent (MeOH, THF, MeCN, pyridine) donors (see Figure 1) in order to analyse the ligand's effect on covalency trends as well as their mutual influence, mainly using single crystal X-ray diffraction (SC-XRD), high-energy-resolution fluorescence detection X-ray absorption near edge spectroscopy (HERFD-XANES), and quantum chemical calculations (QCC).

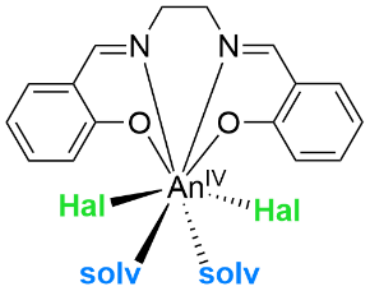

Figure 1: Schematics of [AnHal$_2$(salen)(solv)$_2$] (An = Th, U, Np, Pu; Hal = F, Cl, Br, I; solv = MeOH, THF, MeCN, pyridine). Hydrogen atoms are omitted for clarity.

All syntheses were conducted under inert, water-free atmosphere. SC-XRD results prove that isostructural complex series were achieved in each case, dependent on the solvent and halogen used. In all complexes, one salen ligand coordinates to the An (An = Th, U, Np, Pu) tetradentately with both nitrogen and deprotonated oxygen donor atoms. The vacant coordination sites are occupied by two halogenato ligands for charge compensation as well as two respective solvent molecules, either methanol (MeOH), tetrahydrofuran (THF), acetonitrile (MeCN), pyridine (Py), 4-methylpyridine (Pic), or 3,5-lutidine (Lut), resulting in an eightfold coordination environment (see $[AnCl_2(salen)(Pic)_2]$ as representatives in Figure 2).

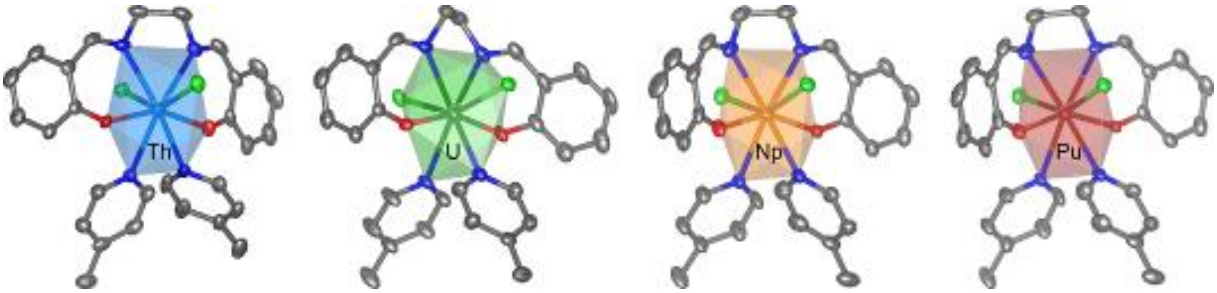

Figure 2: Thermal ellipsoid plots of $[AnCl_2(salen)(Pic)_2]$ (An = Th, U, Np, Pu; Pic = 4-Methylpyridine). Hydrogen atoms are omitted for clarity.

The acquired experimental SC-XRD and IR results as well as supporting quantum chemical calculations (including the Pa(IV) complexes) point to a different bonding situation of the individual donor atoms to the actinide. Whereas the An–$N_{salen/solv}$, An–O_{solv} and the An–Hal bond lengths follow the decrease of the ionic radii, the An–O_{salen} bonds remarkably diverge from this behaviour. These rather follow the trend of decreasing covalent radii, indicating an exceptionally strong bond here. QCC confirm high bond strengths for An–O_{salen} bonds, but also for An–Hal bonds. In addition, QCC indicate a weaker binding strength in the An–solv bonds, explaining the potential solvent exchange and opens up the possibility of further chemical modification at these positions.

Extensive HERFD-XANES data for all complex series show a noteworthy agreement with results from QCC: The trends found indicate covalency dependences on the kind of actinide, halogen, and solvent, but to different extents for both, the experimental and also calculated data. This shows the possibility of proving and understanding covalency in actinide bonding by combining experiments and theory.

[1] L. S. Natrajan, A. N. Swineburn, M. B. Andrews, S. Randall, S. L. Heath, *Coord. Chem. Rev.* **2014**, *266-267*, 171-193.
[2] M. B. Jones, A. J. Gaunt, J. C. Gordon, N. Kaltsoyannis, *Chem. Sci.* **2013**, *4*, 1189-1203.
[3] M. P. Kelley, J. Su, M. Urban, M. Luckey, E. R. Batista, P. Yang, J. C. Shafer, *J. Am. Chem. Soc.* **2017**, *139*, 9901-9908.
[4] T. Radoske, J. März, M. Patzschke, P. Kaden, O. Walter, M. Schmidt, T. Stumpf, *Chem. Eur. J.* **2020**, *26*, 16853.

Acknowledgement

This study was supported by the German Federal Ministry of Education and Research (BMBF) funding under the project No. 02NUK046B (FENABIUM).

Plutonium Metal–Organic Frameworks: a Platform to Harness Hydrolysis and Probe Structural Radiation Stability

Ashley M. Hastings [1], Melissa Fairley [2,3], Jay A. LaVerne [2], Amy E. Hixon [1]

[1] Department of Civil & Environmental Engineering & Earth Sciences, University of Notre Dame, Notre Dame, Indiana 46556, USA
[2] Radiation Laboratory, University of Notre Dame, Notre Dame, Indiana 46556, USA
[3] Materials Physics & Applications Division, Los Alamos National Laboratory, Los Alamos, New Mexico 87545, USA

ahastin1@nd.edu

Actinide-based metal–organic frameworks (MOFs) have demonstrated a repertoire of exotic characteristics due to both their radioactive nature and the interplay of *f*- and *d*-orbital contributions. While some parallel that of transition-metal MOFs, others diverge to yield dazzling and unprecedented architectures, autoluminescence, and spontaneous deinterpenetration of catenated nets [1–3]. The majority of actinide MOFs are assembled from thorium and uranium nodes because of relative ease of handling and accessibility, leaving transuranic MOFs widely underexplored. The intersection of plutonium with the MOF platform presents opportunities that rival the rich chemical complexity of element 94 itself, justifying the stewardship of this high-profile nuclear material for these research endeavors. Plutonium-based MOFs offer the sequestration of plutonium into atomically precise and stable forms, a scaffold for evaluating more elusive properties (e.g., hydrolysis, electronic structure, and catalysis), and the opportunity to probe the radiation stability of hybrid materials composed of an alpha-emitter. Understanding the fundamentals of MOF radiation stability is a tangential, but imperative, need as MOFs continue to offer the modern solutions to the nuclear community and their performance will be subject to high radiation fields [4]. Herein, we describe the synthesis and characterization of the first plutonium MOF, Pu-UiO-66 (Figure 1), and its place in the isostructural radiation stability series of M-UiO-66 (Zr, Ce, Hf, Th, and Pu).

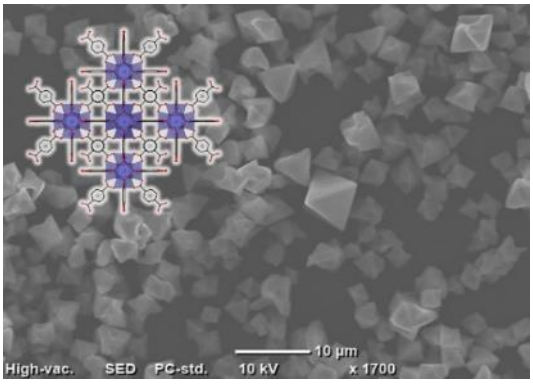

Figure 4. Scanning electron micrograph of Pu-UiO-66 with crystal structure inset.

Solvothermal synthesis of a plutonium(IV) nitrate starting material with the terephthalate ligand, benzoic acid modulator, and *N*,*N*-dimethylformamide (DMF) solvent yielded a pink microcrystalline powder of Pu-UiO-66 [5]. The phase was confirmed with powder X-ray diffraction (PXRD) because the individual crystals were < 10 µm. The synthesis was sensitive to water content, as some water is necessary for the controlled hydrolysis required to form the hexanuclear plutonium-oxo nodes, but too much water causes the plutonium to polymerize out of solution as a green amorphous powder. On one occasion both products formed in the same vial, proving the intricate balance and competition in this system. After fine-tuning synthetic conditions to promote both yield and purity, bulk material (~80 mg) was accumulated from individual synthesis replicates for more extensive characterization – vibrational spectroscopy, thermal gravimetric analysis, and N_2 physisorption isotherms, which yielded

a BET surface area of 710 m^2/g. Density functional theory (DFT) models and Monte Carlo simulations corroborated our experimental findings. While the highly-connected M-UiO-66 structure is known to possess certain defects (e.g., missing linkers and/or clusters) data indicate formate ligands cap defect sites in Pu-UiO-66.

Irradiation of the M-UiO-66 series occurred via gamma and He^{2+} ion methodologies. With the ^{60}Co source and a dose rate of about 70 Gy/min, doses of 1–3 MGy could reasonably be achieved. However, with these doses and the stability of M-UiO-66, little change was observed. Hence, He^{2+} ion irradiation is a pathway to realize much higher doses, up to 85 MGy in this study, with the added benefit of simulating alpha irradiation, although the sample quantity was limited to ~ 0.1 mg. Pu-UiO-66 was irradiated with the gamma methodology and the self-alpha irradiation was taken into account. The isotopically weapons-grade (WG) plutonium used in this study provided a dose rate of 210 Gy/min, substantially more than the ^{60}Co source. This dual-irradiation tactic amounted to a highest dose of 31 MGy for Pu-UiO-66 (Figure 2). PXRD, infrared (IR), and Raman spectroscopy of irradiated samples point to a relative radiation stability of Zr-UiO-66 > Hf-UiO-66 > Th-UiO-66 > Pu-UiO-66 > Ce-UiO-66. Reduction of crystallinity precludes amorphization and the loss of the μ_3-OH stretch and M-OCO components in IR were interpreted as damage to the node-linker connection. DFT models were used to further assess the binding affinity of the linkers to the nodes as a function of metal identity.

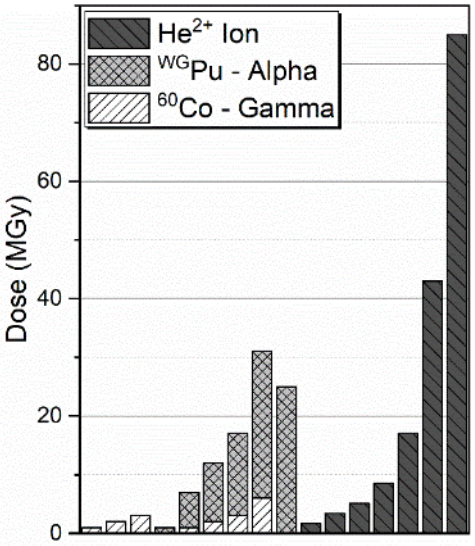

Figure 2. Summary of total radiation doses achieved via different irradiation methodologies.

In this work, we utilized the established foundation of the M-UiO-66 series to enact synthetic conditions that promote the assemblage of an ordered plutonium(IV) MOF over the infamous polymer. This serves as a basis to realize novel plutonium MOF topologies. We also leveraged the radioactivity of Pu-UiO-66 so that its inclusion in the isostructural series allows us to identify the role of metal selection in MOF radiation stability. We hope this informs rational design of radiation-resistant MOF materials for targeted applications. With a firmer scope for the dose range of interest, future work includes the isolation of the plutonium system and the exploitation of different isotopes to explore the effects of dose rates and structural insights of self α-radiolysis in a hybrid material.

Acknowledgements. We recognize contributions from Debmalya Ray, WooSeok Jeong, Dario Campisi, Arup Sarkar, Laura Gagliardi, Zoë C. Emory, Sara E. Gilson, Peter C. Burns, Megan C. Wasson, Timur Islamoglu, Omar K. Farha, Kieran Brunson, and May Nyman as instrumental in this work, supported by the DOE and NNSA under award Number DE-NA0003763.

[1] Gilson et al., *J. Am. Chem. Soc.* **2020**, *142*, 13299–13304. [2] Andreo et al., *J. Am. Chem. Soc.* **2018**, *140*, 14144–14149. [3] Hanna et al., *Chem* **2022**, *8*, 225–242. [4] Fairley et al., *Chem. Mater.* **2021**, *33*, 9285–9294. [5] Hastings et al., *J. Am. Chem. Soc.* **2020**, *142*, 9363–9371.

Synthesis and characterization of ternary M-Pu(VI)-O(H) solid phases in alkaline electrolyte solutions

D. Fellhauer [1], T. Neill [1,2], O. Walter [3], D. Schild [1], J. Rothe [1], X. Gaona [1], M. Altmaier [1]

[1] Karlsruhe Institute of Technology - Institute for Nuclear Waste Disposal (INE), Germany | [2] University of Manchester, Manchester, United Kingdom | [3] European Commission, Joint Research Centre Karlsruhe (JRC-KRU), Germany

david.fellhauer@kit.edu

Within the An(VI) series, the hydrolysis behavior of Pu(VI) in aqueous solution shows some unique features that are clearly different from that of U(VI) and Np(VI). While U(VI) and Np(VI) readily form sparingly soluble An(VI)-(hydr)oxide solid phases in neutral to alkaline solutions, *e.g.* $AnO_2(OH)_2 \cdot xH_2O$(cr), $Na_2An_2O_7 \cdot xH_2O$(cr) with An = U [1] and Np [2], $CaU_2O_7 \cdot 3H_2O$(cr) [3], or Ca_xNpO_{3+x}(s,hyd) [4], the hydrolytic behavior of Pu(VI) is dominated by the formation of dissolved polymeric hydrolysis products $(PuO_2)_y(OH)_x^{2y-x}$(aq). The latter are metastable, but prevalent even at relatively high $[Pu(VI)]_{tot}$ [5], which becomes evident in the kinetically slow formation of Pu(VI)-(hydr)oxides. This challenge may explain why little is reported about the solid phase formation of Pu(VI)-(hydr)oxides. In this contribution we report on the successful preparation and characterization of some ternary M-Pu(VI)-O(H) solid phases obtained in MOH (M = Li, Na, K, Rb, Cs) and $M(OH)_2$ (M = Ca, Sr, Ba) solutions. All experiments were performed under inert Ar atmosphere with ^{242}Pu. Oxidation state pure $^{242}PuO_2^{2+}$ stock solutions were alkalinized with MOH (M = Li-Cs) and $M(OH)_2$ (M = Ca-Ba) solutions. Mild tempering for several weeks resulted in the formation of brownish to blackish precipitates. The precipitates were comprehensively investigated by powder XRD, SEM-EDX, chemical analysis by combined LSC+OES or ICPMS, and Pu L_3-edge XANES and EXAFS at the *INE Beamline for Radionuclide Research at the KIT Light Source*. Additional characterization techniques (solid state Vis/NIR, Raman, thermogravimetric analysis, solubility studies, and single crystal XRD) were applied to selected solids. In all cases, (poly)crystalline Pu(VI) compounds with characteristic powder XRD patterns and distinct SEM morphologies were obtained. EDX of the solid precipitates and quantitative chemical analysis of digested fractions revealed that ternary M-Pu(VI)-O(H) phases with M:Pu ratios ranging from 0.5:1 to 1:1 for M = alkali metal and 0.3:1 to 1:1 for M = alkaline earth metal had formed. The Pu oxidation state in the solids was confirmed to be +VI based on Vis/NIR absorption study of acid digested solid phase fractions. For solids with greater degree of crystallinity (*e.g.* K, Sr), structural models were successfully derived from single crystal XRD analyses. For polycrystalline phases (*e.g.* Li, Na, Ca, Ba), structural parameters were evaluated from the results of EXAFS spectroscopy. In the presentation, the stoichiometries and structures obtained for the different solids will be discussed and compared to the available information for U(VI) and Np(VI) systems.

[1] Altmaier, M., Yalcintas, E., Gaona, X., Neck, V., Müller, R., Schlieker, M., Fanghänel, Th. (2017). "Solubility of U(VI) in chloride solutions. I. The stable oxides/hydroxides in NaCl systems, solubility products, hydrolysis constants and SIT coefficients". J. Chem. Therm. 114: 2-13. [2] Gaona, X., Fellhauer, D., Altmaier, M. (2013). "Thermodynamic description of Np(VI) solubility, hydrolysis, and redox behavior in dilute to concentrated alkaline NaCl solutions", Pure Appl. Chem. 85: 2027-2049. [3] Altmaier, M., Neck, V., Müller, R., Fanghänel, Th. (2005). "Solubility of U(VI) and formation of $CaU_2O_7 \cdot 3H_2O$(cr) in alkaline $CaCl_2$ solutions". Abstract No. A1-3, Migration Conference Avignon (France) 2005. [4] Fellhauer, D., Gaona, X., Rothe, J., Altmaier, M., Fanghänel, Th. (2018). "Neptunium(VI) solubility in alkaline $CaCl_2$ solutions: evidence for the formation of calcium neptunates Ca_xNpO_{3+x}(s,hyd)", Monatshefte für Chemie – Chemical Monthly 149: 237-252. [5] Pashalidis, I. (1992). "Chemisches Verhalten des sechswertigen Plutoniums in konzentrierten NaCl-Lösungen unter dem Einfluß der eigenen Alpha-Strahlung". Bericht 01092, Institut für Radiochemie, Technische Universität München (1992).

High-Valent U, Np, and Pu Imidophosphorane Mono-Oxo Complexes

Henry S. La Pierre,[1][2] and Julie E. Niklas[1]

[1] School of Chemistry and Biochemistry and [2] Nuclear and Radiological Engineering and Medical Physics Program in the School of Mechanical Engineering

Georgia Institute of Technology, Atlanta, Georgia 30332-0400, United States

hsl@gatech.edu

Two-electron oxidative atom transfer reactions are typically restricted to the $3^+/5^+$ couple in molecular uranium chemistry,[1] and reactions of tetravalent uranium complexes to form hexavalent, metal-ligand multiply bonded complexes are rare.[2,3] The development of more reducing ligand frameworks to enable the $4^+/6^+$ couple in mid-actinide complexes is a central issue in the development of high-valent mid-actinide (U, Np, Pu, and Am) complexes in non-aqueous solvents, since the reduction potentials across the mid-actinides become less negative as the series is traversed. As a result, the redox chemistry and small-molecule transformations established in uranium complexes are not directly transferable to neptunium and plutonium complexes. Therefore, in order to enable non-aqueous high-valent Np, Pu, and Am chemistry, ligand systems that both shift redox couples to more negative potentials and sterically and electronically stabilize high-valent actinide ions are necessary to isolate complexes of rare oxidation states and unique metal-ligand bonds of mid-actinide complexes.

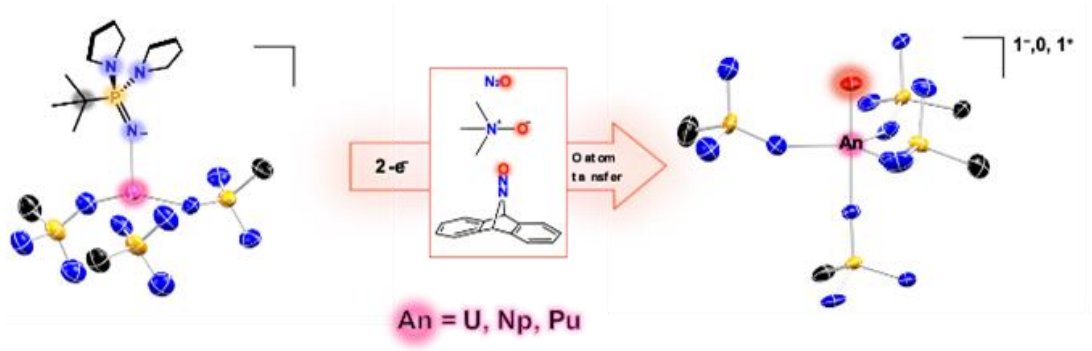

Scheme 1: *Reaction scheme for the oxidation of tetravalent uranium, neptunium, and plutonium homoleptic complexes with two-electron, oxygen atom transfer reagents to form mono-oxide products. The complexes are shown as molecular structures as determined by SC-XRD and thermal ellipsoids are plotted at 50%. The ligands are truncated to core N and C atoms to reveal connectivity at the metal. A single ligand on the homoleptic complex (left) is drawn to depict the full ligand connectivity.*

In this talk, I will present the synthesis of tetrahomoleptic, imidophosphorane complexes of U, Np, and Pu in several formal oxidation states ($[An(NP(t\text{-}Bu)(pyrr_2))_4]^q$, where An = U, Np, and Pu and q can be -1, 0, or +1, pyrr = pyrrolidinyl) and the reactivity of these complexes with two-electron oxygen atom transfer reagents to form high-valent mono-oxo complexes ($([An(O)(NP(t\text{-}Bu)(pyrr_2))_4]^q$, Scheme 1).[4,5] These studies build on my group's recently reported synthesis of hexavalent uranium mono-oxo and mono-imido complexes via two-electron atom transfer reactions.[3] This discussion will include the examination of several oxygen-atom transfer reagents including (nitrous oxide, trimethylamine N-

oxide, dioxygen, and DBABH-NNO (9,10-dihydro-11-nitroso-anthracen-9,10-imine)), the description of ligand design processes to afford high-quality single crystals of the mono-oxo complexes in good yield and on small-scale (10-40 mg of isotope) and the one-electron oxidation and reduction chemistry of the mono-oxo complexes.[6,7,8] Detailed spectroscopic and solution and solid-state structural analyses will address changes in the inverse trans-influence across the mid-actinides – a phenomenon which is uniquely addressable by this series of complexes.[3-5] Additional topics to be covered may include electrochemistry, magnetism, and EPR spectroscopy of selected complexes.

These studies are made possible by the Georgia Tech Transuranic Synthetic Facility which, after three years of construction and a year of COVID shutdown, fully opened in 2020 and the support of the DOE Heavy Element Chemistry Program (DE-SC0019385).

1. La Pierre, H.; Meyer, K., Activation of Small Molecules by Molecular Uranium Complexes. In *Progress in Inorganic Chemistry Volume 58*, 2014; pp 303-416.
2. Mills, D. P.; Cooper, O. J.; Tuna, F.; McInnes, E. J. L.; Davies, E. S.; McMaster, J.; Moro, F.; Lewis, W.; Blake, A. J.; Liddle, S. T., Synthesis of a Uranium(VI)-Carbene: Reductive Formation of Uranyl(V)-Methanides, Oxidative Preparation of a $[R_2C{=}U{=}O]^{2+}$ Analogue of the $[O{=}U{=}O]^{2+}$ Uranyl Ion (R = $Ph_2PNSiMe_3$), and Comparison of the Nature of UIV=C, UV=C, and UVI=C Double Bonds. *J. Am. Chem. Soc.* **2012,** *134* (24), 10047-10054.
3. Rice, N.T.; McCabe, K.; Bacsa, J.; Maron, L.; La Pierre, H.S.; "Two-Electron Oxidative Atom Transfer at a Homoleptic, Tetravalent Uranium Complex," *J. Am. Chem. Soc.* **2020**, *142*, 16, 7368–7373.
4. Niklas, J.E.; Barker, T.B.; Ramanathan, A.; Bacsa, J.; Popov, I. A.; and La Pierre, H.S.; "Inverse-*trans* Influence in an Isostructural Valence Series of Neptunium (Np^{5+}, Np^{6+}, and Np^{7+}) Mono-oxo Complexes," *in preparation* **2022**.
5. Niklas, J.E.; Barker, T.B.; Ramanathan, A.; Bacsa, J.; Popov, I. A.; La Pierre, H.S.; "Reactivity of Homoleptic Plutonium Imidophosphorane Complexes," *in preparation* **2022**.
6. Niklas, J.E.; Barker, T.B.; Bacsa, J.; Popov, I. A.; and La Pierre, H.S.; "Crystal Engineering of Hexavalent Uranium Mono-oxo Complexes," *in preparation* **2022.**
7. Aguirre Quintana, L.M.; Niklas, J.E.; Jiang, N.; Bacsa, J.; Maron, L.; La Pierre, H.S.; "Elemental Chalcogen Reactions of a Tetravalent Uranium Imidophosphorane Complex: Cleavage of Dioxgen," *in preparation* **2022**.
8. Niklas, J.E.; Barker, T.B.; Ramanathan, A.; Bacsa, J.; Popov, I. A.; La Pierre, H.S.; "Inverse-trans influence and weak-field paramagnetism in a pentavalent uranium mono-oxo complex," *in preparation* **2022**.

Electronic Structure of Molecular Plutonium and Actinide Complexes

Ping Yang, Enrique Batista, Jing Su, Ivan A. Popov, Rebecca Carlson, Andrew Gaunt, Stosh A Kozimor

Los Alamos National Laboratory, Los Alamos, NM 87545, USA

pyang@lanl.gov

The complicated electronic structure of actinide complexes leads to their versatility of chemical bonding, reactivity, and spectral properties. Advances in high-performance computing and quantum chemistry have greatly accelerated the understanding of complex systems at the molecular level. In this talk, I will present our recent work on chemical bonding and spectroscopy of heavy elements across the actinide series, with a focus on plutonium, using advanced quantum chemical techniques. Our close collaboration with experimental teams has demonstrated that the synergy between theory and experiments can greatly accelerate the understanding of f-orbital participation in chemical bonding.

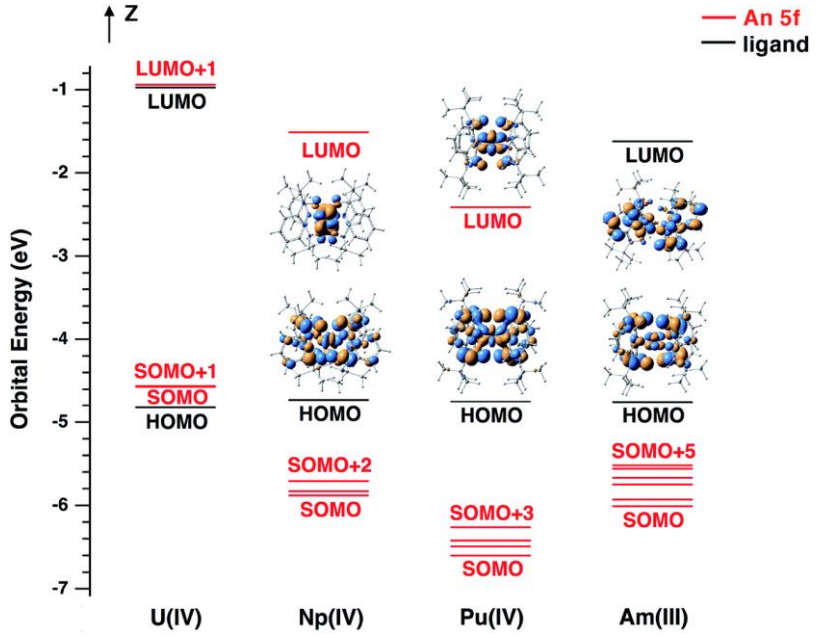

Figure 1. Frontier molecular orbital energy level diagram for An-complexes. [3]

References:

1. MP Kelley, IA Popov, J Jung, ER Batista, P Yang, Nature Communication, 2020, 11, 1558
2. J Su, ER Batista, P Yang, Rare Earth Elements and Actinides: Progress in Computational Applications, 2021, Chapter 14, pg 283-327
3. J Su, T Cheisson, A McSkimming, CAP Goodwin, I DiMucci, T Albrecht-Schoenzart, B Scott, ER Batista, A Gaunt, SA Kozimor, P Yang, EJ Schelter, Chemical Science. 2021, 12, 13343-13359
4. J Su, ER Batista, KS Boland, SE Bone, JA Bradley, SK Cary, DL Clark, SD Conradson, AS Ditter, N Kaltsoyannis, JM Keith, A Kerridge, SA Kozimor, MW Löble, RL Martin, SG Minasian, V Mocko, HS La Pierre, GT Seidler, DK Shuh, MP Wilkerson, LE Wolfsberg, P Yang, Journal of the American Chemical Society, 2018, 140, 17977-17984

Complexation of Actinides with Biologically-Inspired Chelators

J. N. Wacker [1], A. N. Gaiser [1], K. P. Carter [2], Corwin H. Booth [1], R. J. Abergel [1, 3]

[1] Chemical Sciences Division, Lawrence Berkeley National Lab
[2] Department of Chemistry, University of Iowa
[3] Department of Nuclear Engineering, University of California, Berkeley 1 Cyclotron Road, Berkeley, CA 94720, USA

jwacker@lbl.gov; rjabergel@lbl.gov

A fundamental understanding of actinide coordination behaviour underlies efforts to ensure a safe and secure global energy portfolio. Towards this aim, chelators inspired by biological systems are being pursued in an effort to predict, probe, and control the chemical properties of the actinide elements. In particular, multidentate hydroxypyridinone- and catecholamide-based ligands have shown great promise in actinide decorporation treatments as well as in radiotherapeutic applications [1, 2]. By leveraging X-ray absorption spectroscopy (XAS), the oxidation states and coordination chemistries of the actinides (e.g., Pu, Am, Cm, Bk, Cf) in the presence of these chelators were examined [3]. Moreover, changes in actinide redox reactivity and speciation were probed by combining hydroxypyridinone and catecholamide binding groups. Notably, this work highlights the utility of XAS to understand actinide complexation, particularly with the scarce and highly radioactive transplutonium elements. By tailoring the hydroxyl groups of the actinide binding moieties to softer donor atoms, we aim to cater the ligand environment to not only understand differences in complex formation, but also exploit these biologically-inspired chelators for radiochemical separations.

[1] R. J. Abergel, P. W. Durbin, B. Kullgren, S. N. Ebbe, J. Xu, P. Y. Chang, D. I. Bunin, E. A. Blakely, K. A. Bjornstad, C. J. Rosen, D. K. Shuh, K. N. Raymond. *Health Phys.* **2010**, *99*, 401–407.

[2] T. A. Bailey, V. Mocko, K. M. Shield, D. D. An, A. C. Akin, E. R. Birnbaum, M. Brugh, J. C. Cooley, J. W. Engle, M. E. Fassbender, S. S. Gauny, A. L. Lakes, F. M. Nortier, E. M. O'Brien, S. L. Thiemann, F. D. White, C. Vermeulen, S. A. Kozimor, R. J. Abergel. *Nat. Chem.* **2021**, *13*, 284–289.

[3] K. P. Carter, J. N. Wacker, K. F. Smith, G. J.-P. Deblonde, L. M. Moreau, J. A. Rees, C. H. Booth, R. J. Abergel. *J. Synchrotron Rad.* **2022**, *29*, 315–322.

Synthesis and Study of Isostructural F-block Complexes Featuring η^6-Arene Interactions

J. Murillo [1], C.A.P. Goodwin [1,2], B.L. Scott [1], S. Fortier [3], A.J. Gaunt [1]

[1] Los Alamos National Laboratory, Los Alamos, NM 87545, USA [2] Department of Chemistry, University of Manchester, Manchester M13 9PL, United Kingdom [3] Department of Chemistry and Biochemistry, University of Texas at El Paso, El Paso, TX 79968, USA

jmurillo@lanl.gov

Isostructural organometallic complexes that span the actinide series are rare yet informative probes into the nature of f-(p/d/f) bonding. Recently, it has been shown that a growing subset of organometallic complexes possessing uranium-arene interactions have the capability to stabilize unusually low-valent molecular species as well as illicit exotic metal-ligand covalent bonding interactions (i.e. π/δ/ϕ). Such complexes have been established for uranium, yet their extension to transuranium elements remains extraordinarily scarce. We have begun to explore avenues for the synthesis of complexes possessing actinide-arene bonding by use of a bis(anilide)terphenyl ligand platform $[L^{Ar}]^{2-}$, which employs N-atom donors to tether the actinide in a κ^2 -fashion, where the ligand backbone engages the metal via η^6-coordination. Generally, $M(I)_3$ has been shown to react with $K_2[L^{ar}]$ to form the M(III) complexes $L^{Ar}M(I)(THF)$ (**1^M**) (M = Ce, U, Np, Pu), all of which feature η^6-arene interactions with the central ring of the terphenyl backbone. The solid-state metal-arene bond metrics show a distinct bonding trend along the series which diverges from the predicted M-L interactions based on ionic radii. Additionally, synthesis of the closely related "-ate" complexes $[Li(THF)_4][L^{Ar}M(I)_2]$ (**2^M**) (M = La, Ce, Pr, U, Np) are reported along with their chemical redox activity. For the described complexes, spectroscopic (UV-vis/NIR, FT-IR, NMR), structural (SCXRD), and electrochemical (CV) analysis will be discussed. Corresponding features which provide evidence to periodic trends will be examined in detail.

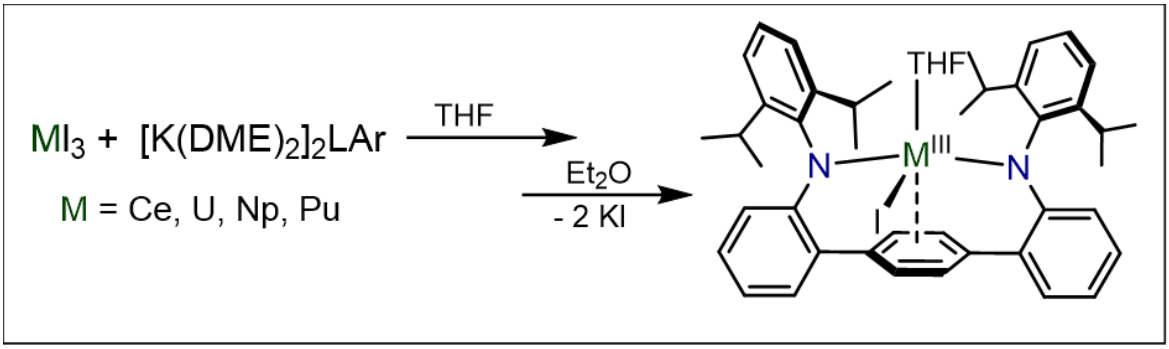

*Figure 1: Synthetic route to the formation of **1^M** complexes.*

The first crystal structure of $Pu(C_2O_4)_2$ and insight into the structural ambiguity of $An(C_2O_4)_2$ sheets – $U(C_2O_4)_2{\cdot}6H_2O$, $Np(C_2O_4)_2{\cdot}6H_2O$ and $Pu(C_2O_4)_2{\cdot}6H_2O$

A. Kirstin Sockwell [1], Teagan F. M. Sweet [2], Brodie Barth [1], Nicole A. DiBlasi [1,3], Jennifer E. S. Szymanowski [1], Ginger Sigmon [1], Allen G. Oliver [2], Peter C. Burns [1], and Amy E. Hixon [1]

[1] Department of Civil & Environmental Engineering & Earth Sciences, University of Notre Dame, Notre Dame, IN 46556 USA [2] Department of Chemistry & Biochemistry, University of Notre Dame, Notre Dame, IN 46556 USA [3] Karlsruhe Institute of Technology, Institute for Nuclear Waste Disposal, Hermann-von-Helmhotz-Platz 1, Eggenstein-Leopoldshafen 76344 Germany

asockwel@nd.edu

Preliminary powder X-ray diffraction crystallographic data for several actinide oxalates with the form $An(IV)(C_2O_4)_2{\cdot}6H_2O$ (An(IV) = Th, U, Pu) was first published in 1963 and later expanded upon in 1965 [1-2]. Due to the assumed isomorphic nature of the compounds, the discussion was based on the Th and U structures due to poor data quality for the Pu compound. Single crystal X-ray data was not published for any of the oxalate hexahydrate compounds until 1997, when the crystallographic data for $Np(C_2O_4)_2{\cdot}6H_2O$ was published [3]. The single crystal structure of the U oxalate was not published until 2008 [4]. In contrast to the U and Np compounds, only powder X-ray data for the Pu oxalate has been published [1].

The Pu oxalate literature has primarily emphasized optimization of a purification method involving the precipitation of Pu oxalate from waste mixtures, followed by calcination to PuO_2. Efforts to optimize the method at an industrial scale have included investigations to understand how various contaminants may alter the Pu oxalate precipitation [5-7]. The crystal structure was not necessary information for these studies. However, interest in understanding the mechanism of the thermal decomposition of Pu oxalate into PuO_2 has created a need to better understand the starting material. Specifically, understanding the placement and subsequent loss of the water and oxalate molecules in the structure will provide more information about the behaviour throughout the decomposition [8-12].

The original powder diffraction data for the Th, U, and Pu hexahydrate structures did not provide the location of the water molecules [1-2]. The exact placement of these water molecules was not provided until the subsequent publication of the Np and U crystal structures. However, despite a relatively straightforward placement of four interlayer and interstitial water molecules, the location of the last two water molecules was more ambiguous due to a high degree of disorder, traditionally attributed to the large mass of the metal center [3-4, 13]. A computational study attempted to model the structure of the Pu oxalate compound starting from the U single-crystal structure but found that one of the six water molecules coordinated to the metal center upon relaxation of the model [13]. The only other attempt at modelling the Pu oxalate structure did not include water, but rather focused on the coordination mode of the oxalate ligands during decomposition [11].

Plutonium(IV) oxalate hexahydrate ($Pu(C_2O_4)_2{\cdot}6H_2O$) was synthesized by first drying down a Pu(VI) stock solution in 3 M HNO_3, followed by several washes in DI water. The final solution was prepared in

0.1 M NaCl. At low pH, a solution of oxalic acid was spiked with the Pu stock and after several days, dark brown, square crystals formed in solution. Dark green, square shaped crystals of $Np(C_2O_4)_2{\cdot}6H_2O$ were synthesized with a similar method. Single crystals of the $U(C_2O_4){\cdot}6H_2O$ were prepared hydrothermally from U_3O_8 and oxalic acid. However, this synthesis did not provide a pure product, but rather a mixture of U(IV) oxalate and U(VI) oxalate. For additional analysis, a pure U(IV) oxalate powder was prepared hydrothermally from UCl_4 and oxalic acid. All single crystals were analyzed by single crystal X-ray diffraction (SC-XRD). The Pu(IV) and Np(IV) oxalate crystals and U(IV) oxalate powder were characterized by Fourier-Transform infrared spectroscopy, Raman spectroscopy, solid-state ultra-violet/visible spectroscopy, powder X-ray diffraction (pXRD), and thermogravimetric analysis (TGA). All powders post-TGA were also characterized by the above methods as well as pXRD.

$Pu(C_2O_4)_2{\cdot}6H_2O$ crystallized in the *C*2/*m* space group with a unit cell of a = 8.9340(5) Å, b = 8.9440(5) Å, c = 7.7920(4) Å, and β = 91.533(5) °. SC-XRD data of this structure provided insight into the location of water molecules within the structure. Unlike previous reports, this new data has shown the coordination of two water molecules to the metal center and four interstitial water molecules. In contrast to previous studies, synthesis and characterization of the isostructural U and Np compounds showed the same coordination of water molecules to the metal center as observed with $Pu(C_2O_4)_2{\cdot}6H_2O$.

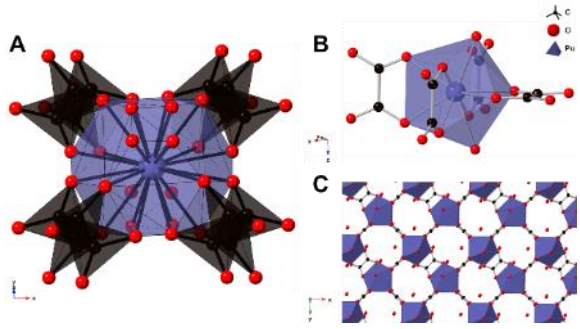

Figure 5: A) Average crystal structure of polymeric $Pu(C_2O_4)_2{\cdot}6H_2O$. B) Coordination environment of Pu(IV) showing three axial and one equatorial oxalates. C) View down z-axis showing a mixture of oxalate coordination modes (randomized).

In addition to the water placement, the Pu crystal data also provided information indicating that the previously published structures represented oversimplifications of the coordination of the oxalate molecules. This new data shows the presence of two coordination modes of the oxalate ligands, where they are coordinated either axially or equatorially to the coordinated waters. The crystal data suggests the presence of three axial oxalates and one equatorial oxalate. Figure 5 shows the average of the oxalate coordination modes (A) and a snapshot of a more realistic representation of the Pu(IV) coordination (B, C). This motif has not previously been seen. While the presence of two coordination modes may not immediately change the chemistry of these compounds, they could result in complications for computational work.

The long sought-after Pu oxalate hexahydrate crystal structure has been isolated and characterized. The single crystal data provided information that suggests previous work overly simplified the $An(C_2O_4){\cdot}6H_2O$ (An = Th, U, Pu) structure. This work provides a better base of understanding for future studies involving Pu oxalate.

[1] I. L. Jenkins, et al., *Chem. Ind.* **1963**, 35-36. [2] I. L. Jenkins, et al., *J. Inorg. Nucl. Chem.* **1965**, *27*, 81-87. [3] M. S. Grigor'ev, et al., *Radiochem.* **1997**, *39*, 420-423. [4] L. Duvieubourg-Garela, et al., *J. Sol. State Chem.* **2008**, *181*, 1899-1908. [5] J. F. Facer, K. M. Harmon, Precipitation of Plutonium(IV) Oxalate. Richland, WA, USA, **1954.** [6] C. A. Nash, Literature Review for Oxalate Oxidation Processes and Plutonium Oxalate Solubility, Savannah River National Laboratory: Aiken, SC, USA, **2012**. [7] F. Abraham, et al., *Coord. Chem. Rev.* **2014**, *266-267*, 28-68. [8] I. L. Jenkins, M. J. Waterman, *J. Inorg. Nucl. Chem.* **1964**, *26*, 131-137. [9] N. Vigier, et al., *J. Alloys Compd.* **2007**, *444-445*, 594-597. [10] R. M. Orr, et al., *J. Nucl. Mater.* **2015**, *465*, 756-773. [11] C. J. South, L. E. Roy, *J. Nucl. Mater.* **2021**, *549*, 152864. [12] J. H. Christian, et al., *J. Nucl. Mater.* **2022**, *562*, 153574. [13] K. E. Garrett, et al., *Comput. Mater. Sci.* **2018**, *153*, 146-152.

Investigation of the *f*-Block Elements with the Biological Ionophore Valinomycin

A. Gaiser [1,2], C. Celis Barros [1], J. Wacker [2], T. Poe [1], J. Sperling [1], E. Oulette [2], M. Boreen [2], T. Albrecht-Schoenzart [1], R. Abergel [2]

[1] Department of Chemistry and Biochemistry, Florida State University, Tallahassee, Florida, 32306, United States [2] Chemical Sciences Division, Lawrence Berkeley National Laboratory, Berkeley, California, 94720, United States

agaiser@lbl.gov

talbrechtschoenzartr@gmail.com; rjabergel@lbl.gov

Valinomycin is a biological ionophore that has been studied with the lanthanides and actinides. Studying these interactions sheds light on a peculiar bonding trend throughout the series as well as elucidating the interaction of *f*-block elements with amino acid moieties. As the lanthanide series is traversed, there is a decrease in denticity between the lanthanide cation and the valinomycin macrocycle (Figure 1). This decrease in denticity is likely due to the decrease in ionic radius across the series. The early lanthanides bind at

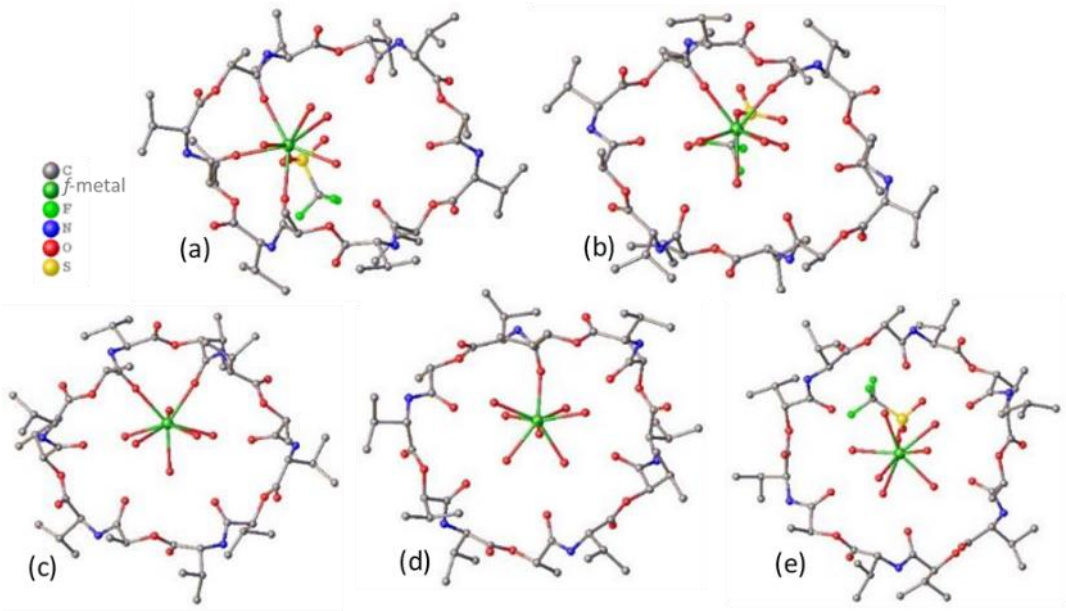

Figure 1: Five of the main crystallized lanthanide valinomycin complexes. Lanthanum and cerium crystallize a unit cell with complexes 1a and 1b disordered with itself. Praseodymium and neodymium crystallize with complexes 1b, 1c, and 1b disordered with 1a. Samarium crystallizes with two 1b molecules. Europium through lutetium crystallize with complexes 1d and 1e within the unit cell. Noteworthy, californium crystallizes 1b as the unit cell, being most similar to that of samarium.

two and three of the six amide carbonyl groups of valinomycin; whereas, at europium onward the lanthanide valinomycin complex contains one bond to an amide carbonyl group and a fully hydrated metal center stabilized through hydrogen bonding with valinomycin in the same unit cell.

Of the actinides, uranium and californium were crystallographically characterized with valinomycin. Californium adopts the same interaction with valinomycin as observed with samarium—a purely bidentate interaction. With respect to ionic radius, californium is more frequently compared to the slightly larger europium and gadolinium than to samarium, making this finding rather distinctive.[1,2]

Uranium expresses two different binding motifs with valinomycin. One, where the uranium starting material is not recrystallized prior to the experiment, yields a structure like those observed with alkaline earth metals—two metal centers inside the valinomycin cavity, each bound to three consecutive amide carbonyl groups, but with a bridging hydroxide molecule. The other, where the uranium starting material is recrystallized, yields a stacked structure with uranium nitrate hydrogen bonding between valinomycin molecules. The old uranium starting material in this case had a build up of peroxide from years of radiolytic degradation that had been mostly expelled when the starting material was recrystallized, resulting in the two binding motifs.

This work also led to an interest of the interaction of valinomycin with radium. Radium, in the form of radium chloride, is an FDA-approved targeted alpha-therapy used for treating bone metastasized cancers. Since it behaves like calcium in the body, naturally accumulating in the bones, it would be beneficial to elucidate the fundamental chemistry of radium to potentially target other parts of the body. With this in mind, barium was used as a non-radioactive analog of radium to optimize the chemistry with valinomycin to shed light on how radium may interact with this biological ionophore, most importantly the amino acid moieties.

Further radium work was performed to make strides in getting the first radium single crystal structure. Preliminary results on this front hint at radium adopting a twelve-coordinate structure in the hydrated chloride.

[1] Edelstein, N. M. Comparison of the Electronic Structure of the Lanthanides and Actinides. *J. Alloys Compd.* **1995**, *223* (2), 197–203.

[2] Sperling, J. M.; Warzecha, E.; Windorff, C. J.; Klamm, B. E.; Gaiser, A. N.; Whitefoot, M. A.; White, F. D.; Poe, T. N.; Albrecht-Schönzart, T. E. Pressure-Induced Spectroscopic Changes in a Californium 1D Material Are Twice as Large as Found in the Holmium Analog. *Inorg. Chem.* **2020**, *59* (15), 10794–10801.

Condensed Matter Physics

	Conference room #2: CHAMBRE DU TRÉSORIER
INVITED TALK **10:00 – 10:30**	**Johann BOUCHET (CEA)** *"Simulating plutonium at high temperature"*
INVITED TALK **11:00 – 11:30**	**Adam P. DIOGUARDI (LANL)** *"^{239}Pu nuclear magnetic resonance in the candidate topological insulator PuB_4"*
11:30 – 11:50	**Alexander LANDA (LLNL)** *"Ab initio study of advanced metallic nuclear fuels for fast breeder reactors"*
11:50 – 12:10	**Boris MAIOROV (LANL)** *"Thermodynamic and dynamic studies of delta-Pu and its alloys using Resonant Ultrasound Spectroscopy"*
12:10 – 12:30	**Emeric BOURASSEAU (CEA)** *"Thermodynamic properties of (U,Pu) mixed-oxide fuel: empirical interatomic potential calculations"*
PLENARY TALK **14:00 – 14:50**	*Conference room #1: CELLIER BENOIT XII* **Bernard AMADON (CEA)** *"Role of electronic interaction on structural properties of actinides and phases of plutonium"*
	Conference room #2: CHAMBRE DU TRÉSORIER
INVITED TALK **15:00 – 15:30**	**Per SODERLIND (LLNL)** *"Density-functional theory for plutonium"*
15:30 – 15:50	**Eric Bauer (LANL)** *"Nuclear magnetic resonance studies of plutonium compounds"*
16:20 – 16:40	**Jason JEFFRIES (LLNL)** *"Magnetic dichroism in Ga-stabilized delta-Pu"*
16:40 – 17:00	**Baptiste LABONNE (CEA)** *"Atomic-scale modelling investigation of structural and thermodynamic properties of Americium-bearing oxides "*
17:00 – 17:20	**Roxanne TUTCHTON (LANL)** *"Electronic Correlation Induced Expansion of Fermi Pockets in delta-Pu"*

Chair persons:

Alexander LANDA and Bernard AMADON

Simulating plutonium at high temperature

J. Bouchet [1], F. Bottin [2], B. Amadon [2], A. Castellano [2]

[1] CEA, DES, IRESNE, DEC F-13108 Saint-Paul-Lez-Durance, France
[2] CEA, DAM, DIF, F-91297 Arpajon, France, and Université Paris-Saclay, CEA, Laboratoires des Matériaux en Conditions Extrêmes, 91680 Bruyères-le-Châtel, France.

johann.bouchet@cea.fr; francois.bottin@cea.fr

The theoretical description of the plutonium phase diagram still represents a major challenge to modern electronic structure theories. On the one hand, plutonium exhibits six different allotropic phases at ambient pressure, with each phase transition marked by a significant change in the electronic behaviour, so that a unified theory able to correctly describe all six phases has yet to be developed. On the other hand, each of the six phases of plutonium represents in itself a major challenge, with the face-centered-cubic (fcc) δ phase being one striking example of the difficulties encountered. Indeed, it was only after 40 years of theoretical studies (combined with experimental measurements) that the underlying phenomena governing the ground state of δ-Pu could be unveiled [1,2].

One of the key parameters in successfully determining a phase diagram is, of course, temperature. If the pressure can be taken into account simply by modifying the lattice parameter in density functional theory (DFT) calculations, taking into account the temperature turns out to be much more difficult. Some assumptions have to be made, for example that the atomics vibrations are harmonic and the frequencies only dependent of the volume (quasi-harmonic approximation) to obtain the phonon spectra. Paradoxically, these approximations make it possible to take into account the temperature only thanks to calculations performed at 0 K! Unfortunately, applied to plutonium, this strategy is too crude and can at best provide qualitative results.

To offer a better modelling of thermal effects at the atomic scale, more sophisticated methods have been developed in the last fifteen years based on the formalism developed in the 60's [3]. In particular, we have implemented [4] the Temperature Dependent Effective Potential (TDEP) developed by O. Hellman *et al.* [5]. This method, based on a sampling of the Born-Oppenheimer energy surface using *ab initio* molecular dynamics (AIMD), is able to capture the explicit temperature effects at the level of the phonon spectrum. Applied to plutonium [6] this method gives good results (see Fig. 1) but the computational time required for the molecular dynamics limits its application, and some crucial effects have to be neglected as the spin-orbit coupling.

To circumvent this limitation we introduce a new method named Machine Learning Assisted Canonical Sampling (MLACS), which accelerates the sampling of the potential surface in the canonical ensemble by iteratively training a Machine Learning Interatomic Potential [10]. We show that MLACS is able to reproduce the temperature dependent phonon spectrum and pair distribution function of AIMD with an *ab initio* accuracy at a fraction of its computational cost (about one hundred of *ab initio* calculations using MLACS compared to thousands AIMD time steps).

By applying MLACS, associated with a unified description of electronic correlations for plutonium [11], we are able to reproduce several key thermodynamic properties of δ-Pu which were not unveiled in our previous work [6] (see Fig. 1). In particular, we find all the unusual features noted by J. Wong *et al.* [9]: "a large elastic anisotropy, a small-shear elastic modulus C', a Kohn-like anomaly in the T1 [011]

branch, and a pronounced softening of the [111] transverse modes". In addition, we recover the negative thermal expansion of the δ-Pu phase and give insight of the mechanisms responsible for the stabilization of the fcc structure by alloying with Ga [12].

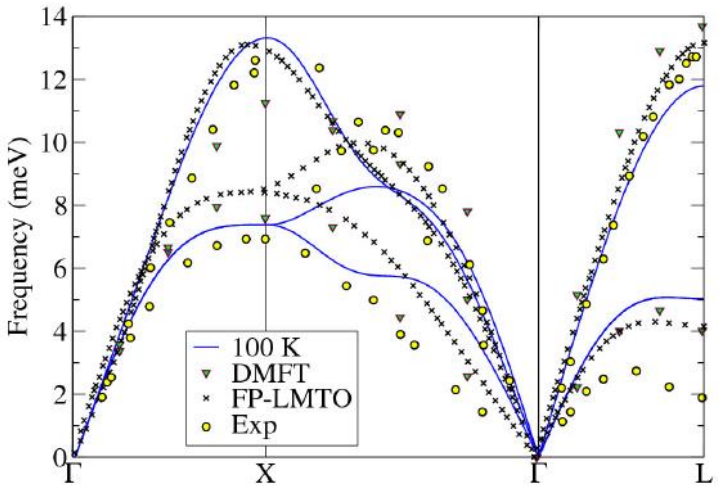

Figure 1: Phonon spectrum of δδ-Pu at 100 K calculated with LDA+U using TDEP [6] and compared to that obtained from DMFT [7], full-potential approach (FP-LMTO) [8], as well as experiments measured on a Pu-2 at.%Ga sample [9].

[1] J. H. Shim, K. Haule, and G. Kotliar, Nature **446**, 513 (2007).
[2] M. Janoschek, P. Das, B. Chakrabarti, D. L. Abernathy, M. D. Lumsden, J. M. Lawrence, J. D. Thompson, G. H. Lander, J. N. Mitchell, S. Richmond, M. Ramos, F. Trouw, J.-X. Zhu, K. Haule, G. Kotliar, and E. D. Bauer, Sci. Adv. **1**, e1500188 (2015).
[3] A.A. Maradudin, A.E. Fein, Phys. Rev. **128** , 2589 (1962).
[4] F. Bottin, J. Bieder and J. Bouchet, Comput. Phys. Comm. **254**, 107301 (2020).
[5] O. Hellman, I.A. Abrikosov and S.I. Simak, Phys. Rev. B **84**, 180301 (2011).
[6] B. Dorado, F. Bottin, J. Bouchet, Phys. Rev. B **95**, 104303 (2017).
[7] X. Dai, S. Y. Savrasov, G. Kotliar, A. Migliori, H. Ledbetter, and E. Abrahams, Science **300**, 953 (2003).
[8] P. Söderlind, F. Zhou, A. Landa, and J. E. Klepeis, Sci. Rep. **5**, 15958 (2015).
[9] J. Wong, M. Krisch, D. L. Farber, F. Occelli, A. J. Schwartz, T.-C. Chiang, M. Wall, C. Boro, and R. Xu, Science **301**, 1078 (2003).
[10] A. Castellano, F. Bottin, J. Bouchet, A. Levitt and G. Stoltz, submitted (2022).
[11] B. Amadon and B. Dorado, *J. Phys.: Condens. Matter* **30**, 405603 (2018).
[12] F. Bottin, J. Bouchet, A. Castellano and B. Amadon, in preparation (2022).

^{239}Pu nuclear magnetic resonance in the candidate topological insulator PuB_4

A. P. Dioguardi [1,2], H. Yasuoka [1,3], S. M. Thomas [1], H. Sakai [1,4], S. K. Cary [1], S. A. Kozimor [1], T. E. Albrecht-Schmitt [5], H. C. Choi [1], J.-X. Zhu [1], J. D. Thompson [1], E. D. Bauer [1], and F. Ronning [1]

[1] Los Alamos National Laboratory, Los Alamos, New Mexico 87545, USA
[2] IFW Dresden, Institute for Solid State Research, 01171 Dresden, Germany
[3] Max Planck Institute for Chemical Physics of Solids, 01187 Dresden, Germany
[4] Advanced Science Research Center, Japan Atomic Energy Agency, Tokai, Naka, Ibaraki 319-1195, Japan
[5] Department of Chemistry and Biochemistry, Florida State University, 95 Chieftan Way, Tallahassee, Florida 32306, USA
Los Alamos National Laboratory, Los Alamos, New Mexico 87545, USA

adioguardi@gmail.com

We present a detailed nuclear magnetic resonance (NMR) study of ^{239}Pu in bulk and powdered single-crystal plutonium tetraboride (PuB_4), which has recently been investigated as a potential correlated topological insulator [1,2]. This study constitutes the second-ever observation of the ^{239}Pu NMR signal, and provides unique on-site sensitivity to the rich *f*-electron physics and insight into the bulk gaplike behavior in PuB_4.The ^{239}Pu NMR spectra are consistent with axial symmetry of the shift tensor showing for the first time that ^{239}Pu NMR can be observed in an anisotropic environment and up to room temperature. The temperature dependence of the ^{239}Pu spin shift (K_s), combined with a relatively long spin-lattice relaxation time (T_1), indicate that PuB_4 adopts a nonmagnetic state with gaplike behavior consistent with our density functional theory calculations. The temperature dependencies of K_s and T_1–microscopic quantities sensitive only to bulk states–imply bulk gaplike behavior confirming that PuB_4 is a good candidate topological insulator. The large contrast between the ^{239}Pu orbital shifts (K_0) in the ionic insulator PuO_2 (∼+24.7%) [3] and PuB_4 (∼−0.5%) indicates that NMR is sensitive to the nature of chemical bonding in plutonium materials.

[1] A. P. Dioguardi, H. Yasuoka, S. M. Thomas, H. Sakai, S. K. Cary, S. A. Kozimor, T. E. Albrecht-Schmitt, H. C. Choi, J.-X. Zhu, J. D. Thompson, E. D. Bauer, and F. Ronning, ^{239}Pu nuclear magnetic resonance in the candidate topological insulator PuB_4, Phys. Rev. B **99**, 035104 (2019).
[2] Hongchul Choi, Wei Zhu, S. K. Cary, L. E. Winter, Zhoushen Huang, R. D. McDonald, V. Mocko, B. L. Scott, P. H. Tobash, J. D. Thompson, S. A. Kozimor, E. D. Bauer, Jian-Xin Zhu, and F. Ronning, Experimental and theoretical study of topology and electronic correlations in PuB_4, Phys. Rev. B **97**, 201114(R) (2018).
[3] H. Yasuoka, G. Koutroulakis, H. Chudo, S. Richmond, D. K. Veirs, A. I. Smith, E. D. Bauer, J. D. Thompson, G. D. Jarvinen, and D. L. Clark, Observation of ^{239}Pu Nuclear Magnetic Resonance, Science **336**, 901 (2012).

Ab initio study of advanced metallic nuclear fuels for fast breeder reactors

A. Landa [1], P. Söderlind [1], E.E. Moore [1], A.P. Perron [1]

[1] Lawrence Livermore National Laboratory, Livermore, California 94550, USA

landa1@llnl.gov

The RERTR program requires implementation of LEU fuels to minimize the risk of nuclear proliferation. The U-TRU-Zr and U-TRU-Mo alloys proved to be very promising fuels for TRU-burning liquid metal fast breeder reactors. The optimal composition of these alloys is determined from the condition for which the fuel remains stable in the bcc phase (*γ*-U) in the temperature range of stability of *α*-U phase. In other words, both Zr and Mo play the role of 'γ-stabilizers' helping to keep U in the metastable bcc phase upon cooling. The main advantage of U-Pu-Mo fuels over U-Pu-Zr fuels lies in much lower constituent redistribution due to the existence of a single *γ*-phase with bcc structure over typical fuel operation temperatures. The nucleation time for the decomposition of the metastable alloys, which controls the constituent redistribution process, is directly connected to the excess enthalpy of solution of these alloys.

In the present study, we perform KKR-ASA-CPA, EMTO-CPA, and FPLMTO-SQS calculations of the ground state properties of *γ*-U-Zr and *γ*-U-Mo alloys and compare their heats of formation with CALPHAD assessments. We discuss how the heat of formation in both alloys correlates with the charge transfer between the alloy components, how magnetism influences the deviation from Zen's law for the equilibrium atomic volume, and how the specific behavior of the density of states in the vicinity of the Fermi level promotes the stabilization of the U_2Mo compound. Our calculations prove that due to the existence of a single *γ*-phase over the typical fuel operation temperatures, *γ*-U-Mo alloys should indeed have much lower constituent redistribution than *γ*-U-Zr alloys where a high degree of constituent redistribution takes place. The binodal decomposition curves for *γ*-based U-Zr and U-Mo solid solutions are derived from Ising-type Monte Carlo simulations incorporating effective cluster interactions obtained from the Screened Generalized Perturbation and Connolly-Williams methods. We also explore the idea of stabilizing the *δ*-UZ_2 compound against the *α*-Zr (hcp) structure due to increase of Zr d-band occupancy by the addition of U to Zr. Analogous stabilization of the *ω*-phase in Zr under compression is made.

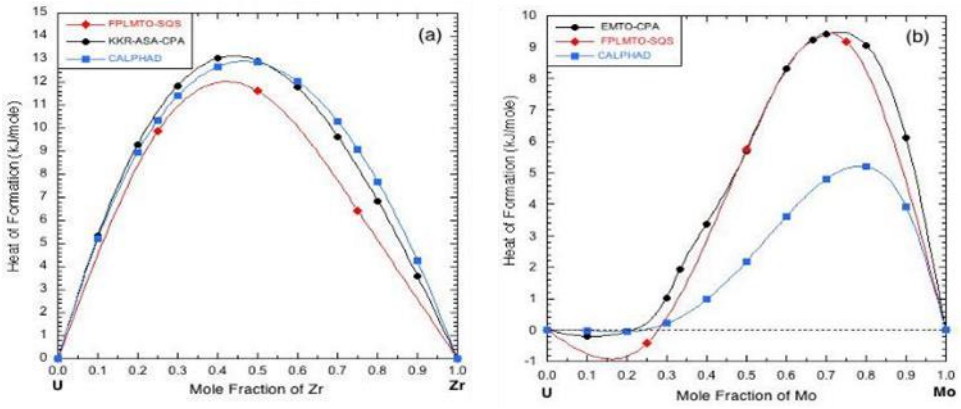

Figure 1: The heat of formation versus composition calculated at T = 0 K for (bcc-based): (a) γ-U-Zr and (b) γ-U-Mo alloys. The full lines are guides to the eye only.

Though the U-Pu-Zr and U-Pu-Mo alloys can be used as nuclear fuels, a fast reactor operating on a closed fuel cycle will, due to the nuclear reactions, contain significant amount of MA (Np, Am, Cm). Calculated heats of formation of bcc Pu-U, Pu-Np, Pu-Am, Pu-Cm, Pu-Zr, Pu-Mo, Np-Zr, Np-Mo, U-Am, Np-U, Np-Am, Am-Zr, Am-Mo as well as U-Ti, U-Nb, alloys are also presented and compared with CALPHAD assessments. Figure 1 shows results of our calculations of the heat of formation of *γ*-U-Zr(Mo) solid solutions.

Finally, various CALPHAD assessments have been proposed for the U-Mo, U-Zr, and Mo-Zr systems, leading to multiple possible extrapolations of the U-Mo-Zr phase stability depending on the selected binary assessments (an example of an isothermal section for T = 1073 K is presented in Figure 2). As previously demonstrated, a*b initio* electronic calculations can be used to inform the CALPHAD interaction parameters (i.e., heat of mixing) for the BCC phase and evaluate the consistency of the existing binary assessments. Thus, a*b initio* and CALPHAD calculations for the U-Mo-Zr will be presented and discussed.

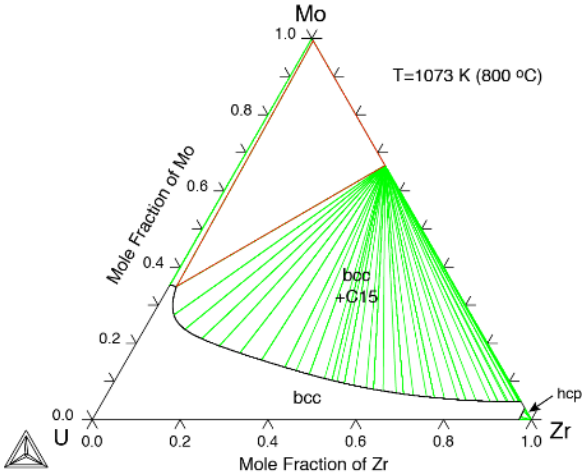

Figure 2: Example of a calculated isothermal section at T = 800 C of the U-Zr-Mo system.

Acknowledgments: This work was performed under the auspices of the US Department of Energy by Lawrence Livermore National Laboratory under Contract DE-AC52-07NA27344 and was partially funded by the Laboratory Directed Research and Development Program at LLNL under Project Tracking Code 12-SI-008.

Thermodynamic and dynamic studies of δ-^{239}Pu and its alloys using Resonant Ultrasound Spectroscopy

Boris Maiorov

Los Alamos National Laboratory, Los Alamos, NM 87545, United States

maiorov@lanl.gov

Determining the elastic properties of Pu alloys and their changes as a function of temperature and time is a powerful tool to study thermodynamic and dynamic changes. Temperature dependence informs the nature of the free energy of the different phases, as elastic moduli are fundamental thermodynamic susceptibilities and connect directly to thermodynamics, electronic structure, and mechanic properties. Changes occurring as a result of self-irradiation can change the elastic moduli and affect thermodynamic phase transitions. Similarly, sound attenuation provides information about dynamic processes such as dissipation associated with defect movement, annealing or re-crystallization.

Thus, measurements of elastic moduli and sound attenuation help determine the origin of the phenomena found in ^{239}Pu and its Ga alloys. The Resonant Ultrasound Spectroscopy (RUS) technique is based on the measurement of mechanical resonance frequencies that can be made with extreme precision and used to compute the elastic moduli without corrections. From the resonant frequencies we can extract elastic moduli while the resonance peak's width is directly associated with sound attenuation/internal friction.

Using RUS we perform time- and temperature-dependent measurements of the mechanical resonance frequencies of polycrystalline δ-PuGa. From these measurements, elastic moduli and the sound attenuation can be extracted. I will show the changes in elastic moduli and sound attenuation with time for samples with different ages. I will also show the temperature dependence of moduli and sound attenuation for different Ga concentrations, microstructures and ages and the changes in the δ–α' transition.

Thermodynamic properties of (U,Pu) mixed-oxide fuel: empirical interatomic potential calculations

E. Bourasseau, D. Bathellier, G. Porto, M. Freyss, J. Bouchet [1]

[1] CEA, DES, IRESNE, DEC F-13108 Saint-Paul-Lez-Durance, *emeric.bourasseau@cea.frl*

Uranium and Plutonium Mixed-oxide fuel (MOX) is the reference fuel for fast breeder reactors and is envisaged in France to implement plutonium multi-recycling in light water reactors. For these purposes, it is necessary to determine accurately its thermodynamic properties, including under irradiation. We focus in this work on the calculation of heat capacity (Cp) over the entire range of Pu content and a large range of stoichiometry (in the hypostoichiometric domain) and temperature (from 300 K to the melting temperature) using classical molecular dynamics (CMD).

For $U_{1-y}Pu_yO_{2-x}$ CMD with the CRG interatomic potential [1], [2] predicts a full Bredig transition [3] at high temperature (T > 1800 K) and an effect of Pu and O contents solely on this transition [4], [5]. For UO_2, the occurrence of the complete Bredig transition is in good agreement with recent available experimental studies [6]. CMD results have also been confirmed by Ab Initio Molecular Dynamics calculations in the cases of UO_2 and PuO_2. An analytical expression Cp(T,y,x) is fitted from our CMD data, valid from 700 K to the melting temperature and for any Pu and O contents. The resulting law is then tested in the fuel performance code GERMINAL [5] by simulating transient tests operated with MOX fuel for fast reactors. In the case of Reactivity-Initiated Accident power transients, and taking into account the effect of the Pu content, the new law of heat capacity induces a quicker temperature increase until melting point and a larger radial propagation of the liquid phase in the fuel pellets. On the opposite, it has no significant effect for slow power transients.

[1] M. W. D. Cooper, M. J. D. Rushton, et R. W. Grimes, « A many-body potential approach to modelling the thermomechanical properties of actinide oxides », *J. Phys.: Condens. Matter*, vol. 26, n° 10, p. 105401, mars 2014, doi: 10.1088/0953-8984/26/10/105401.

[2] C. Takoukam-Takoundjou, E. Bourasseau, M. J. D. Rushton, et V. Lachet, « Optimization of a new interatomic potential to investigate the thermodynamic properties of hypo-stoichiometric mixed oxide fuel U1−y Pu y O2−x », *J. Phys.: Condens. Matter*, vol. 32, n° 50, p. 505702, sept. 2020, doi: 10.1088/1361-648X/abace3.

[3] A. S. Dworkin et M. A. Bredig, « Diffuse transition and melting in fluorite and antifluorite type of compounds. Heat content of potassium sulfide from 298 to 1260.degree.K », *J. Phys. Chem.*, vol. 72, n° 4, p. 1277-1281, avr. 1968, doi: 10.1021/j100850a035.

[4] C. Takoukam-Takoundjou, E. Bourasseau, et V. Lachet, « Study of thermodynamic properties of U1-yPuyO2 MOX fuel using classical molecular Monte Carlo simulations », *Journal of Nuclear Materials*, vol. 534, p. 152125, juin 2020, doi: 10.1016/j.jnucmat.2020.152125.

[5] D. Bathellier, M. Lainet, M. Freyss, P. Olsson, et E. Bourasseau, « A new heat capacity law for UO2, PuO2 and (U,Pu)O2 derived from molecular dynamics simulations and useable in fuel performance codes », *Journal of Nuclear Materials*, vol. 549, p. 152877, juin 2021, doi: 10.1016/j.jnucmat.2021.152877.

[6] T. R. Pavlov *et al.*, « Measurement and interpretation of the thermo-physical properties of UO 2 at high temperatures: The viral effect of oxygen defects », *Acta Materialia*, vol. 139, p. 138-154, oct. 2017, doi: 10.1016/j.actamat.2017.07.060.

Role of electronic interaction on structural properties of actinides and phases of plutonium.

B. Amadon, B. Dorado and R. Outerovitch

CEA DAM DIF F-91297 Arpajon, France, Université Paris-Saclay, CEA, Laboratoire Matière en Conditions Extrêmes, 91680 Bruyères le Châtel, France

bernard.amadon@cea.fr

The description of pure actinides is complex for electronic structure calculations because of the interplay of electronic interaction, spin orbit coupling and complex crystal structure. Being able to describe the variety of the phases of plutonium, their spectral properties and their non magnetic ground state is thus a challenge and represents a striking example of this complexity.

We discuss the theoretical description of the experimental transition from low volume early actinides (uranium, neptunium, α-plutonium) to high-volume late actinides (δ-plutonium, americium, and curium) and the volume of phases of plutonium. We will compare methods using an explicit 5*f* electronic interactions, such as the combination of Density Functional Theory (DFT) with Dynamical Mean Field Theory (DMFT) to other approaches. We will comment the relative importance of direct and exchange Coulomb interaction and their calculation, as well as the importance of crystal structure, spin orbit coupling and magnetism on structural properties.

Density-functional theory for plutonium

P. Söderlind [1], A. Landa, [1], B. Sadigh [1], L. H. Yang [1]

[1] Lawrence Livermore National Laboratory Livermore, California 94550, USA
soderlind@llnl.gov

We review developments in the theoretical description and understanding of plutonium in terms of a metal with bonding and itinerant (band) 5f electrons. Within this picture, many facets of this stunning and non-intuitive material are accurately described by first-principle, parameter-free, density-functional-theory (DFT) calculations. We show that the approach explains plutonium's phase stability, elasticity, lattice vibrations, electronic structure, alloy properties, and magnetism. Fluctuations are addressed by means of constrained-DFT calculations and new light is shed on the anomalous properties of *d*-plutonium, including explaining its negative thermal expansion. Effects of alloying and point defects in plutonium are also addressed. It is further emphasized that strong electron correlations, originating from a large intra-atomic Coulomb repulsion (~ 4 eV) of the 5f electrons, that has often been assumed for plutonium in the literature, is inconsistent with the experimental phase diagram of plutonium. We note that even a very small U (~0.2 eV), in the most popular DFT+U formulation, results in the wrong ground state for plutonium.

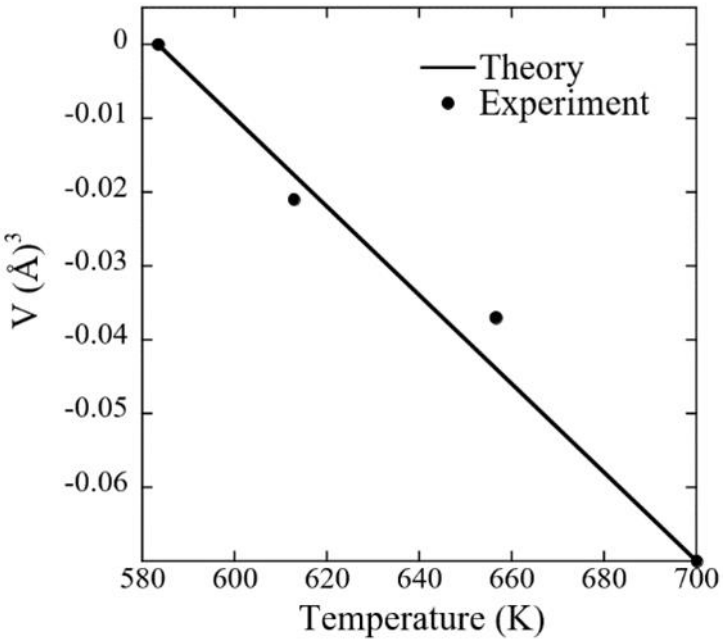

Figure 1: Calculated [1] and measured [5] volume change (DV) for d-plutonium.

Many of the results shown in this presentation originates from recent works [1,2,3] and in this abstract we highlight two of these. First, one of the most peculiar aspects of plutonium is the existence of negative thermal expansion. For example, *d*-plutonium demonstrates a weak but significant volume decrease with temperature in roughly the 600-700 K temperature range. Employing a spin-fluctuation model [1,4], coupled with a quasi- harmonic Debye-Grüneisen (DG) approach, we calculate the thermal expansion from first- principles density-functional theory for the *d* phase. For an illuminating comparison between experiment and theory we show in Fig. 1 the change in the atomic volumes as functions of temperature for the experimental [5] and theoretical [1] methods. The negative thermal expansion is very similar and also the absolute volumes are close [1].

Second, phonons for the anomalous *a* phase have been measured [6] but never been calculated by any method. In Fig. 2, we show the first calculation of the phonon density of states for *a*-plutonium together with inelastic x-ray measurements [6]. The agreement is very encouraging, and we explain [3] that plutonium atom number 8, in the standard enumeration, plays an important role for the shape of the phonon density of states.

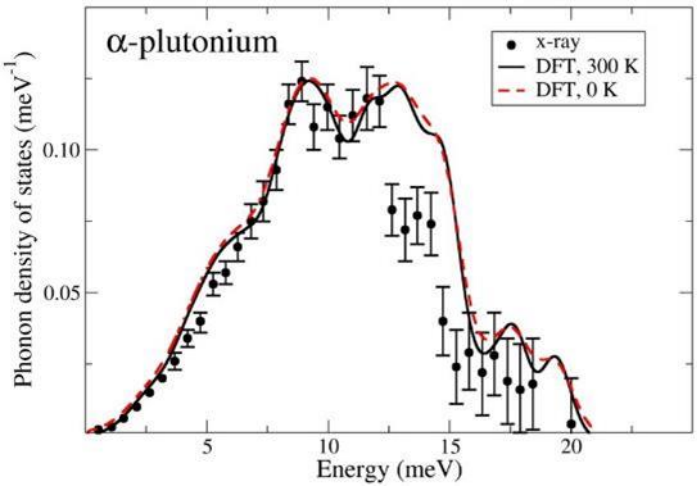

Figure 2: Calculated [3] and measured [6] phonon density of states for α-plutonium.

Acknowledgments: This work was performed under the auspices of the U.S. DOE by LLNL under Contract DE-AC52-07NA27344 and was partly funded by the Laboratory Directed Research and Development Program at LLNL under Project Tracking Code No. 17-ERD- 041.

[1] P. Söderlind, A. Landa, B. Sadigh, Adv. Phys. 68, 1 (2019).
[2] B. Sadigh, A. Kutepov, A. Landa, P. Söderlind, Appl. Sci. 9, 3914 (2019).
[3] P. Söderlind and L.H. Yang, Sci. Rep. 9, 18682 (2019). [4] A. Migliori et al., PNAS 113, 11158 (2016).
[4] D.C. Wallace, Phys. Rev. B 58, 15433 (1998).
[5] M.E. Manley et al., Phys. Rev. B 79, 052301 (2009).

Nuclear magnetic resonance studies of plutonium compounds

Eric D. Bauer [1], R. Yamamoto [1], S. B. Blackwell [1], A. P. Dioguardi [1,2], E. Bowes [1], I. M. DiMucci [1], S. M Greer [1], M. Hirata [1], H. Yasuoka [1,3], S. M. Thomas [1], F. Ronning [1], S. K. Cary [1, 4], S. A. Kozimor [1], J. N. Mitchell [1], P. H. Tobash [1], T. A. Martinez [1], C. Archuleta [1], M. Ramos [1], and J. D. Thompson [1]

[1] Los Alamos National Laboratory, Los Alamos, New Mexico 87545, USA
[2] IFW Dresden, Institute for Solid State Research, 01171 Dresden, Germany
[3] Max Planck Institute for Chemical Physics of Solids, 01187 Dresden, Germany
[4] Oak Ridge National Laboratory, Oak Ridge, Tennessee 37831, USA

e-mail:edbauer@lanl.gov

The discovery of the direct Pu-239 nuclear magnetic resonance (NMR) signal in PuO_2 [1] and PuB_4 [2,3], provides a new opportunity to explore and understand the bonding, electronic structure, and self-irradiation damage of plutonium-based materials at the atomic scale. We present a detailed study of the anisotropy of the ^{239}Pu NMR resonance of PuB_4 confirming the local tetragonal symmetry inferred from previous polycrystalline measurements. The temperature dependence of the ^{239}Pu Knight shift (K_s) and spin-lattice relaxation time (T_1) indicate that PuB_4 adopts a nonmagnetic state with gap like behavior, consistent with the insulating behavior observed in electrical resistivity measurements. Additionally, the temperature dependence of T_1 and the Knight shift reflect a gap that is twice as large for $B//c$ than for $B//b$ within the tetragonal crystal structure of PuB_4. Our results also reveal the existence of static disorder through the presence of at least five distinct Pu local environments in PuB_4. While spin-lattice relaxation measurements of PuB_4 show clear signs of aging over the time frame of ~20 months, isochronal annealing up to 250 K is unable to influence the NMR spectra or relaxation dynamics over a time scale of two months, likely due to the high melting point (~2400 K) of PuB_4.

We are also continuing our search for other compounds in which the Pu-239 NMR signal may be found. The compound $[Et_4N]_4[Pu^{IV}(NCS)_8]$ is particularly promising. It hosts a highly symmetric, square prismatic Pu environment with 8 Pu-N bonds at 2.36 Å [4]. Point-charge calculations of the Pu(IV) crystalline electric field (CEF) scheme indicate a singlet ground state with dominant $|M_J=0>$ character that is separated by ~135 meV from a magnetic triplet excited state. This CEF scheme proposed for $Pu^{IV}(NCS)^{4-}_8$ is similar to that of PuO_2 [5], where the direct Pu-239 NMR signal was observed. The measured temperature independent magnetic susceptibility of $Pu^{IV}(NCS)_8^{4-}$ with χ_0~0.001 emu/mol is consistent with the proposed CEF scheme and is similar in magnitude to that of PuO_2 (χ_0~0.0005 emu/mol). These data suggest that $Pu^{IV}(NCS)^{4-}_8$ is a good candidate for the observation of the Pu-239 NMR resonance. Preliminary measurements on $Pu^{IV}(NCS)^{4-}_8$ reveal the presence of two overlapping spectra for the nuclear spin-1 signal of N-14, as expected for the tetraethyl ammonium (Et_4N) and thiocyanate (NCS) environments. Details of the NMR investigation, including the search for the Pu-239 signal and the effect of self-irradiation on the spectra and dynamics of the nitrogen environment, will be presented.

Previous NMR measurements on δ-Pu stabilized by 1.7 at.-% Ga revealed a distribution of electric field gradients of the ^{69,71}Ga nuclei, suggesting that the Ga reside in locally distorted, non-cubic symmetric environments [6]. The Ga spectra also appeared to change due to increased self-irradiation damage at low temperature [6]. Results of our recent investigation the ^{69,71}Ga spectra of δ-Pu stabilized by 7 at.-% Ga will be presented.

[1] H. Yasuoka *et al.* Science **336**, 901 (2012).

[2] A. P. Dioguardi *et al.* Phys. Rev. B **99**, 035104 (2019).

[3] H. Choi *et al.* Phys. Rev. B **97**, 201114(R) (2018).

[4] T. J. Carter and R. E. Wilson, Chem. Eur. J. **21**, 15575 (2015).

[5] S. Kern *et al.* Phys. Rev. B **59**, 104 (1999).

[6] N. J. Curro and L. Morales, Mat. Res. Soc. Symp. Proc. **802**, 53 (2004).

Magnetic dichroism in Ga-stabilized δ-Pu

J. R. Jeffries [1], A. A. Baker [1], G. Fabbris [2], and D. Haskel [2]

[1] Lawrence Livermore National Laboratory, Livermore, CA USA
[2] Argonne National Laboratory, Argonne, IL USA

jeffries4@llnl.gov

No element in the Periodic Table has so affected the last century of humanity as has plutonium. Since its discovery in 1940, plutonium has had an outsized influence on global events as a weapon of war, as a deterrent to enable peace, as a National Security fulcrum, as a source of carbon-free power, and as a vehicle to power exploration beyond the Solar System. Plutonium is on one hand a marvel of human ingenuity, and on the other an enigma that refuses to yield. Given its utmost importance in the global arena, our understanding of the fundamental physics and chemistry of Pu is inadequate.

Plutonium exhibits an unprecedented six solid crystallographic phases at ambient pressure, a property that has been known for seven decades, but a fact that remains difficult to predict from first-principles to this day. Modern theories are challenged with describing this narrow free energy landscape correctly, and then using that basis to extrapolate into untested conditions in an effort to solve real-world problems. A major roadblock in Pu science is thus the accurate description of elemental Pu, but recent theoretical advances have led to two contending theories: (a) one in which the electronic states of Pu fluctuate between different valence configurations [1]; and (b) one in which orbital polarization leads to a local, on-site cancellation of the spin and orbital magnetic moments [2]. Both of these theories reproduce some of the observed structural features of Pu, but both predict distinct magnetic behavior. The subtleties of magnetism thus become a distinguishing characteristic of these competing models, and the problem of magnetism in Pu once again is at the forefront of our understanding of this mysterious element.

In the case of the spin and orbital cancellation model, a local, on-site cancellation of the spin and orbital magnetic moments yields a near net-zero moment for Pu that precludes long-range order, but which describes the free energy sufficiently to predict structural evolution. The hallmark of this spin/orbit cancellation model is the presence of anti-parallel, on-atom spin and orbital moments of identical magnitude (or nearly so) near 3 Bohr magnetons each. Such an offsetting magnetic configuration would be invisible to bulk probes that see only the total moment, but x-ray magnetic circular dichroism (XMCD) can offer a glimpse into the local, atomic magnetic configuration.

Herein, we will discuss the results of dichroism measurements at the M4 and M5 edges of Ga-stabilized δ-Pu acquired at a temperature of 2 K and in magnetic fields up to 60 kOe.

This work was performed under the auspices of the U.S. Department of Energy by Lawrence Livermore National Laboratory under Contract DE-AC52-07NA27344. This research used resources of the Advanced Photon Source, a U.S. Department of Energy (DOE) Office of Science user facility operated for the DOE Office of Science by Argonne National Laboratory under Contract No. DE-AC02-06CH11357.

[1] M. Janoscheck, et al., Science Advances 1, e1500188 (2015).
[2] P. Soderlind, et al., Sci. Rep. 5, 15958 (2015).

Atomic-scale modelling investigation of structural and thermodynamic properties of Americium-bearing oxides

B. Labonne [1], M. Bertolus [1], J. Bouchet [1]

[1] CEA, DEs, IRESNE, DEC, SESC, LM2C - Centre de Cadarache, 13108 Saint-Paul-lez-Durance Cedex, France

baptiste.labonne@cea.fr

Americium is a chemical element produced by neutron capture in nuclear reactors, whose strong radiotoxicity is a major issue for the management of nuclear waste. One solution envisaged to reduce the amount of americium in the waste is to re-irradiate it in fast neutron reactors in order to transform it into a less radiotoxic element thanks to a transmutation reaction [1]. Two main transmutation approaches are currently studied. Homogeneous transmutation consists in including a small Americium content (< 5%) into the nuclear fuel to transmute it during power production. Heterogeneous transmutation aims at including higher percentages (around 10 to 20%) of Americium into either a matrix located in specific pins inside the core, or in minor actinides bearing blankets located on the core periphery. Another possibility would be to use an accelerator driven system, an under-critical reactor core driven by a proton accelerator coupled to a spallation source and used for the transmutation of compounds containing high concentrations of minor actinides (up to 50%) [2].

It is therefore necessary to evaluate the impact of Americium on the behaviour of nuclear fuels, and in particular on their high temperature thermal properties. This requires, among other things, a very good knowledge of the Uranium – Plutonium – Americium - Oxygen thermodynamic system. For this, a reliable description of the ternary systems (U-Pu-O), (U-Am-O) and (Pu-Am-O) is a prerequisite. The (U-Pu-O) system has been revisited extensively in recent years and is relatively well described. Much less data is available on the Americium-bearing oxides, especially at high temperature [3].

Atomic scale modelling methods are now essential tools to complement experimental characterizations of nuclear fuels and get further insight into their properties and behaviour. We will present the results of the investigation of structural and thermodynamic properties of Americium bearing oxides using a state-of-the-art combination of electronic structure calculations and empirical interatomic potentials. Concerning electronic structure calculations, we used the DFT+U method combined with the orbital control scheme [4]. For empirical atomic potentials, we developed a potential in the Cooper-Rushton-Grimes formalism [5] to allow for the study of Uranium-Americium mixed oxides.

This project has received funding from the Euratom research and training programme 2019-2020 under grant agreement No 945077.

[1] Report on sustainable radioactive-waste-management (2012): http://www.cea.fr/english/Documents/corporate-publications/report-sustainable-radioactive-waste-management.pdf
[2] CEA, Séparation et transmutation des éléments radioactifs à vie longue, 2012
[3] C. Guéneau, A. Chartier, L. Van Brutzel, Thermodynamic and thermophysical properties of the actinide oxides
[4] B. Dorado, Etude des propriétés de transport atomique dans le dioxyde d'uranium par le calcul de structure électronique : influence des fortes corrélations, PhD Thesis, Université Aix-Marseille II, 2010
[5] M.W.D. Cooper, M.J.D. Rushton, R.W. Grimes, J. Phys.: Condens. Matter 26, 105401 (2014)

Electronic Correlation Induced Expansion of Fermi Pockets in δ-Pu

Roxanne M. Tutchton [1], Wei-ting Chiu [2], R.C. Albers [1], G. Kotliar [3], Jian-Xin Zhu [1,4]

[1] Theoretical Division, Los Alamos National Laboratory, Los Alamos, New Mexico 87545, USA | [2] Department of Physics, University of California, Davis, California 95616, USA | [3] Department of Physics and Astronomy, Rutgers University, Piscataway, New Jersey 08854, USA | [4] Center for Integrated Nanotechnologies, Los Alamos National Laboratory, Los Alamos, New Mexico 87545, USA | Theoretical Division, Los Alamos National Laboratory, Los Alamos, New Mexico 87545, USA

rtutchton@lanl.gov

LA-UR-20-20656

With six allotropic crystal phases at ambient pressure, Pu is the most complex elemental solid in the periodic table. Much of its exotic behavior is driven by a large anisotropy natural in its *f*-electron bonding whose strength is tuned by strong electronic correlations, which arise from its 5 *f*-electron behavior existing between the metallic-like itinerant character of the light actinides and the localized atomic-like character of the heavy actinides. Consequently, the local moments and their impact on Pu's electronic structure is difficult to model [1-3]. In addition, these correlations are highly temperature dependent and give rise to a strong atomic volume dependence for the different phases. In particular, the 25% volume expansion between the α and δ phases gives rise to exotic physics that has appealed to experimentalists and theorists for decades [1, 4-7].

Using sophisticated Gutzwiller wavefunction approximation (GutzA) and dynamical mean-field theory (DMFT) correlated theories, we study, for the first time, the Fermi surface topologies (Figure 1) and associated mass renormalizations of δ-Pu together with calculations of the de Haas-van Alphen (dHvA) frequencies (Table 1). Each of the correlated electron theories predict, approximately, the same hole pocket placement in the Brillouin zone, which is different from that obtained in conventional density-functional band-structure theory. Conversely, the electron pockets from all theories are in, roughly, the same area of the Brillouin Zone (Figure 1). We see a large (~200%) correlation-induced volume expansion in both the hole and electron pockets of the Fermi surface in addition to an intermediate mass enhancement (Table 1). This is in agreement with the band renormalization theory for strongly correlated systems and provides significant electronic structure features that may be compared to experimental explorations of quantum magnetic oscillations in δ-Pu.

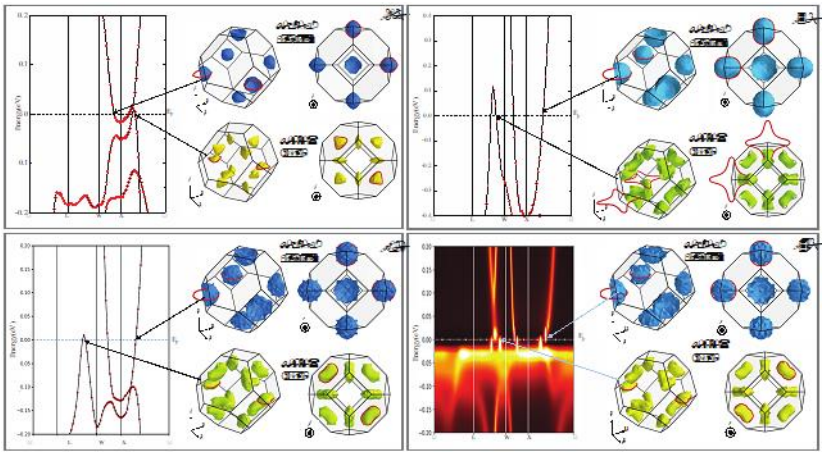

Figure 1: The Fermi surface topologies and corresponding, band dispersions for (a) the generalized gradient approximation (GGA) method, (b) the GGA+U method, (c) the GutzA methods, and (d) the DMFT method. Each panel shows the hole (bands 15 and 16) and electron (bands 17 and 18) isosurfaces for two orientations as indicated by the coordinates to the bottom left of each Brillouin zone (BZ). The arrows from the Fermi surfaces to the band structures indicate the band intersections with the Fermi energy that correspond to each Fermi surface. Red lines are interposed on the Fermi surfaces to indicate the cross-sections related to the dHvA extremal frequencies for an external B field parallel to the z-axis (B ∥ z).

	DFT			GGA+U			GGA+GutzA			GGA+DMFT		
Band	f	m^*	V_{FS}	f	m^*	V_{FS}	f	m^*	V_{FS}	f	m^*	V_{FS}
15, 16	1.74	3.19	0.31	10.2	2.35	1.02	3.12	2.00	0.91	3.07	1.84	0.95
17, 18	2.87	5.32	0.31	6.65	1.54	1.02	6.27	2.48	0.91	6.18	2.17	0.95

Table 1: The dHvA and volume data for Fermi surface calculations at zero temperature. Frequencies are given in kilotesla (kT), and corresponding effective masses are in units of electron mass (m_e). Reciprocal occupied (electron bands 17 and 18) and unoccupied (hole bands 15 and 16) Fermi surface volumes are given in units of $A^{\circ -3}$. Calculations for δ-Pu done with DFT, GGA+U, GutzA, and DMFT are compared. All measurements were taken for a magnetic field parallel to the z axis (B ∥ z). The results for T = 0 K were extrapolated from the DMFT calculation at T = 116 K, where the sensitivity of electronic self-energy to temperature is negligible since this temperature is already far below the coherence temperature [8]. The Fermi energy was shifted by −3.36 meV to maintain the conservation of the number of electrons as T → 0 K.

[1] S. Y. Savrasov, G. Kotliar, and E. Abrahams, Nature 410, 793
[2] J.-X. Zhu, P. H. Tobash, E. D. Bauer, F. Ronning, B. L. Scott, K. Haule, G. Kotliar, R. C. Albers, and J. M. Wills, EPL (Europhysics Letters) 97, 57001 (2012).
[3] M. Janoschek, P. Das, B. Chakrabarti, D. L. Abernathy, M. D. Lumsden, J. M. Lawrence, J. D. Thompson, G. H. Lander, J. N. Mitchell, S. Richmond, M. Ramos, F. Trouw, J.-X. Zhu, K. Haule, G. Kotliar, and E. D. Bauer, Science Advances 1 (2015), 10.1126/sciadv.1500188.
[4] P. Weinberger, A. Gonis, A. Freeman, and A. Boring, Physica B+C 130, 13 (1985).
[5] G. Kotliar, S. Y. Savrasov, K. Haule, V. S. Oudovenko, O. Parcollet, and C. A. Marianetti, Rev. Mod. Phys. 78, 865 (2006).
[6] P. S¨oderlind, F. Zhou, A. Landa, and J. E. Klepeis, Scientific Reports 5, 15958 (2015).
[7] P. S¨oderlind, A. Landa, and B. Sadigh, Advances in Physics 68, 1 (2019).
[8] J. H. Shim, K. Haule, and G. Kotliar, Nature 446, 513 (2007).

Metallurgy and Materials Science

	Conference room #1: CELLIER BENOIT XII
PLENARY TALK 9:00 – 09:50	**Franz FREIBERT (LANL)** *"Thermodynamics of Plutonium and its Metal Alloys"*
	Conference room #1: CELLIER BENOIT XII
INVITED TALK 10:00 – 10:30	**Michel FREYSS (CEA)** *"First-principles modeling of actinide mixed oxide bulk properties and radiation effects"*
INVITED TALK 11:00 – 11:30	**Aurelien PERRON (LLNL)** *"Alloyed Plutonium: Thermodynamics and Application to Transformations"*
11:30 – 11:50	**Najeb ABDUL-JABBAR (LANL)** *"Recovery of Thermal Expansion in Aged and Pre-Conditioned Pu-Ga Alloys"*
11:50 – 12:10	**Lucas SWEET (PNNL)** *"Crystallite Size Distributions of PuO2 Evaluated by X-Ray Diffraction Line Profile Analysis and Microscopy"*
12:10 – 12:30	**Alice SMITH (LANL)** *"Kinetic Response of the δ-phase ^{239}Pu-Ga Alloys Lattice to Self-Irradiation and Thermal Processes"*
	Conference room #1: CELLIER BENOIT XII
INVITED TALK 15:00 – 15:30	**Scott McCALL (LLNL)** *"Dimensional changes due to radiation damage in naturally aged δ-Pu (Ga) and α-Pu"*
15:30 – 15:50	**Guillaume BERNARD-GRANGER (CEA)** *"MOX fuel sintering investigations"*
INVITED TALK 16:20 – 16:50	**Dallas REILLY (PNNL)** *"Nano/Atom-Scale Investigation of Pu-Fe Inclusions in δPu"*
16:50 – 17:10	**Leonid BURAKOWSKY (LANL)** *"Systematics of the ambient melting points of soichiometric mixed oxide (MOX) fuel"*
17:10 – 17:30	**Pierrick CHEVREUX (CEA)** *"Study of carbochlorination of Plutonium oxide and electrochemistry of Pu in molten salt for Molten Salt Reactor (MSR) applications"*
17:30 – 17:50	**Alexandria MARCHI (LANL)** *"Isothermal Dilatometry of δ-^{239}Pu: Evidence of Contraction at Early Ages"*

Chair persons:

Paul ROUSSEL and Benoit OUDOT

Thermodynamics of Plutonium and its Metal Alloys

F.J. Freibert and S.C. Hernandez

Los Alamos National Laboratory - MS T001 PO Box 1663, Los Alamos, NM 87545 USA,

freibert@lanl.gov

Plutonium in its elemental form is semi-metallic in nature and exhibits many confounding behaviors for a single component system when exposed to temperature and pressure. One informative concept which enables researchers to better understand this system is that of thermodynamics. The most useful thermodynamic potential is the Gibb's Free energy G defined in terms of internal energy U and intensive parameters of temperature T, pressure P and chemical potential μ that act to compel heat, volume and matter flow, respectively. The expression of G for any phase of Pu is given by

$$G=U-TS+PV+\mu N$$

in terms of extensive parameters entropy S, volume V and numbers of component atom N. Alloying Pu (i.e., adding solute atoms to the system and component species $\mu_s N_s$ terms into G) produces materials that may reduce extreme behaviors for a more applicable material; but other puzzling behaviors appear. Important to the application of thermodynamics in Pu are the thermophysical properties of bulk modulus B, thermal expansion α, specific heat C_p defined as higher order intensive parameter derivatives of G and density $\rho=1/V$.[1]

Thermophysical quantities are derivable from first-principles calculations, thus electronic structure and phonon (i.e., lattice vibration) spectrum modeling should be verified against them. Modern theoretical tools such as the electronic structure theory implemented via Density Functional Theory (DFT) are extremely useful as a direct connection between quantum mechanics and thermodynamics. Pu crystallographic and defected structures minimized by DFT will provide U at T=0K and with the application of hydrostatic stress P revealing local minimum energies for volumes and energies of formation.[2] Due to the spin-orbit coupling of Pu, 5f electrons play a significant role in atomic interactions responding with varied bonding or non-bonding configurations via energy minimized structures whether crystalline or defects of broken global symmetry.[3] Collectively, the physics of electron correlations in Pu as exhibited in diverse lattice structures, defects and magnetism in Pu is not understood and thus driving current research.

As intensive parameters T or P are varied thus lowering the G of one Pu phase relative to another, structural instabilities arise and phase transformations occur. The perceived order of these transformations is based on the curvature of G at critical point in phase space, critical point behavior of the related thermophysical properties and as suggested by Fig.1, the characteristics of these transformations indicate potential underlying physical mechanisms.[4] Multiple phases may coexistence in Pu and its alloys [5] resultant from local compositional variation with solute heterogeneity from coring, nucleation and growth kinetic barriers of super-cooling and super-heating and defects and damage from plastic deformation and lattice disruption. Exploration of these and related phenomena are important to the ultimate understanding of metastability and anharmonicity in plutonium.

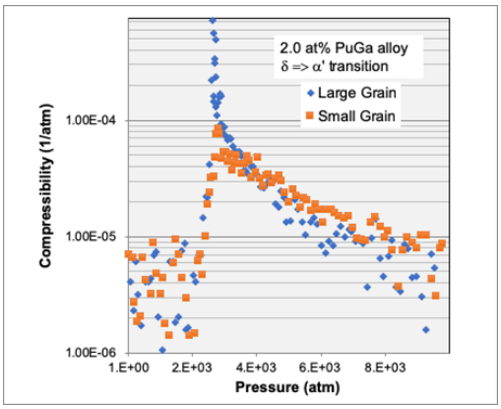

Figure 6 : Plot showing grain size influence on divergence of compressibility at the δ→α' critical pressure of 2.0at% PuGa alloy. Data taken from Hecker, et al. [4].

Self-irradiation of Pu is via a radioactive α-particle decay process resulting in a recoil uranium nucleus with a decay energy of 85keV and a 5MeV α-particle which captures two electrons to become a helium atom within the lattice. After each decay, there is a collision cascade and follow-on Frenkel pair recombination. It has also been shown that self-irradiation damage in δ-Pu alloys does not completely annihilate by room temperature, but continues to accumulate to higher temperatures.[6],[7] DFT calculations have enabled the determination of Pu defect formation energies or enthalpy and volume.[8] Extending DFT by Nudged Elastic Band (NEB) techniques, Pu defect migration transition states are calculable to obtain

defect energy of activation energies or enthalpy necessary for phenomena such as diffusion, creep and anelasticity. Current models suggest that migration of defects in unalloyed and alloyed δ-Pu are highly dependent on the electronic and magnetic interactions that induce associated low-symmetry structures and consequently influence the diffusional properties of these metal. [9],[10] Thus, typical face-centered cubic defect diffusion mechanisms do not apply to defects in the complex strongly correlated 5*f* δ-Pu system. In Pu and its alloys, solid state diffusive or inelastic processes are due to stress-strain coupling through an internal variable, such as a short or long-range order, or a parameter describing the electronic structure, atomic bonding, or magnetic moment interactions.

These and related topics of the thermodynamics of Pu and its metal alloys will be discussed during this presentation.

[1.] Freibert, F.J., S. C. Hernandez, A. Migliori, Thermophysical Properties of Plutonium Metal and Alloys, Plutonium Handbook, Vol. 2, 2nd ed., D. L. CLARK, D. A. GEESON, and R. J. HANRAHAN Jr., Eds., pp. 641–752, American Nuclear Society, La Grange Park, Illinois (2019).

[2.] Hernandez, S.C., F.J. Freibert, J.M. Wills, Density functional theory study of defects in unalloyed δ-Pu. Scripta Materialia, 2017. ***134****, p. 57.*

[3.] Söderlind, P., A. Landa, B. Sadigh, Density-functional theory for plutonium, Advances in Physics, 2019. ***68****, p. 1.*

[4.] Hecker, S.S., D.R. Harbur, T.G. Zocco, Phase stability and phase transformations in Pu– Ga alloys. Progress in Materials Science, 2004. ***49****: p. 429.*

[5.] Freibert, F.J., et al., Thermophysical properties of coexistent phases of plutonium. Actinides 2009. ***9****: p. 6.*

[6.] Maiorov, B., et al., Elastic moduli of δ-Pu239 reveal aging in real time. Journal of Applied Physics, 2017. ***121****: p. 125107.*

[7.] Freibert, F.J., D.E. Dooley, D.A. Miller, Formation and recovery of irradiation and mechanical damage in stabilized δ-plutonium alloys. Journal of Alloys and Compounds, 2007. ***444–445****: p. 320.*

[8.] Hernandez, S.C., et al., Spin density stabilization of local distortions induced by a monovacancy in δ-Pu. Physical Review Materials, 2018. ***2****: p. 085005.*

[9.] Hernandez, S.C., et al., Role of electronic and magnetic interactions in defect formation and anomalous diffusion in δ-Pu, Journal of Nuclear Materials, 2020. ***532****: p. 152027.*

[10.] Hernandez, S.C., F.J. Freibert, Ab Initio Study of the Effect of Mono-Vacancies on the Metastability of Ga-Stabilized δ-Pu. Appl. Sci. 2020. ***10****: p. 7628.*

First-principles modeling of actinide mixed oxide bulk properties and radiation effects

M. Freyss, M. S. Talla Noutack, G. Jomard [1], G. Geneste [2,3]

[1] CEA, DES, IRESNE, DEC, Centre de Cadarache, 13108 Saint-Paul-lez-Durance, France
[2] CEA, DAM, DIF, 91297 Arpajon, France
[3] Université Paris-Saclay, CEA, Laboratoire Matière en Conditions Extrêmes, 91680 Bruyères-le-Châtel, France

michel.freyss@cea.fr

We present applications of first-principles calculations aiming at determining material properties and radiation effects of actinide mixed oxides, in particular $(U,Pu)O_2$. Mixed U and Pu oxides (MOX) are one of the current nuclear fuels used in French pressurized water nuclear reactors and they are considered for future reactors with a higher Pu content. They contain a few percent of americium due to neutron irradiation effects and to the fabrication process from spent fuels. In MOX fuels with high Pu contents (25-30 at.%), the influence of americium on thermal properties is not well established and needs to be monitored precisely in order to increase safety margins. Using first-principles DFT+*U* calculations, we determine the influence of Am on bulk properties of Am-bearing oxides, such as structural, elastic, magnetic, thermodynamic properties. We also study the stability of electronic defects and point defects with various charge states. We consider the Am bearing-oxides AmO_2, $(U,Am)O_2$ and $(U,Pu,Am)O_2$.

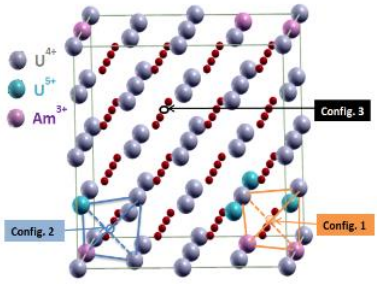

Figure 1: Periodic simulation box for $(U,Am)O_2$ illustrating the various oxygen vacancy configurations studied. Configuration 1: two Am(+III) and two U(+IV) first-neighbors. Configuration 2: one (U+V), one Am(+III) and two U(+IV) first-neighbors. Configuration 3: four U(+IV) first-neighbors.

We show that self-trapped electron polarons (which locally correspond to reducing one Am(+IV) cation into Am(+III)) are found very stable in AmO_2 [1]. As a result, $(U,Am)O_2$ oxides display particular mixed cation valence states which are fundamentally different from $(U,Pu)O_2$. A systematic study of $(U,Am)O_2$ as a function of the Am content [2] reveals a large value of the mixing enthalpy of $(U,Am)O_2$, much larger than the value obtained for $(U,Pu)O_2$, thus showing that $(U,Am)O_2$ does not behave as an ideal solid solution. The formation of oxygen vacancies is also found to be favoured in presence of Am in $(U,Am)O_2$ and $(U,Pu,Am)O_2$ [3]. $(U,Am)O_2$ is more easily reduced to a hypostoichiometric compound than UO_2, which could have a significant influence on the speciation of fission products and on the melting temperature.

[1] M.S. Talla Noutack, M. Freyss, G. Jomard, G. Geneste, Phys. Rev. B 101, 024108 (2020);
[2] M.S. Talla Noutack, G. Jomard, M. Freyss, G. Geneste, J. Phys.: Condens. Matter 31, 485501 (2019)
[3] M.S. Talla Noutack, G. Geneste, G. Jomard, M. Freyss, to be published (2022)

Alloyed Plutonium: Thermodynamics and Application to Transformations

Aurélien Perron, Patrice E.A. Turchi

Lawrence Livermore National Laboratory, 7000 East Avenue, Livermore, CA 94550, USA

perron1@llnl.gov

INTRODUCTION

A new edition of the "Pu Handbook – A Guide to the Technology" is now available. The original Chapter 7 (first edited in 1967 and reedited in 1980 with minor modifications) entitled "Alloying Behavior of Plutonium" and authored by F. H. Ellinger, C. C. Land, and K. A. Gschneidner, Jr., was of particular interest for the CALPHAD (CALculation of PHAse Diagrams) community as it was focused on phase diagrams of plutonium alloys. Indeed, with the body of experimental work that exists on plutonium-based alloys, the best systematic way of recording this information and making it useful to daily practice in alloy design is to use the phase diagram representation. This way of recording the information allows the scientist to quickly find out, as a function of temperature and composition (and possibly other variables, such as pressure), about phase stability and also, in a qualitative way, the microstructure that may develop.

The present talk will provide an historical note (up to 1967) and an update of the Pu-based phase diagrams, both experimental and theoretical, that are detailed in the Chapter 8 of the new Pu Handbook: "Alloyed Plutonium: Thermodynamics and Application to Transformations". As little was said about modeling in the 1967 chapter and because modeling has made substantial progress with the advent of commercial software to ease the thermodynamic assessment of phase diagrams and, more recently, with quantum mechanical *ab initio* electronic structure calculations aiding the assessment process, this has been corrected in the current chapter. After a general survey on experimental phase diagrams that are currently approximately known, CALPHAD modeling (phase diagrams and transformations) of Pu-based alloys will be discussed during this presentation.

RESULTS

Experimental phase diagrams

Most of the work on experimental phase diagram characterization was performed in the 1960s and 1970s with little done since then. Most effort has been spent on plutonium-rich regions of the phase diagrams of plutonium alloyed with other elements, except in a few rare cases. The resulting sparsity of data has resulted in poorly defined overall phase diagrams with dashed lines in most regions away from pure plutonium. In other instances, it was assumed, based on the location of an element in the periodic table, that the phase diagram would look similar to those associated with nearby elements. This is the case for several classes of elements associated with plutonium, including the six alkali metals (group 1 elements, except hydrogen: lithium, sodium, potassium, rubidium, cesium, and francium), the six alkaline earth metals (some of the group 2 elements: calcium, strontium, barium, and radium), the six bcc transition metals (TMs) (vanadium, niobium, tantalum, chromium, molybdenum, and tungsten), and the seventeen rare earth elements (REEs) (i.e., the 15 lanthanides, plus scandium and yttrium). These alloys that form classes in themselves will be discussed first, while specific systems of interest (e.g. Pu-Zr) for the Pu community will be presented individually.

CALPHAD thermodynamic studies

After a general description of the method, a brief review of the phase and property diagrams that have been generated by the CALPHAD community, including those that were obtained as part of a thermodynamic assessment activity carried out at Lawrence Livermore National Laboratory will be

given [1-4]. New insights into uncertainty quantification of CALPHAD model parameters and its propagation to phase stability predictions will also be presented. Knowledge of the thermodynamic driving force (through CALPHAD modeling) versus temperature and composition is critical to carrying out studies on transformations, kinetics of transformation, and microstructure evolution in alloys, among others. Examples of such extensions [5,6] will be briefly discussed in the case of Pu–Ga alloys, including: (i) kinetics associated with the predicted eutectoid invariant reaction in plutonium-rich Pu–Ga alloys, and (ii) temperature-induced α′ martensitic transformation and α′ → δ reversion transformations. Finally, predictions of phase stability for multicomponent Pu-Ga systems will be presented as functions of daughter products (U, Am) and impurities (Fe, Ni).

ACKNOWLEDGEMENTS

Prepared by LLNL under Contract DE-AC52-07NA27344.

REFERENCES

[1] A. Perron *et al.*, “Thermodynamic re-assessment of the Pu–U system and its application to the ternary Pu–U–Ga system,” *J. Nucl. Mater*. **454**, 81 (2014).
[2] A. Perron *et al.*, “The Pu–U–Am system: An *ab initio* informed CALPHAD thermodynamic study,” *J. Nucl. Mater*. **458**, 425 (2015).
[3] A. Perron *et al.*, “Thermodynamic assessments and inter-relationships between systems involving Al, Am, Ga, Pu, and U,” *J. Nucl. Mater*. **482**, 187 (2016).
[4] E.E. Moore *et al.*, “Development of a CALPHAD Thermodynamic Database for Pu-U-Fe-Ga Alloys”, *Appl. Sci.* **9**, 5040 (2019).
[5]. B. Ravat *et al.*, “Phase transformations in PuGa 1 at.% alloy: Study of whole reversion process following martensitic transformation,” *J. Alloys Comp*. **580** 298 (2013).
[6] A. Perron *et al.*, “Phase transformations in Pu–Ga alloy: Synergy between simulations and experiments to elucidate direct and indirect reversion competition,” *Acta Mat*. **61**, 7109 (2013).

Recovery of Thermal Expansion in Aged and Pre-Conditioned Pu-Ga Alloys

Najeb M. Abdul-Jabbar* and Jeremy N. Mitchell

Los Alamos National Laboratory - Los Alamos, New Mexico 87545, USA

najeb@lanl.gov

Stabilized δ Pu-Ga alloys are the predominant form of Pu that is used in scientific and engineering applications owing to a face-centered cubic structure that yields desirable mechanical properties for machining and fabrication. Nevertheless, the kinetics and thermodynamics that drive δ stabilization via tri-valent cations (e.g., Al^{3+} and Ga^{3+}) are still not fully understood. This is especially highlighted in the discrepancy that emerged between the Western and Russian versions of the Pu-Ga equilibrium phase diagram (Figure 1) in the 1960s. In the Western version, the δ phase can be retained to ambient conditions while the Russian diagram predicts a eutectoid decomposition into the Pu_3Ga intermetallic compound and pure α-Pu (the latter exhibits a monoclinic structure that results in poor mechanical properties). The decomposition is driven by the sluggish kinetics of Ga diffusion, where the timescale for it to proceed is on the order of ~10^4 years. Western efforts to reproduce the Russian diagram in the next two decades failed, but in the late 1990s, renewed scientific exchanges with Russia and the West revealed that Russian researchers were subjecting δ alloys to pre-conditioning treatments that would enhance the kinetics of eutectoid decomposition [1]. Based on these findings, it was concluded that the Russian diagram represents the thermodynamic equilibrium in the Pu-Ga system, while the Western diagram depicts the metastable scenario that is encountered in real-world engineering applications.

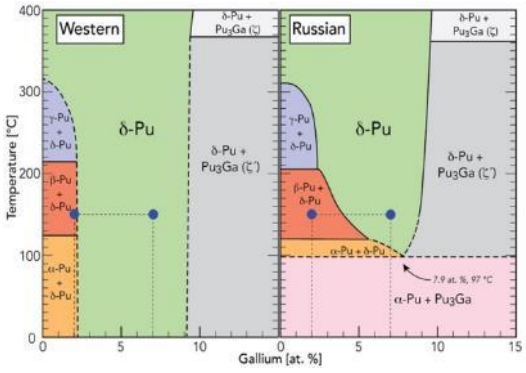

Figure 1: Comparison between the Western and Russian Pu-Ga phase diagrams, where alloy compositions measured in this investigation are plotted

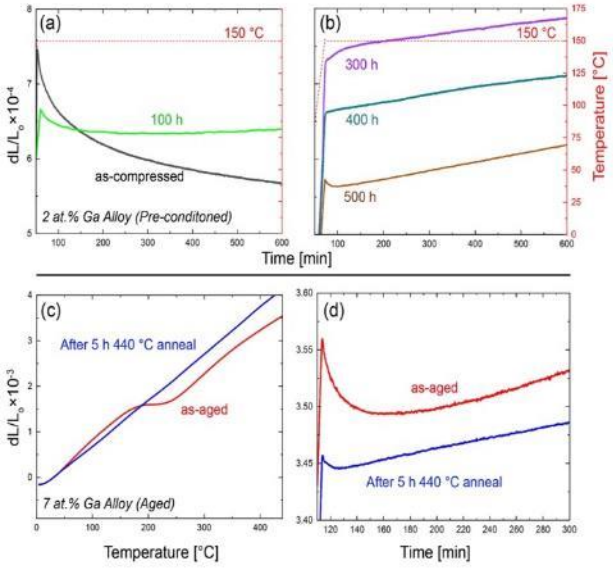

Figure 2: (a)-(b) Thermal expansion behavior of a pre-conditioned Pu-Ga alloy (c)-(d) Thermal expansion of a naturally aged Pu-Ga alloy.

While the new insights behind the variations in the Pu-Ga phase diagram have been valuable, understanding of mechanisms that would lead to eutectoid decomposition of the δ phase remains elusive. It has been posited that the Russian pre-conditioning treatments induce residual monoclinic distortions that act as nucleation sites for the transformation to occur [1, 2]. However, direct observation of such defect embryos has yet to be reported. Renewed efforts at Los Alamos National Laboratory (LANL) have sought to probe such materials phenomena using high-precision dilatometry to measure thermal expansion behavior in pre-conditioned Pu-Ga alloys. The data are then compared with naturally aged material to assess if radiation damage has the potential to initiate δ decomposition. In Figure 2, a set of dilatometry experiments is shown for two Pu-Ga alloys: one with ~2 at. % Ga (Figure 2 a-b) and one containing ~7 at. % Ga (Figure 2 c-d). The 2 at. % Ga alloy was pre-conditioned via compressive plastic deformation at room-temperature, then isothermally annealed at 150 °C for up to 500 h. The 7 at. % Ga alloy was aged for 10 years, and dilatometry curves were collected in the as-aged condition and after a 5 h anneal at 440 °C. In the pre-conditioned alloy, noticeable contraction is observed during the 150 °C isotherm, which is indicative of recovery to a state prior to compressive deformation (Figure 2a). As anneal times are increased, contraction during the isotherm diminishes (Figure 2b) and the material reverts to its pre-deformed condition. Analogous behavior is observed in the naturally aged 7 at. % Ga alloy. Specimen contraction is observed on heating (Figure 2c) and during isothermal annealing (Figure 2d), where it is initiated at temperatures ranging from 150-225 °C. After annealing for 5 h at 440 °C, the recovery features do not reappear upon reheating. Similar trends have been observed in electrical resistivity measurements on cold-worked Pu-Ga alloys within the same temperature range and has been attributed to the migration of point defects, dislocations, and vacancy clusters [3]. Moreover, these effects have also been observed in neutron irradiated aluminum [4], which suggests that radiation damage can create equivalent defect structures to those seen Pu-Ga alloys after pre-conditioning. Whether interactions between defects produced by pre-conditioning or natural aging can develop into α-like embryos that facilitate eutectoid decomposition remains to be seen. Consequently, ongoing thermal analysis work is being conducted at LANL on a comprehensive series of pre-conditioned and naturally age Pu-Ga alloys and the ensuing results in the context of δ phase stability will be further discussed.

References

[1] S. S. Hecker and L. F. Timofeeva, "A tale of two phase diagrams," *Los Alamos Science,* vol. 26, pp. 244-251, 2000.
[2] L. F. Timofeeva, "Phase transformations in Pu–Ga and Pu–Al alloys Effects of pressure and temperature on kinetics of δ-phase decomposition," *Journal of Alloys and Compounds,* vol. 444-445, pp. 124-128, 2007.
[3] W. N. Seery, "The recovery of electrical resistivity in plutonium-1 wt. % gallium after plastic deformation," *Journal of the Less-Common Metals,* vol. 18, pp. 373-379, 1969.
[4] R. Vandermeer and J. Ogle, "The kinetics of void annealing in neutron irradiated aluminum," *Acta Metallurgica,* vol. 28, pp. 151-161, 1980.

Crystallite Size Distributions of PuO_2 Evaluated by X-Ray Diffraction Line Profile Analysis and Microscopy

Lucas E. Sweet [1], Jordan F. Corbey[1], Matteo Leoni [2], Edgar C. Buck[1], Amanda J. Casella[1], Ana L. Arteaga[1], Dave E. Meier[1], Robert G. Surbella[1], Gregg J. Lumetta[1], Joel M.Tingey[1], Forrest D. Heller[1], Aaron D. Nicholas[1], Dallas D. Reilly[1], Richard A. Clark[1], Karl Pitts[1]

[1] Pacific Northwest National Laboratory, 902 Battelle Blvd., Richland, WA 99354, USA [2] University of Trento, Italy, Via Mesiano, 77 - 38123 Trento, Italy

Lucas.sweet@pnnl.gov

The microstructure of PuO_2 has been studied since the Manhattan era and is still a focus today, although our drivers have changed. Today we are interested in how the micro-structural properties of PuO_2, including various colloidal hydrolysis products, impact environmental fate and transport of particulates for environmental clean up sites and waste repositories.[1-3] In addition, performance and safety testing associated with proposed uses of mixed oxide nuclear fuels in power reactors, as a route for plutonium disposition, also rely on accurate measurements of microstructural properties of PuO_2.[4, 5] In the vein of national security, there have been indications that the microstructural properties of PuO_2 could be of significance in nuclear forensics technologies.[6] Due to the hazards, expense in handling, rarity of plutonium samples and need for validated analytical techniques, there is motivation to improve the level of sophistication in analytical techniques used in plutonium research in order to maximize the amount of useful information one can obtain from a minimal number of measurements and minimal handling.

Advances in microstructure property quantification through X-ray diffraction line profile analysis (LPA) has opened the door to a more in depth understanding of materials properties. In this study we use the Whole Powder Pattern Modelling (WPPM) approach [7-9] to evaluate the factors that influence crystallite size distributions of PuO_2 (shown in Figure 1). Previous studies on the crystallite size of PuO_2 as a function of process history reported average crystallite sizes and used LPA methods such as the Scherer method. By applying the WPPM approach to quantifying crystallite size we get insight into the shape of the distribution of crystallite sizes.

The work presented here evaluates the crystallite size distributions of PuO_2 prepared under several different conditions. Some validation work on the WPPM method will be presented in addition to an assessment of factors that could influence crystallite size distributions in PuO_2. At this point, we have more questions about how different processing conditions perturb microstructure properties of PuO_2, but the methods developed in this work have the potential to start answering those questions.

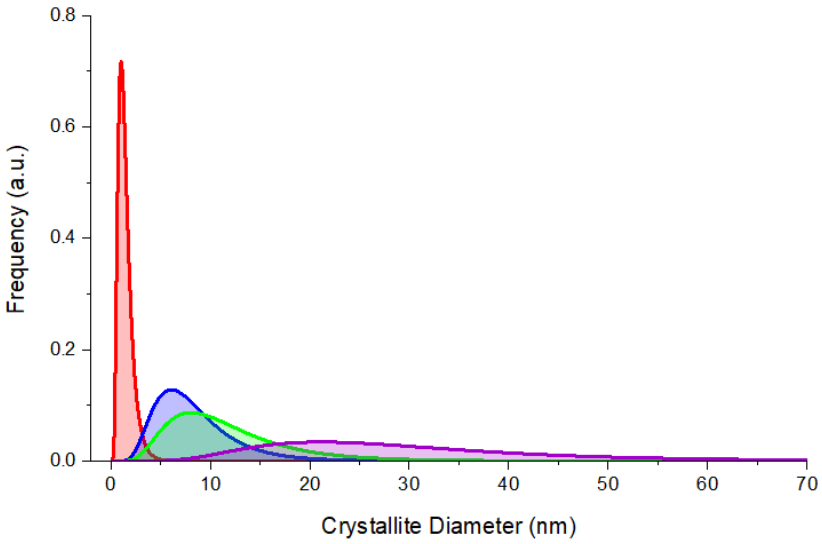

Figure 1. Crystallite size distributions of PuO_2 prepared by heating Pu(IV) oxalate to 300°C (red), Pu(III) oxalate to 641°C (blue), Pu(III) oxalate to 655°C (green) and Pu(III) oxalate to 850°C (purple)

1. Delegard, C. H., Effects of aging on PuO2·xH2O particle size in alkaline solution. *Radiochim. Acta* **2013,** *101* (5), 313-322.
2. Hixon, A. E.; Powell, B. A., Plutonium environmental chemistry: mechanisms for the surface-mediated reduction of Pu(V/VI). *Environ. Sci.: Processes Impacts* **2018,** *20* (10), 1306-1322.
3. Kersting, A. B., Plutonium Transport in the Environment. *Inorg. Chem.* **2013,** *52* (7), 3533-3546.
4. Cina, B., Decomposition effects in PuO2 on sintering. *J. Nucl. Mater.* **1963,** *9* (1), 85-100.
5. Machuron-Mandard, X.; Madic, C., Plutonium dioxide particle properties as a function of calcination temperature. *J. Alloys Compd.* **1996,** *235* (2), 216-24.
6. Mayer, K.; Wallenius, M.; Varga, Z., Nuclear forensic science: Correlating measurable material parameters to the history of nuclear material. *Chem. Rev. (Washington, DC, U. S.)* **2013,** *113* (2), 884-900.
7. Scardi, P.; Leoni, M.; Dong, Y. H., Whole diffraction pattern-fitting of polycrystalline fcc materials based on microstructure. *Eur. Phys. J. B* **2000,** *18* (1), 23-30.
8. Scardi, P.; Leoni, M., Whole powder pattern modelling. *Acta Crystallogr A* **2002,** *58* (Pt 2), 190-200.
9. Leoni, M.; Di Maggio, R.; Polizzi, S.; Scardi, P., X-ray diffraction methodology for the microstructural analysis of nanocrystalline powders: Application to cerium oxide. *J. Am. Ceram. Soc.* **2004,** *87* (6), 1133-1140.

Kinetic Response of the δ-phase ^{239}Pu-Ga Alloys Lattice to Self-Irradiation and Thermal Processes

Alice I. Smith[1], F. J. Freibert[1-2], S. C. Vogel[3], J. Zhang[3], J. E. Siewenie[4], S. Richmond[1], and M. Ramos[1]

[1]MST-16:Nuclear Materials Science
[2] NSEC: National Security Education Center
[3]MST-8: Materials Science in Radiation&Dynamics Extremes
[4]P-27:LANSCE Weapons Physics
Los Alamos National Laboratory, Los Alamos NM 87545 USA
aismith@lanl.gov

Self-irradiation in plutonium metal at room temperature introduces defect accumulation into the lattice, such as He bubbles and other daughter product impurities, interstitials and vacancies. X-ray diffraction and dilatometry studies have shown that the room temperature self-irradiation of δ-phase Pu-Ga alloys results in swelling of the lattice that saturates after 0.1-0.2 dpa of accumulated lattice damage. For a more complete picture of the poorly understood "aging" processes of defect accumulation and damage evolution δ-phase Pu-Ga alloys, dose, dose rate, thermal history and alloy composition must be considered. This work is a time-of-flight neutron diffraction investigation of δ-phase ^{239}Pu- Ga alloys as associated with a varied history of storage time at ambient temperature, elevated temperature annealing, and repeated alternating-temperature exposure.

In-situ time-of-flight neutron diffraction measurements were performed on the High-pressure Preferred Orientation (HIPPO) diffractometer at Lujan Neutron Scattering Center facility, Los Alamos National Laboratory. Data were collected between room temperature and 35K in an investigation of ambient aging impact on the lattice effects on the lattice of a δ-phase ^{239}PuGa alloys.

Repeated alternate temperature measurements of ^{239}Pu−Ga alloys (2 and 7at.%Ga) immediately after annealing at 450°C exhibits lattice swelling similar to ambient temperature isothermal lattice swelling, but at much shorter time scales. Reported here, the amount of lattice swelling for each temperature sequence decreased in magnitude relative to the time before indicative of a saturating strain due to stress of local defect evolution to damage accumulation and impact on long-range order.

This study is an attempt at unravelling the complex history dependence of induced stress states and corresponding lattice strain on the kinetic processes of self-irradiation damage, as a result of repeatedly alternating the temperature between room temperature and cryogenic values.

Dimensional changes due to radiation damage in naturally aged δ-Pu(Ga) and α-Pu

S. K. McCall, J. E. Schnackenberg, D. Ruddle, B.W. Chung

Lawrence Livermore National Laboratory - 7000 East Avenue, Livermore CA USA 94550

mccall10@llnl.gov

Radiation damage is a complicated process where the final state depends on impurity concentrations, dose, dose rate, temperature, as well as the processing and thermal history of the material. One well documented effect is a change in density due to swelling from the accumulated damage in the atomic structure and in the case of α-decay, helium in-growth. In some materials, void growth has been shown to develop, where after a period of incubation, the material swells at a rapid rate. To determine if this is a risk for plutonium, accelerated aging experiments have been performed where δ-Pu has been enriched in Pu-238 to generate a higher dose rate. The results have shown initial rapid swelling with a length change of ~$2x10^{-4}$ per year, primarily due to the formation of helium bubbles. This rate slows to less than 10^{-5} per year after the first several equivalent years of aging[1, 2]. However, the higher dose is not a perfect match for natural aging and presents a challenge when trying to tease out the influence of other terms such as temperature and history.

Temperature is an excellent example. At very low temperatures near 4K, α-Pu has been shown to swell at an initial rate >$3x10^{-6}$ per hour with a saturation in swelling predicted to result in a volume increase of ~10%[3]. At such low temperatures, large volumes of radiation damage are retained in both α- and δ-Pu, which largely anneals away when warmed to room temperature. More remarkably, the volume in stabilized δ-Pu(6at.%Al) due to radiation damage at similar cryogenic temperatures has been shown to decrease[3, 4] with a saturation value approaching 15%. Apart from radiation damage, δ-Pu stabilized by 3at% or less Ga is thermodynamically unstable and partially transforms to the ~20% denser α'-Pu phase. This has been observed repeatedly at temperatures below zero Celsius, with notable transitions occurring after only a day at -20°C in 1at.%Ga doped δ-Pu[5]. Earlier measurements had shown that thermal cycling leads to the beginning of reversion by around 50°C for Ga concentrations near 2at.%[6]. The influence, if any, that radiation damage has on this process is not yet understood. Longer term measurements on δ-Pu(1.9at%Ga) have shown a very small contraction occurs even near ambient temperature (22-30°C) and that this reverts to swelling once temperatures reach 60°C. By contrast, specimens of the denser α-Pu phase readily expand at both cryogenic and room temperatures. The results of careful dilatometry measurements at temperatures above zero Celsius will be discussed in the context of long-term self-damage of α-Pu and stabilized δ-Pu(Ga) alloys.

This work was performed under the auspices of the U.S. Department of Energy by Lawrence Livermore National Laboratory under Contract DE-AC52-07NA27344.

***1**. Chung, B.W., et al., Density changes in plutonium observed from accelerated aging using Pu-238 enrichment. Journal of Nuclear Materials, 2006. 355(1-3): p. 142-149. **2**.Chung, B.W., K.E. Lema, and P.G. Allen, Effects of self-irradiation in plutonium alloys. Journal of Nuclear Materials, 2016. 471: p. 239-242. **3**. Marples, J.A.C., et al. Length Changes in the Actinide Metals Due to Self-Irradiation at 4K. in Proceedings of the 4th International Conference on Plutonium and other Actinides. 1970. Metallurgical Society AIME **4** Jacquemin, J. and R. Lallement. Length change of a, b, and d Plutonium at 1.4K and 4.2K. in Proceedings of the 4th International Conference on Plutonium and other Actinides. 1970. Metallurgical Society AIME. **5**. Lalire, F., et al., Phase transformations in PuGa 1 at.% alloy: New valuable insight into the isothermal martensitic δ→α' transformation. Acta Materialia, 2017. 123(Supplement C): p. 125-135. **6**. Mitchell, J.N., et al., Phase stability and phase transformations in plutonium and plutonium-gallium alloys. Metallurgical and Materials Transactions A, 2004. 35(8): p. 2267-2278.*

MOX fuel sintering investigations

Guillaume Bernard-Granger [1], Laure Ramond [1], Florent Lebreton [2], Marion Le Guellec [1] & Julie Simeon [2]

[1] CEA/DES/ISEC/DMRC/SPTC/LSEM, [2] CEA/DES/ISEC/DMRC/SASP/LMAT

CEA Marcoule, 30207 Bagnols sur Cèze, France

guillaume.bernard-granger@cea.fr

MOX (UO_2-PuO_2) freeze granulated powders have been elaborated, shaped by uniaxial pressing and sintered at high temperatures under different oxygen potential values. The Pu/(U+Pu) content ranged between 11 and 33 mol%. Two kinds of UO_2 powder were used.

The sintering map strategy enabled to determine the activation energy for densification and the mechanism controlling densification. Using the master sintering curve approach enabled to determine an optimized sintering cycle to obtain a target microstructure characterized by a (relative density, grain size) pair.

Finally, the sintered microstructures have been deeply characterized using SEM, EMPA and TEM investigations.

Nano/Atom-Scale Investigation of Pu-Fe Inclusions in δPu

D. Reilly [1], K. Holliday [2], T. Lach [3], L. Kovarik [1], M. Olszta [1], D. Perea [1], S. Stout [2], E. Smith [1]

[1] Pacific Northwest National Laboratory, 902 Battelle Blvd, Richland, WA 99354
[2] Lawrence Livermore National Laboratory, 7000 East Avenue, Livermore, CA 94550
[3] Oak Ridge National Laboratory, 1 Bethel Valley Rd, Oak Ridge, TN 37830

Dallas.Reilly@pnnl.gov

Plutonium (Pu) interactions with iron (Fe) have been studied extensively since the discover of the former[1-6]. Since Fe is a common contaminant in many nuclear processes, these studies are important to better understand how Fe incorporates and the properties of the resulting Pu-Fe phases and their impact on performance and processing. At low Fe concentrations, a commonly identified phase is Pu_6Fe. This intermetallic has a slightly lower melting point (610 °C) than Pu (640 °C)[7] and therefore tends to migrate to grain boundaries[8] upon solidification. However, discussions with colleagues at LLNL indicated that a second type of Fe-rich inclusion has been observed in samples of Pu, but until now has not been characterized extensively. In this study, we applied commonly available microscopic techniques such as scanning electron microscopy (SEM) and transmission electron microscopy (TEM) along with more recently established techniques like atom probe tomography (APT) to the study of these inclusions.

Our laboratory received a ~110 mg sample of gallium (Ga)-stabilized δPu from colleagues at LLNL. This sample was mounted in epoxy and polished to a 3 μm finish in aqueous-based solutions, followed by oil-based polishing to a 250 nm polycrystalline diamond finish. The sample was cleaned in ethanol and carbon coated prior to SEM analysis. Although the previously uncharacterized Fe-rich phase had been described as angular inclusions, our images showed that this was not always the case (potentially due to corrosion in the aqueous-based polishing steps). Figure 1 shows the difference between traditional Pu_6Fe inclusions and the previously uncharacterized Fe-rich inclusions.

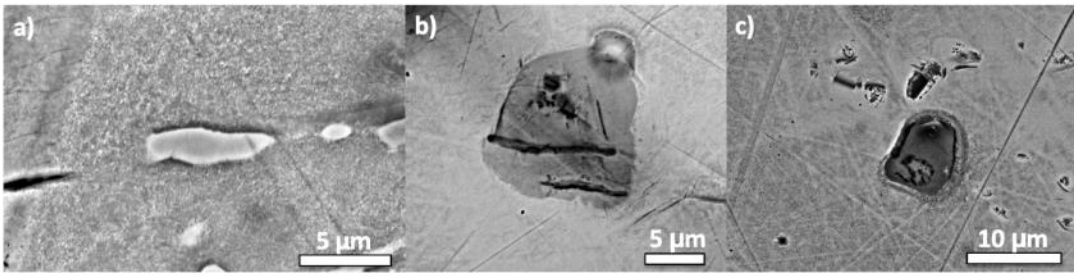

Figure 1. a) traditional Pu_6Fe inclusions and b/c) the other Fe-rich inclusions.

All images in Figure 1 were taken in backscattered electron (BSE) imaging mode at similar contrast/brightness settings. There are clear differences of the uncharacterized inclusions when compared to traditional Pu_6Fe, namely they are 1) larger, 2) darker, 3) angular or globular instead of

elongated, and 4) intragranular instead of distributed along grain boundaries. They were also much more dilute.

In an effort to gain as much information on these inclusions as possible, we focused on capturing samples of the δPu-inclusion interface for both inclusion types. Sample geometries for both TEM and APT were initially APT specimens: needle-shaped samples on the order of 0.1 picograms of material. However, TEM is not always ideal on this geometry, so eventually traditional TEM lamella were fabricated across the interface. Both sample types were made using focused ion beam (FIB)/SEM, Figure 2. Samples were transferred quickly in air to each instrument, and only slight oxidation occurred.

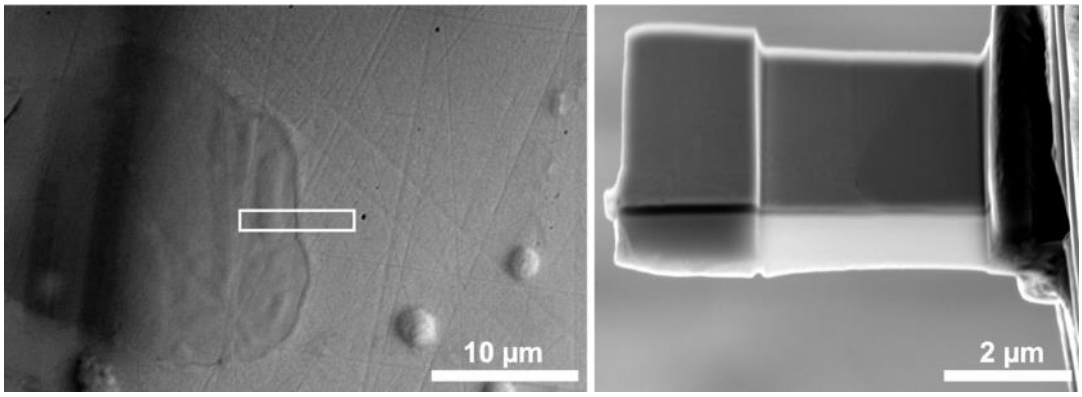

Figure 2. Location and sample of FIB/SEM-produced lamella across the interface of the Fe-Pu inclusion and metal matrix.

This study revealed the structure and chemical composition of both inclusions including information related to the interfacial chemistry. Ultimately, this study confirmed that the unknown inclusion type is also Pu_6Fe via APT and TEM atomic resolution imaging. Our Presentation will focus on the finer details of this study and the reason(s) why these particular inclusions appear to be dramatically different than traditional Pu_6Fe.

1. ASM Handbook, Volume 3: Allohy Phase Diagrams, ed. H.S. Okamoto, M.E. Mueller, E.M. Vol. 3. 2016.
2. Mitchell, J.N.S., D.S., Thermophysical Properties of Plutonium Alloys. 2013, LANL: Los Alamosm, NM.
3. Moore, E., et al., Development of a CALPHAD Thermodynamic Database for Pu-U-Fe-Ga Alloys. Applied Sciences, 2019. **9**: p. 5040.
4. Moore, K., M. Wall, and A. Schwartz, Experimental verification of the existence and structure of ζ Pu 6Fe in a Pu–Ga alloy. Journal of Nuclear Materials - J NUCL MATER, 2002. **306**: p. 213-217.
5. Nakamura, K., et al., Reactions of Uranium-Plutonium Alloys with Iron. Journal of Nuclear Science and Technology, 2001. **38**(2): p. 112-119.
6. Schwartz, D., P. Tobash, and S. Richmond, Thermal Analysis of Pu6Fe Synthesized from Hydride Precursor. MRS Proceedings, 2014. **1683**.
7. Milewski, J.O. and D.A. Javernick, The microstructural response of delta-stabilized plutonium to pulsed laser welding. Metallurgical and Materials Transactions A, 2004. **35**(8): p. 2445-2454.
8. Boehlert, C.J., et al., Initial electron backscattered diffraction observations of a plutonium alloy. Scripta Materialia, 2001. **45**(9): p. 1107-1115.

Systematics of the ambient melting points of stoichiometric mixed oxide (MOX) fuel

L. Burakovsky*, S.D. Ramsey, and R.S. Baty [1]

[1] P.O. Box 1663, Los Alamos National Laboratory, Los Alamos, NM 87545, USA

**burakov@lanl.gov*

Of all its alternatives, nuclear power seems to be one of the most reliable energy sources to achieve our goal of a world free of man-made CO_2 emissions. The choice between the two possible nuclear fuels, uranium and mixed oxide (MOX), has been under debate. MOX has the advantage of being less waste disposable as it produces less intermediate- and high-level waste. Also, MOX is planned to be the fuel for the new generation of fast breeder reactors such as ASTRID. Uranium-plutonium MOX is the system $U_{1-x}Pu_xO_{2-y}$, where x is the plutonium fraction; y=0 and y>0 correspond to stoichiometric and sub-stoichiometric MOX, respectively. With low plutonium content (x<0.1) it is used as nuclear fuel in several thermal neutron reactors around the world. MOX with higher plutonium content is expected to be a favorable fuel for fast neutron reactors (FNRs).

Of all the physical properties of a material, melting behavior is a fundamental property closely related to its structure and thermodynamic stability, and therefore has always been a crucial research subject. The ambient (zero pressure) melting point (T_m) is also an important engineering parameter, as it defines the operational limits of a material in its application environment. It becomes critical in nuclear engineering where the thermo-mechanical stability of a nuclear fuel element is a key factor determining fuel performance and safety. Also, PuO_2 and UO_2 are two endpoints of the phase diagram of MOX, therefore their ambient T_ms are fundamental reference points.

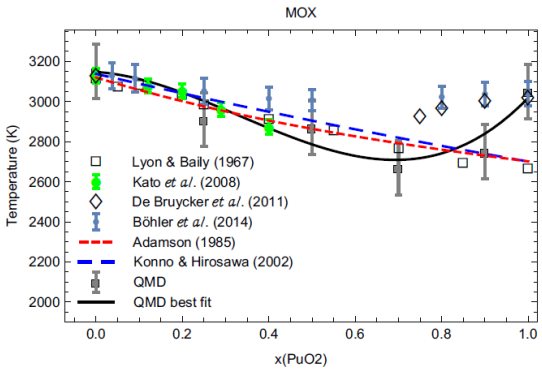

Figure 1: Ab initio melting points of stoichiometric MOX.

In our study we calculated the ambient melting points of MOX at several values of x, 0<x<1, including the two end points (x=0, x=1), using the *ab initio* Z method based on quantum molecular dynamics (QMD) simulations implemented with VASP (Vienna Ab initio Simulation Package). The details of the QMD simulations and the LDA+U methodology used in our study will be given during the talk. Our results shown in Figure 1 will be compared with experimental and theoretical results available in the literature. Our study suggests a potential ambient density-melting point systematics of MOX which will be also discussed; it may be useful in subsequent research on MOX such as its thermoelasticity modeling.

Study of carbochlorination of Plutonium oxide and electrochemistry of Pu in molten salt for Molten Salt Reactor (MSR) applications

P. Chevreux [1], J. Serp [1]

[1] CEA, DES, ISEC, DMRC, Univ Montpellier, Marcoule, France - CEA Marcoule BP 17 171, 30 207 Bagnols sur Cèze CEDEX

pierrick.chevreux@cea.fr

Among many innovative designs for Generation-IV reactors, Molten Salt Reactors (MSR) have a strong renewed interest in the nuclear energy worldwide community (China, USA, Russia, Canada). MSR operating with a liquid fuel and a fast neutron spectrum might be used as burner/converter or breeder reactors. While fluoride salts were often considered based on the Molten Salt Reactor Experiment (MSRE) operated in the 60's at Oak Ridge National Laboratory, chloride salts are investigated nowadays by several start-ups (Terrapower, Moltex). Whatever the salt composition is, liquid MSR fuels will require actinide bearing salts synthesis, purification and processing techniques. This paper deals with the synthesis of plutonium trichloride ($PuCl_3$) and its electrochemical properties in the NaCl-$CaCl_2$ eutectic.

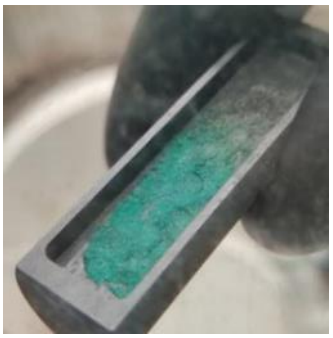

Plutonium trichloride synthesized by carbochloration at 700 °C

The development of synthetic routes for pure $PuCl_3$ used as fuel for chlorides fast molten salt reactor is necessary to properly prepare the salt composition. Carbochlorination, a well-known solid-gas reaction in the field of metallurgical industry, is the studied way for synthetizing $PuCl_3$ from Plutonium oxide (PuO_2). Chlorination experiments were carried out in a static bed reactor with chlorine as a chlorinating agent and reaction conditions were optimized to enhance the conversion of PuO2 to PuCl3. The influence of temperature, amount of chlorine and carbon were investigated. Reaction products were characterized by chemical analysis after leaching and X-ray diffraction measurements. Conversion efficiency of PuO_2 to $PuCl_3$ is evaluated as the function of the synthesis parameters.

Measurements of Pu electrochemistry in the molten NaCl-$CaCl_2$ were also performed in the range of temperature of 550-650 °C. Fundamental thermodynamics properties such as the apparent standard potential, and diffusion coefficient of Pu^{3+} are determined.

Isothermal Dilatometry of δ-239Pu: Evidence of Contraction at Early Ages

A. Marchi [1], A. Migliori [1], G. Goff [1], B. Scott [1]

[1] Materials Physics and Applications Division, Los Alamos National Laboratory, PO Box 1663, Bikini Atoll Road, SM-30, Los Alamos, NM 87545, United States

alexm@lanl.gov

The radioactive decay of plutonium metal self-induces an accumulation of damage that is not fully understood. Through the decay of 239Pu into uranium and an alpha particle, a large amount of energy is produced and deposited in the surrounding material, which leads to defects or imperfections in the metal. This study, combined with complimentary measurements, aims to address questions regarding where damage accumulates, at what rates, and how the damage affects mechanical properties long-term. To monitor bulk density changes with time, we performed high-precision length measurements of δ-239Pu samples at constant temperature using a capacitance-based dilatometry cell.[1] The samples were observed to contract at a high rate initially, with the contraction rate slowing over time (see Figure 1). The measured contraction of these samples is contrary to previous immersion density and dilatometry studies.[2-4] However, this work complements more recent reports showing density increases with time of delta-Pu samples, which have been naturally aged.[5] Additionally, resonant ultrasound spectroscopy has shown stiffening moduli with time, which may correlate to an increase in density. This talk will present results from our first measurements using a previously published dilatometer cell design. I will also discuss potential mechanisms for this contraction and density increase. In parallel with this effort, we designed a unique dilatometer cell that should provide greater precision to the measurement. Preliminary results from these upgraded cells will also be presented.

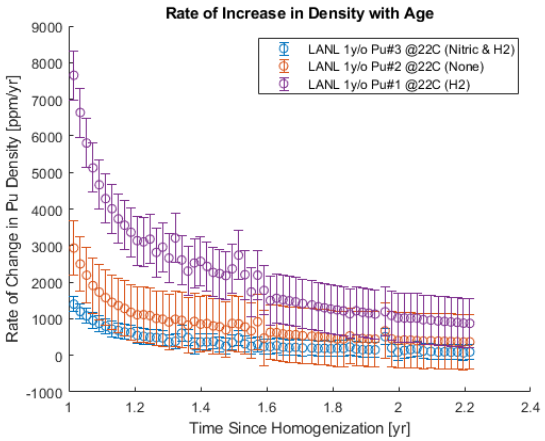

Figure 1: Three delta-Pu samples, cast and homogenized one year prior to measurements, show an initially large contraction rate that slows with time towards an asymptotic rate of contraction. Fluctuations in rate are because of poor temperature control over those measurement timelines. A new cell and environmental chamber design will bring more precision to future measurements.

[1] Schmiedeshoff, G. M. et al. Versatile and compact capacitive dilatometer. *Rev. Sci. Instrum*. **77**, (2006).
[2] Mulford, R. N. Radiation damage in plutonium alloys determined from bulk density. *Los Alamos National Laboratory Internal Report*, LA-UR-02-1045 (2002).
[3] Freibert, F. J., Dooley, D. E. & Miller, D. A. Immersion Density Measurements of Self-heating Samples. *Los Alamos National Laboratory Internal Report*, LA-UR-05-9007 (2005).
[4] Chung, B. W., Thompson, S. R., Lema, K. E., Hiromoto, D. S. & Ebbinghaus, B. B. Evolving density and static mechanical properties in plutonium from self-irradiation. *J. Nucl. Mater.* **385**, 91–94 (2009).
[5] McCall, S. K., Lema, K., Mirkarmi, P., Ruddle, B., Chung, W. Nanodilatometry to measure length changes due to radiation damage in naturally agerd Pu specimens. *Lawrence Livermore National Laboratory Internal Report,* LLNL-TR-739179 (2017).

Environmental Behavior and Chemistry

	Conference room #2: CHAMBRE DU TRÉSORIER
INVITED TALK 10:00 – 10:30	**Nicolas DACHEUX (Univ Montpellier)** *"Formation of $PuSiO_4$: lessons coming from chemical analogues"*
INVITED TALK 11:00 – 11:30	**Xavier GAONA (KIT)** *"Aquatic chemistry and thermodynamics of plutonium: applications to repository science and environmental studies"*
11:30 – 11:50	**Aurélie DIACRE (CEA)** *"Characterization of the Pu and Cs tempOral talk: evolution in sediment transiting the Ukedo and Takase Rivers, Japan"*
11:50 – 12:10	**Donald REED (LANL)** *"The Role of Pu (III) in Groundwater Contaminant and Repository Assessments"*
12:10 – 12:30	**Jean AUPIAIS (CEA)** *"Transferrin and Fetuin: potential vectors for Pu accumulation in liver and skeleton"*
PLENARY TALK 14:00 – 14:50	*Conference room #1: CELLIER BENOIT XII* **Kristina KVASHNINA (HZDR)** *"Plutonium Chemistry by Innovative Synchrotron Methods"*
	Conference room #2: CHAMBRE DU TRÉSORIER
INVITED TALK 15:00 – 15:30	**Enrica BALBONI (LLNL)** *"Plutonium fate and transport in the environment: from the desert to salt marshes"*
15:30 – 15:50	**Marcus ALTMAIER (KIT)** *"Complexation speciation and thermodynamics of tri- and tetravalent plutonium with EDTA and citrate in high ionic strength systems"*
INVITED TALK 16:20 – 16:50	**Christophe DEN AUWER (Université Côte d'Azur)** *"Actinide speciation in marine radioecology"*
16:50 – 17:10	**Francesca QUINTO (KIT)** *"Retention and Near-Field Release of ^{99}Tc, ^{233}U, ^{237}Np, ^{242}Pu and ^{241}Am from the Long-Term In-Situ Test at the Grimsel Test Site"*
17:10 – 17:30	**Manon COT-AURIOL (CEA)** *"Isotopic effect on the formation kinetics of Pu (IV) intrinsic colloids"*
17:30 – 17:50	**Jeremiah BEAM (LANL)** *"Plutonium Oxidation State Distribution in High Ionic Strength Environments"*

Chair persons:

David L. CLARK & Mavrik ZAVARIN

Formation of $PuSiO_4$: lessons coming from chemical analogues

N. Dacheux [1], P. Estevenon [1;2], E. Welcomme [2], S. Szenknect [1], A. Mesbah [1], P. Moisy [2], C. Poinssot [2]

[1] ICSM, Univ Montpellier, CEA, CNRS, ENSCM, Site de Marcoule, Bagnols-sur-Cèze, France.
[2] CEA, DEN, DMRC, Univ Montpellier, Marcoule, France.

nicolas.dacheux@umontpellier.fr

Actinides, including plutonium, are the main contributors to the long-term radiotoxicity of spent nuclear fuels. In geological conditions, the interactions between these radioelements and silicate species could influence their mobility in environmental conditions and could affect the safety of the storage facilities. Especially, the formation of actinide silicate, $AnSiO_4$, has to be considered carefully, since thorium and uranium silicates are rather abundant in environmental silicate rich media and under reductive conditions [1]. Moreover, the natural formation mechanism of coffinite $USiO_4$, which involves the alteration of UO_2 in reductive and silica rich media, rose important questions about the radionuclides' behavior under geological repository conditions [2]. Additionally, the formation of actinide oxy-hydroxy-silicate colloids has been observed for thorium, uranium and neptunium in weakly basic carbonate media at room temperature [3]. Due to their low isoelectric point compared to the respective oxides ($pH_{PIE} \approx 4$ against $pH_{PIE} \approx 8$), these colloids are suspected to play a huge role on the actinide mobility in environmental conditions. Therefore, the synthesis and the determination of the thermodynamic properties of $PuSiO_4$ could be a crucial issue to study the behavior of plutonium in the environment.

However, even if $PuSiO_4$ has been hydrothermally synthesized once in 1963 [4] and if the formation of silicate based compounds has been suspected for Pu-containing precipitates, the conditions associated to the formation of this phase remain largely unknown. In order to provide more information on the plutonium-silicate system and to determine suitable conditions of synthesis, we investigated the conditions of synthesis of $PuSiO_4$ first considering the three usual surrogates: thorium, uranium and cerium. Those surrogates allow to represent Pu(IV) aqueous chemistry and to form zircon type silicates, $ThSiO_4$, $USiO_4$ and $CeSiO_4$, which crystallize with the same zircon type-structure as $PuSiO_4$ (space group $I4_1/amd$) [4,5].

For each surrogate element, optimized conditions of synthesis of the silicate-based samples were determined by varying several experimental parameters: pH of the starting mixture, ligand concentrations (including carbonate ions), reactant concentrations, temperature and duration of the heating/hydrothermal treatment, redox conditions…), so that they could be transposed to the plutonium system.

- For thorium, two different optimized sets of conditions, which allow the formation of $ThSiO_4$, have been determined: the first one in acidic media without any complexing agent [6] and the second one in weakly basic media in the presence of large quantities of carbonate ions [7];

- For uranium, the optimized conditions of formation of $USiO_4$ were more specific than for $ThSiO_4$. Indeed, only weakly basic carbonate media allowed the formation of coffinite [1];
- For cerium, the conditions of formation of $CeSiO_4$ were significantly different as the synthesis starting from Ce(IV) reactants did not succeed due to the rapid and efficient hydrolysis of Ce(IV). On the contrary, the use of Ce(III) reactants led to the formation of $CeSiO_4$ in very specific conditions in terms of pH, concentrations and temperature [8;9]. Using Ce(III) reactants, and especially solid Ce(III) silicate precursors, promoted the formation of cerium silicate complexes, which counterbalanced the hydrolysis of Ce(IV) and allowed the formation of pure $CeSiO_4$.

The transposition of the four optimized protocols to the plutonium system was conducted in the hot-laboratories of the ATALANTE facility. While it failed when applying the protocols developed for $ThSiO_4$ and $USiO_4$, it succeeded starting from solid Pu(III) silicate precursors, as observed for cerium counterpart. Thus, the study provided key information on the formation of silicate based phases and enabled to identify differences in terms of reactivity between plutonium and the considered surrogate elements. Since the conditions of synthesis allowing the formation of $PuSiO_4$ were very close to those obtained for $CeSiO_4$ (Figure 1), it may be inferred that cerium constitutes the best surrogate of plutonium in silicate ions rich environment. Moreover, experiments performed in alkaline conditions have proved that Pu-silicate based colloids can be formed and exhibit the same structure as their thorium, uranium and neptunium counterparts.

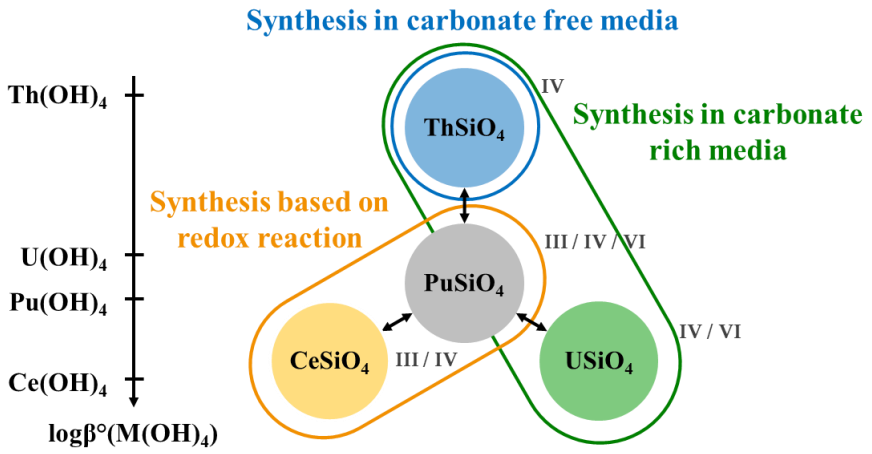

Figure 1: Summary of the conditions of synthesis of $MSiO_4$ for plutonium and its surrogate elements (Ce, U, Th).

[1] A. Mesbah et al., Inorganic Chemistry, 2015, 54, 6687–6696
[2] J. Janeczek, R. Ewing, MRS Symposium Proceedings, 1992, 257, 497–504
[3] H. Zänker et al., Chemistry Open Reviews, 2016, 5, 174–182
[4] C. Keller, Nukleonik, 1963, 5, 41–48
[5] J. Skakle et al., Powder Diffraction, 2000, 15, 234–238
[6] P. Estevenon et al., Inorganic Chemistry 2018, 57, 9393–9402
[7] P. Estevenon et al., Inorganic Chemistry 2018, 57, 12398–12408
[8] P. Estevenon et al., Dalton Transactions, 2019, 48, 7551–7559
[9] P. Estevenon et al., Dalton Transactions, 2019, 48, 10455–10463

Aquatic chemistry and thermodynamics of plutonium: applications to repository science and environmental studies

X. Gaona, A. Tasi, N. A. DiBlasi, R. Guidone, I. Androniuk, D. Fellhauer, M. Altmaier, H. Geckeis

Karlsruhe Institute of Technology - Institute for Nuclear Waste Disposal (INE), Germany

xavier.gaona@kit.edu

Comprehensive reviews dedicated to the aquatic chemistry and thermodynamics of plutonium were recently published in the context of the OECD NEA-TDB project [1] and the Plutonium Handbook of the American Nuclear Society [2]. These reference volumes summarize the very significant progress achieved in this field within the last decades, whilst highlighting data gaps and most relevant limitations in the existing thermodynamic models.

Due to its electronic configuration, several oxidation states of plutonium (+III to +VII) can exist in aqueous solution, which results in unique chemical behaviour as a function of the redox boundary conditions. This contribution targets the redox chemistry, solubility and sorption phenomena of plutonium in alkaline, anoxic to very reducing conditions relevant in underground repositories for nuclear waste disposal as well as in given environmental systems. Under these conditions, thermodynamic calculations predict the formation of both Pu(IV) and Pu(III), with (pe + pH) being the main parameters controlling the redox distribution of plutonium. Additionally, the presence of inorganic or organic ligands as well as mineral surfaces can significantly affect the redox boundary between both oxidation states, thus requiring a thorough understanding of the solution chemistry as well as the molecular level processes occurring at the interface.

The stability of the $Pu(OH)_3(s)$ solid phase in alkaline reducing systems has been controversially discussed in the literature [3-8]. The current thermodynamic selection in the NEA-TDB Update volume supports the stability of this Pu(III) solid phase above the border of water reduction [1], although the co-existence of $PuO_2(s)$ and $Pu(OH)_3(s)$, or alternatively the formation of a mixed valence $PuO_{2-x}(s)$ phase, have been proposed at (pe + pH) ≈ 2 based on advanced spectroscopic methods [7]. This contribution will elaborate on the interplay between $PuO_2(s)$ and $Pu(OH)_3(s)$, and further on the coupling with Fe(0) chemistry and corresponding corrosion products under conditions potentially relevant for nuclear waste disposal.

The complexation with organic ligands can importantly affect the redox border between Pu(IV) and Pu(III). Pu(IV) is characterized by a much stronger hydrolysis than Pu(III). This may suggest a net stabilization of the Pu(III) redox state by complexation with organic ligands in near-neutral pH conditions where Pu(IV) is already fully hydrolysed while Pu(III) is not. However, recent comprehensive solubility experiments conducted at KIT-INE confirm the systematic formation of ternary complexes Pu(IV)-OH-L (with L = ISA, GLU, EDTA), which allow these organic ligands to overcome the strong competition with hydrolysis even in hyperalkaline conditions [9-12]. This emphasizes the need for complete chemical and thermodynamic models to precisely evaluate the retention / mobilization properties of plutonium. This contribution will also elaborate on the role of environmentally relevant

major cations, *e.g.* Ca, Mg or Fe, which can act as competitors but may also contribute to the further stabilization of negatively charged Pu(III/IV)-OH-L complexes.

Sorption is a key process that contributes to the retention of plutonium in nuclear waste repositories and environmental systems, and thus extensive research at KIT-INE and elsewhere focusses on numerous sub-systems and relevant mineral phases. Dedicated experimental efforts are on-going at KIT-INE to quantitatively assess the uptake of plutonium in cementitious systems relevant in the context of low and intermediate level wastes (L/ILW) [12-14]. Sorption is significantly decreased in the presence of polyhydroxocarboxylic acids such as ISA or GLU, in line with the formation of the aforementioned stable ternary or quaternary complexes (Ca-)Pu-OH-ISA/GLU in the aqueous phase. Differences observed for the uptake in systems containing hydroquinone (with pe + pH ≈ 9) or Sn(II) (with pe + pH ≈ 2) as redox-buffers underpin that the reduction of Pu(IV) to Pu(III) is also feasible in hyperalkaline systems, and highlight the need for conducting experiments with plutonium instead of using redox-stable analogues such as Th(IV) or Eu(III). Molecular dynamics (MD) calculations arise as a suitable tool to gain insight on the mechanisms driving the uptake of plutonium by different surfaces. On-going MD studies and future activities at KIT-INE targeting C-S-H phases (as main component of cement) and clay minerals will be also presented.

Acknowledgements: Some of the studies in this contribution were partly funded by SKB (Sweden). The project (EURAD-CORI) leading to some of the examples has received funding from the European Union's Horizon 2020 research and innovation programme under grant agreement No 847593.

[1] Grenthe, I., Gaona, X., Plyasunov, A.V., Rao, L., Runde, W.H., Grambow, B., Konings, R. J. M., Smith, A.L., Moore, E.E. (2020). Second Update on the Chemical Thermodynamics of Uranium, Neptunium, Plutonium, Americium and Technetium, Chemical Thermodynamics. OECD Nuclear Energy Agency, Boulogne-Billancourt, France.
[2] Altmaier, M., Gaona, X., Fellhauer, D., Clark, D.L., Runde, W.H., Hobart, D.E. (2019). Chapter 22. Aqueous solution and coordination chemistry of plutonium. In: Clark, D.L., Geeson, D.A., Hanrahan Jr., R.J. (Eds.), Plutonium Handbook. American Nuclear Society, La Grange Park, IL, USA.
[3] Felmy, A. R., Rai, D., Schramke, J. A., Ryan, J. L. (1989). Radiochim. Acta, 48, 29.
[4] Neck, V., Altmaier, M., Fanghänel, T. (2007). C. R. Chim., 10, 959.
[5] Fellhauer, D. (2013). PhD Thesis University of Heidelberg, Heidelberg (Germany).
[6] Cho, H. R., Young, Y. S., Jung, E. C., Cha, W. (2016). Dalton Trans., 45, 19449.
[7] Tasi, A., Gaona, X., Fellhauer, D., Böttle, M., Rothe, J., Dardenne, K., Schild, D., Grivé, M., Colàs, E., Bruno, J., Källström, K., Altmaier, M., Geckeis, H. (2018). Radiochim. Acta, 106, 259–279.
[8] Schramke, J. A., Santillan, E. F. U., Peake, R. T. (2020). Applied Geochemistry, 116, 104561.
[9] Tasi, A., Gaona, X., Fellhauer, D., Böttle, M., Rothe, J., Dardenne, K., Polly, R., Grivé, M., Colàs, E., Bruno, J., Källström, K., Altmaier, M., Geckeis, H. (2018). Applied Geochemistry, 98, 247–264.
[10] Tasi, A., Gaona, X., Fellhauer, D., Böttle, M., Rothe, J., Dardenne, K., Polly, R., Grivé, M., Colàs, E., Bruno, J., Källstrom, K., Altmaier, M., Geckeis, H. (2018). Applied Geochemistry, 98, 351–366.
[11] DiBlasi, N. A., Tasi, A. G., Gaona, X., Fellhauer, D., Dardenne, K., Rothe, J., Reed, D. T., Hixon, A. E., Altmaier, M. (2021). Science of the Total Environment, 783, 146993.
[12] Guidone, R. E., Tasi, A., Gaona, X., Lothenbach, B., Altmaier, M., Geckeis, H. (2022). Book of Abstracts NUWCEM Conference, Avignon, May 2022.
[13] Tasi, A., Gaona, X., Fellhauer, D., Böttle, M., Rothe, J., Dardenne, K., Polly, R., Grivé, M., Colàs, E., Bruno, J., Källstrom, K., Altmaier, M., Geckeis, H. (2021). Applied Geochemistry, 126, 104862.
[14] Tasi, A., Szabo, P., Gaona, X., Altmaier, M., Geckeis, H. (2022). Book of Abstracts NUWCEM Conference, Avignon, May 2022.

Characterization of the Pu and Cs temporal evolution in sediment transiting the Ukedo and Takase Rivers, Japan

Aurélie Diacre [1,2], Soazig Burban [1], Anne-Claire Humbert [1], Amélie Hubert [1], Irène Lefevre [2], Anne-Laure Faure [1], Fabien Pointurier [1], Olivier Evrard [2]

[1] Commissariat à l'Energie Atomique et aux énergies alternatives (CEA, DAM, DIF), F-91297 Arpajon, France.
[2] Laboratoire des Sciences du Climat et de l'Environnement (LSCE/IPSL), Unité Mixte de Recherche 8212 (CEA/ CNRS/UVSQ), Université Paris-Saclay, Gif-sur-Yvette, France.

aurelie.diacre@lsce.ipsl.fr

Eleven years ago, the Fukushima Dai-Ichi Nuclear Power Plant (FDNPP) accident released significant quantities of radionuclides into the environment[1]. Japanese authorities decided to progressively reopen the difficult-to-return zone without obligatory decontamination. This zone includes the initially highly contaminated municipalities to the north of the FDNPP, including Namie Town, an area mainly drained by Ukedo and Takase Rivers. Several research questions emerged regarding (1) the contribution of the sediment transiting this river to the radionuclide supply to the Pacific Ocean, and (2) the temporal evolution of contamination levels in a fully abandoned zone since the accident. So far, studies focused on the spatial distribution of Pu and Cs at both the *bulk* [2–4] and particle scales[5,6] at individual locations. The objectives of the current research are to (1) highlight the temporal variation of inorganic markers (Pu and Cs) in sediment transiting the Ukedo and Takase River outlets between 2013 and 2020, and to (2) investigate the relationship between the Pu concentration, the $^{240}Pu/^{239}Pu$ isotopic ratios, the ^{137}Cs weight activity, the particle size, carbon content properties of sediment and rainfall occurring in the zone.

In this study, 22 sediment samples were analyzed at the *bulk* scale by gamma spectrometry and Multi-Collection Inductively Coupled Plasma Mass Spectrometry (MC-ICP-MS) to respectively determine the ^{137}Cs weight activity and the $^{240}Pu/^{239}Pu$ isotopic ratios and Pu contents. These results obtained are combined with other parameters like granulometry, carbon contents of sediment and rainfall conditions in order to identify potential factors controlling the variations of cesium and plutonium signature found in sediments.

The first results highlighted a global decrease of the Pu content and ^{137}Cs weight activity in sediment with years. In Takase River, the results showed (1) lower ^{137}Cs weight activities and Pu concentrations in sediment than in the nearby Ukedo River, and (2) a correlation between ^{137}Cs weight activity and the median particle size.

[1] M. Yamamoto, Overview of the Fukushima Dai-ichi Nuclear Power Plant (FDNPP) accident, with amounts and isotopic compositions of the released radionuclides, J Radioanal Nucl Chem. 303 (2015) 1227–1231. https://doi.org/10.1007/s10967-014-3639-3.
[2] S. Schneider, C. Walther, S. Bister, V. Schauer, M. Christl, H.-A. Synal, K. Shozugawa, G. Steinhauser, Plutonium release from Fukushima Daiichi fosters the need for more detailed investigations, Sci Rep. 3 (2013) 2988. https://doi.org/10.1038/srep02988.
[3] G. Yang, H. Tazoe, K. Hayano, K. Okayama, M. Yamada, Isotopic compositions of 236U, 239Pu, and 240Pu in soil contaminated by the Fukushima Daiichi Nuclear Power Plant accident, Sci Rep. 7 (2017) 13619. https://doi.org/10.1038/s41598-017-13998-6.
[4] J. Zheng, K. Tagami, Y. Watanabe, S. Uchida, T. Aono, N. Ishii, S. Yoshida, Y. Kubota, S. Fuma, S. Ihara, Isotopic evidence of plutonium release into the environment from the Fukushima DNPP accident, Sci Rep. 2 (2012) 304. https://doi.org/10.1038/srep00304.

[5] Y. Kurihara, N. Takahata, T.D. Yokoyama, H. Miura, Y. Kon, T. Takagi, S. Higaki, N. Yamaguchi, Y. Sano, Y. Takahashi, Isotopic ratios of uranium and caesium in spherical radioactive caesium-bearing microparticles derived from the Fukushima Dai-ichi Nuclear Power Plant, Scientific Reports. 10 (2020) 1–10. https://doi.org/10.1038/s41598-020-59933-0.
[6] E. Kurihara, M. Takehara, M. Suetake, R. Ikehara, T. Komiya, K. Morooka, R. Takami, S. Yamasaki, T. Ohnuki, K. Horie, M. Takehara, G.T.W. Law, W. Bower, J.F. W. Mosselmans, P. Warnicke, B. Grambow, R.C. Ewing, S. Utsunomiya, Particulate plutonium released from the Fukushima Daiichi meltdowns, Science of The Total Environment. 743 (2020) 140539. https://doi.org/10.1016/j.scitotenv.2020.140539.

The Role of Pu(III) in Groundwater Contaminant and Repository Assessments

D. T. Reed and J. Beam

Actinide Chemistry and Repository Science Project team

Los Alamos National Laboratory, 1400 University Drive, Carlsbad NM, 88220 USA

dreed@lanl.gov

The data that support or contradict a critical role for Pu(III) in the fate and migration of plutonium in groundwater contaminant and repository assessment scenarios is presented and assessed. For many years it has been understood that the dominant form of plutonium in the subsurface is Pu(IV) mostly in the oxide form. This explains its apparent biogeochemical stability and high immobility under many near-surface groundwater conditions. Recent reviews of the environmental chemistry of plutonium [1, 2] largely ignore a possible role for Pu(III) under environmentally-relevant conditions. There, however, is growing evidence [3-8] that appear challenge this understanding. For this reason, a discussion is needed within the field of actinide environmental chemistry to account for and explain these data in the context of current environmental assessments and repository evaluations. This will help ensure that a proper weighting of the potential impacts of Pu(III) speciation on plutonium mobility are included in overall environmental assessments.

There are many key and critical data that support the long-held belief and understanding that the environmental chemistry should be dominated by the Pu(IV) oxidation state. Plutonium oxide is a highly insoluble and stable form of plutonium that is readily formed under most environmental conditions and is often the form of plutonium that will be disposed in a permanent geologic repository. Although some evidence of plutonium mobility exists, it is often linked to physical process rather than solubility and groundwater mobility. The most important evidence of its predominance in many near-surface contaminant sites is its relatively low mobility (in many cases its immobility) when compared with other actinides that are present as co-contaminants. There are many site-specific data, particularly in the US, where this has been observed.

The data for the possible importance of Pu(III) that at least point to its further consideration in long-term performance assessments comes from two general areas of research. The first is from microbial studies of metal-reducing and sulfate reducing bacteria where the bioreduction of PuO_2 has been shown to be possible under anaerobic conditions. These results, for plutonium, were most recently summarized [9]. There are however still questions about the exact mechanism of this process and it is not clear that the reduction of Pu(IV) to Pu(III) under these circumstances lead to a long-term and enduring effect that results in enhanced mobility.

The second source of data that raise questions about the possible role for Pu(III) in the environmental fate and transport of plutonium is from the long-term Fe (0, II) dominated repository studies that show a sustainable presence of Pu(III) species [3-8]. Pu(III) hydroxide, as an amorphous phase, can be readily precipitated in pH > 8 systems. A crystalline phase has however not been identified at high pH and the stability field of stability for Pu(III) phases appears to be quite small and at/near the water line (See Fig. 1) which is difficult to envision as a sustainable E_h in most environments. Additionally the measured solubilities under these conditions is often more consistent with a Pu(IV) phase even when

the solid phase if predominantly Pu(III). This chemistry is not yet fully understood and continues to be the focus of ongoing studies.

The iron dominated system and anaerobic microbial data both show that Pu(III) can be produced under the broad range of environmentally relevant conditions. The question however, for site-specific assessments is not only can they be formed but are they also important contributors to potential repository release or subsurface migration. This is a much more difficult question that probably cannot be answered at this point in time and is perhaps a very site-specific or scenario-specific question and issue.

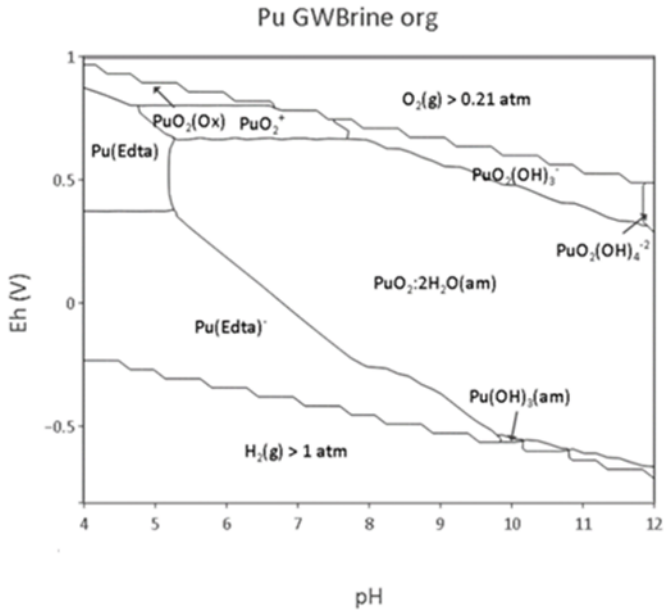

Figure 1. Pourbaix diagram for plutonium solids in simulated GWB high ionic strength brine in the presence of EDTA. This shows a very large stability field for Pu(IV) solids with a small area of stability for Pu(III) at the lower (most reducing) boundary [7].

References:

[1] Runde, W.; Neu, M. P. Actinides in the Geosphere. In *The Chemistry of the Actinide and Transactinide Elements*, 4th ed.; Morss, L. R., Edelstein, N. M., Fuger, J. Katz, J. J., Eds.; Springer: Netherlands, 2011; Vol. 1–6, pp 3475–3593.

[2] Geckeis, H., M. Zavarin, B. Salbu, O. Lind, and L. Skipperud. "Environmental Chemistry of Plutonium." Chapter 25 in Plutonium Handbook, D. Clark, D. Geeson and R. Hanranhan, eds., American Nuclear Society, pp. 1979, 2019.

[3] Reed, D.T., M. Borkowski, J. Swanson, M. Richmann, H. Khaing, J.f. Lucchini and D. Ams. 2011. Redox-controlling processes for multivalent metals and actinides in the WIPP. 3rd Annual Workshop Proceedings, 7th EC FP - ReCosy CP, pp. 1-12.

[4] D.T. Reed. 2018. *Plutonium Oxidation State Distribution in the WIPP: Conceptual Model, Project-Specific Data, and Current/Ongoing Issues*. LA-UR-18-25748. Los Alamos National Laboratory; Carlsbad, NM.

[5] Cho, H.-R., Youn, Y.-S., Chang Jung, E., Cha, W., 2016. Hydrolysis of trivalent plutonium and solubility of Pu(OH) 3 (am) under electrolytic reducing conditions. Dalton Transactions 45, 19449–19457. https://doi.org/10.1039/C6DT03992H

[6] Tasi, A., Gaona, X., Fellhauer, D., Böttle, M., Rothe, J., Dardenne, K., Schild, D., Grivé, M., Colàs, E., Bruno, J., Källström, K., Altmaier, M., Geckeis, H. 2018. "Redox Behavior and Solubility of Plutonium under Alkaline, Reducing Conditions". *Radiochimica Acta* 106: 259-279.

[7] Colas, E., D. Garcia and L. Duro. 2020. "Systematic Calculation of Pu Pourbaix Diagrams: Modelling Support for the LANL ACRSP Team." Los Alamos report LA-UR-20-26859.

[8] J.A. Schramke, E.F.U. Santillan, R.T. Peake. "Plutonium oxidation states in the Waste Isolation Pilot Plant repository." Applied Geochem, (116) 104561.

[9] Reed, D.T., R. Kinder, J. Lloyd, and J.S. Swanson, "Plutonium Microbial Interactions in the Environment", Chapter 26 in Plutonium Handbook, D. Clark, D. Geeson and R. Hanranhan, eds., American Nuclear Society, pp. 2119, 2019.

Transferrin and Fetuin: potential vectors for Pu accumulation in liver and skeleton

Jean Aupiais [1], Claude Vidaud [2], Laurent Miccoli [3], Florian Brulfert [1]

[1] CEA, DAM, DIF, F-91297 Arpajon, France [2] CEA, DRF, BIAM-Marcoule, F-30207 Bagnols sur Cèze, France, [3] Laboratoire de RadioToxicologie, CEA, Université de Paris-Saclay, F-91297 Arpajon, France

jean.aupiais@cea.fr

Plutonium, as a toxic radioactive metal, creates damages inside the human body. It is therefore important to understand why plutonium accumulates mainly in liver and bone. It is well known that a transferrin-mediated system is implicated in accumulation of plutonium in the liver but this is probably not true for bone. We show that fetuin (Fet) – a serum protein that participates in mineralization by conveying calcium to bone – competes with transferrin (Tf) for plutonium binding and could the protein responsible for bone Pu deposit.

By means of capillary electrophoresis coupled with an ICPMS, we have determined at pH 7.0 the binding constants between plutonium at the tetravalent state and transferrin and fetuin (see Table 1). Concerning the complexation of plutonium by transferrin we show that the experimental value is consistent with the trends observed for other metals (see Figure 1) for which the affinity of transferrin for metal cation depends on their first hydrolysis constants.

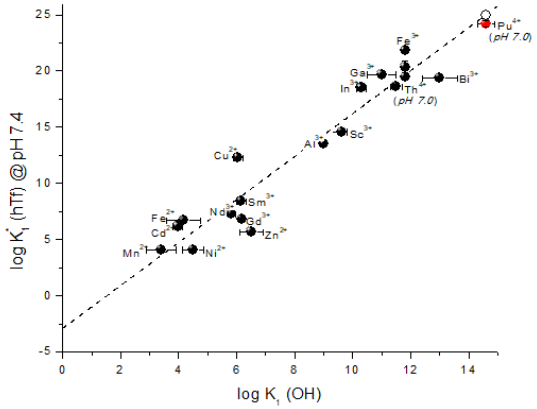

Figure 1: Variation of the conditional constant K_1 as a function of the first hydrolysis of metal. At pH 7.4 (○), the binding constant is expected to be $\log_{10} \boldsymbol{K_1^*} = 25.0$. At pH 7.0, the value 24.17 ± 0.30 was found (red point).*

According to Table 1, Fet and Tf present almost the same affinity for plutonium. We can hypothesise that these two proteins may be competing for Pu in serum. In order to confirm this hypothesis, competition reactions were carried out with various protein concentration ratios. We can assume that if thermodynamics drives the competition between these proteins, then the relative distribution of plutonium between them will obey the law of mass action according to the relation:

$$\frac{[PuTf]}{[PuFet]} = \frac{K^*_{PuTf}[Pu][Tf]}{K^*_{PuFet}[Pu][Fet]} = \frac{10^{26.44}}{10^{26.20}} \times \frac{[Tf]}{[Fet]} = 1.738 \times \frac{[Tf]}{[Fet]}$$

At equilibrium, the [PuTf]/[PuFet] ratio increases linearly with the [Tf]/[Fet] ratio by a constant factor of 1.738. The slope calculated from the data (1.81 ± 0.27) is in excellent agreement with the expected slope (see Figure 2). We can conclude that the chemical equilibria are attained and that the distribution of plutonium between these two proteins is driven only by the binding constants.

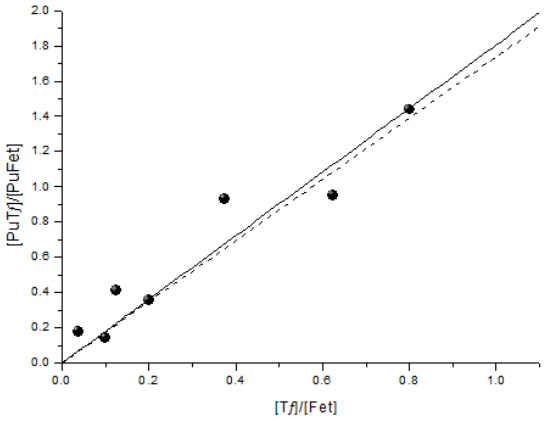

Figure 2: Variation of $\frac{[PuTf]}{[PuFet]}$ as function of $\frac{[Tf]}{[Fet]}$; dashed line corresponds to expected slope based on binding constants with log_{10} K_{PuTf} = 26.44 and log_{10} K_{PuFet} = 26.20 (slope = 1.738); straight line corresponds to linear regression based on data slope = 1.81 (●).

Table 1: Experimental conditional binding constants K at pH 7.0, I = 0.1 M, 25°C.[1]*

Equilibrium	log_{10} K*
$Pu + Fet \rightleftharpoons PuFet$	26.20 ± 0.24
$Pu + Tf \rightleftharpoons Pu_CTf$ $log_{10}K_1^* = log_{10}K_{PuTf}^* + log_{10}\alpha_c$ [#]	26.44 ± 0.28 $logK_1^* = 24.17 \pm 0.30$

[#] $\alpha_c = K_c \frac{[HCO_3^-]}{1+K_c[HCO_3^-]}$, with K_c the binding constant of bicarbonate with Tf.

These results provided fruitful information suggesting that the driving force between both proteins is only thermodynamic. This observation led us to postulate that the fate of Pu in a body depends mainly on the relative concentrations of these two proteins in the blood.

To conclude, even if the involvement of the Tf-mediated system cannot be totally excluded for bone cell functions, the accumulation of Pu in bone in such a proportion cannot be attributed to Tf alone. On the contrary, Fet is very highly concentrated in the bone matrix, and its high affinity for Pu could now convincingly explain Pu accumulation in the bones. We propose that Pu is conveyed to the bones not only through the citrate species present in serum, but through Fet as a protein carrier.

[1] Claude Vidaud, Laurent Miccoli, Florian Brulfert, Jean Aupiais, Sci. Rep. 9 (2019) 17584.

Plutonium Chemistry by Innovative Synchrotron Methods

K. O. Kvashnina [1,2]

[1] The Rossendorf Beamline at ESRF – The European Synchrotron, Grenoble, France
[2] Helmholtz Zentrum Dresden-Rossendorf (HZDR), Institute of Resource Ecology, Dresden, Germany

kristina.kvashnina@esrf.fr

Over the past several years, our understanding of plutonium chemistry at the atomic level was greatly improved. This is partly due to the expansion of advanced analytical techniques, developed at the large-scale synchrotron facilities, which recently become available for the investigation of radioactive materials. This contribution will give an overview of those experimental methods available at various synchrotrons and applicable to studying physico-chemical processes of radionuclides behaviour in the environment.

I will mainly focus on high energy resolution fluorescence detected (HERFD) X-ray absorption spectroscopy and Resonant Inelastic X-ray Scattering (RIXS) methods[1], which probe the local and electronic structure of actinide materials at the L_3 and M_4 actinide absorption edges. HERFD and RIXS techniques have high sensitivity towards oxidation state detection and can provide unprecedented information on the ground state configuration, electron-electron interactions, and hybridization between molecular orbitals. I will show the results of recently performed studies on plutonium oxide nanoparticles[2–5], which were achieved by the combination of HERFD, RIXS, EXAFS, XRD, HEXS (PDF) synchrotron methods together with results on thorium[6,7] and uranium[8] oxide nanoparticles. The experimental results were analyzed using electronic structure calculations [9,10]. It might be of interest for fundamental research in chemistry and physics of actinides as well as for applied science.

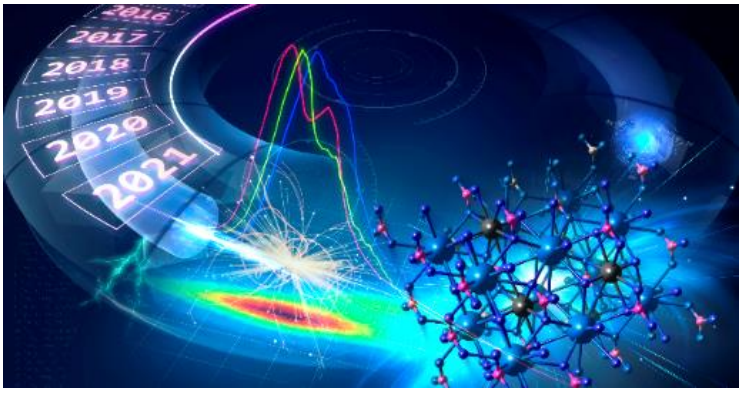

Cover Image of the recently published article [1]

References:

(1) Kvashnina, K. O.; Butorin, S. M. High-Energy Resolution X-Ray Spectroscopy at Actinide M 4,5 and Ligand K Edges: What We Know, What We Want to Know, and What We Can Know. *Chem. Commun.* **2022**, No. 58, 327–342. https://doi.org/10.1039/D1CC04851A.

(2) Kvashnina, K. O.; Romanchuk, A. Y.; Pidchenko, I.; Amidani, L.; Gerber, E.; Trigub, A.; Rossberg, A.; Weiss, S.; Popa, K.; Walter, O.; Caciuffo, R.; Scheinost, A. C.; Butorin, S. M.; Kalmykov, S. N. A Novel Metastable Pentavalent

Plutonium Solid Phase on the Pathway from Aqueous Plutonium(VI) to PuO 2 Nanoparticles. *Angew. Chemie Int. Ed.* **2019**, *58* (49), 17558–17562. https://doi.org/10.1002/anie.201911637.

(3) Gerber, E.; Romanchuk, A. Y.; Pidchenko, I.; Amidani, L.; Rossberg, A.; Hennig, C.; Vaughan, G. B. M.; Trigub, A.; Egorova, T.; Bauters, S.; Plakhova, T.; Hunault, M. O. J. Y.; Weiss, S.; Butorin, S. M.; Scheinost, A. C.; Kalmykov, S. N.; Kvashnina, K. O. The Missing Pieces of the PuO 2 Nanoparticle Puzzle. *Nanoscale* **2020**, *12* (35), 18039–18048. https://doi.org/10.1039/D0NR03767B.

(4) Pidchenko, I.; März, J.; Hunault, M. O. J. Y.; Bauters, S.; Butorin, S. M.; Kvashnina, K. O. Synthesis, Structural, and Electronic Properties of K4PuVIO2(CO3)3(Cr) : An Environmentally Relevant Plutonium Carbonate Complex. *Inorg. Chem.* **2020**, *59* (17), 11889–11893. https://doi.org/10.1021/acs.inorgchem.0c01335.

(5) Gerber, E.; Romanchuk, A. Y.; Weiss, S.; Kuzenkova, A.; Hunault, M. O. J. Y.; Bauters, S.; Egorov, A.; Butorin, S. M.; Kalmykov, S. N.; Kvashnina, K. O. To Form or Not to Form: PuO 2 Nanoparticles at Acidic PH. *Environ. Sci. Nano* **2022**, *00*, 1–10. https://doi.org/10.1039/D1EN00666E.

(6) Amidani, L.; Vaughan, G. B. M.; Plakhova, T. V.; Romanchuk, A. Y.; Gerber, E.; Svetogorov, R.; Weiss, S.; Joly, Y.; Kalmykov, S. N.; Kvashnina, K. O. The Application of HEXS and HERFD XANES for Accurate Structural Characterisation of Actinide Nanomaterials: The Case of ThO 2. *Chem. – A Eur. J.* **2021**, *27* (1), 252–263. https://doi.org/10.1002/chem.202003360.

(7) Amidani, L.; Plakhova, T. V.; Romanchuk, A. Y.; Gerber, E.; Weiss, S.; Efimenko, A.; Sahle, C. J.; Butorin, S. M.; Kalmykov, S. N.; Kvashnina, K. O. Understanding the Size Effects on the Electronic Structure of ThO 2 Nanoparticles. *Phys. Chem. Chem. Phys.* **2019**, *21* (20), 10635–10643. https://doi.org/10.1039/C9CP01283D.

(8) Gerber, E.; Romanchuk, A. Y.; Weiss, S.; Bauters, S.; Schacherl, B.; Vitova, T.; Hübner, R.; Shams Aldin Azzam, S.; Detollenaere, D.; Banerjee, D.; Butorin, S. M.; Kalmykov, S. N.; Kvashnina, K. O. Insight into the Structure–Property Relationship of UO 2 Nanoparticles. *Inorg. Chem. Front.* **2021**, *8* (4), 1102–1110. https://doi.org/10.1039/D0QI01140A.

(9) Amidani, L.; Retegan, M.; Volkova, A.; Popa, K.; Martin, P. M.; Kvashnina, K. O. Probing the Local Coordination of Hexavalent Uranium and the Splitting of 5f Orbitals Induced by Chemical Bonding. *Inorg. Chem.* **2021**, *60* (21), 16286–16293. https://doi.org/10.1021/acs.inorgchem.1c02107.

(10) Butorin, S. M. 3d-4f Resonant Inelastic X-Ray Scattering of Actinide Dioxides: Crystal-Field Multiplet Description. *Inorg. Chem.* **2020**, *59* (22), 16251–16264. https://doi.org/10.1021/acs.inorgchem.0c02032.

Plutonium fate and transport in the environment: from the desert to salt marshes

E. Balboni

Glenn T. Seaborg Institute, Physical & Life Sciences Directorate, Lawrence Livermore National Laboratory, P.O. Box 808, Livermore, CA 94550, USA.

balboni1@llnl.gov

Plutonium (Pu) has been discharged to and transported in the environment in a wide array of initial forms, concentrations, and hydrologic and geologic environments.[1] To resolve the global and national concerns regarding Pu in our environment, the Scientific Focus Area at Lawrence Livermore National Laboratory (LLNL) is identifying and quantifying the biogeochemical processes and underlying mechanisms that control Pu mobility at a series of biogeochemically diverse contaminated sites.

My research efforts have recently focused on understanding Pu mobility and migration at two different sites: the Nevada National Security Site (NNSS) and the Ravenglass saltmarsh, located 10 km south of the Sellafield site, U.K. The two sites both have a long-term contamination history (~60 years) but are characterized by very different environmental conditions (hydrogeology, organic content, ionic strength). The goal of this work is to develop the necessary predictive understanding of actinide behavior across a range of relevant environmental conditions so as to address long-term risk to the environment.

The migration of low levels of Pu has been observed at the NNSS and attributed to colloids. To understand why Pu is migrating, experiments were performed using mineral colloids produced from nuclear melt glass collected directly from underground nuclear test cavities at the NNSS. Results indicate that the formation of zeolites and clays hydrothermally altered at 200 °C will lead to a more stable association of plutonium with colloids than previously thought and could give rise to more extensive colloid-facilitated transport[2]. These insights help explain why trace levels of plutonium are found downgradient from their original source decades after a nuclear detonation.

The Ravenglass saltmarsh is a low energy, intertidal region that accumulates Sellafield-derived contamination.[3] Since 1952, authorized liquid radioactive effluents have been discharged from Sellafield into the Irish Sea resulting in the largest discharge of Pu in all of western Europe (276 kg Pu).[1] Salt marshes like Ravenglass are dynamic systems which are vulnerable to external agents (sea level changes, erosion, sediment supply and fresh water inputs), and there are uncertainties about their stability under current rising sea levels and possible increases in storm activity[4].Thus far, studies on Sellafield impacted sediments in the Ravenglass saltmarsh have focused on sediment concentration measurements with little detailed study of processes impacting radionuclide mobilization[5, 6]. Shifting redox profiles together with changing hydrological regimes (sea level rise, increased storm activity) have the potential to impact the speciation and mobility of the redox active elements, such as, Pu.

At this site, we are examining the factors affecting Pu mobility in redox stratified soils by conducting desorption experiments of contaminated Ravenglass sediments under both oxic and anoxic conditions. Desorption experiments were conducted over 9 months. The experiments were periodically sampled to determine the amount of desorbed Pu via MC-ICP-MS – (Multi Collector Inductively Couple Mass Spectrometry) along with redox indicators (Eh, pH and extractable Fe(II)). The microbial community

composition was also characterized at both the beginning and end of the desorption experiments. In these experiments the desorption of Pu (and other radionuclides) may be influenced by redox conditions, organic content and microbial community composition. Pu desorption (and mobilization) increases under anoxic conditions and is enhanced in the top 10 cm of sediments.

The results presented in this talk provide information on the potential mobilization and re-mobilization of Pu in biogeochemically diverse and dynamic environments over long timescales. Understanding the behavior of Pu in diverse environmental and hydrological conditions remains a challenge. However, detailed studies of historical contaminated field sites across a range of environmental conditions is providing the necessary insight into the long-term processes controlling Pu migration in the environment.

1. Geckeis, H.; Zavarin, M.; Salbu, B.; Lind, O. C.; Skipperud, L., Environmental chemistry of Plutonium. In *Plutonium Handbook*, 2nd ed.; American Nuclear Society: 2019.
2. Joseph, C.; Balboni, E.; Baumer, T.; Treinen, K.; Kersting, A. B.; Zavarin, M., Plutonium Desorption from Nuclear Melt Glass-Derived Colloids and Implications for Migration at the Nevada National Security Site, USA. *Environmental Science & Technology* **2019,** *53* (21), 12238-12246.
3. Hamilton, E. I.; Clarke, K. R., THE RECENT SEDIMENTATION HISTORY OF THE ESK ESTUARY, CUMBRIA, UK - THE APPLICATION OF RADIOCHRONOLOGY. *Science of the Total Environment* **1984,** *35* (3), 325-386.
4. Leonardi, N.; Defne, Z.; Ganju, N. K.; Fagherazzi, S., Salt marsh erosion rates and boundary features in a shallow Bay. *Journal of Geophysical Research-Earth Surface* **2016,** *121* (10).
5. Aston, S. R.; Stanners, D. A., Plutonium transport to and deposition and immobility in Irish Sea intertidal sediments. *Nature* **1981,** *289*, 581.
6. Morris, K.; Butterworth, J. C.; Livens, F. R., Evidence for the remobilization of Sellafield waste radionuclides in an intertidal salt marsh, West Cumbria, UK. *Estuarine Coastal and Shelf Science* **2000,** *51* (5), 613-625.

Work was performed under the auspices of the U.S. Department of Energy by Lawrence Livermore National Laboratory under Contract DE-AC52-07NA27344

Complexation speciation and thermodynamics of tri- and tetravalent plutonium with EDTA and citrate in high ionic strength systems

N.A. DiBlasi [1], D. Fellhauer [1], X. Gaona [1], M. Altmaier [1]

[1] Karlsruher Institut für Technologie, Institut für Nukleare Entsorgung - Hermann-von-Helmholtz-Platz 1, 76344 Eggenstein-Leopoldshafen, Germany

nicole.diblasi@kit.edu

Understanding the formation, stability, and behavior of aqueous complexation between Pu(III/IV) and strongly complexing organic molecules such as ethylenediaminetetraacetic acid (EDTA) and citrate and the effects of various ionic media on this behavior is essential for accurate determination of the long-term fate and transport of plutonium (Pu) in environmental and underground repository systems where significant inventories of EDTA or citrate may be present. In low ionic strength media, the formation of very stable Pu(III)- and Pu(IV)-EDTA aqueous complexes in reducing to anoxic conditions is described in the literature [1-5]. However, little to no reliable thermodynamic information is available for Pu(III)- and Pu(IV)-citrate complex(es), both under low- and high-ionic strength conditions. After closure, deep geologic repositories are expected to develop reducing conditions due to the anoxic corrosion of iron and steel components. In the case of repository concepts in salt-rock formations, high ionic strength aqueous systems may form upon water intrusion scenarios [6-7]. As detailed thoroughly within the literature, high ionic strengths can greatly impact radionuclide solubility and aqueous speciation [8-9], thus emphasizing the importance of continued investigation into the impact of high ionic strength on the chemistry and mobility of Pu. In addition to ion-ion interaction processes, the electrolytes contained within the ionic media can also greatly impact plutonium speciation. For example, (qua)ternary Ca-Pu-(OH)-EDTA complex(es) have been recently identified and shown to increase solubility under alkaline, reducing conditions [4-5]. Thus, it is not only necessary to understand the impact of high ionic strength but also to thoroughly investigate other major cations of environmental relevance (i.e., Mg) to determine whether additional, (qua)ternary complexes form that may in turn affect the solubility and mobility of plutonium under repository-relevant conditions.

This contribution aims at evaluation the solubility and complexation behavior of Pu(III) and Pu(IV) (hydr)oxide solid phases in the presence of EDTA or citrate under low- to high-ionic strength conditions using both NaCl and $MgCl_2$ background electrolytes. Modelling exercises are performed with the goal of developing reliable thermodynamic and activity models.

Pu-organic complexation for EDTA and citrate is investigated using undersaturation solubility experiments conducted under inert gas atmosphere (Ar) with < 2 ppm O_2 at T = (23 ± 2) °C. Solubility experiments are performed using well-defined ^{242}Pu solid phases ($Pu(OH)_3$(am) or PuO_2(ncr,hyd)) equilibrated in aqueous solutions with $5 < pH_m < 13$ (where $pH_m = -\log m[H^+]$), $0 \leq [org] \leq 0.1$ M, and either $0.5 \leq [NaCl] \leq 5.0$ M or 4.5 M $MgCl_2$. Redox conditions are buffered with either hydroquinone (HQ, moderately reducing), tin(II) or sodium dithionite (Sn(II), $Na_2S_2O_4$, very reducing). pH and E_h (as pe) are measured at regular time intervals and Pu concentrations are monitored over time with inductively coupled plasma mass spectrometry (ICP-MS) after 10 kD ultrafiltration. Solid phases are characterized using powder X-ray diffraction (pXRD) and/or X-ray photoelectron spectroscopy (XPS).

Equilibrium thermodynamic calculations are conducted using constants reported in the literature [1,13] or generated within this work. The PHREEPLOT-PHREEQC Interactive software package was applied for solubility calculations and data analysis/modeling (version 3.4.0, svn 12927) [10], and the Medusa/Spana software package was applied for calculation of Pourbaix (pe-pH_m) diagrams [11]. In a first step, activity models were derived using the Specific Ion-interaction Theory approach [12].

Figures 1A and 1B show preliminary solubility data for the Pu(IV)-citrate system as a function of ionic strength and citrate concentration, respectively. The figures also include solubility calculations conducted for the Th(IV)-citrate system with available thermodynamic data [1,13], which only includes only binary and protonated complexes: $Th(cit)_n^{(4-3n)}$ and $Th(Hcit)_n^{(4-2n)}$. From this comparison, it is clear that additional work is necessary to construct thermodynamic models that effectively describe Pu behavior in the presence of citrate, possibly requiring the definition of ternary Pu(IV)-OH-citrate complexes as predominant Pu(IV) species in near-neutral to hyperalkaline pH conditions. Further experimental results including data on Pu total concentration, aqueous and solid phase characterization (UV-Vis-NIR, pXRD, XPS), and generation of new thermodynamic and activity models for Pu(III/IV)-citrate and -EDTA systems will be discussed in this contribution.

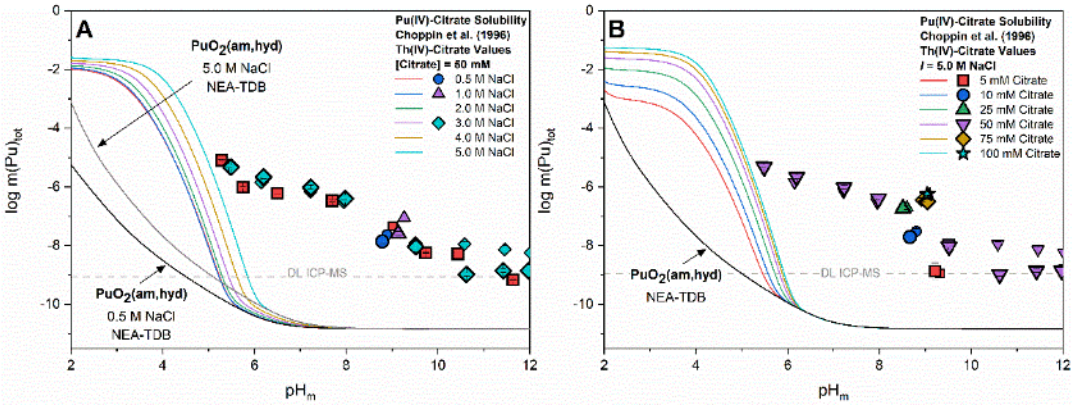

Figure 1: Experimentally measured $m(Pu)_{tot}$ in equilibrium with PuO_2(ncr,hyd) at (A) [Citrate] = 50 mM and 0.5 M ≤ [NaCl] ≤ 5.0 M or (B) [NaCl] = 5.0 M and 5 ≤ [Citrate] ≤ 100 mM. Solid lines correspond to thermodynamically calculated solubility of PuO_2(am,hyd) under different solution conditions based on citrate protonation constant values from the NEA-TDB [1] and Th(IV)-citrate complexation values from Choppin et al. (1996) [13]. Gray dashed lines represent the ICP-MS detection limits for the experimental analyses and all error bars are contained within data symbols.

Acknowledgement: This work has been financially supported by Bundesgesellschaft für Endlagerung (BGE).

[1] W. Hummel, et al., Chemical Thermodynamics, Vol. 9 (2005).

[2] D. Rai, et al., Solution Chem. 37, 957 (2008).
[3] D. Rai, et al., Solution Chem. 39, 778 (2010).
[4] N.A. DiBlasi, et al., Sci. Tot. Environ. 783, 146993 (2021).
[5] N.A. DiBlasi, et al., RSC Advances, in press (2022).
[6] Appendix SOTERM. 40CFR191 (2019).
[7] J.F. Lucchini, et al., U.S. Department of Energy, LA-UR-13-20620 (2013).
[8] I. Grenthe, et al., Chemical Thermodynamics, Vol. 14, (2020).
[9] A.R. Felmy, et al., Radiochim. Acta, 48, 29 (1989).
[10] S.R Charlton and D.L. Parkhurst, Comput. Geosci., 37, 1653 (2011).
[11] I. Puidgomenech, Medusa/Spana (2020).
[12] L. Ciavatta, Ann. Chim., 70, 551 (1980).
[13] G.R. Choppin, et al., Radiochim. Acta, 74, 123 (1996).

Actinide speciation in marine radioecology

M. R. Beccia [1], C. Berthomieux [2], C. Den Auwer [1], T. Dumas [3], M. Maloubier [4], D. K. Shuh [5], M. Monfort [6], C. Moulin [6$], B. Reeves [1,6], P. L. Solari [7], R. Stefanelli [1,6] M. Virot [8]

[1] Université Côte d'Azur, CNRS, ICN, 06108 Nice, France
[2] Commissariat à l'Energie Atomique, DRF, CNRS, BIAM, Cadarache 13108, St Paul lez Durance, France
[3] Commissariat à l'Energie Atomique, DES, Marcoule, 30207 Bagnols sur Cèze, France
[4] Université Paris Saclay, IJCLab, 91405 Orsay, France
[5] Lawrence Berkeley National Laboratory, Chemical Sciences Division, Berkeley, CA94720, USA
[6] Commissariat à l'Energie Atomique, DAM/DIF/DASE, 91297 Arpajon, France
$ secondment at SGDSN, Paris, France
[7] Synchrotron SOLEIL, MARS beam line, 91047 Gif sur Yevette, France
[8] ICSM, CEA, CNRS, UM, 30207 Bagnols sur Cèze, France

christophe.denauwer@univ-cotedazur.fr

The mechanisms of dissemination of radionuclides resulting from an accidental release in the environment, in particular in sea water, is a scientific but above all political and social issue. Hence, the need for managing the risk, for controlling the environmental fate and transport of radionuclides, and for preventing human exposure through direct contact and indirectly through the food chain is essential. Among the different environmental matrices, seawater represents the largest proportion of the hydrosphere, it covers by itself about 71% of the earth's surface and it is the final repository of pollution. It is therefore crucial to understand the transfer and accumulation mechanisms of radionuclides in marine environment and to attempt to perform direct speciation analysis in seawater. But speciation is poorly described in seawater systems but also more generally in the environment because of its complexity and large dilution factors that preclude direct determination. Therefore, it is required to shift from a purely descriptive radioecology approach to a mechanistic approach and this can be performed with the use of speciation tools in model (eco)systems.

Figure 1 : Picture of a sea urchin Paracentrotus lividus (total diameter equals about 7 cm).

Our group has been investigating the impact of contamination of several actinides (uranium, neptunium, plutonium, americium and surrogate europium), fission products (cesium) and activation products (cobalt) on marine species (sponge, sea urchin, mussels) in well-controlled marine systems. By describing the speciation of the above metallic radionuclides, we explored the speciation of soluble and insoluble species in seawater leading to potentially bioavailable and bio-transferred species [1]. We have addressed this question in semi natural systems by doping natural seawater with the radionuclides of interest in order to be able to perform direct spectroscopic investigation and thus to decipher their molecular speciation [2]. We have also monitored the uptake mechanisms of metallic radionuclides, *in vivo* [3]. For instance, the sea urchins *Paracentrotus Lividus* is known as a possible sentinel species for heavy metal accumulation has been selected (Figure 1). After a specific contamination procedure, contaminated gonads of *P. lividus* were analyzed by X ray Absorption Spectroscopy (XAS) and Scanning Transmission X-ray Microscopy (STXM), a technique that couples XAS and microscopy in order to localize the element of interest in a 2-D space and define its speciation at the same time. Such a technique is suitable for element-selective imaging studies with a spatial resolution down to a few tens of nm. EXAFS data analysis at the U L_{II} edge of contaminated gonads further suggested that the metal is coordinated to carboxylate residues of a biomolecule. The toposome protein, the main protein in *P. lividus* was identified as a possible target for U complexation because of its ability to store Ca^{2+} ions with carboxylate chemical functions

Overall, we have combined several spectroscopic techniques mostly based on X ray Absorption Spectroscopy (XAS) in bulk mode and spatially resolved mode (imaging), together with electron microscopy images, speciation modeling and quantum chemical models. The major limitation to this methodology is certainly the validation of representativeness for contaminated ecosystems. For that purpose, much care should be taken to complement such approaches with field data, as much as possible.

In conclusion, obtaining speciation data calls for a methodological compromise. Nevertheless, the input data so gathered is essential and can impact calculation codes developed on a larger scale.

[1] M. Maloubier, P. L. Solari, P. Moisy, M. Monfort, C. Den Auwer, C. Moulin, *Dalton Trans*., **2015**, *44*, 5417-5427

[2] M. Maloubier, D. K. Shuh, S. G. Minasian, J. I. Pacold, P.-L. Solari, H. Michel, F. R. Oberhaensli, Y. Bottein, M. Monfort, C. Moulin, C. Den Auwer, *Env. Sci. Technol*. **2016**, *50*, 10730-10738

[3] B. Reeves, M. R. Beccia, P. L. Solari, D. E. Smiles, D. K. Shuh, L. Mangialajo, S. Pagnotta, M. Monfort, C. Moulin, C. Den Auwer, *Environ Sci. Technol.* **2019**, *16*, 7974-7983

Retention and Near-Field Release of ^{99}Tc, ^{233}U, ^{237}Np, ^{242}Pu and ^{241}Am from the Long-Term In-Situ Test at the Grimsel Test Site

F. Quinto [1]*, I. Blechschmidt [2], T. Faestermann [3], K. Hain [4], G. Korschinek [3], S. Kraft [1], B. Lanyon [5], J. Pitters [4], M. Plaschke [1], G. Rugel [6], T. Schäfer [7], P. Steier [4], H. Geckeis [1]

[1] Karlsruhe Institute of Technology (KIT), Institute for Nuclear Waste Disposal (INE), Karlsruhe, Germany [2] NAGRA (National Cooperative for the Disposal of Radioactive Waste), Wettingen, Switzerland [3] Technical University of Munich (TUM), Physics Department, Garching, Germany [4] University of Vienna, Faculty of Physics, VERA Laboratory, Vienna, Austria [5] Fracture Systems Ltd, Tregurrian, Ayr, TR26 1EQ St. Ives, United Kingdom [6] Helmholtz-Zentrum-Dresden, Accelerator Mass Spectrometry and Isotope Research, Dresden, Germany [7] Friedrich-Schiller-Universiy (FSU), Institute for Geosciences (IGW), Applied Geology, Jena, Germany

**francesca.quinto@kit.edu*

The CFM (Colloid Formation and Migration) Long-Term In-Situ Test (LIT) consisted in a packer-system containing compacted Febex bentonite rings (2 cm thick, each) partly spiked with conservative and radionuclide (RN) tracers and emplaced in the granodiorite at the Grimsel Test Site (Switzerland) [1]. The LIT source intersected a water-conducting shear zone, allowing for the saturation of the bentonite with Grimsel groundwater (GGW) and the consequent possible diffusion of the RN tracers. During ~4.5 years, groundwater was regularly collected from two near-field boreholes placed at a distance of 4 cm from the LIT source. In these samples, composed of GGW mixing with a small proportion of bentonite pore water (mixed water, MW), we have investigated the concentration of the conservative fluorescent tracer Amino-G (AGA) and the RN tracers ^{99}Tc, ^{233}U, ^{237}Np, ^{242}Pu and ^{241}Am, originally emplaced in the bentonite as Tc(VII), U(VI), Np(V), Pu(III) and Am(III). Considering the setup of LIT, a signal of the RN tracers in the MW samples would account for a near-field release from the bentonite followed by the transport/retention through the shear zone under advective transport conditions.

Some of the investigated RNs are expected to show slow diffusion through bentonite and therefore ultra-trace levels in the MW samples. This analytical challenge was addressed with AMS that provides detection efficiency for actinide nuclides and ^{99}Tc at the level of ~1 × 10^4 atoms (25 ag) and 3 × 10^6 atoms (0.5 fg) in a sample, respectively [2, 3]. Fig. 1 shows extremely low concentrations of the RN tracers determined in the MW samples for example for ^{99}Tc with values spanning from a maximum of (1.2 ± 0.6) × 10^9 atoms/mL at 206 days and down to (4.5 ± 1.2) × 10^6 atoms/mL at 1600 days after the start of the experiment. Similar trends are observed for ^{233}U and ^{237}Np with a possible maximum in the first phase of LIT and decreasing levels towards the end, while ^{242}Pu shows a more or less flat concentration profile. Levels higher than detection limits for ^{241}Am are determined in samples collected up to ~900 days with concentrations generally lower than (8.3 ± 5.5) × 10^4 atoms/mL. Based on those analytical data collected over ~4.5 years, the fraction of RN tracers in MW relative to the emplaced inventory corresponds to ~8.5 × 10^{-5} for ^{99}Tc, 3.4 × 10^{-4} for ^{233}U, 1.9 × 10^{-5} for ^{237}Np, 6 × 10^{-5} for ^{242}Pu and 2.4 × 10^{-5} for ^{241}Am (with AGA recovery equal to ~ 3.7× 10^{-2} [1]). Whether the measured concentrations can be considered entirely as near-field releases from the LIT is a matter of discussion.

In particular, the possible background from previous in situ RN tracer tests [2] performed during the last 21 years in various dipoles intersecting the shear zone may play an important role by contributing to a "shear zone background". This "background" cannot be univocally estimated, since it can only be determined in GGW samples collected before or during the LIT in far-field boreholes located at a certain distance to the LIT experiment. While the concentrations of most of the RNs in samples collected after ~700 days are close or below the respective "background" levels, the concentrations of ^{99}Tc lie significantly above its "background" equal to ~1.6 × 10^5 atoms/mL and, thus, point to a clear release of ^{99}Tc from the bentonite source over the entire experimental period.

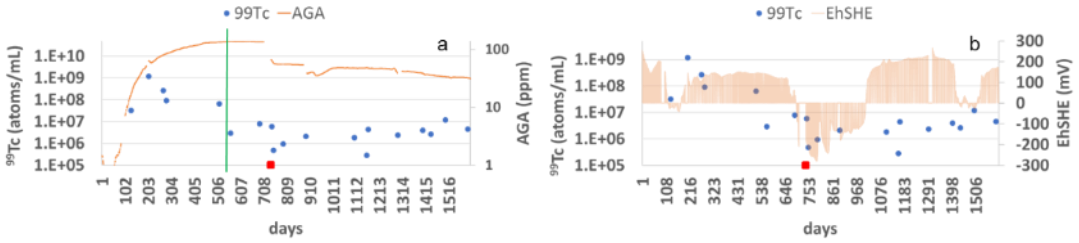

Figure 1: Concentration of ^{99}Tc and the conservative tracer AGA a) and the Eh_{SHE} b) in near-field MW samples. The red square represents the date of the increase of the extraction rate of the groundwater.

However, the shape of the ^{99}Tc release curve differs from that of the conservative, non-sorbing tracer AGA. In fact, as shown in Fig. 1a, the concentrations of ^{99}Tc (as well as of ^{233}U, ^{237}Np and ^{241}Am, not depicted here) significantly decrease within ~550 days, indicated with a green vertical line. The concentration of AGA reaches a steady state at 400-500 days and decreases by 60% after 738 days due to an increase of the extraction rate of the MW samples from 20 to 50 µl/min. At this time, indicated in Fig. 1 with a red square, a clear decrease in the ^{99}Tc concentration cannot be recognized, though possibly due to the scatter in analytical data. The initial elution curve shapes of the RNs could be ascribed to the inhomogeneous swelling in the early phase of bentonite saturation with the GGW [1], possibly opening preferential transport pathways for the RNs and AGA. At the same time, redox conditions in the bentonite varied due to oxygen consumption that may have an impact mainly on the speciation of Tc and Np. The enhanced RN retardation observed in the actual experiment after ~550 days would occur when the swelling of the fully saturated bentonite closes the pathways and the Eh_{SHE} values decrease in bentonite pore water. It is important to note that the expected establishment of increasingly reducing conditions in the bentonite cannot be inferred from the evolution of the Eh_{SHE} values determined in the MW samples, as shown in Fig. 1b. In fact, the Eh_{SHE} values measured in the borehole may not necessarily reflect the redox conditions in the bentonite. This study addresses a complex *in situ* system simulating the behaviour of compacted bentonite in contact with a water-conducting feature in which the possible release and retention of the RN tracers is investigated with unprecedented sensitivity. Experimental data suggest that ^{233}U, ^{237}Np, ^{242}Pu and ^{241}Am are strongly captured by the bentonite. While trace fractions of ^{99}Tc, ^{233}U, ^{237}Np and ^{241}Am are released during the early phase when the bentonite is not fully saturated, for ^{99}Tc also a steady state concentration establishes pointing to the diffusive transport of a small fraction of non-reduced TcO_4^-.

[1] U. Noseck, T. Schäfer (eds.), 2019, KOLLORADO-e2 Final report. KIT Open Report 7757, Karlsruhe

[2] F. Quinto et al., Anal. Chem., 2017, **89**, 7182

[3] F. Quinto et al., Anal. Chem., 2019, **91**, 4585

Isotopic effect on the formation kinetics of Pu(IV) intrinsic colloids

M. Cot-Auriol [1], M. Virot [1], T. Dumas [2], O. Diat [1], D. Menut [3], P. Moisy [2], S.I. Nikitenko [1]

[1] ICSM, Univ Montpellier, CEA, CNRS, ENSCM, Marcoule, France.
[2] CEA of Marcoule, BP17171, 30207 Bagnols-sur-Cèze, France.
[3] Synchrotron SOLEIL, MARS beamline, l'Orme des Merisiers, Saint Aubin BP 48, 91192 Gif-sur-Yvette, France.

Corresponding author: manon.cotauriol@cea.fr

Fundamental knowledge of the intrinsic colloids of plutonium is a major issue in predicting their behavior in the environment.[1,2] It has been demonstrated that these species are spherical nanoparticles measuring *ca.* 2 nm with a local structure similar to the one of bulk PuO_2.[3,4] Recent studies have questioned the contribution of small Pu clusters in the formation mechanism of Pu(IV) intrinsic colloids.[5] The current work draws attention to this issue by investigating an unprecedented kinetic isotopic effect (KIE) observed during the preparation of Pu(IV) colloids in light (H_2O) or heavy (D_2O) water.

Plutonium colloids have been synthetized by the dilution of acidic Pu(IV) solutions in H_2O and D_2O.Time dependent measurements carried out with UV-Vis absorption spectroscopy demonstrated a much lower formation rate of the Pu(IV) colloids in D_2O compared to H_2O (Figure 1a). The observed KIE was attributed to the difference in zero-point energies of O-H and O-D bonds. This finding has confirmed that the formation of Pu(IV) colloids is limited by the rupture of O-H bonds during hydrolysis and polymerization of Pu(IV) species. In addition, formation of some unstable intermediate Pu(IV) species was observed during colloid formation. A thorough investigation of this intermediate using synchrotron SAXS and XAS techniques revealed the presence of an hexanuclear Pu(IV) cluster of quasi-spherical shape measuring *ca.* 0.8 nm and agreeing with the literature (Figure 1b).[6,7]

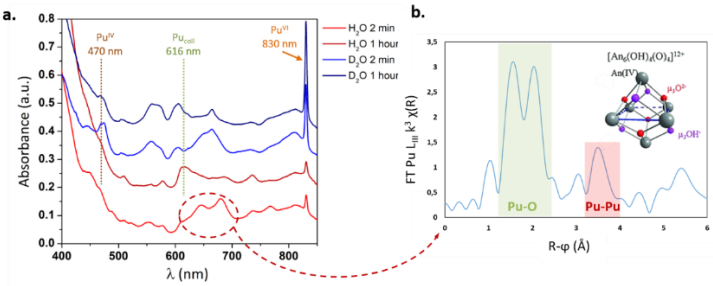

Figure 1: (a) UV-Vis absorption spectra acquired during the synthesis of 5 mM Pu(IV) hydrolytic colloids in H_2O (red lines) and D_2O (blue lines). (b) k^3-weighted Fourier transform (FT) of the intermediate species observed in H_2O by UV-Vis absorption spectroscopy (dashed circle).[6]

References:

[1] C. Walther *et al., Chem. Rev.* **113**, 995–1015 (2013).
[2] A.Y. Romanchuk *et al., Front. Chem.* **8**, 630 (2020).
[3] E. Dalodière *et al.*, *Sci Rep* **7**, 43514 (2017).
[4] C. Micheau *et al.*, *Environ. Sci.: Nano* **7**, 2252 (2020).
[5] K.E. Knope *et al., Inorg. Chem.* **52**, 6770-6772 (2013).
[6] C. Tamain *et al.*, *Eur. J. Inorg. Chem.* **2016**, 3536-3540 (2016).
[7] T. Dumas *et al.*, *J. Synchrotron Rad.* **29**, 30-36 (2022).

Plutonium Oxidation State Distribution in High Ionic Strength Environments

Jeremiah C. Beam [1], Adrianne Navarrette [1], Donald T. Reed [1]

[1] Actinide Chemistry and Repository Sciences Program, Los Alamos National Laboratory

1400 University Drive Carlsbad, NM 88220

jbeam@lanl.gov

Plutonium can be found in several oxidation states in the environment (+III, +IV, +V, +VI, +VII), The solubility and chemistry differences of these oxidation states have large impacts when calculating release from deep geological repositories such as the Waste Isolation Pilot Plant (WIPP). The redox environment in the WIPP is dominated by the chemistry of the iron waste canisters, radiolysis from the actinide waste, and the presence of organic ligands (acetate, citrate, EDTA, and oxalate). For performance assessment calculations, it is useful to set upper and lower limits for the oxidation state distribution. In the case of the WIPP, the high redox scenario can be approximated with a system that contains Pu-239 with no reducing conditions. This allows brine radiolysis to control the upper bound of Pu oxidation states. Similarly, the low redox scenario can be approximated by a system that contains Pu-242 and iron metal. The reducing environment produced by the iron metal, with minimal radiolysis from Pu, sets the lower bound of Pu oxidation states. Finally, a realistic WIPP redox environment can be approximated by the use of Pu-239 along with mixed Fe(II/III) phase and the presence of the major organic components found in the waste. X-ray absorption near-edge spectroscopy (XANES) analysis indicates that in the lower bounding redox environment, a mixture of Pu(III) and Pu(IV) solids are present (Figure 1). In the upper bounding redox environment, all Pu(III) solids have been converted to Pu(IV). These results indicate that over a wide range of redox environments, Pu(IV) solids are expected to dominate in the WIPP.

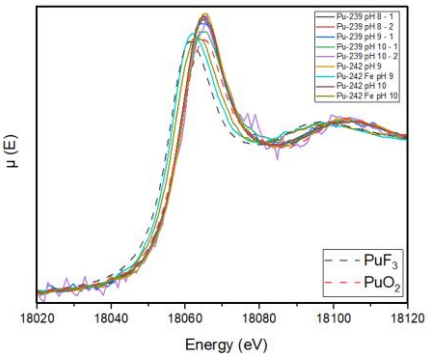

Figure 1: *X-ray absorption near-edge spectroscopy spectra of initially Pu(III) solids in a variety of redox environments*

References

[1] Reed, D. 2018. Plutonium Oxidation State Distribution in the WIPP: Conceptual Mode, Project-Specific Data, and Current/Ongoing Issues. Los Alamos National Laboratory; Carlsbad, NM. LA-UR-18-25748

[2] Di Blasi, N.A.; Tasi, A.G.; Trumm, M.; Schnurr, A.; Gaona, X.; Fellhauer, D.; Dardenne, K.; Rothe, J.; Reed, D.T.; Hixon, A.E.; Altmaier, M. Pu(III) and Cm(III) in the presence of EDTA: aqueous speciation, redox behavior, and the impact of Ca(II). *RSC Advances*. **2022**, 12, 9478-9493.

[3] Reed, D.T.; Lucchini, J.-F.; Aase, S.B.; Kropf, A.J. Reduction of Plutonium (VI) in Brine under Subsurface Conditions. *Radiochimica Acta.* **2006**, 94, 591-597.

LA-UR-22-23116

Nuclear Fuel Cycle

	Conference room #1: CELLIER BENOIT XII
PLENARY TALK 9:00 – 09:50	**Gilles BORDIER (CEA)** *"Stakes and scientific challenges for a sustainable use of Uranium and Plutonium in the French nuclear fuel cycle"*
	Conference room #1: CELLIER BENOIT XII
INVITED TALK 10:00 – 10:30	**Gregory HORNE (INL)** *"Recent Advances in Radiation-Induced Actinide Redox Chemistry"*
INVITED TALK 11:00 – 11:30	**Philippe MARTIN (CEA)** *"Extreme multi-valence states in mixed actinide oxides $U_{1-y}M_yO_{2\pm x}$"*
11:30 – 11:50	**Luther McDonald (U. UTAH)** *"Morphology Signatures of the Nuclear Fuel Cycle"*
11:50 – 12:10	**Catherine SABATHIER (CEA)** *"TEM characterization of MOX fuel irradiated to 13.1% FIMA in the PHENIX reactor"*
12:10 – 12:30	**Pablo VACAS ARQUERO (CIEMAT)** *"First gamma irradiation studies of AmSel extraction system"*
	Conference room #1: CELLIER BENOIT XII
INVITED TALK 15:00 – 15:30	**Hannah COLLEDGE (NNL)** *"Preparation of Homogenous (U,Pu) Mixed Oxides via Oxalate Precipitation"*
15:30 – 15:50	**Meghann FUCINA (CNRS)** *"Synthesis of plutonium trichloride for molten salt reactor technology"*
16:20 – 16:40	**Russel JOHNS (LANL)** *"A Contemporary Investigation of Clementine"*
16:40 – 17:00	**Marie-Margaux DESAGULIER (CEA)** *"Manufacturing of $(U,Pu)O_{2-x}$ mixed oxides with high plutonium contents (> 60 mol.%)"*
17:00 – 17:20	**Hope RASMUSSEN (LANL)** *"Effects of salt concentration and ionic strength on transuranic separations from aqueous chloride waste streams using a quaternary ammonium ionic liquid"*
17:20 – 17:40	**Jean-Philippe BAYLE (CEA)** *"Modelling of (U-Pu)O2 powder die compaction for nuclear fuel fabrication and characterization method for elasto-plastic model identifications"*

Chair persons:

Christophe JOUSSOT-DUBIEN and Gregory HORNE

Stakes and scientific challenges for a sustainable use of Uranium and Plutonium in the French nuclear fuel cycle

G. Bordier

[1] CEA – DES/EC/DSE - Saclay Research Centre 91191 Gif-sur-Yvette cedex

gilles.bordier@cea.fr

The current French recycling strategy takes advantage of the 10 MT of plutonium produced annually by the irradiation of the UOX fuel in the French LWR fleet. This recycling strategy aims at saving natural uranium resources as well as decreasing the net production of plutonium, safely recovered and recycled in the MOX fuels. It also limits the necessary interim storage and future final disposal capacities and prevents any residual plutonium content in the high-level nuclear glass waste. Although the feasibility of MOX reprocessing is already considered proven at an industrial scale, the used MOX fuel (100-120 t/y), which still contains a fraction of potentially reusable plutonium, is currently untreated and stored.

The French Energy Transition Act and the Multi-annual Energy Program (2019-2028) make several commitments and notably:

I. net zero CO2 emissions by 2050,
II. Decreasing the share of nuclear energy in the electric mix down to 50% by 2035, and shutting down 14 LWRs by 2035 consequently; recent presidential announcements are however in favor of extending the lifetime of existing reactors and building soon new EPRs (6 initially with a study of 8 more).
III. Increasing the amount of renewable energies in the mix consequently.
IV. Maintaining the recycling strategy at least until the years 2040.

The MOX fuel is currently used in the 900 MWe LWRs, which will be shut down first; partially “MOXing” the 1300 MWe LWRs will compensate this.

In the long run (on the horizon of the end of the 21st century), the nuclear industry has to be prepared for a potential forthcoming lack of natural uranium available at an economically viable cost. Therefore, a sustainable closed fuel cycle strategy makes it necessary to introduce the 4th Generation fast neutron reactors into the fleet, which are able to take the best benefit of every actinide isotopes through a better neutron fission/absorption ratio. The option of using molten salt reactors to carry out the transmutation of actinides is also under study, with specific scientific challenges at stake.

Meanwhile, French industry should pave the way for multi-recycling Pu and U in the current LWRs. The option of multi-recycling plutonium in LWRs implies an increase in the plutonium flux and a degradationof the plutonium isotopic composition, which induces several hurdles concerning the safety, radiation protection and operating conditions of the reactors and the fuel cycle (reprocessing and fabrication). In particular, concerning the fuel cycle, a dedicated R&D program addresses innovative options for reprocessing (dissolution of more refractory oxide pellets, simplified separation process). In this talk, we address the main scientific challenges associated with this step-by-step strategy towards a sustainable Pu « full recycling » and highlight the need for improvements and simplifications in the MOX fuel reprocessing and manufacturing operations required by the notably increasing quantity of degraded plutonium in the fuel cycle.

Recent Advances in Radiation-Induced Actinide Redox Chemistry

Gregory P. Horne

Center for Radiation Chemistry Research, Idaho National Laboratory, Idaho Falls, ID, P.O. Box 1625, 83415, USA.

gregory.horne@inl.gov

The actinide series boasts many unique physical and chemical features worthy of both fundamental and applied study. However, the chemical influence of their inherent radiation field is often overlooked, especially as we begin to explore the late actinides in more detail than ever possible before. From the perspective of used nuclear fuel reprocessing, the absorption of ionizing radiation induces the formation of a variety of transient and steady-state excited states, radicals, ions, and molecular degradation products, many of which are highly redox active and can lead to significant changes in a reprocessing solvent system's physical and chemical properties. For example, radiolysis of the actinides can drive steady-state redox distributions and the formation of non-traditional oxidation states which can complicate their separation and recovery from fission products.[1-3] This scenario is further exacerbated when complexation is taken into account.[4] Consequently, a molecular-level understanding of radiation effects on the actinides over multiple time, distance, and material domains is essential for supporting innovation in used nuclear fuel reprocessing technologies.

Attaining this knowledge necessitates a firm grasp of actinide radiation chemistry to develop predictive, mechanistic, multiscale models to support engineering efforts. Presented here are several recent studies that highlight recent advances in actinide radiation chemistry, in particular, the effect of actinide complexation on ligand reactivity towards radiation-induced transients.

[1] Horne, G. P.; Grimes, T. S.; Mincher, B. J.; Mezyk, S. P., *Journal of Physical Chemistry B*, **2016**, *120 (49)*, 12643-12649.

[2] Grimes, T. S.; Horne, G. P.; Dares, C. J.; Pimblott, S. M.; Mezyk, S. P.; Mincher, B. J., *Inorganic Chemistry*, **2017**, *56 (14)*, 8295-8301.

[3] Horne, G. P.; Grimes, T. S.; Bauer, W. F.; Dares, C. J.; Pimblott, S. M.; Mezyk, S. P.; Mincher, B. J., *Inorganic Chemistry*, ***2019***, 58*, 8551-8559.*

{4] Celis-Barros, C.; Pilgrim, C.D.; Cook, A.R.; Grimes, T.S.; Mezyk, S.P., Horne, G.P., *Physical Chemistry and Chemical Physics*, **2021**, *23*, 24589-24597.

Extreme multi-valence states in mixed actinide oxides $U_{1-y}M_yO_{2\pm x}$

Ph. Martin [1], L. Medyk [1], P. Fouquet-Métivier [1], Enrica Epifano [2], F. Lebreton [1], M.O.J.Y Hunault [3], P.L. Solari [3], D. Manara [4], C. Guéneau [5], A.C. Scheinost [6], C. Hennig [6], D. Prieur [6], T. Vitova [7], K. Dardenne [7], J. Rothe [7]

[1] CEA, DES, ISEC, DMRC, Univ. Montpellier, Marcoule, France [2] CIRIMAT, UMR CNRS 5085, Univ. Toulouse III, France [3] Synchrotron SOLEIL, France [4] European Commission, JRC, Ispra, Italy [5] Université Paris Saclay, CEA, DES, ISAS, DPC, Gif-sur-Yvette, France [6] HZDR, Institute of Resource Ecology, Dresden, Germany [7] INE, KIT, Eggenstein-Leopoldshafen, Germany.

philippe-m.martin@cea.fr

In order to ensure the safety of nuclear reactors using oxide fuels, the knowledge of the atomic-scale properties of $U_{1-y}M_yO_{2\pm x}$ (with M=Pu, Am) materials is essential. These compounds show complex chemical properties, as actinides may be present in different oxidation states. In these reactors, $UO_{2\pm x}$ and various ternary (or higher order) $U_{1-y}M_yO_{2\pm x}$ solid solutions can be encountered, such as fresh fuels (M = Pu), transmutation targets (M = Np or Am) or irradiated fuels (M = fission products, as d-transition metals and lanthanides). These materials are formed by substitution of uranium atoms (U^{4+}) with other cations, which are not necessarily in a tetravalent state. In these $U_{1-y}M_yO_{2\pm x}$ compounds, presenting mostly an ionic character, a direct connection exists between the cationic oxidation state and the oxygen stoichiometry, generally referred to as Oxygen/Metal (O/M) ratio. This is a crucial point for the safety assessment of nuclear fuels as changes in the O/M ratio can dramatically affect their thermal properties, for instance the melting point and the thermal conductivity, which determine their behaviour in reactors and safety margins.

By combining XRD, Raman microscopy, X-ray Absorption Spectroscopy (XANES, HERFD-XANES and EXAFS) in-depth study of atomic-scale properties of $U_{1-y}M_yO_{2\pm x}$ compounds can be performed. The first application of this methodology is dedicated to $U_{1-y}Am_yO_{2\pm x}$ on a wide compositional domain ($y \leq 0.70$) [1]. We provide evidences of the systematic co-existence of at least three different cations (U^{4+}, U^{5+} and Am^{3+}), even for stoichiometric compounds (O/M ratio = 2.00). As illustrated in Figure 1, for Am contents higher than 50 mol. %, the presence of four cations (U^{4+}, U^{5+}, Am^{3+} and Am^{4+}) is demonstrated. Nevertheless, the fluorite structure is maintained through the whole composition range. Indeed, both XRD and EXAFS results show that the cationic sublattice is unaffected by the extreme multi-valence states, whereas complex defects are present in the oxygen sublattice.

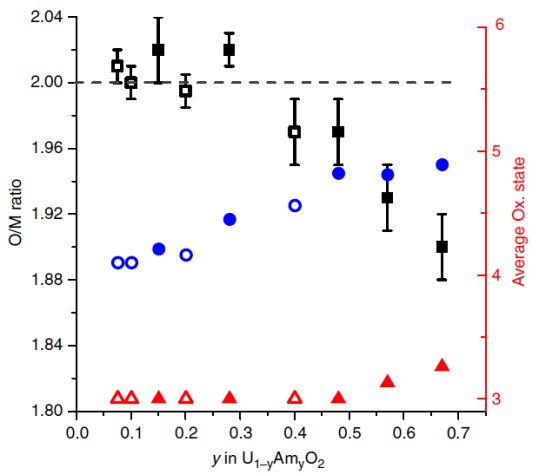

Figure 1: Compositions of $U_{1-y}Am_yO_{2-x}$ oxides. The O/M ratios are represented on the left axis scale, the average oxidation states (AOS) of U and Am are shown on the right axis scale [1–4].

The second application focuses on $U_{1-y}Pu_yO_{2\pm x}$ fuels dedicated to fast neutron reactors. In such materials, the accepted convention is a U^{4+}-Pu^{4+} configuration for stoichiometric (O/M=2.00) and the coexistence of Pu^{3+}, Pu^{4+} and U^{4+} for hypo-stoichiometric face centred cubic materials. However, our recent results clearly show a situation more similar to $U_{1-y}Am_yO_{2-x}$. Thanks to the gain in sensitivity brought by HERFD-XANES at actinide M edges, the systematic presence of U^{5+}/Pu^{3+} even for stoichiometric samples (O/M ratio = 2.00) is evidenced for Pu content up to 40 mol%, as illustrated in Figure 2. We observe that the relative presence of U^{5+} and Pu^{3+} increases with the Pu content, reaching 10% for Pu/(U+Pu) = 0.40. One should note that the O/M ratios calculated from O/Pu, O/U and O/Am determined by HERFD-XANES are equal to the Raman [5] an XRD derived [6] values. Furthermore, the analysis of the microstructure (EPMA, µ-Raman) demonstrates that this multi-valence phenomenon cannot be attributed to the slight inhomogeneity of the samples, but really to a charge-compensation mechanism.

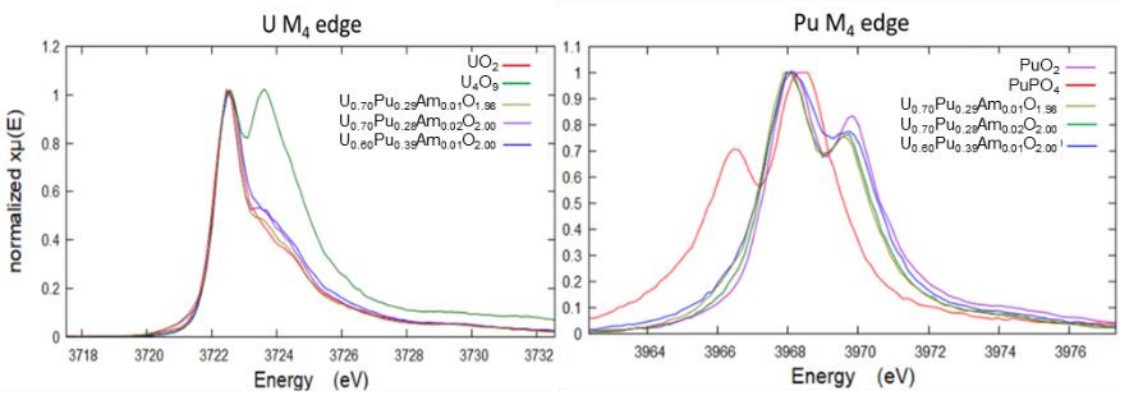

Figure 2: U and Pu M_4 HERFD-XANES data obtained on $U_{1-y}Pu_yO_{2-x}$ oxides.

[1] E. Epifano et al., Commun. Chem. 2 (2019) 59.
[2] D. Prieur et al., Inorg. Chem. 50 (2011) 12437–12445.
[3] D. Prieur et al., J. Nucl. Mater. 434 (2013) 7–16.
[4] F. Lebreton et al., Inorg. Chem. 54 (2015) 9749-9760.
[5] C. Duriez et al., J. Nucl. Mater. 277 (2000) 143–158.
[6] L. Medyk et al., J. Nucl. Mater. 541 (2020) 152439.

Morphology Signatures of the Nuclear Fuel Cycle

L. W. McDonald IV

[1] University of Utah Department of Civil and Environmental Engineering – Nuclear Engineering Program, 201 President's Circle, Salt Lake City, UT 84112. United States

luther.mcdonald@utah.edu

Particle morphology is emerging as a powerful signature to aid nuclear forensic investigations. Traditionally, forensic signatures such as parent-daughter isotope ratios have provided accurate means of determining the processing age of nuclear materials. Nonetheless, these traditional signatures provide limited information regarding the chemical processing history. Particle morphology can help reveal the process history, but a detailed understanding of factors impacting the morphology, coupled with high throughput data processing capabilities, are needed for this signature to be viable. Replicating many commercial production routes, we have built a database of morphological signatures for the production of U-oxides from ammonium diuranate (ADU), ammonium uranyl carbonate (AUC), uranyl peroxide (UO_4), sodium diuranate (SDU), and magnesium diuranate (MDU)[1] and evaluated the impact of process variables (i.e., temperature, impurities, aging)[2,3] on these signatures. Results highlighting the current data and efforts to process it using human guided segmentation, supervised machine learning[4] and unsupervised machine learning[5] will be discussed.

[1] Schwerdt, Ian J., et al. "Uranium oxide synthetic pathway discernment through thermal decomposition and morphological analysis." Radiochimica Acta 107.3 (2019): 193-205.

[2] Hanson, Alexa B., et al. "Quantifying impurity effects on the surface morphology of α-U3O8." Analytical chemistry 91.15 (2019): 10081-10087.

[3] Hanson, Alexa B., Cody A. Nizinski, and Luther W. McDonald IV. "Effect of Diel Cycling Temperature, Relative Humidity, and Synthetic Route on the Surface Morphology and Hydrolysis of α-U3O8." ACS omega 6.28 (2021): 18426-18433.

[4] Ly, Cuong, et al. "Determining uranium ore concentrates and their calcination products via image classification of multiple magnifications." *Journal of Nuclear Materials* 533 (2020): 152082.

[5] Girard, M., et al. "Uranium Oxide Synthetic Pathway Discernment through Unsupervised Morphological Analysis." *Journal of Nuclear Materials* 552 (2021): 152983.

TEM characterization of MOX fuel irradiated to 13.1% FIMA in the PHENIX reactor.

C. Sabathier, D. Reyes, D. Drouan, C. Onofri, K. Hanifi, I. Zacharie, T. Blay, I. Viallard, J. C. Dumas

CEA, DES, IRESNE, Cadarache F-13108 Saint Paul lez Durance, France

catherine.sabathier@cea.fr

Mixed oxide fuels with a composition of $(U_{0.78}Pu_{0.22})O_{1.975}$ were irradiated in an experiment called NESTOR3 in the PHENIX sodium cooled reactor during 758 Equivalent Full Power Day at high burn-up (13.1 %) Fissions per Initial Metal Atom (FIMA) at the pin maximum flux plane.

Complementary analysis were done at the LECA-STAR hot cell facility at the CEA Cadarache Centre (EPMA, SEM-FIB-EBSD,TEM) on this fuel (Figure 1). More specifically, two lamellas taken at two radial positions (0.33R and 0.98R) were characterized, i.e in the columnar grains region and in the High Burn-up Structure (HBS), respectively.

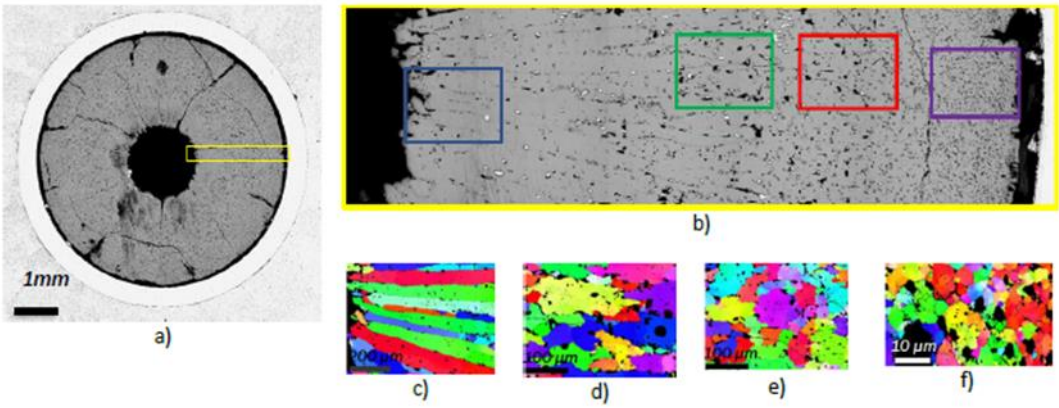

Figure 1: a) Ceramography image, b) SEM image on a specific radius of the pellet, EBSD maps at c) 0.33R in the columnar grains region, d) 0.63R at the end of the columnar grains region, e) 0.82R in the equiaxis grains region, f) 0.98R in the HBS region.

Near the centre hole of the pellet, the presence of a low dislocation lines density is measured, thanks to the determination of the local thickness [1] using EELS (Electron Energy Loss Spectrometry) technique. This low dislocation density is probably due to the high temperature (≈2000°C) at the EOL (End Of Life) computed with the GERMINAL fuel performance code [2]. This high level of temperatures can induce an annealing of these defects. An over concentration of Pu is measured in agreement with EPMA measurements and at the nanoscale no metallic precipitates are observed into the grains.

In return, near the periphery, in the HBS region where the temperature at the EOL is around 850°C, the grains that are subdivided are free from dislocation lines (Fig.2a) and some grains not yet subdivided present dislocation lines with some dislocations rearranged into a network (Fig.2b). A very low disorientation angle (equal to 2.35°) is calculated with the *pycotem* [3] disorientation module using the specific stereo projections on areas located on both sides of this dislocation network. This low disorientation value suggests that the grain subdivision process is in its early stages. Based on our TEM observations, we can also suppose that the metallic precipitates can hinder the movement of

dislocations because they are anchored to them. Moreover, a part of the xenon is found at a grain boundary enclosed into bubbles/cavities.

Thanks to the nanoscale characterization of the MOX fuel, a comprehensive view and deeper insight on the RNR fuel microstructure and associated mechanisms is reached and complements microscale characterizations.

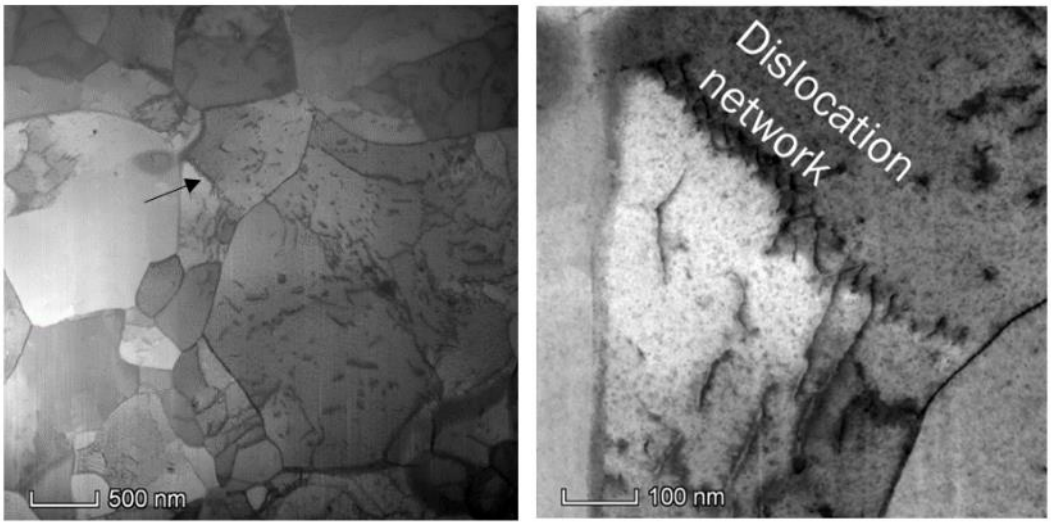

Figure 2: TEM bright field images of the lamella taken at 0.98R, a) with small grains free from dislocation lines and grains larger with dislocations b) zoom on a dislocation network.

[1] “Determination of the inelastic mean free path in (U, Pu)O_2 fuels by means of electron energy loss spectroscopy (EELS) and Convergence beam electron diffraction” D. Reyes, M. Angleraud, C. Onofri, D. Drouan, C. Sabathier, Abstract Plutonium Futures 2022, 26-29 September in Avignon.

[2] GERMINAL, a fuel performance code of the PLEIADES platform to simulate the in-pile behaviour of mixed oxide fuel pins for sodium-cooled fast reactors", M. Lainet, B. Michel, J.-C. Dumas, M. Pelletier, I. Ramière, JNM 516, 2019, 30-53.

[3] Mompiou F, Xie R-X. "pycotem: An open source toolbox for online crystal defect characterization from TEM imaging and diffraction ". Journal of Microscopy. 2020, 1–14.

First gamma irradiation studies of AmSel extraction system

P. Vacas-Arquero [1], I. Sánchez-García [1], H. Galán [1]

[1] Centro de Investigaciones Energéticas, Medioambientales y Tecnológicas (CIEMAT)

Pablo.Vacas@ciemat.es

One of the main issues nowadays towards the future of Nuclear Power is the proper and efficient management of nuclear waste. As one of the most sustainable solutions, the scientific community is working on advanced nuclear fuel cycles. Particularly, on the demonstration of totally closed fuel cycles, where the recovery of valuable fissile and fertile materials are not the only main goals, but also the reduction of the volume and radiotoxicity of the waste to be emplaced in the geological disposal facility. For this purpose, the separation of the most relevant minor actinides (MA: Np, Am, and Cm) from fission products like lanthanides (Ln) is required. From the different possible scenarios, the heterogeneous recycling one comes with the reuse of uranium and plutonium and the burning of MA as specific fuels or targets. Additionally, this situation implies the separation of curium from americium, since the presence of Cm during fuel manufacturing would difficult a lot the manage because of its high decay heat and neutron emission and its contribution to long term heat load and radiotoxicity is not really significant. Therefore, curium should be routed with the fission products for final disposal after decay storage [1].

However, due to the similar chemical behaviour between americium and curium, their separation means one of the biggest challenges for the scientific community, reason why several new strategies based on liquid-liquid extractions are currently being developed. This is the case of the AmSel (*Americium Selective Extraction*) process [2]. In the first stage of the AmSel process, the trivalent lanthanides and actinides from PUREX raffinate are co-extracted by using TODGA (*N*,*N*,*N*,*N*-tetraoctyl diglycolamide) based solvent. After that, a hydrophilic tetra-*N*-dentate ligand, the water soluble SO_3-Ph-BTBP (6,6'-bis(5,6-di(sulfophenyl)-1,2,4-triazin-3-yl)-2,2'-bipyridine), is proposed to selectively strip Am(III) from Cm(III) and the Ln(III). This separation is achieved thanks to the inverse selectivity of BTBP ligands and TODGA towards Am and Cm (Figure 1).

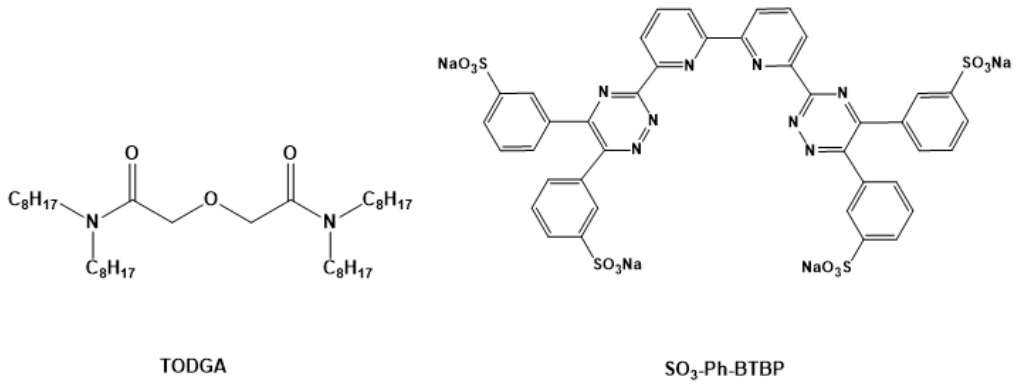

Figure 1: Current reference molecules in the key step of AmSel process [2].

Since both, aqueous and organic, phases are in continuous contact with highly radioactive solutions and high nitric acid concentrations, the suitability of extractants is determined, not only by their good

extraction properties, but also by their degradation resistance. The degradation of these molecules can lead to undesirable effects such as decrease of selectivity, third phase formation, degradation compounds generation, etc, which could increase the volume of secondary wastes and process costs. Most often, the new species generated could have extracting properties that markedly differ from those of the original ligands. TODGA based solvents have been successfully employed for different separation strategies because of its good extraction properties, but also, its high resistance to radiation, which has been widely studied by many authors [3-7]. This is not the case of the selected stripping agent selected for AmSel process, only a preliminary study of SO_3-Ph-BTBP stability has been described until now [8].

In this work, we summarize the first stability studies of the reference AmSel system, which have been designed and performed to obtain conclusions about the aqueous phase resistance. For such studies, we have first explored the stability against gamma radiation of SO_3-Ph-BTBP and compared with its analogue, the An stripping agent SO_3-Ph-BTP ((2,6-bis(5,6-di(sulfophenyl)-1,2,4-triazin-3-yl) pyridine)). Moreover, it is shown the initial results of the first stability studies of the full AmSel systems applying the recent methodology described for TODGA/SO_3-Ph-BTP systems, where the most relevant process conditions have been simulated. For that, the extraction behaviour after gamma radiation has been checked by gamma-ray and alpha spectrometry (using ^{152}Eu, ^{241}Am and ^{244}Cm) and the change in solvent composition have been analysed by HPLC-MS and Raman spectroscopy.

This project has received funding from the Euratom research and training programme 2019-2020 under grant agreement No 945077.

1. Collins, E., et al., *State-of-the-Art Report on the Progress of Nuclear Fuel Cycle Chemistry*. 2018, Organisation for Economic Co-Operation and Development.
2. Wagner, C., et al., Solvent Extraction and Ion Exchange, 2016. **34**(2): p. 103-113.
3. Galán, H., et al., Procedia Chemistry, 2012. **7**: p. 195-201.
4. Sugo, Y., Y. Sasaki, and S. Tachimori, Radiochimica Acta, 2002. **90**(3): p. 161-165.
5. Modolo, G., et al., Solvent Extraction and Ion Exchange, 2007. **25**(6): p. 703-721.
6. Zarzana, C.A., et al., Solvent Extraction and Ion Exchange, 2015. **33**(5): p. 431-447.
7. Sánchez-García, I., et al., EPJ Nuclear Sciences & Technologies, 2019. **5**: p. 19.
8. Jose, J., et al., Journal of Radioanalytical and Nuclear Chemistry, 2021. **328**(3): p. 1127-1136.

Preparation of Homogenous (U,Pu) Mixed Oxides via Oxalate Precipitation

H. Colledge [1], M. Sarsfield [1], C. Maher [1], R. Taylor [1] and R. Sanderson [1]

[1] National Nuclear Laboratory, Central Laboratory, Sellafield, Seascale, Cumbria, CA20 1PG, UK

Hannah.m.colledge@uknnl.com

---

n co-operation with the National Nuclear Laboratory, UK Government has initiated an "Advanced Fuel Cycle Programme" (AFCP) looking at future options for advanced fuel manufacture and spent fuel recycle and waste management. The development of advanced reprocessing flowsheets for future actinide recycling is a key element of this programme. It is anticipated that these separation processes will produce a range of mixed transuranic (TRU) actinide nitrate products rather than the pure plutonium stream produced in current reprocessing plants. This will help reduce perceived proliferation risks associated with current reprocessing plants that produce separate uranium and plutonium products and simplify the downstream mixed oxide (MOX) fuel manufacturing process.

Investigations presented here have focused on the 'finishing' process using the oxalate precipitation route enabling co-conversion of actinides. It is envisaged that advanced separation processes will allow part of the uranium stream to flow with the plutonium stream, so that co-precipitation as the oxalate will ensure a homogenous distribution of the two actinides at the molecular scale. This will be followed by joint conversion of uranium and plutonium to the dioxide powder form by thermal decomposition. One advantage is that this can remove the complicated downstream step of blending and grinding the two distinct oxide powders, as currently used in MOX fuel fabrication.

Experimental work has focused on the co-precipitation of uranium(IV) and plutonium(III) and characterisation of the resultant oxalates and oxides. The co-precipitation of U(IV) and Pu(III) at varying concentrations has been investigated on both a small scale (up to 26g/L heavy metal concentration) to prove the experimental set up and conditions, followed by a series of larger scale experiments (up to 150 g/L heavy metal concentration) that are closer to pilot scale concentrations from the advanced reprocessing flowsheet created as part of the separations programme. Uranium(VI) and plutonium(IV) were electrochemically conditioned at -1 V to uranium(IV) and plutonium(III), in the presence of hydrazine. The reduced uranium(IV) and plutonium(III) nitrates were combined with oxalic acid using the direct strike method, at ambient temperature to promote precipitation to the mixed oxalate.

All the mixed uranium-plutonium oxalate solid products have been characterised by Infrared spectroscopy and a portion by X-Ray diffraction to confirm the phase of the oxalate solid. The (U,Pu) oxalates were then calcined to the oxide under different atmospheres (air and argon) and temperatures (650, 700 and 900 °C) and characterised to determine if a homogenous mixed oxide was produced. In the next phase, experimental work will look at the pelleting and dissolution of the mixed oxides produced under this programme.

Synthesis of plutonium trichloride for molten salt reactor technology

M. Fucina[2]a, P. Souček[1], A. Rodrigues[1], E. Capelli [3], O. Beneš[1], O.Walter[1] , O. Tougait[2], R.J.M. Konings[1]

[1] European Commission, Joint Research Centre (JRC), Karlsruhe, Germany[1] Visiting scientist at the Joint Research Center
[2] Univ. Lille, CNRS, UMR 8181 - UCCS - Unité de Catalyse et Chimie du Solide, F-59000, Lille, France
[3] Orano, 92320, Châtillon, France

meghann.fucina@ext.ec.europa.eu, meghann.fucina@univ-lille.fr

---

The nuclear energy future will strongly benefit from the closure of the fuel cycle, reducing the natural resources needs and the amount of the generated radioactive waste to be disposed. Even though some solutions to reuse fissile Pu239 as mixed oxide fuel (MOX) are employed at present, significant improvement in fissionning all the Pu isotopes and minor actinides can be achieved with the introduction of fast-spectrum advanced reactor systems. A molten salt reactor (MSR) using chloride salts is a very promising advanced reactor system aiming to reuse and valorise plutonium from the spent fuel and other sources. Chloride salts are often retained for the fast spectrum concepts, as they provide harder neutron spectra and higher solubility of actinides. For the design and safety assessment of this reactor, the knowledge of thermodynamic and thermo-physical properties of actinide chlorides and their mixtures is required. Nevertheless, few experimental data are available. Obtaining pure $PuCl_3$ is key for accurate determination of the fuel properties and it is nowadays still a challenge.

In this work, plutonium trichloride was synthesized based on a gas-solid reaction, proposed by West *et al.* [1] in 1988. Nanometric plutonium dioxide was used as starting material and various combinations of Ar, Cl_2 and CCl_4 gas were used as chlorinating agent. Different reactions parameters were investigated, such as temperature, excess and composition of the reaction gases, and the results are presented in this work. Thermodynamic calculations were also performed to assess the reaction conditions and support interpretation of the results.

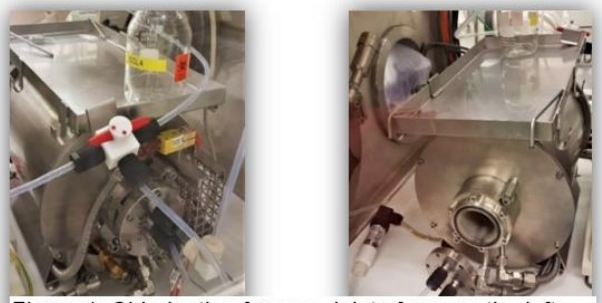

Figure 1: Chlorination furnace, inlet of gas on the left, outlet on the right

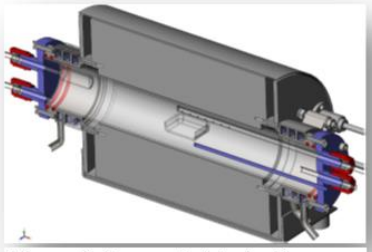

Figure 2: Draw of chlorination furnace

The syntheses took place in a horizontal furnace in a glovebox filled with nitrogen atmosphere (see Figure 1). The flanges on each side of the furnace are from Inconel 750, selected to minimize corrosion while the reaction is carried out in a 35 cm removable quartz tube. The PuO_2 powder was inserted in

a 5 cm quartz boat which was then placed in the centre of the tube in a homogeneous temperature zone. The gas was led directly above the boat through a quartz inlet tube (see Figure 2).

Results of many different chlorination runs showed that a mixture of Cl_2/CCl_4 avoiding the use of Ar during the chlorination shows satisfactory results yielding a $PuCl_3$ product with conversion efficiency up to 97%, while a multi-phase containing products were obtained when using Ar as a carrier gas.

Nevertheless, some plutonium dioxide remain in the $PuCl_3$ product even with a large excess of CCl_4. A method of extraction by an organic solvent, tetrahydrofuran (THF) was attempted, followed by heat treatment under a flow of chlorine. Powder x-ray diffraction (PXRD) of such obtained final product revealed a phase pure $PuCl_3$ (see Figure 3).

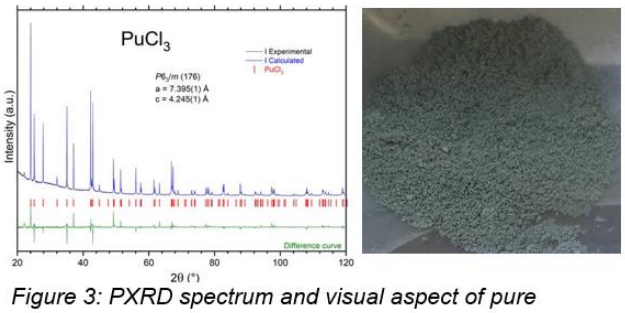

Figure 3: PXRD spectrum and visual aspect of pure plutonium trichloride

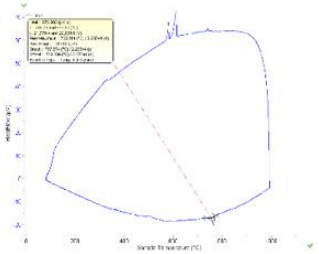

Figure 4: DSC measurement on $PuCl_3$ after purification by solvent extraction

However, evidence of a reaction occurring at high temperature measured by differential scanning calorimetry, showed that traces of another phase or moisture were still present in the product. This resulted in two peaks at the DSC curve during the cooling (see Figure 4).

It can be explained by a presence of residual THF in the product not detected by PXRD, as the remaining moisture usually present in THF would lead to partial conversion of $PuCl_3$ to PuOCl and consequently to formation of $PuCl_3$-PuOCl solution at high temperature. This explanation is strongly supported by the fact that the detected melting temperature corresponds to the eutectic temperature of this solution.

[1] H.West, Michelle D. Ferran, K. W. F. Mike “The Chlorination of Plutonium Dioxide,” *Nature*, vol. 412, no. 6848, pp. 681–681, 1988, doi: 10.1038/35089124.

A Contemporary Investigation of Clementine

R.C. Johns [1], F.J. Freibert [1] and H. Patenaude [2]

[1] Los Alamos National Laboratory, PO Box 1663, Los Alamos, NM 87545 USA

[2] University of Nevada, Las Vegas 4505 S Maryland Pkwy, Las Vegas, NV 89154 USA

johns@lanl.gov

At the end of WWII, a group of Los Alamos pioneering researchers led by Jane and David Hall designed and built the world's first fast reactor nicknamed "Clementine". This reactor was unique in many aspects as a critically important high intensity fission-neutron source and novel platform to prove the adaptability of plutonium as a reactor fuel. Fast reactor fission is accomplished with high-energy neutrons, and so Clementine was designed as a Pu alloy core with no moderating material. Thus, the neutrons in its core had a fission energy spectrum desirable for nuclear research and for acquiring nuclear cross-section data needed by the bomb designers. Furthermore, Clementine provided information about fast reactors, i.e., control characteristics and nuclear breeding properties required for post-war production of power and generation of fissile materials. With the aid of well-archived design information and experimental data, we are conducting a modern reactor analysis of Clementine to further explore and characterize this singularly unique experimental device.

Manufacturing of $(U,Pu)O_{2-x}$ mixed oxides with high plutonium contents (> 60 mol.%).

M-M. Desagulier [1], P.M. Martin [1], J. Martinez [1], C. Guéneau [2], N. Clavier [3]

[1] *CEA, DES, ISEC, DMRC, Université Montpellier,* Marcoule, France
[2] *Université Paris Saclay, CEA, DES, ISAS, DPC*, Gif-sur-Yvette, France
[3] *Institut de chimie séparative de Marcoule, ICSM, CEA, CNRS, ENSCM, Université de Montpellier*, Marcoule, France

marie-margaux.desagulier@cea.fr

Uranium-Plutonium mixed oxides $U_{1-y}Pu_yO_{2-x}$ (MOX) are considered as reference fuels for Sodium-cooled Fast neutron Reactors (SFRs). Their plutonium content and their Oxygen/Metal ratio (O/M with M = U + Pu) must range between 20 to 35 mol. % and $1.94 \leq O/M < 2.00$, respectively. Under irradiation, a thermal gradient along the fuel pellets radius (typically ~4 mm) occurs, with a temperature reaching 773 K close to the cladding and 2073-2273 K at the center [1]. This thermal gradient induces a redistribution of plutonium and oxygen atoms along the radius. Therefore, the center of the pellet is enriched in plutonium with a local Pu content in the 30-70 mol. % range (depending on the location in the core and its initial Pu content and O/M ratio) and depleted in oxygen leading to a reduced O/M ratio (< 1.95). Close to the cladding, Pu content is ~20 mol. %, and the O/M ratio is close to 2.00. These mass transport phenomena lead to significant heterogeneities in the thermo-physical properties of the fuel along the pellet radius. For instance, the local melting point will be modified as it depends upon both the O/M ratio and the Pu content of the mixed oxide. In particular, an enriched local plutonium content induces a decrease in the melting temperature and thus a decrease in the safety margin of the reactor. As shown in Figure 7, up to y ~ 50% a decrease of the $(U,Pu)O_2$ melting point is experimentally observed. However, above 60%, values available in the literature show large discrepancies, with deviations up to 300K. The investigation of the thermodynamic and structural properties of U-Pu mixed oxides with high plutonium content is thus mandatory.

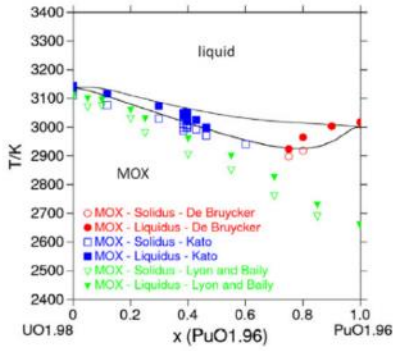

Figure 7. Calculated $UO_{1.98}$–$PuO_{1.96}$ section by Gueneau et al. [7].

The main difficulty lies in the lack of experimental data (enthalpy, heat capacity, conductivity or melting temperature, …) for MOX fuels with Pu content greater than 60 mol. % [2-6]. To fill this lack and further improve the thermodynamic modelling of the U-Pu-O system, it is necessary to provide new experimental input data for the fuel behavior simulation codes [8]. The first step consists in

manufacturing single-phase and dense MOX pellets with Pu contents between 60-70 mol . %. Due to the complexity of the U-Pu-O phase diagram in the oxygen hypo-stoichiometric domain (O/M < 2.00) the main difficulties lie in the determination of the appropriate manufacturing parameters [9].

The optimized manufacturing process based on powder metallurgy allowing to obtain such dense and monophasic MOX pellets with Pu content of 60, 65 and 70 mol.% will be detailed. The associated multi-scale characterization results will be described in order to demonstrate that the targeted properties could be obtained. As an example, pseudo-quantitative maps obtained by Electron Probe Micro-Analysis are presented in Figure 8. It shows the homogeneous distribution of cations with U-rich agglomerates (< 80 µm) and confirms the Pu targeted.

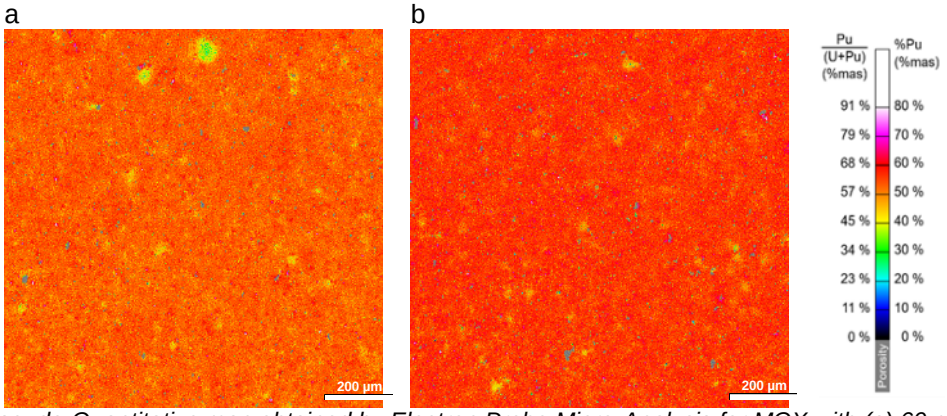

Figure 8. Pseudo-Quantitative map obtained by Electron Probe Micro-Analysis for MOX with (a) 60 mol. % of Pu and (b) 65 mol. % of Pu.

This research is carried out as part of the European PuMMA project (Plutonium Management for More Agility) which has received funding from the European Union's Horizon 2020 (grant agreement No 945022).

[1] Y. Guerin, Comprehensive Nuclear Materials, 2012, p. 547-578, Elsevier Ltd.

[2] F. De Bruycker *et al.*, *J. Nucl. Mater.*, 2011, vol. 419, p. 186-193.

[3] T. Truphémus *et al., J. Nucl. Mater.*, 2013, vol. 432, p. 378-387.

[4] R. Böhler *et al., J. Nucl. Mater.*, 2014, vol. 448, p. 330-339.

[5] R. Vauchy *et al., Ceram. Int.*, 2014, vol. 40, p. 10991-10999.

[6] M. Strach *et al., Nucl. Instrum. Methods Phys. Res. B*, 2016, vol. 374, p. 125-128.

[7] C. Guéneau *et al., J. Nucl. Mater.*, 2011, vol. 419, p. 145-167.

[8] M. Lainet *et al., J. Nucl. Mater.*, 2019, vol. 516, p. 30-53.

[9] C. Guéneau *et al.*, Comprehensive Nuclear Materials, 2012, vol. 2 chap. 02, p. 21-59, Elsevier Ltd.

Effects of salt concentration and ionic strength on transuranic separations from aqueous chloride waste streams using a quaternary ammonium ionic liquid

H. Rasmussen [1], J. Droessler [1], G. Goff [1], A. Nichols [1]

[1] Material Physics and Applications Division, Los Alamos National Laboratory

P.O. Box 1663, Bikini Atoll Road, SM-30, Los Alamos, NM 87545

hrasmussen@lanl.gov

Separation of plutonium (Pu) and its daughter products, particularly americium (Am), from other radionuclides and metals in aqueous chloride waste streams is of pressing importance for recovery of valuable products and reduction of hazard classification for end-of-life disposal of nuclear waste. Many current separation techniques involve chromatographic separation using ion exchange with extractants mounted on resins. These processes can be inefficient in speed and product yield and create high-level solid waste from resin disposal. Los Alamos National Laboratory (LANL) has been investigating alternative solvent-extraction chemistries to the traditional PUREX-like process chemistry. Pyrochemical separations generate chloride-based waste streams, and improvements in current hydrometallurgical process are necessary to decrease the time needed for separation and thus dose to the operator while greatly increasing the throughput of waste and overall product recovery [1].

This study analyzes the use of the quaternary ammonium ionic liquid Aliquat 336® for the extraction of Pu through anion exchange and ion association of metal chloride species in a range of hydrochloric acid (HCl) and chloride salt concentrations [2, 3]. The design of the system aims to selectively recover Pu(IV) over Am(III) and other transition metal impurities. Aqueous chloride separations in this study are simulated with surrogate metals and potential co-contaminants in process-appropriate ranges of HCl and salt eutectic matrices prior to testing with plutonium [1]. Thermodynamic studies explore the effect of ionic strength and pH on the extraction efficiency. Primary analytical techniques include inductively coupled plasma - optical emission spectrometry (ICP-OES) and ultraviolet – visible spectroscopy (UV-VIS).

Batch extractions were performed for 3 wt % and 10 wt % Aliquat 336® in xylenes contacted with single and multi-element combinations of Fe(II), Fe(III), U(IV), U(VI), and Nd(III) dissolved in various concentrations of HCl with and without the presence of chloride salts. From these extractions, distribution ratios (K_D) were obtained as shown in Equation 1, where $[Me]_{org}$ and $[Me]_{aq}$ are the concentrations of metal in the final organic and aqueous phases, respectively.

$$K_D = \frac{[Me]_{org}}{[Me]_{aq}} \quad (1)$$

For these extractions, Nd(III) serves as an Am(III) surrogate, while the other metals serve dual purposes as both Pu surrogates and co-contaminants. Figure 1 shows distribution ratio results for Fe(II), Fe(III), and Nd(III) in a range of HCl and NaCl/KCl compositions contacted with 3 wt % Aliquat 336® in xylenes, plotted as a function of total chloride concentration.

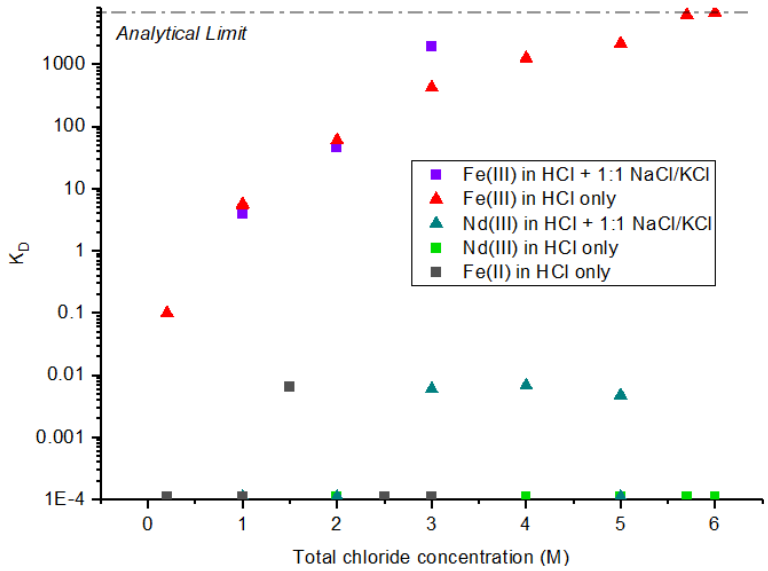

Figure 9 - Distribution ratios (K_D) for Fe(II), Fe(III), and Nd(III) in a range of HCl and 1:1 mole sodium chloride:potassium chloride (NaCl/KCl) salt eutectic mixtures contacted with 3 wt % Aliquat 336 in xylenes. K_D is equal to the concentration of metal in organic divided by the concentration of metal in the aqueous after 10 minutes of mixing of 1:1 organic:aqueous fractions.

This work provides the foundation for the eventual system design for Pu loading and recovery under aqueous chloride waste stream relevant conditions. Results thus far from surrogate testing indicates that Aliquat 336® in xylenes is a promising extractant for separation of Pu from Am that would provide subsequent high yield recovery of Pu from chloride waste streams.

Acknowledgements: We thank the U.S. Department of Energy, National Nuclear Security Agency, Plutonium Program Office (NA-191) for their support of this project.

[1] Reichley-Yinger, L. and G.F. Vandegrift, *Recovery of Plutonium and Americium from Chloride Salt Wastes by Solvent Extraction.* Separation Science and Technology, 1988. **23**(12-13): p. 1409-1421.
[2] Bhandiwad, V.R., R. Swarup, and S.K. Patil, *Extraction of actinides by quaternary amines from hydrochloric acid medium.* Journal of Radioanalytical Chemistry, 1979. **52**(1): p. 5-14.
[3] Seeley, F.G. and D.J. Crouse, *Extraction of Metals from Chloride Solutions and Amines.* Journal of Chemical & Engineering Data, 1966. **11**(3): p. 424-429.

Modelling of (U-Pu)O_2 powder die compaction for nuclear fuel fabrication and characterization method for elasto-plastic model identifications

J-Ph. Bayle [1], A. Haultcoeur [2], F. Ledrappier [3], [4]

[1] CEA, DES, ISEC, DMRC, Université de Montpellier, Marcoule, France

[2] Université de Lorraine, Polytech Nancy, Material structure and mechanic, France

[3] Technetics Group France, Laboratoire d'Etanchéité, 2 rue James Watt, F-26700 Pierrelatte, France

[4] CEA, DES, ISEC, DE2D, Université de Montpellier, Pierrelatte, France - CEA Marcoule, DES/ISEC/DMRC/SPTC/LSEM, BP 1717, 30207 Bagnols sur cèze cedex

Jean-philippe.bayle@cea.fr

The nuclear fuel is produced by the ceramic process, which includes the grinding, pressing and sintering stages. Due to the presence of actinides in the fuel powder to be shaped, the grinding of the pellets to fit with the cylindricity requirements is prohibited after sintering. Therefore, the sintered pellets must be considered as «Net shape» or at the final dimension without grinding [4]. In order to predict the influences of the PuO_2 percentage on the pellet final shape, the finite element method simulates the shaping by integrating the geometry of the tools as well as the kinematic parameters of the compaction press. In addition, it is necessary to have a constitutive model of the (U-Pu)O_2 powder during its densification. We chose to use the Drucker Prager cap model [1], [2], [3], [6] for which we have to identify a number of parameters. The identification of these parameters requires doing of a large number of pellets with a sacrifice of the powder. Through this study, an alternative is proposed in order to minimize the number of tests while maintaining an equivalent representativeness of the model [5], [7]. The annular pellet simulation results by Abaqus code are shown and compared to the manufacturing results obtained with instrumented die set on the hydraulic press in LN0 Atalante facility laboratory.

[1] L.H. Han, J.A. Elliott, "A modified Drucker-Prager Cap model for die compaction simulation of pharmaceutical powders" - International Journal of Solids and Structures 45, Science Direct, 2008

[2] J-Ph. Bayle, "Nuclear fuel shaping: specific die press development and modelling" - Shaping VI-Sixth international conference on shaping and advanced ceramics, July 2016.

[3] P-R. Brewin, O. Coube, P. Doremus, J-H. Tweed, Modelling of Powder Die Compaction, Engineering Material and Processes, Springer, 2008

[4] J-Ph. Bayle, G. Delette, Finite element modelling and experiments for shaping nuclear powder pellets, application in technological tool developments to minimize damage during ejection and geometrical tolerances, Procedia Chemistry 7 (2012) 444-455

[5] C-L. Martin, O. Lame, D. Bouvard. Cohesion and dilatation of powder compacts containing hard phase particules under highly deviatoric stress states. Article Mechanics of materials 32 (2000) 405-421. 2000.

[6] Mengcheng Zhou and all. A density-dependent Drucker-Prager Cap model for die compaction of Ag57.6-Cu22.4-Sn10-Ln10 mixed metal powders. Article Powder Technology, 305 (2017) 183-196. 2017.

[7] G. Bernard-Granger and all, Rheological properties of alumina powder mixtures investigated using shear tests, Powder technology, 345(2019) 300-310

Detection and Analysis

	Conference room #2: CHAMBRE DU TRÉSORIER
INVITED TALK 10:00 – 10:30	**Mike SAVINA (LLNL)** *"Nuclear fuel analysis by resonance ionization mass spectrometry"*
INVITED TALK 11:00 – 11:30	**Michael KRACHLER (European Commission - JRC)** *"Analytical Strategies for Bulk and Spatially-resolved Analysis of U and Pu Isotopes in Nuclear Samples"*
11:30 – 11:50	**Sarah HICKAM (LANL)** *"Local structure and distribution of impurities in PuO_2: forensic signatures of formation conditions"*
11:50 – 12:10	**Bianca SCHACHERL (KIT)** *"Pu M4 and M5 edge Resonant Inelastic X-ray Scattering of PuO_2"*
12:10 – 12:30	**Sébastien PICART (CEA)** *"Coulometry analysis of plutonium in the presence of excess uranium: focus on the effect of sulfate complexation"*
	Conference room #1: CELLIER BENOIT XII
PLENARY TALK 14:00 – 14:50	**Peter MARTIN (University of Bristol)** *"Advances in the Micro-Analysis of Environmentally Sourced Nuclear Materials"*
	Conference room #2: CHAMBRE DU TRÉSORIER
INVITED TALK 15:00 – 15:30	**David MEIER (PNNL)** *"Recent Developments on the Production and Morphological Analysis of Plutonium Oxalate and Oxide Compounds"*
15:30 – 15:50	**Brandon CHUNG (LLNL)** *"Morphological Provenance Signatures from Plutonium and Uranium Oxide Scales"*
16:20 – 16:40	**Matthew HIGGINSON (AWE)** "Development of Direct Analysis Approaches on Solid Plutonium Samples for Actinide Analysis"
16:40 – 17:00	**Eliel VILLA-ALEMAN (Savannah River National Laboratory)** *"Spectroscopy Research of Pu-bearing Compounds at the Savannah River National Laboratory"*
17:00 – 17:20	**Lav TANDON (LANL)** *"Challenges Associated with Plutonium Pyrochemical Process Monitoring Deploying Unique Analytical Tools & Techniques"*
17:20 – 17:40	**Adah ZHANG (Sandia National Laboratories)** *"A Functional Statistical Modelling Approach to Using Plutonium Particle Features from Scanning Electron Microscope Images"*

Chair persons:

Klaus LUETZENKIRCHEN and Jean AUPIAIS

Nuclear fuel analysis by resonance ionization mass spectrometry

M. Savina [1], B. Isselhardt [1], D. Z. Shulaker [1]

[1] Lawrence Livermore National Laboratory, 7000 East Ave. Livermore California USA

savina1@llnl.gov

Most nuclear reactor fuel begins as fairly pure uranium oxide or metal and accumulates fission and neutron capture products as it self-irradiates. The isotopic compositions of those products provide valuable information on reactor operation history for comparison with declared activity. Because spent fuel is extremely radioactive, methods that maximize information obtained from small samples and minimize handling are valuable.

Resonance Ionization Mass Spectrometry (RIMS) is a mass spectrometric method that operates directly on solid materials without sample pre-treatment. In brief, surface material is removed from a solid by a pulsed ion or laser beam and ionized above the surface by one or more lasers tuned to electronic resonances in the element of interest. The photo-ions created by the lasers are detected by time-of-flight mass spectrometry. Because the ionization is resonant, the element of interest is detected with far higher efficiency than other elements present in the sample. There are several characteristics that make RIMS an extremely useful and unique mass spectrometric method. Firstly, isobaric interference is greatly suppressed, such that sample preparation (i.e. elemental separation) is unnecessary. Also, resonant ionization is very efficient, resulting in higher detection efficiency than other forms of mass spectrometry. For example, RIMS has a maximum U detection efficiency of 38% [1], compared to ~2% for other forms of mass spectrometry (SIMS, TIMS, ICPMS). RIMS is a microbeam technique, applicable to spatially resolved analyses. Finally, the sputtering and ionization processes during RIMS are pulsed, so that the time of birth of various ions, and thus their arrival times at the detector, can be controlled and isobars resolved. For example, delaying the ionization of Pu with respect to U and Am enables the simultaneous analysis of isobaric pairs such as $^{238}U/^{238}Pu$ and $^{241}Pu/^{241}Am$.

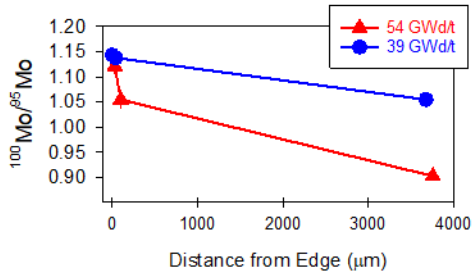

Figure 1: Mo isotope ratios as a function of radial position in a fuel pellet. Pellet center at ~4000 μm.

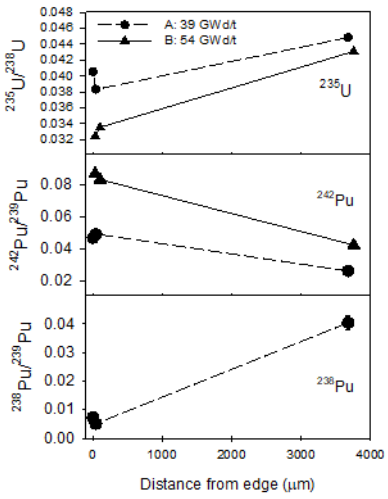

Figure 2: U and Pu isotope ratios as a function of radial position in a fuel pellet. Pellet center is at ~4000 μm.

The isotopic analysis of small (10 μm) samples of solid fuel from a PWR reactor show characteristic spatial variations due to the uneven neutron flux [2]. Figure 1 shows selected U and Pu isotope ratios from two different fuel pellets with burnups of 39 and 54 GWd/t. The $^{235}U/^{238}U$ is lower for the higher burnup sample, as expected since more ^{235}U was consumed. The ratio drops at the pellet edge reflecting the higher burnup experienced in that region of the pellet due to the skin effect. Two different neutron capture effects are seen in Pu. The Pu isotopes $^{239\text{-}242}Pu$ are seeded by ^{238}U, such that the $^{242}Pu/^{239}Pu$ ratio increases strongly at the pellet edge where epithermal neutrons are captured efficiently by ^{238}U due to a resonance in that region of the neutron energy spectrum. The opposite trend is seen in $^{238}Pu/^{239}Pu$, because ^{238}Pu is seeded by ^{235}U, which lacks such a resonance. In fact, this difference in seed nuclei can be exploited so that the radial change in $^{238}Pu/^{239}Pu$ seen in Fig. 1 can be used as a proxy for the overproduction of ^{239}Pu near the pellet edge [2].

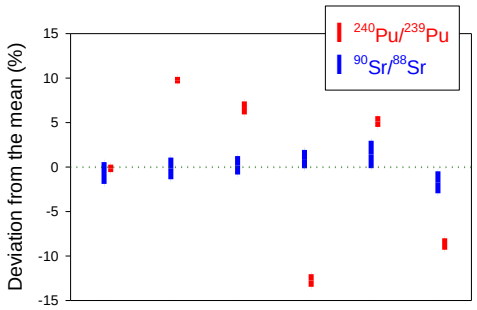

Figure 3: Deviations in the Pu (blue) and Sr (red) isotopic ratios from the mean of six samples. Samples were 10 μm cubes of BR3 fuel from a single fuel rod. Uncertainties are 1σ.

Fission products also show strong spatial effects, due to neutron capture and to differences in the relative fission yields from ^{235}U and ^{239}Pu. For example, the $^{100}Mo/^{95}Mo$ ratio rises at the pellet edge due to the increased contribution of ^{239}Pu fission (Fig.2), which is overproduced at the pellet edge as described above. Analyses of this and other fission products provide additional constraints on reactor operation history.

In contrast to most other isotopic systems, the Sr isotopic composition is spatially homogeneous across a reactor. The $^{90}Sr/^{88}Sr$ ratio is largely unaffected by neutron capture, and only minimally affected by the parent fissile isotope (e.g., ^{235}U or ^{239}Pu). By far the largest factors determining the $^{90}Sr/^{88}Sr$ ratio are the irradiation and the cooling times. Figure 3 shows Pu and Sr isotope ratios measured in six samples of spent fuel. One cannot ascertain from the Pu isotopics alone whether the samples come from a single reactor core. However, the $^{90}Sr/^{88}Sr$ ratio (red bars) is consistent across the set, clearly indicating the common irradiation and cooling history of all six samples. Further, simple reactor modeling of the Sr isotopics yields an accurate cooling time (40.8 yr) within 0.4 years.

This work was supported by the NNSA Office of Defense Nuclear Nonproliferation Research and Development. LLNL-ABS-833155

References:

1. Savina, M.R., et al., *Analytical Chemistry*, 2018, **90**(17): p. 10551-10558.
2. Savina, M.R., B.H. Isselhardt, and R. Trappitsch, *Analytical Chemistry*, 2021, **93**(27): p. 9505-9512.

Analytical Strategies for Bulk and Spatially-resolved Analysis of U and Pu Isotopes in Nuclear Samples

M. Krachler, Z. Varga, A. Nicholl, M. Wallenius, K. Mayer

European Commission - Joint Research Centre,
P.O. Box 2340, 76125 Karlsruhe, Germany

michael.krachler@ec.europa.eu

Mass spectrometric techniques such as inductively coupled plasma-mass spectrometry (ICP-MS), multi-collector (MC)-ICP-MS and thermal ionization mass spectrometry (TIMS) are commonly applied to determine U and Pu isotopes in a large variety of samples. Such analyses are often complemented by measurements using α- and γ-spectrometry. However, also commercial high resolution (HR)-ICP-optical emission spectrometers allow for the isotopic determination of actinides such as U and Pu [1,2]. The isotopic splitting of emission lines of different U and Pu isotopes can be resolved with such instruments. Because U and Pu are emitting light in different wavelength regions, ^{238}U and ^{238}Pu can be analysed simultaneously without a prior chemical separation of the two elements from each other. This presentation will highlight selected applications of HR-ICP-OES analysis of U and Pu isotopes including the assessment of diverse U enrichments and the determination of the production age (^{234}U/^{238}Pu age-dating) of ^{238}Pu samples (Fig. 1). Although HR-ICP-OES measurements do not provide the precision achievable with mass spectrometry, they are fit-for-purpose for above-mentioned applications employing relatively cheap instrumentation.

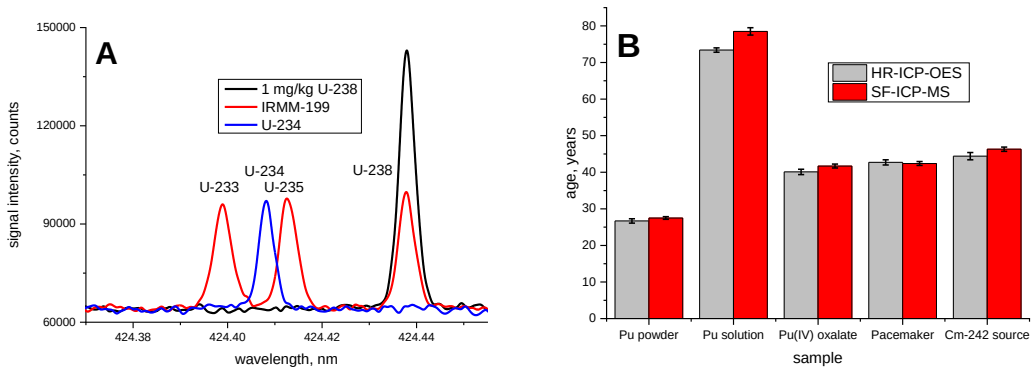

Figure 1: (A) Highly-resolved optical emission spectrum highlighting the isotope-specific identification of the ^{238}Pu daughter product ^{234}U [2]. (B) Comparison of ^{234}U/^{238}Pu ages (years) of five selected Pu-bearing samples as determined using high resolution ICP-OES and sector field ICP-MS [2].

While most U and Pu isotopic analyses with atomic spectrometry methods consider the entire sample or a fragment thereof (bulk measurements), spatially-resolved analysis on the µm scale provides additional insights into the production and homogeneity of nuclear forensic samples, for example. Coupling laser ablation (LA) to a (MC)-ICP-MS instrument is a straightforward way to achieve this goal [3-6]. Such an analytical approach not only is much faster than conventional solution-based analysis, requiring dissolution and chemical separation of the analyte, but also avoids generation of additional radioactive waste when working with nuclear material. Differences in isotopic enrichments can be identified within a few hours while the sample remains virtually unchanged, a key aspect in nuclear forensic investigations [7].

Employing "line scan" analysis, a small laser beam of a few nm is continuously moved across the sample surface generating numerous individual, spatially-resolved U isotopic ratios. This talk will present selected examples of the assessment of the U isotopic inhomogeneity of various UO_2 pellets and scrap metal samples using LA-MC-ICP-MS. Results will be put into perspective by comparing them to both bulk analysis using TIMS and γ-spectrometry as well as particle analysis employing secondary ion mass spectrometry (SIMS).

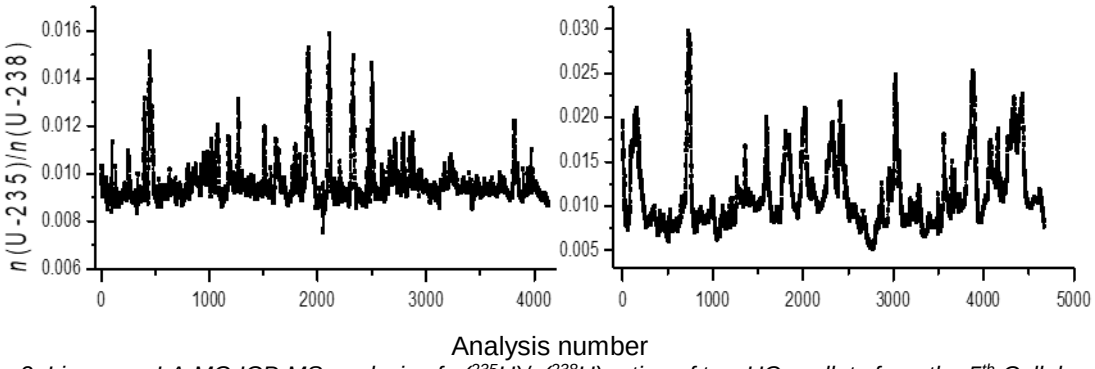

Figure 2: Line scan LA-MC-ICP-MS analysis of n(^{235}U)/n(^{238}U) ratios of two UO_2 pellets from the 5th Collaborative Materials Exercise (CMX-5). more (left) and less (right) homogeneous pellet [4].

References:

[1] M. Krachler, P. Carbol, Validation of isotopic analysis of depleted, natural and enriched uranium using high resolution ICP-OES, J. Anal. At. Spectrom. 26 (2011) 293-299.
[2] M. Krachler, R. Alvarez-Sarandes, G. Rasmussen, High resolution inductively coupled plasma optical emission spectrometry for ^{234}U/^{238}Pu age dating of plutonium materials and comparison to sector field inductively coupled mass spectrometry, Anal. Chem. 88 (2016) 8862-8869.
[3] Z. Varga, M. Krachler, A. Nicholl, M. Ernstberger, T. Wiss, M. Wallenius, K. Mayer, Accurate measurement of uranium isotope ratios in solid materials by laser ablation multi-collector inductively coupled plasma mass spectrometry, J. Anal. Atom. Spec. 33 (2018) 1076-1080.
[4] M. Krachler, Z. Varga, A. Nicholl, M., M. Wallenius, K. Mayer, Spatial distribution of uranium isotopes in solid nuclear materials using laser ablation multi-collector ICP-MS, Microchem. J. 140 (2018) 24-30.
[5] M. Krachler, Z. Varga, A. Nicholl, M., K. Mayer, Analytical considerations in the determination of uranium isotope ratios in solid nuclear materials using laser ablation multi-collector ICP-MS, Anal. Chim. Acta X 2 (2019) 100018.
[6] M. Krachler, A. Bulgheroni, A.I. Martinez Ferri, Y. Ma, A. Miard, Ph. Garcia, Single shot laser ablation MC-ICP-MS for depth profile analysis of U isotopes in UO_2 single crystals, J. Anal. At. Spectrom. 34 (2019) 1965-1974.
[7] Z. Varga, M. Wallenius, M. Krachler, N. Rauff-Nisthar, L. Fongaro, A. Knott, A. Nicholl, K. Mayer, Trends and perspectives in Nuclear Forensic Science, Trends Analyt. Chem. 146 (2022) 116503.

Local structure and distribution of impurities in PuO_2: forensic signatures of formation conditions

S. Hickam[1], K. Hanson[1], H. Jang[1,2], A. van Veelen[1], D.T. Olive[1], K.F. Smith[3], R. Sykes[1], N.P. Edwards[4], C.H. Booth[3], A.L. Pugmire[1]

[1] Los Alamos National Laboratory, Los Alamos, NM, USA
[2] University of Nevada, Las Vegas, NV 89154 USA
[3] Lawrence Berkeley National Laboratory, Berkeley, CA 94720, USA
[4] SLAC National Accelerator Laboratory, Menlo Park, CA 94025, USA

shickam@lanl.gov

Nuclear forensic signatures can be identified using a combination of destructive and non-destructive techniques; however, there is a need to collect information rapidly with little to no sample preparation.[1] Particle samples pose challenges of limited volume and sample preparation steps that are needed to locate the particles or extract them from swipes before they can be analyzed.[2] Synchrotron x-ray methods are being developed to help address these challenges. Specifically, synchrotron x-ray fluorescence (XRF) imaging and x-ray absorption spectroscopy (XAS) can be combined to quickly identify particles with 1 µm resolution and then obtain local structure information from individual points. This approach was previously demonstrated for environmental actinide samples acquired from the McGuire Air Force Base, Chernobyl, and other sites.[4] Our work explores the application of these techniques to materials of interest including plutonium dioxide that has been oxidized from plutonium metal. PuO_2 can be formed from metal by processes including corrosion during storage in ambient conditions and by intentional oxidation of Pu^0 at high temperatures, such as in the Advanced Recovery and Integrated Extraction System (ARIES) program at Los Alamos National Laboratory.[3] Using synchrotron XRF and XAS methods, we show the types of information that can be rapidly extracted from PuO_2 particle samples and identify possible signatures that can distinguish between these sample histories.

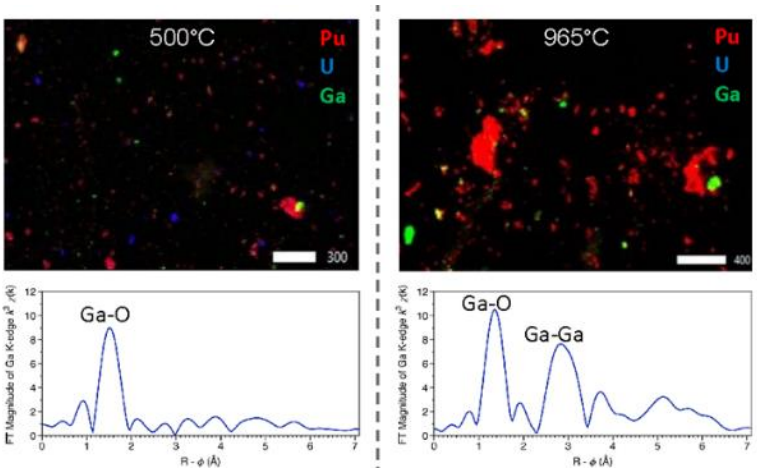

Figure 10. XRF maps and corresponding Ga K edge XAS spectra for two ARIES samples are shown. The Fourier transform of the Ga XAS for the 500°C sample (bottom left) was acquired on a green spot (a gallium-rich particle) in the upper left figure. The 965°C EXAFS figure (bottom right) corresponds to a green spot in the 965°C XRF map (upper right).

Prior to particle analysis, our bulk XAS studies of the Pu L_{III} edge for PuO_2 samples showed that Pu exhibits local structure differences when oxidized at low or high temperatures that could largely be attributed to particle size. However, we also hypothesized that we could take advantage of the low detection limits and element specific nature of XAS to examine the local structure of ppm-level impurities that form discrete particles or are incorporated in the PuO_2 matrix, which may provide new nuclear forensics signatures of sample provenance or processing history. Our first element of interest was gallium, which can be used as a phase-stabilizer of δ-Pu^0 and has been shown to oxidize to a Ga^{III} oxide when an oxide layer forms on δ-Pu^0 surfaces.[5] By leveraging samples from the ARIES program and samples corroded Pu metal, we probed Ga local structure and distribution at a particle level. Our results show differences in Ga distribution when comparing corrosion in ambient conditions to oxidation at higher temperatures. We also observe differences in local structure between the ARIES samples that were oxidized at 500°C and those that were calcined to 965°C (Figure 1). Ga local structure is best described as amorphous at 500°C, and it becomes a crystalline sesquioxide phase at temperatures around 965°C. These clear distinctions in local structure and distribution of Ga in PuO_2 particles provide a foundation for studying other impurities in these samples and show the potential of synchrotron particle analysis to provide new nuclear forensics signatures.

[1] National Academies of Sciences, Engineering, and Medicine 2021. *Restoring and Improving Nuclear Forensics to Support Attribution and Deterrence: Public Summary*. Washington, DC: The National Academies *Press. DOI: 10.17226/26167.*
[2] Zendel, M.; Donohue, D. L.; Kuhn, E.; Deron, S.; Biro, T. Nuclear Safeguards Verification Measurement Techniques. In Handbook of Nuclear Chemistry; Vértes, A., Nagy, S., Klencsár, Z., Lovas, R. G., Rösch, F., Eds.; Springer US: Boston, 2011; pp 2896−3015, DOI: 10.1007/978-1-4419-0720-2.
[3] ARIES turns 10. *Actinide Research Quarterly* **2008,** *1st/2nd quarters 2008*.
[4] Batuk, O. N.; Conradson, S. D.; Aleksandrova, O. N.; Boukhalfa, H.; Burakov, B. E.; Clark, D. L.; Czerwinski, K. R.; Felmy, A. R.; Lezama-Pacheco, J. S.; Kalmykov, S. N.; Moore, D. A.; Myasoedov, B. F.; Reed, D. T.; Reilly, D. D.; Roback, R. C.; Vlasova, I. E.; Webb, S. M.; Wilkerson, M. P., Multiscale speciation of U and Pu at Chernobyl, Hanford, Los Alamos, McGuire AFB, Mayak, and Rocky Flats. *Environmental Science & Technology* 2015, 49 (11), 6474-6484.
[5] Donald, S. B.; Stanford, J. A.; Talbot, W. A.; Saw, C. K.; Chung, B. W.; McLean, W., Evidence of an oxidation induced phase transformation for a delta phase plutonium-gallium alloy. *Corrosion Science* 2022, 194, 109923.

Pu M_4 and M_5 edge Resonant Inelastic X-ray Scattering of PuO_2

B. Schacherl [1], A. Beck [1], M. Trumm [1], P. Bagus [2], M. Tagliavini [3], M. Haverkort [3], A. Seibert [4], D. Schild [1], A. Tasi [1], H. Ramanantoanina [1], D. Fellhauer [1], H. Geckeis [1], T. Vitova [1]

[1] Karlsruhe Institute of Technology (KIT), Institute for Nuclear Waste Disposal (INE), P.O. Box 3640, 76021 Karlsruhe, Germany. [2] Center for Advanced Scientific Computing and Modeling (CASCaM) Department of Chemistry University of North Texas, Denton, Texas 76203-5017, USA. [3] Heidelberg University, Institute for Theoretical Physics, P.O. Box 105760, 69047 Heidelberg, Germany. [4] European Commission, Joint Research Centre Karlsruhe, P.O. Box 2340, 76125 Karlsruhe, Germany.

bianca.schacherl@kit.edu

Resonant inelastic X-ray scattering (RIXS) is a valuable tool and can lead to a deeper understanding of the electronic structure of materials as shown e.g. for transition metal compounds.[1] For uranium, the first M_5-edge core-to-core 3d4f RIXS spectra were measured in 1996[2], but for plutonium the first M_5-edge RIXS was published only in 2017.[3] This technique holds a high potential for actinide spectroscopy, which is not yet thoroughly explored. The aim of this work is an enhanced understanding of the Pu 3d4f RIXS maps measured at the Pu M_4 and M_5 absorption edges.

The Pu $M_{4,5}$-edge core-to-core 3d4f RIXS consists of electronic transitions from 3d to 5f (3d→5f) states followed by X-ray emission via 4f→3d transitions fulfilling the dipole selection rule (ΔJ = 0, ±1). As unoccupied 5f valence states of Pu are directly probed, the Pu oxidation state and its chemical bonding have a large effect on the RIXS maps. In the PuO_2 3d4f RIXS in Figure 1 it is visible that the maximum of the resonant X-ray emission intensity (line A) is shifted to a higher emission energy in comparison to the normal emission (line B). For uranium this shift appears to be correlated to a lower electronic density around the metal, corresponding to a higher uranium oxidation state.[3] In addition, previous results suggest that the energy shift between lines A and B increases for more localised 5f states.[3]

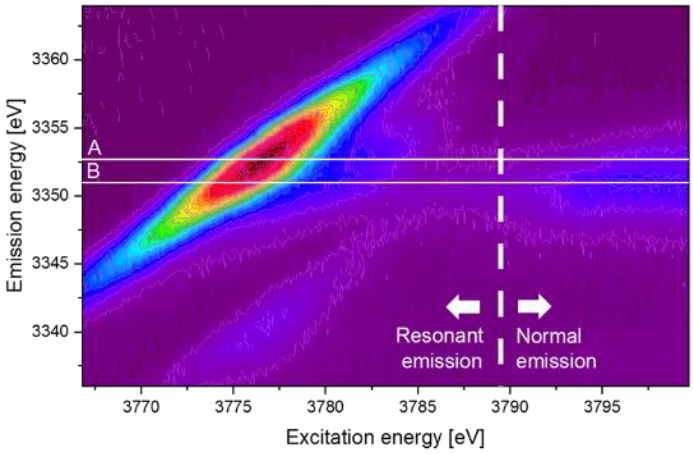

Figure 1: 3d4f RIXS of PuO_2, the maximum of the resonant emission feature is marked with line A, the maximum of the normal emission feature is marked with line B.[3]

This study focuses on the analysis of how different parameters affect the 3d4f RIXS map of PuO_2. To understand the origin of the different spectral features, calculations based on *ab initio* multiplet calculations (MOLCAS and CLIPS) and semi-empirical multiplet approaches (Quanty) are applied. The

effect of different contributions to the experimental resolution is studied and the impact of the physical state of PuO_2 and its contact with water on the RIXS maps are discussed.

X-ray absorption spectroscopy experiments were performed with powdered $^{239}PuO_2$. To investigate potential size effects, PuO_2 thin film samples of 65–100 nm thickness where prepared by direct-current (dc) sputter deposition from a ^{242}Pu metal target with Ar/O_2 mixtures as sputter gas on SiN/Si wafers.[4] An experimental setup where $^{242}PuO_2$ thin films are in contact with H_2O under anaerobic conditions was designed. In addition, a colloidal Pu suspension (5 mmol/L) at pH 1.5 was investigated. It was obtained by aging of amorphous, hydrated $^{242}PuO_2$ precipitates in $HClO_4$ at pH 1.5 and E_h=0.78 V for 9 months. The XAS experiments were performed at the INE and CAT-ACT beamlines at the KIT Light Source in Karlsruhe Germany.[5,6]

3d4f RIXS spectra for the PuO_2 powder measured with various experimental resolutions, revealed that different broadening effects have a large influence on the shape of the spectra and the energy position of the main resonant feature. Theoretical calculations and simulation of different broadening effects will be compared to the experimental results. For the Pu colloids and PuO_2 thin films similar spectra are obtained. In comparison to the PuO_2 powder sample the resonant emission is shifted by 1.8 eV to higher emission energies. The RIXS spectrum of the PuO_2 thin film in contact with water also changes compared to the as prepared dry film. It has been a long-standing discussion if and at which conditions PuO_{2+x} is stable.[7–9] The spectral differences will be discussed as a potential presence of PuO_{2+x} and/or changes in the geometric structure or differences in the 5f electron localization.[10]

Acknowledgements: The authors acknowledge funding from the ERC Consolidator Grant 2020 under the European Union's Horizon 2020 research and innovation programme (grant agreement No. 101003292). This project has received funding from the European Union's Horizon 2020 research and innovation programme under grant agreement No 847593. PSB acknowledges support from the U.S. Department of Energy, Office of Science, Office of Basic Energy Sciences, Chemical Sciences, Geosciences, and Biosciences (CSGB) Division through the Geosciences program at Pacific Northwest National Laboratory. We thank the Institute for Beam Physics and Technology (IBPT), KIT for the operation of the storage ring, the Karlsruhe Research Accelerator (KARA).

(1) Glatzel, P.; Sikora, M.; Fernández-García, M. Resonant X-Ray Spectroscopy to Study K Absorption Pre-Edges in 3d Transition Metal Compounds. *Eur. Phys. J. Spec. Top.* **2009**, *169* (1), 207–214. https://doi.org/10.1140/epjst/e2009-00994-7.
(2) Butorin, S. M.; Mancini, D. C.; Guo, J. H.; Wassdahl, N.; Nordgren, J.; Nakazawa, M.; Tanaka, S.; Uozumi, T.; Kotani, A.; Ma, Y.; Myano, K. E.; Karlin, B. A.; Shuh, D. K. Resonant X-Ray Fluorescence Spectroscopy of Correlated Systems: A Probe of Charge-Transfer Excitations. *Phys. Rev. Lett.* **1996**, *77* (3), 574–577. https://doi.org/10.1103/PhysRevLett.77.574.
(3) Vitova, T.; Pidchenko, I.; Fellhauer, D.; Bagus, P. S.; Joly, Y.; Prüßmann, T.; Bahl, S.; Gonzalez-Robles, E.; Rothe, J.; Altmaier, M.; Denecke, M. A.; Geckeis, H. The Role of the 5f Valence Orbitals of Early Actinides in Chemical Bonding. *Nat. Commun.* **2017**, *8* (1), 16053. https://doi.org/10.1038/ncomms16053.
(4) Seibert, A.; Gouder, T.; Huber, F. Interaction of PuO2 Thin Films with Water. *Radiochim. Acta* **2010**, *98* (9–11), 647–654. https://doi.org/10.1524/ract.2010.1765.
(5) Rothe, J.; Butorin, S.; Dardenne, K.; Denecke, M. A.; Kienzler, B.; Löble, M.; Metz, V.; Seibert, A.; Steppert, M.; Vitova, T.; Walther, C.; Geckeis, H. The INE-Beamline for Actinide Science at ANKA. *Rev. Sci. Instrum.* **2012**, *83* (4), 043105. https://doi.org/10.1063/1.3700813.
(6) Zimina, A.; Dardenne, K.; Denecke, M. A.; Doronkin, D. E.; Huttel, E.; Lichtenberg, H.; Mangold, S.; Prüßmann, T.; Rothe, J.; Spangenberg, T.; Steininger, R.; Vitova, T.; Geckeis, H.; Grunwaldt, J.-D. CAT-ACT — A New Highly Versatile X-Ray Spectroscopy Beamline for Catalysis and Radionuclide Science at the KIT Synchrotron Light Facility ANKA. *Rev. Sci. Instrum.* **2017**, *88* (113113), 1–12. https://doi.org/10.1063/1.4999928.
(7) Haschke, J. M.; Allen, T. H.; Morales, L. A. Reaction of Plutonium Dioxide with Water: Formation and Properties of PuO2+x. *Science (80-.).* **2000**, *287* (5451), 285–287. https://doi.org/10.1126/science.287.5451.285.
(8) Neck, V.; Altmaier, M.; Fanghänel, T. Thermodynamic Data for Hydrous and Anhydrous PuO2+x(S). *J. Alloys Compd.* **2007**, *444–445* (SPEC. ISS.), 464–469. https://doi.org/10.1016/j.jallcom.2007.01.159.
(9) Vitova, T.; Pidchenko, I.; Fellhauer, D.; Prüßmann, T.; Bahl, S.; Dardenne, K.; Yokosawa, T.; Schimmelpfennig, B.; Altmaier, M.; Denecke, M.; Rothe, J.; Geckeis, H. Exploring the Electronic Structure and Speciation of Aqueous and Colloidal Pu with High Energy Resolution XANES and Computations. *Chem. Commun.* **2018**, *54* (91), 12824–12827. https://doi.org/10.1039/C8CC06889E.
(10) Bagus, P. S.; Schacherl, B.; Vitova, T. Computational and Spectroscopic Tools for the Detection of Bond Covalency in Pu(IV) Materials. *Inorg. Chem.* **2021**, *60* (21), 16090–16102. https://doi.org/10.1021/acs.inorgchem.1c01331.

Coulometry analysis of plutonium in the presence of excess uranium: focus on the effect of sulfate complexation

G. Canciani, Y. Davrain, M. Crozet, C. Rivier, S. Picart

[1] CEA, DEN, DMRC, CETAMA, Univ. Montpellier, Marcoule, France

sebastien.picart@cea.fr

Controlled Potential Coulometry (CPC) is an analytical technique used to determine very accurately the amount content of an electroactive species in a solution by measuring the amount of charge required for this species to undergo a quantitative electrochemical reaction [1]. The quantity of electricity involved in the studied reaction, *Q*, is related to the mass of an element in solution, *m*, by a modified version of Faraday's law, as shown in equation 1 where *M* is the molar mass of the species studied, *n*, is the number of electrons exchanged during the electrochemical transformation, *F*, is Faraday's constant, and the f term, is a corrective factor (derived from Nernst's law) which takes into account the fraction of species non-electrolysed during the analysis.

$$m = \frac{Q\,M}{n\,F\,f} \qquad (1)$$

The technique's use of physical parameters (time and current) allows to attain high degrees of accuracy with biases close to, or below, 0.1% even on small quantities of matter (typically a few milligrams) [2], [3]. In the light of these good performances, CPC has become the subject of renewed interest in the field of nuclear analysis [1], [2]. In particular, the technique has been successfully adopted for the determination of the plutonium (Pu) content of certified reference materials produced by metrology laboratories such as the French Alternative Energies and Atomic Energy Commission (CEA)'s Committee for the Establishment of Analytical Methods (CETAMA) [4], [5].

With an increasing demand in diverse certified reference materials, there has been a growing interest for the application of CPC to more complex actinide solutions. At the CETAMA, the technique's applicability to the determination of Pu in aqueous acidic solutions (HNO_3, 0.9 mol L^{-1}) in the presence of high concentrations of uranium (U) has received particular interest. Preliminary studies performed by Ruas *et al.* showed that whilst it was possible to perform high accuracy CPC analysis of Pu in mixed U/Pu solutions with moderate concentrations of U (U:Pu ratios up to 10:1), significant interferences occurred [5]. It was suggested that these interferences arose from the sulfate species introduced into the system with the U and their interaction with the Pu cations [5].

The present study expands on Ruas *et al.*'s work by combining experimental results with computational simulations in order to provide a comprehensive understanding of the Pu and UO_2^{2+} complexation with sulfates during CPC. It was thus possible to quantify the speciation of the different species in the solutions of U/Pu in HNO_3 used for CPC in relation sulphate concentration (as shown in figure 1 for significant Pu species). The simulations allowed to demonstrate the direct correlation between a shift in the formal potential of the Pu(IV)/Pu(III) redox couple, (denoted $E^{0\prime}_{Pu(IV)/Pu(III)}$) and the concentration of sulfates in the system. Experimentally, this shift results in an increased fraction of non-electrolysed species during CPC analysis which can be taken into account through the f term

(equation 1) if $E^{0\prime}_{Pu(IV)/Pu(III)}$ is precisely known for the studied solution. In the light of the increased importance of the f factor with respect to analyses in pure Pu nitrate solutions, $E^{0\prime}_{Pu(IV)/Pu(III)}$ needs to be measured individually for each different U/Pu nitrate solution analysed in order to achieve a high degree of accuracy.

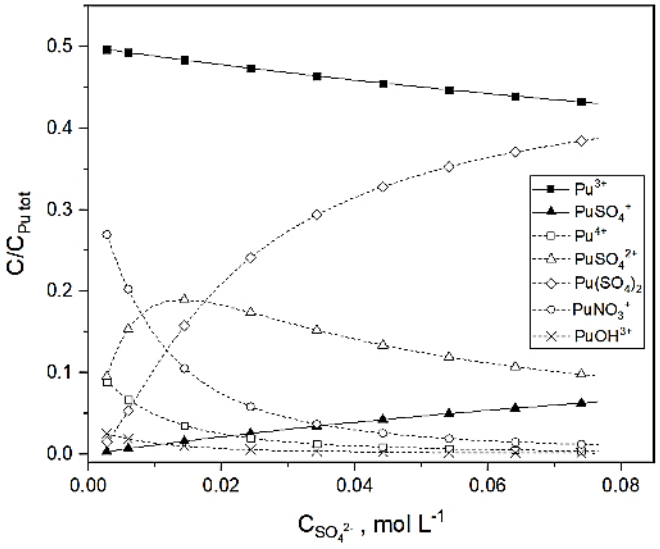

Figure 1: Speciation distribution of significant Pu(III) and Pu(IV) species in an aqueous HNO_3 solution (0.9 mol L^{-1}) in relation to the [SO_4^{2-}] in solution.

Ultimately it was possible to establish an experimental protocol for the high accuracy CPC analysis of Pu in the presence of large quantities of U (U:Pu ratios up to 100:1). This protocol, as well as the increased understanding of the speciation of Pu in U/Pu aqueous acidic solutions in relation to sulfates in a nitric acid medium, will be particularly important for the future adoption of CPC as a cornerstone in the metrology of mixed U/Pu solutions [6].

[1] V. N. Momotov and E. A. Erin, 'Coulometric methods for uranium and plutonium determination', *Radiochemistry*, vol. 59, no. 1, pp. 1–25, Jan. 2017.
[2] K. Zhao, M. Penkin, C. Norman, and S. Balsley, 'International Target Values 2010 for Measurement Uncertainties in Safeguarding Nuclear Materials', *ESARDA Bull.*, pp. 3–24, 2012.
[3] M.K. Holland, J.R. Weiss, C.E. Pietri, 'Controlled-potential coulometric determination of plutonium', *Analytical Chemistry* vol. 50, no. 2, pp. 236–240, 1978.
[4] S. Picart, M. Crozet, G. Canciani, Y. Davrain, L. Faure, and D. Roudil, 'Accurate determination of plutonium by Controlled Potential Coulometry: uncertainty evaluation by the Monte Carlo Method approach', *Journal of Radioanalytical and Nuclear Chemistry*, vol. 324, vol. 2, pp. 747–758, 2020.
[5] A. Ruas, N. Leguay, R. Sueur, N. Vedel, V. Dalier, and P. Moisy, 'High accuracy plutonium mass determination by controlled-potential coulometry', *Radiochim. Acta*, vol. 102, no. 8, pp. 691–699, Jan. 2014
[6] G. Canciani, Y. Davrain, M. Crozet, D. Roudil, S. Picart, 'Controlled Potential Coulometry for the accurate determination of plutonium in the presence of uranium: The role of sulfate complexation', *Talanta*, vol. 222, p.121490, 2021.

Advances in the Micro-Analysis of Environmentally Sourced Nuclear Materials

P.G. Martin,T.B. Scott

Interface Analysis Centre and South West Nuclear Hub, University of Bristol, Tyndall Avenue, Bristol, BS8 1TL, UK.

peter.martin@bristol.ac.uk

Both routine and accidental releases have distributed a considerable inventory of radioactive material into the local and wider global environments over nuclears varied, controversial and extensive history. While the most high-profile releases are the result of IAEA INES rated incidents such as Chernobyl and Fukushima, as well as from permitted discharges at reprocessing sites including Le Hague (France) and Sellafield (UK), the greatest combined source of radioactivity in the environment is the result of historic weapons testing during the 1950's and 1960's [1].

This source of anthropogenic and actinide-containing nuclear particulate material into the environment represents the birth of the field more recently termed "nuclear forensics". Since its inception, decades of research have been performed on material from various sources, each with differing release characteristics which, together with their source term, influence the particulates properties within the specific environment. Dependent upon their source, such radioactive particles (typically existing on the sub-mm scale) can contain extreme levels of radioactivity (GBq in some instances) owing to the gamma-emitting fission product content introduced into the actinide material, and therefore represent highly mobile point-sources of extreme health concern. In contrast to other forms of radioactive particulate that may exist in the environment, such as ionic species, colloids, and pseudo-colloids [2], particles represent the largest physio-chemical form of radioactive material, which may undergo significant and continuous transformational processes under environmental conditions.

The analytical techniques (and resultant levels of insight gained into such nuclear particulate) have evolved significantly since the earliest works in the field. Some of the earliest work was undertaken during the 1960's on fallout material associated with the Nevada Test Site and Eniwetok Proving Grounds [3], [4], employing primitive electron microscopy, autoradiography, x-ray diffraction and light microscopy techniques on mm-scale glassy particulate. The accident at the Chernobyl Nuclear Power Plant Reactor 4 in 1986 provided a new inventory of (highly) radioactive particulate for analysis and for the application of advancements in analytical techniques to be applied – including enhanced electron microscopy [5], as well as novel synchrotron x-ray based characterisation methods, including fluorescence, absorption and diffraction mapping [6].

Recent examination of material released from Japan's Fukushima Daiichi Nuclear Power Plant (FDNPP), Sellafield and other legacy operations has further applied the advancements in analytical capability. Through such advancements, it is now possible to resolve sub-micron actinide particulate embedded within a matrix, as well as attribute specific portions of a sample to individual reactor components (Figure 1). This spatial and spectral resolution has permitted for a heightened understanding of how actinide materials released into the environment behave over varying timescales. While formerly only possible to be performed within national laboratories established for examining such actinide or highly active materials, advancements in laboratory instrumentation have removed such prohibitive requirements and allowed for many experiments to be performed 'in-house'.

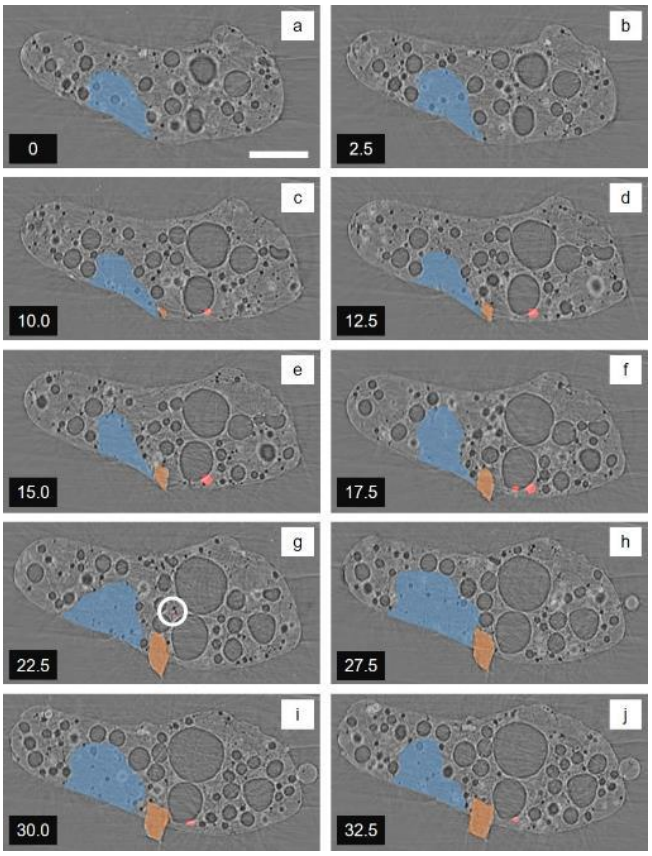

Figure 1: Synchrotron radiation x-ray tomography (ptychography) slices through a Fukushima Daiichi derived fallout particle, overlain with x-ray fluorescence compositional data. Blue = cement, orange = steel, and pink = uranium. Scale bar = 100 μm.

[1] Q.-H. Hu, J.-Q. Weng, and J.-S. Wang, "Sources of anthropogenic radionuclides in the environment: a review.," *J. Environ. Radioact.*, vol. 101, no. 6, pp. 426–37, Jun. 2010.
[2] B. Salbu, "Speciation of radionuclides – analytical challenges within environmental impact and risk assessments," *J. Environ. Radioact.*, vol. 96, no. 1–3, pp. 47–53, Jul. 2007.
[3] C. E. Adams, N. H. Farlow, and W. R. Schell, "The compositions, structures and origins of radioactive fall-out particles," *Geochim. Cosmochim. Acta*, vol. 18, pp. 42–56, Jan. 1960.
[4] J. Mackin, P. Zigman, D. Love, D. Macdonald, and D. Sam, "Radiochemical analysis of individual fall-out particles," *J. Inorg. Nucl. Chem.*, vol. 15, no. 1–2, pp. 20–36, Sep. 1960.
[5] T. Raunemaa, S. Lehtinen, H. Saari, and M. Kulmala, "2–10 μm sized hot particles in chernobyl fallout to Finland," *J. Aerosol Sci.*, vol. 18, no. 6, pp. 693–696, Dec. 1987.
[6] B. Salbu *et al.*, "High energy X-ray microscopy for characterisation of fuel particles," *Nucl. Instruments Methods Phys. Res. Sect. A Accel. Spectrometers, Detect. Assoc. Equip.*, vol. 467–468, pp. 1249–1252, Jul. 2001.

Recent Developments on the Production and Morphological Analysis of Plutonium Oxalate and Oxide Compounds

David E. Meier, Richard A. Clark, Lucas E. Sweet, Matthew K. Edwards, Forrest D. Heller, Edgar C. Buck, Alex R. Hagen, Ian J. Schwerdt, Jason M. Lonergan, Jordan F. Corbey, Cyrena M. Parker, Amanda J. Casella, Joel M. Tingey, Gregg J. Lumetta

Pacific Northwest National Laboratory, U.S.A.

David.meier@pnnl.gov

Pacific Northwest National Laboratory (PNNL) has established plutonium processing capabilities at two different scales to study nuclear forensics signatures. The processing capabilities emulate historical efforts used by Hanford, Savannah River, and Rocky Flats. This capability is a flexible system that can process various flow sheets associated with the plutonium nitrate precipitation methods including Pu (III) and Pu (IV) oxalate and peroxide. Key operations for this capability include dissolution, ion exchange, precipitation, filtration, and calcination. Processing parameters include precipitation and operation temperatures, reagent addition flow rates, agitation speed, digestion time, and calcination temperatures. A comprehensive suite of analytical capabilities including inorganic, radiochemical, and physical analysis, as well as state-of-the art microscopy systems are used to characterize the feed, process, and product materials. Additionally, machine learning algorithms are being employed to further understand the correlation between morphologies and the various processes.

The system was designed with the ability to include on-line instrumentation for monitoring key process parameters such as the Pu oxidation state and nitric acid (HNO3) concentration. Over 100 processing experiments have been conducted including a 76-experiment parametric statistical design study focusing on the plutonium (III) oxalate precipitation method. Data, images, and observations from various processing experiments will be presented.

Morphological Provenance Signatures from Plutonium and Uranium Oxide Scales

Brandon W. Chung [1], Debra L. Rosas [1], Scott B. Donald [1]

[1] Lawrence Livermore National Laboratory, Livermore, CA 94551

chung7@llnl.gov

We are investigating changes in the interior morphology of the oxide scale formed on plutonium (Pu) and uranium (U) metals following exposures to various environments anticipated under the loss-of-institutional-control scenarios. Using focused ion beam (FIB) and multiplatform microanalysis techniques, our work shows the distinguishing morphological and chemical characteristics between the original oxide scale formed from the controlled storage environment and the oxide scale that is formed during subsequent exposures to external environments. Internal chemical composition, structure, and pore geometry of oxide scales are different, attributable to oxidative corrosion from exposure to outside the storage environment. This information is of potential use in predicting and discovering discriminating material characteristics related to the history and provenance of an interdicted nuclear materials.

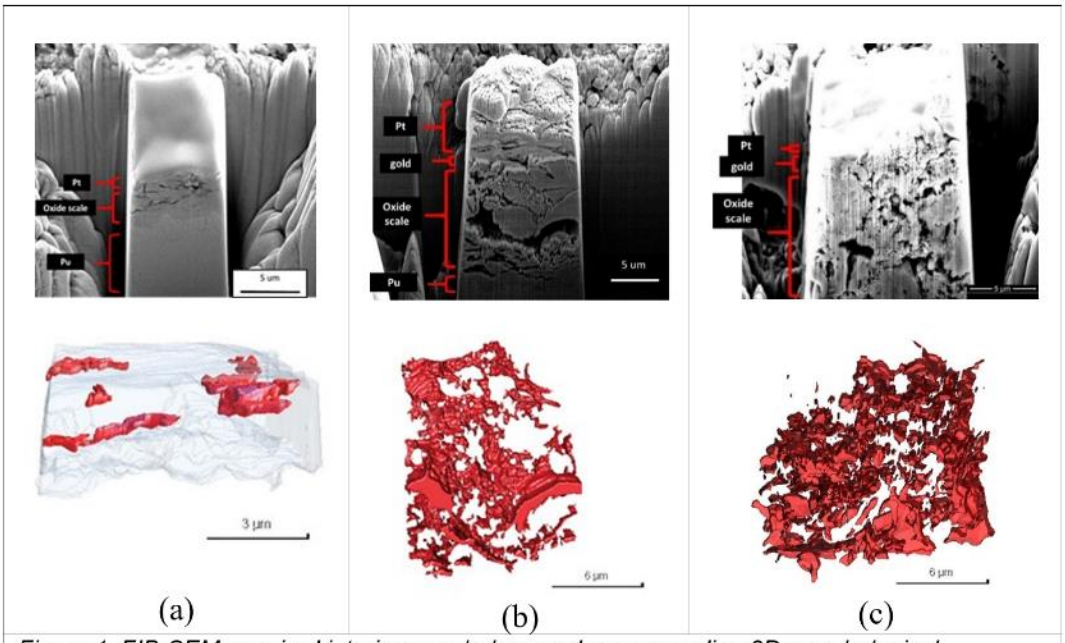

Figure 1. FIB-SEM acquired interior morphology and corresponding 3D morphological representation from the oxide scale formed on the delta-stabilized Pu (~2 atomic % Ga) metal sample. Oxide scale formed from (a) nitrogen inert storage, (b) exposure to air, and (c) exposure to water [1].

Figure 1 demonstrates applicability of focused ion beam and scanning electron microscopy (FIB-SEM) to identify primary morphological features formed from the Pu metal's exposure to various environments: (1) an outer shell-like layer, (2) a porous core, (3) a corroded floor, and (4) longitudinal microcracks. By using the FIB's ion sputtering capability [2-4], we can expose subsurface features in bulk nuclear materials [1, 5]. It is clear from Figure 1 that there are clear differences in the interior morphology of the oxide scale after exposure to outside the controlled storage environment.

With elemental analysis from Auger Emission Spectroscopy (AES), we found that the Pu oxide scale is composed of hyper-stoichimetric plutonium oxide, PuO_{2+x}. This shell-like layer can have either a dense or porous morphology, including longitudinal microcracks. The lower morphological boundary of the shell-like layer is longitudinal microcracks. In some samples, we saw significant modification to the internal scale structure with presence of a porous core after exposure to air and water (Figure 1). This porous core is a dominant morphological feature that contains a porous mass made up of agglomerates of small PuO_2 particles of different morphologies comingled with pores and microcracks. The porous core is formed because of the continual influx of oxygen from a new source of air during the repackaging process. Below the outer shell-like layer is a corroded floor. This inner layer is a mixture of PuO_2, PuO_{2-x}, and Pu_2O_3 interfaced with plutonium.

Our work shows that the original oxide scale structure is influenced by the source environment. Under the standard inert (nitrogen) atmosphere glove box operations and storages, the oxide scale is composed of the outer shell-like layer covering the corroded floor. Under the well-controlled storage conditions, the original scale features could remain for many years. The appearance of a porous core in the subsurface indicates exposure to an influx of air, anticipated under one of the loss-of-institutional-control scenarios.

Currently our major aim is to quantify the morphological properties, such that those can be utilized for elucidating the recent environmental changes experienced by Pu and U metals. This quantification is performed by 3D analysis of measured shape and size of pores and cracks. Furthermore, we will describe our efforts to study discriminating material features from an individual grain/inclusion from the bulk and a single particle from the population.

Prepared by LLNL under Contract DE-AC52-07NA27344. This work was supported by the Office of Defense Nuclear Nonproliferation Research and Development within the U.S. Department of Energy's National Nuclear Security Administration. This support does not constitute an express or implied endorsement on the part of the Government. LLNL-ABS-831909

[1] S.B. DONALD and B.W. CHUNG, *J. Nucl. Mater.*, **559**, 153473 (2022)
[2] C.A. VOLKERT and A.M. MINOR, *MRS Bulletin*, **32**, 389 (2007)
[3] B. LICH, *Microscopy Today*, 26 (2007).
[4] M.D. UCHIC et. al., *MRS Bulletin*, **32**, 408 (2007).
[5] B.W. CHUNG, et. al., *J. Nucl. Mater.*, **473**, 264 (2016).

Development of Direct Analysis Approaches on Solid Plutonium Samples for Actinide Analysis

M Higginson [1], B Dawkins [1] T Shaw [1] L Ingman [1] S Dunn [1] P Thompson [1] and P Kaye [1]

[1] AWE, Aldermaston, RG7 4PR,

matthew.higginson@awe.co.uk

The precise analysis of plutonium materials for process development, fundamental research, regulatory and specification requirements currently rely on destructive, wet chemistry methodologies. These processes add considerable complexity and cost to plutonium analysis as well as generating waste.

We will present innovations to this conventional approach. Firstly, we have developed scalable sample containment systems to allow multiple analysis techniques to be applied to a sample. The sample can be cleared from glovebox containment and can be handled in the open laboratory. Actinide samples were consistently produced and prepared to a precise geometry to enable calibration approaches to reference standards to be established.

Radiometric, x-ray fluorescence, spectroscopic and microscopic techniques can then be applied to the same sample. Using high-resolution gamma spectrometry we can complete assay, isotopic and trace actinide measurements rapidly and non-destructively, avoiding wet chemical processing of the sample.

The main challenge of the radiometric analysis is the precise assay of ^{240}Pu to which we will present approaches. The results show that despite not meeting the precision of other benchmark destructive techniques, the approach is promising as a parallel, rapid, low-cost methodology for sample analysis and allows a platform for direct plutonium analysis on conventional laboratory instrumentation.

Figure 1: Example sample containment system for direct plutonium analysis in the open laboratory [1]

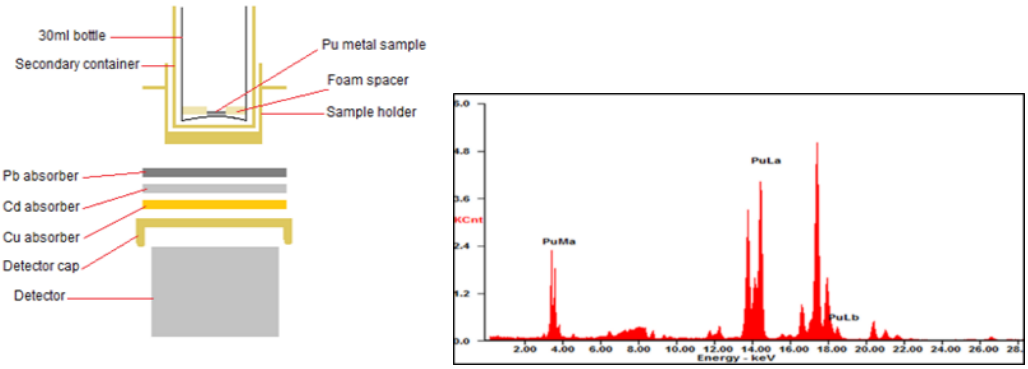

Figure 2: Example detector setup for direct plutonium analysis by high resolution gamma spectrometry (left) [1] [2] Example direct energy dispersive x-ray fluorescence of plutonium in sample containment (right)

Sample ID	Standard A (in duplicate)		Standard B (in duplicate)	
Isotope	%Difference from known value	Standard deviation (n=4)	%Difference from known value	Standard deviation (n=4)
238	0	0.0001	0	0.0001
239	0.1	0.11	0.18	0.052
240	2.8	0.20	2.1	0.057
241	0.1	0.002	0.1	0.001
242 (by correlation)	0.1	0.003	0.1	0.001
Assay	0.21	0.42	0.31	0.31

Table 1: Example isotopic measurement results on plutonium metal and alloy standards by direct solid HRGS [1]

References

[1] Higginson, M., Dawkins, B., Shaw, T. et al. Development of assay, isotopic and trace actinide measurements on solid plutonium and uranium samples by high resolution gamma spectrometry. J Radioanal Nucl Chem 330, 901–911 (2021). https://doi.org/10.1007/s10967-021-08043-w
[2] Higginson and Rim et al. The Plutonium Handbook, 2nd Edition, Chapter 46.3, Gamma Spectroscopy, ISBN: 978-0-89448-201-4

Spectroscopy Research of Pu-bearing Compounds at the Savannah River National Laboratory

Eliel Villa-Aleman, Don D. Dick, Jason R. Darvin, Jonathan H. Christian, Bryan J. Foley
Savannah River National Laboratory, Aiken, SC 29808, USA

The physical properties of plutonium-bearing compounds depend on several production parameters and can change with time due to alpha decay that induces decomposition resulting in the formation of PuO_2 nanoparticulates. Many of these changes can be probed with spectroscopic techniques such as Raman, luminescence, and diffuse reflectance spectroscopy in the visible, shortwave, and infrared regions. These spectroscopic tools can also be used to study temperature dependent material properties and can provide complementary and distinct information on material crystallinity and the nature of charge defects. This presentation will discuss the dynamic spectroscopic attributes of Pu-bearing materials and the value that different spectroscopic techniques add for nuclear forensics applications.

1. Raman spectroscopy is a valuable tool to study PuO_2 and can provide important information regarding crystal lattice structure.
    a. Raman spectra of PuO_2 were measured in our laboratory with 9 wavelengths (244, 325, 405, 457, 488, 514, 561, 633, 785 nm). The laser wavelength can affect band intensity ratios and defect band intensities.
    b. Four defect bands were identified at 535, 580, 625, and 650 cm^{-1}. The band ratio intensity of the 580 and the 650 cm^{-1} bands were highly dependent on the excitation wavelength. The 650 cm^{-1} band became the most intense using laser excitation wavelengths longer than 561 nm. Meanwhile the 580 cm^{-1} band became the most intense using laser excitation wavelengths shorter than 561 nm.
    c. Raman spectroscopy can be used to estimate temperature of the material using the Stokes and anti-Stokes bands. This measurement can help identify laser-induced annealing of the material.
    d. Raman spectroscopy can be used to follow alpha decay-induced damage in the crystal lattice by following the T_{2g} band properties (FWHM, band position, and intensity) as well as the ratio of the defect bands to the T_{2g} band. This information can be used to identify the age of PuO_2 since last calcination.
    e. Electronic Raman bands were observed by our group for the first time with laser excitation wavelengths beyond the optical band gap of 438 nm. The spectrum acquired with a 405 nm laser wavelength was confirmed with a 457 nm and 514 nm laser.
2. Luminescence spectroscopy is a new tool in the analysis of PuO_2. A broad luminescence spectral band from ~438 – 700 nm grows with time. The intensity of the luminescence is related to the age of the PuO_2 sample since last calcination.
3. Diffuse reflectance in the visible, shortwave, and infrared spectral regions provide information on the Pu compounds.
    a. The infrared region is extremely useful in the analysis of vibrational modes corresponding to oxalates, nitrates, and oxides and also provides understanding about the number of water molecules present in the system and the electronic bands of PuO_2. Additionally, bands corresponding to carbon molecular species can be observed during decomposition of the oxalate to the oxide.

b. The shortwave spectral region (930 – 1600 nm) provides valuable information on the electronic bands and those bands originating from water molecules. The most interesting aspect of this region is the band located at ~7000 cm^{-1} (1430 nm), which corresponds to PuO_2. This band can be used to observe the transition from PuO_2 precursors, such as plutonium oxalate as they convert to PuO_2. This band has been used to correlate the FWHM with calcination temperature. Although we do not have an assignment for this band at this time, we have coined this band the "V" band.
c. The 400 – 930 nm region provides information regarding the electronic transitions with sharper bands corresponding to different Pu-bearing compounds. This region has been useful in the clear differentiation between the Pu (III) and Pu (IV) oxalates.

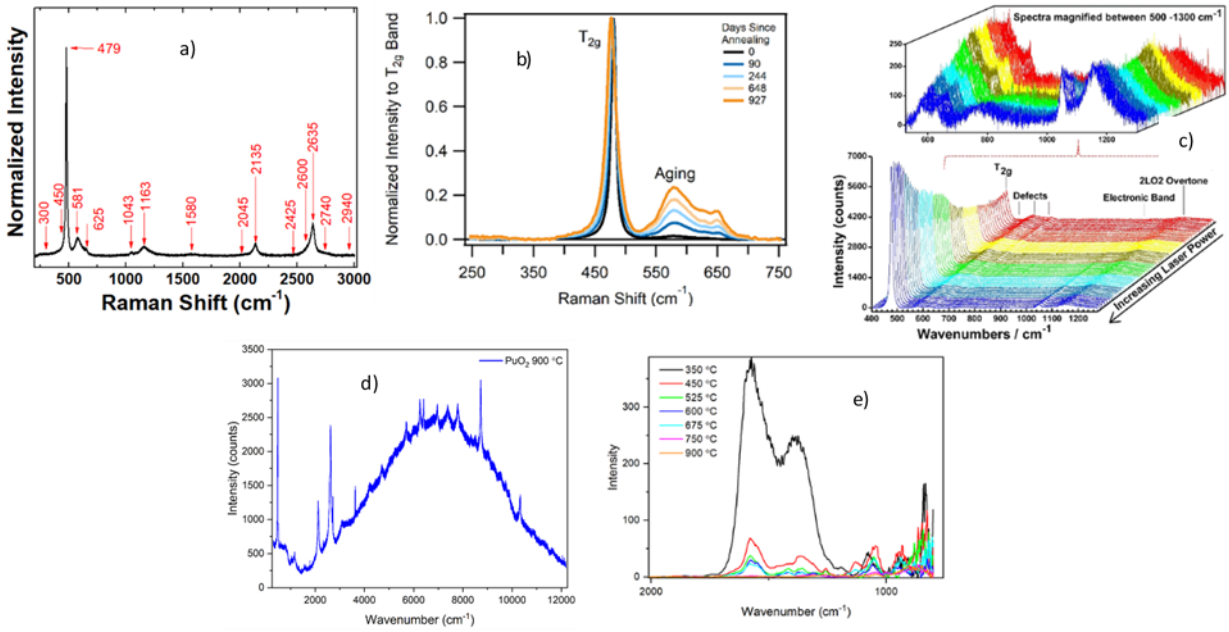

Figure 1: a) Raman spectrum of PuO_2, b) time dependent age defects, c) laser annealing of PuO_2, d) luminescence and electronic Raman bands, and e) calcination of carbon features in the infrared spectrum of Pu oxalate to PuO_2.

References

1. Villa-Aleman E, Dick DD, Christian JH, Foley BJ *Journal of Raman Spectroscopy*, *52*, 1486.
2. Villa-Aleman E, Bridges NJ, Shehee TC, Houk AL *Journal of Nuclear Materials* **2019**, *515*, 140.
3. Villa-Aleman E, Houk AL, Shehee TC, Bridges NJ *Journal of Nuclear Materials* **2021**, *551*, 152969.
4. Villa-Aleman E, Houk AL, Bridges NJ, Shehee TC *Journal of Raman Spectroscopy* **2019**, *50*.
5. Christian JH, Foley BJ, Ciprian E, Dick DD, Said M, Darvin J, Hixon, AE, Villa-Aleman E *Journal of Nuclear Materials* **2022**, 562, 153574.

Challenges Associated with Plutonium Pyrochemical Process Monitoring Deploying Unique Analytical Tools & Techniques

L. Tandon [1], A. C. Olson [1], F. R. Rocha [1], N. H. Anderson [1], C. E. Lledo [1], J. H. Rim [1], J. R. Mason [1], R. Winkler [1], T. R. Wenz [1], S. E.Betts [1], D. Patel [1], M. F. Schappert [1], M. S. Rearick [1], E. J. Lujan [1], M. A. Knaak [1], A. D. Wall [1], P. T. Martinez [1] L. Colletti [1], D. R. Porterfield [1], J. M. Jackson [1], C. G. Worley[1]

[1] P.O. Box 1663, Los Alamos National Laboratory, Los Alamos, NM,87545 USA,

tandon@lanl.gov

Nuclear facilities depend on nuclear material attribute measurements within the context of formal international safeguards, material processing, nuclear security and environmental compliance requirements. Fundamental property measurements are necessary to: 1) meet specifications for intermediate or product materials, 2) meet regulatory requirements, and 3) track material inventory within a facility. It is important that characteristics such as actinide assay and isotopic composition, trace element content, grain/particle size and shape measurement be determined with a high degree of confidence.

Pyrochemical processing of plutonium involves a set of high temperature operations including chemical and electrochemical reactions in molten salts for the production and purification of metal [1]. Numerous impurities may be present in this process, originating from impure plutonium feed (metal or oxide or halide), the solvent alkali or alkaline earth chloride salts, or the metals used as reductants. All these operations are carried out in unique assemblies capable of performing thermite reactions. The challenge lies in tracking the various stages of production and refinement using novel tools and techniques. This is because the starting nuclear material composition will change depending on processing or operating conditions. The objective of this study is to evaluate, validate, and deploy in-line and robust analytical capabilities (that include assay, isotopics, trace metal, trace actinide, and non-metal impurity characterization along with full material science laboratory) to analyze all products from these processes to track product quality for developing greater understanding of the processes, material accountability and meeting regulatory requirements. The ultimate goal of this study is to update understanding of these chemical reactions and to feed into models using thermodynamics, kinetics and electrochemical data. The processes under investigation include direct oxide reduction, metal chlorination, molten salt extraction and electrorefining**.** The most unusual aspect of this study was to develop methods to determine what information could be inferred by studying smaller quantities of materials collected for health and safety evaluations of these processes which includes plutonium particles from the differing operations. The results from both traditional and novel approaches to characterization will be discussed in terms of accuracy, precision, uncertainty and the limitations of the deployed techniques.

'LA-UR-22-22333'

[1] Paget, T.; McNeese, J.; Fife, K.; Jackson, J. M.; Watson, R. *Molten Salt Chemistry of Plutonium*; Chapter 6: Molten Salt Chemistry of Plutonium, In Plutonium Handbook, Second Edition; Clark, D.L, Geeson, D.A., Hanrahan, Jr. R.J., Eds,; American Nuclear Society, La Grange Park, IL, USA; p 201-286; 2019.

A Functional Statistical Modelling Approach to Using Plutonium Particle Features from Scanning Electron Microscope Images

A. Zhang [1], K. Shuler [1], D. Ries [1], J. D. Tucker [1], Gabriel Huerta [1], Katherine Goode [1], and M. Ausdemore [2]

[1] Sandia National Laboratories [2] Los Alamos National Laboratory

[1] 1515 Eubank Blvd. SE, Albuquerque, NM 87123

[2] P.O. Box 1663 Bikini Atoll Road, SM-30, Los Alamos, NM 87545

azhang@sandia.gov

In nuclear forensics, it is of interest to be able to determine the processing conditions under which interdicted material, such as Plutonium (Pu), was produced. Such determinations can aid in material attribution, which allows for making inference about material origins, which, in turn, can lead to answering questions of who, when, and where the material was produced. By studying the morphological characteristics of a sample Pu, we can begin to make such inferences.

The morphological characteristics can be studied with a Scanning Electron Microscope (SEM) image. SEM images magnify the particle, thus allowing for close study of morphological features, such as the shape, texture, and physical properties of the sample. These features can be directly measured from the raw image or quantitatively measured using the Morphological Analysis for Material Attribution (MAMA) software [1]. By properly representing these features and considering them within the framework of a statistical model, these measurements can be used to make inferences on the material's production process.

To achieve this, we propose a Functional Inverse Prediction (FIP) modelling framework for inferring material processing conditions [2]. This framework uses functional representations of the morphological characteristics of Pu that are obtained using Scanning Electron Microscope (SEM) images to quantitatively model the relationship between the sample of Pu and the processing conditions. This framework is particularly useful in that it does not rely on a specific set of conditions or models, and only requires a minimal set of assumptions that allow for comparing different inverse modelling approaches, such as those reviewed in [3]. The FIP framework, mapped out in Figure 1, divides the problem of determining material processing conditions into two phases: (1) A training phase under which a functional statistical model is fit to relate morphological features to material processing conditions using a basis representation of these Pu morphological features and (2) An inference phase which utilizes the forward model to predict the unknown processing conditions from a new Pu sample.

We illustrate the usefulness of this method using data collected from an optimally designed statistical experiment that allows for studying the shape, texture, and MAMA feature responses associated with the processing conditions of PuO_2. The novel representations of these morphological features obtained directly from SEM imagery, along with a comparison to standard approaches of using a mean-only summary gathered from MAMA are demonstrated in this framework. These experiments show that: (1) the fitted model is useful for recovering the original processing conditions, and (2): given a new

interdicted sample, the fitted model is useful for inferring the processing conditions that were used to produce that sample.

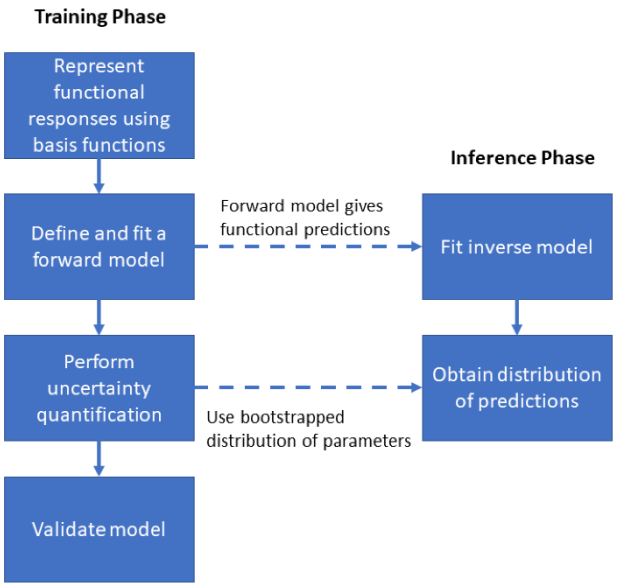

Figure 1: FIP Framework

[1] Gaschen, Brian Keith, et al. *MAMA User Guide v2. 0.1*. No. LA-UR-16-25116. Los Alamos National Lab.(LANL), Los Alamos, NM (United States), 2016.

[2] Ries, D., Zhang, A., Tucker, J. D., Shuler, K., and Ausdemore, M. (February 3, 2022). "A framework for inverse prediction using functional response data." ASME. J. Comput. Inf. Sci. Eng. doi: https://doi.org/10.1115/1.4053752

[3] Lewis, J. R., Zhang, A., & Anderson-Cook, C. M. (2018). Comparing multiple statistical methods for inverse prediction in nuclear forensics applications. *Chemometrics and Intelligent Laboratory Systems*, *175*, 116-129.

This paper describes objective technical results and analysis. Any subjective views or opinions that might be expressed in the paper do not necessarily represent the views of the U.S. Department of Energy or the United States Government.

Sandia National Laboratories, a multi-mission laboratory managed and operated by National Technology & Engineering Solutions of Sandia, LLC, a wholly owned subsidiary of Honeywell International, Inc., for the U.S. Department of Energy's National Nuclear Security Administration under contract DE-NA0003525. SAND2022-3664 A.

Los Alamos National Laboratory strong supports academic freedom and a researcher's right to publish; as an institution, however, the Laboratory does not endorse the viewpoint of a publication or guarantee its technical correctness.